

Paolo Di Barba
Antonio Savini
Sławomir Wiak

Field Models in Electricity and Magnetism



Springer

Field Models in Electricity and Magnetism

Paolo Di Barba • Antonio Savini • Sławomir Wiak

Field Models in Electricity and Magnetism

 Springer

Paolo Di Barba
University of Pavia
Dept. Electrical Engineering
Via Ferrata, 1
27100 Pavia
Italy
paolo.dibarba@unipv.it

Antonio Savini
University of Pavia
Dept. Electrical Engineering
Via Ferrata, 1
27100 Pavia
Italy

Sławomir Wiak
Technical University of Lodz
Inst. Mechatronics and
Information Systems
ul. Stefanowskiego 18/22
90-924 Lodz
Poland

ISBN 978-1-4020-6842-3

e-ISBN 978-1-4020-6843-0

Library of Congress Control Number: 2008922192

© 2008 Springer Science+Business Media, LLC

No part of this work may be reproduced, stored in a retrieval system, or transmitted in any form or by any means, electronic, mechanical, photocopying, microfilming, recording or otherwise, without written permission from the Publisher, with the exception of any material supplied specifically for the purpose of being entered and executed on a computer system, for exclusive use by the purchaser of the work.

Printed on acid-free paper.

9 8 7 6 5 4 3 2 1

springer.com

To our wives

Contents

1	Introduction	1
2	Vector Fields	3
2.1	Basic Operators and Equations	3
2.1.1	Vector Fields and Operators	3
2.1.2	Definition of a Vector Field	5
2.1.3	Decomposition of a Field	7
2.1.4	Scalar and Vector Potentials	8
2.1.5	Green's Theorem	9
2.1.6	Green's Formula	9
2.2	Electrostatic Field	10
2.2.1	Maxwell's Equations for Electrostatics	10
2.2.2	Electrostatic Potentials	13
2.2.3	Electrostatic Energy	15
2.2.4	Field of a Charged Plane in a Rectangular Domain	16
2.2.5	Field of a Point Charge in a Spherical Domain	16
2.2.6	Field of a Dipole	18
2.2.7	Field of a Line Charge in a Cylindrical Domain	19
2.2.8	Field of a Surface Charge on a Sphere	20
2.2.9	Energy and Forces in the Electrostatic Field	22
2.2.10	Force between the Plates of a Capacitor	24
2.2.11	Force at the Interface between Two Dielectric Materials	25
2.3	Magnetostatic Field	28
2.3.1	Maxwell's Equations for Magnetostatics	28
2.3.2	Magnetostatic Potentials	30
2.3.3	Magnetostatic Energy	32
2.3.4	Field of a Line Current in a Three-Dimensional Domain: Differential Approach	33
2.3.5	Energy and Forces in the Magnetostatic Field	34
2.3.6	Force on an Electromagnet	37
2.3.7	Test Problems	38

2.4	Steady Conduction Field	39
2.4.1	Maxwell's Equations for Conduction Field	39
2.4.2	Potentials	40
2.4.3	Power Loss	42
2.4.4	Analytic Functions of Complex Variable	42
2.4.5	Field of a Cylindrical Conductor	42
3	Analytical Methods for Solving Boundary-Value Problems	45
3.1	Method of Green's Function	45
3.1.1	Green's Formula for Electrostatics	46
3.1.2	Green's Functions for Boundary-Value Problems	46
3.1.3	Field of a Point Charge Surrounded by a Spherical Surface at Known Potential	54
3.1.4	Field of a Surface Dipole Distributed on a Sphere of Radius R	56
3.1.5	Green's Formula for Two-Dimensional Magnetostatics	57
3.1.6	Field of a Line Current in a Three-Dimensional Domain: Integral Approach	57
3.1.7	Field of a Current-Carrying Conductor of Rectangular Cross-Section	59
3.2	Method of Images	60
3.2.1	Magnetic Field of a Line Current in a Slot	67
3.2.2	Magnetic Field of a Line AC Current over a Conducting Half-Space	70
3.3	Method of Separation of Variables	71
3.3.1	Magnetic Field of a Current Uniformly Distributed in a Slot	73
4	Numerical Methods for Solving Boundary-Value Problems	77
4.1	Variational Formulation in Two-Dimensional Magnetostatics	77
4.2	Finite Elements for Two-Dimensional Magnetostatics	80
4.2.1	Discretization of Energy Functional	80
4.2.2	Local Shape Functions in Rectangular Coordinates	82
4.2.3	Coefficient Matrix and Source Vector	84
4.2.4	From Potential to Field	85
4.2.5	Magnetic Field in a Slot Solved by the Finite Element Method	86
4.3	Finite Elements for Three-Dimensional Magnetostatics	95
4.3.1	Surface and Solid Modelling	95
4.3.2	Local Shape Functions in Rectangular Coordinates	95
4.3.3	Comparison of 2D and 3D Simulations of an Electromagnet	97

5	Time-Varying Electromagnetic Field	101
5.1	Maxwell's Equations in Differential Form	101
5.2	Poynting's Vector	103
5.3	Maxwell's Equations in the Frequency Domain	103
5.4	Plane Waves in an Infinite Domain	105
5.5	Wave and Diffusion Equations in Terms of Vectors \vec{E} and \vec{H}	106
5.6	Wave and Diffusion Equations in Terms of Scalar and Vector Potentials	108
5.7	Electromagnetic Field Radiated by an Oscillating Dipole	110
5.8	Diffusion Equation in Terms of Dual Potentials	113
5.9	Weak Eddy Current in a Conducting Plane under AC Conditions ...	115
5.10	Strong Eddy Current in a Conducting Plane under AC Conditions ..	116
5.11	Eddy Current in a Cylindrical Conductor under Step Excitation Current	122
5.12	Electromagnetic Field Equations in Different Reference Frames ...	125
5.12.1	A Relativistic Example: Steady Motion and Magnetic Diffusion	129
5.12.2	Galileian and Lorentzian Transformations in Electromagnetism	132
6	Inverse Problems	135
6.1	Direct and Inverse Problems	135
6.2	Well-Posed and Ill-Posed Problems	135
6.3	Fredholm's Integral Equation of the First Kind	137
6.4	Case Study: Synthesis of the Source Producing a Magnetic Field in Two Dimensions	137
6.5	Under- and Over-Determined Systems of Equations	138
6.6	Least-Squares Solution	139
6.7	Classification of Inverse Problems	141
7	Optimization	143
7.1	Solution of Inverse Problems by the Minimization of a Functional	143
7.2	Constrained Optimization	144
7.3	Multiobjective Optimization	145
7.4	Gradient-Free and Gradient-Based Methods	145
7.5	Deterministic vs Non-Deterministic Search	146
7.6	A Deterministic Algorithm of Lowest Order: Simplex Method	147
7.7	A Non-Deterministic Algorithm of Lowest Order: Evolution Strategy	147
7.8	Numerical Case Studies	149
7.8.1	Identification of the B–H Curve of the Iron Region of a Magnetic Pole	150
7.8.2	Shape Design of a Magnetic Pole (Static Optimization)	153

7.8.3	Shape Design of a Magnetic Pole (Dynamic Optimization)	156
7.8.4	A Multiobjective Approach to the Shape Design of a Magnetic Pole	159
8	Conclusion	161
	Appendix	163
	References	167
	Acknowledgements	169
	Index	171

Chapter 1

Introduction

The subject of computation in electricity and magnetism has so advanced in the past 40 years, since the advent of digital computers and thanks to the development of numerical methods, that today it urges and deserves adequate collocation also in curricula for electrical engineering. However, the time allotted to the subject in general is not very large in undergraduate studies, where more emphasis is still usually attributed to circuits and systems than to fields. Moreover, field models are generally not very popular among students, who are by far more familiar with circuit models. Even if one considers the quasi-static case, however, not only is electromagnetism fundamental for people dealing with electric and magnetic devices, but it provides the basis for, e.g. semiconductor device design, bioengineering applications and so forth.

In the authors' opinion, therefore, time has come to present field models in electricity and magnetism, in the frame of an introductory textbook to be used by senior undergraduate or graduate students in the area of electrical and computer engineering. Elementary electromagnetism, basic vector analysis and fundamentals of numerical analysis are assumed to be known subjects.

Having this in mind, the authors have collected the experience they have accumulated in teaching electromagnetic theory at various levels and in different countries; they intend to offer a book on applied electricity and magnetism, describing the problems of calculating electromagnetic fields and the integral parameters connected with them in sufficiently clear and short form.

The aim is that of writing a textbook containing the necessary background, i.e. laws explaining electromagnetic phenomena, mathematical operators and equations as well as methods for electromagnetic field calculation. The latter include both analytical and numerical methods applied to the analysis as well as to the synthesis of electromagnetic devices.

Classical analytical methods are first presented and closed-form solutions to some problems are obtained by making the simplifying assumptions required. Numerical methods are then discussed and it is shown how they are able to provide a solution to practically any complicated problem. Special emphasis, among the numerical schemes, is attributed to the finite element method because it is largely and commonly used for field simulation. A peculiar feature of the book is the fact that the accent

is always put on field vectors rather than potentials, because the former represent the quantity of main physical interest; consequently, the differential formulation of Maxwell's equations is preferred with respect to the integral one. An effort is accordingly made to develop both analytical and numerical methods for solving the electromagnetic problem in terms of field components directly.

Chapter 2 starts with a basic introduction to the world of vector fields. The reader is guided through definitions, properties, theorems and equations in simply connected domains, both bounded and unbounded. Scalar and vector potentials associated to fields are presented as well. Then electric, magnetic and conduction fields under steady conditions are considered separately.

Chapter 3 presents the most common analytical methods for solving boundary-value problems which are applicable to simple domains.

For more complicated domains, numerical methods are required. Accordingly, Chapter 4 deals with the finite-element method which has become the most general and powerful method to solve field problems in these domains.

A general introduction to time-varying electromagnetic fields is presented in Chapter 5, where Maxwell's equations are presented and solved in some fundamental cases.

Finally, in Chapters 6 and 7 the authors move from direct to inverse problems, which in the past decade have increasingly attracted the attention not just of researchers but also of practitioners in the field of electricity and magnetism. Nowadays, in fact, the association of powerful low-price and high-speed computers with available advanced numerical methods makes it possible to try solutions for inverse problems of various kind, with the ultimate target of offering engineers the possibility of implementing the so-called automated optimal design. In these two chapters, after giving definitions and a general presentation of the background, strategies to solve inverse problems are presented and some case studies are solved.

Throughout the book theoretical concepts are illustrated by practical examples, following a problem-solving approach and never forgetting that the engineering task is just that of formulating and solving electromagnetic problems in a computational fashion. It has been decided, in particular, to solve a single test problem by different methods so that, from the comparison, limitations and advantages of each approach are made clear.

The book is mainly recommended and addressed to undergraduate and graduate students of electrical and computer engineering; however, it could also be helpful for students preparing their Ph.D. projects, as well as for researchers and engineers working in the broad area of electromagnetism. Finally the book, although written by the authors who had in mind their own students in Italy and Poland, is intended hopefully to be valid for a wider international audience.

Pavia, Łódź
August 2007

Paolo Di Barba, Antonio Savini, Sławomir Wiak

Chapter 2

Vector Fields

2.1 Basic Operators and Equations

2.1.1 Vector Fields and Operators

In a three-dimensional domain (Fig. 2.1), given a reference frame, a vector function \bar{V} can be defined in

- (i) a system of rectangular coordinates

$$\bar{V} = V_x \bar{i}_x + V_y \bar{i}_y + V_z \bar{i}_z \quad (2.1)$$

- (ii) a system of cylindrical coordinates

$$\bar{V} = V_r \bar{i}_r + V_\phi \bar{i}_\phi + V_z \bar{i}_z \quad (2.2)$$

- (iii) a system of spherical coordinates

$$\bar{V} = V_r \bar{i}_r + V_\phi \bar{i}_\phi + V_\theta \bar{i}_\theta \quad (2.3)$$

Two first-order differential operators, namely curl and divergence, can be defined for a given vector function \bar{V} , hereinafter assumed to be regular enough.

In a system of rectangular coordinates, introducing the operator $\bar{\nabla}$ which is defined as

$$\bar{\nabla} \equiv \frac{\partial}{\partial x} \bar{i}_x + \frac{\partial}{\partial y} \bar{i}_y + \frac{\partial}{\partial z} \bar{i}_z \quad (2.4)$$

curl and divergence are expressed by the following formulas

$$\text{curl } \bar{V} \equiv \bar{\nabla} \times \bar{V} = \left(\frac{\partial V_z}{\partial y} - \frac{\partial V_y}{\partial z} \right) \bar{i}_x + \left(\frac{\partial V_x}{\partial z} - \frac{\partial V_z}{\partial x} \right) \bar{i}_y + \left(\frac{\partial V_y}{\partial x} - \frac{\partial V_x}{\partial y} \right) \bar{i}_z \quad (2.5)$$

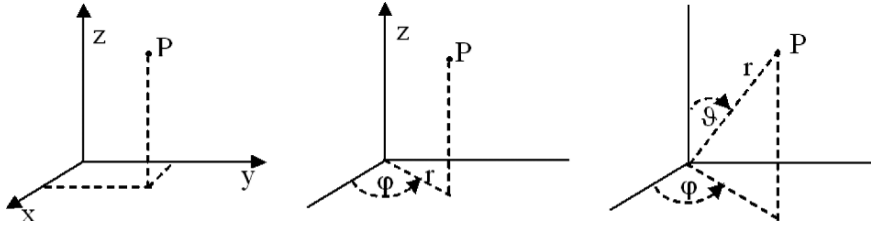


Fig. 2.1 Three systems of coordinates

and

$$\operatorname{div} \bar{V} \equiv \bar{\nabla} \cdot \bar{V} = \frac{\partial V_x}{\partial x} + \frac{\partial V_y}{\partial y} + \frac{\partial V_z}{\partial z} \quad (2.6)$$

respectively.

A vector function \bar{V} can be obtained from a scalar function U by means of the differential operator gradient:

$$\bar{V} \equiv \operatorname{grad} U = \bar{\nabla} U = \frac{\partial U}{\partial x} \bar{i}_x + \frac{\partial U}{\partial y} \bar{i}_y + \frac{\partial U}{\partial z} \bar{i}_z \quad (2.7)$$

Two second-order differential operators can be also defined, as follows

Laplacian of a scalar function

$$\nabla^2 U \equiv \operatorname{div}(\operatorname{grad} U) = \bar{\nabla} \cdot (\bar{\nabla} U) \quad (2.8)$$

Laplacian of a vector function

$$\bar{\nabla}^2 \bar{V} \equiv \bar{\nabla} (\bar{\nabla} \cdot \bar{V}) - \bar{\nabla} \times (\bar{\nabla} \times \bar{V}) \quad (2.9)$$

In a system of rectangular coordinates, the former operator becomes

$$\nabla^2 U = \frac{\partial^2 U}{\partial x^2} + \frac{\partial^2 U}{\partial y^2} + \frac{\partial^2 U}{\partial z^2} \quad (2.10)$$

while the latter, if $\bar{\nabla} \cdot \bar{V} = 0$, reduces to

$$\bar{\nabla}^2 \bar{V} = \left(\nabla^2 V_x \right) \bar{i}_x + \left(\nabla^2 V_y \right) \bar{i}_y + \left(\nabla^2 V_z \right) \bar{i}_z \quad (2.11)$$

Surfaces to which \bar{V} is tangent are called flux (or field) surfaces. In each point of the domain we can draw one and only one flux surface. In rectangular coordinates, the equations of a flux surface are

$$\frac{dx}{V_x} = \frac{dy}{V_y} = \frac{dz}{V_z} \quad (2.12)$$

In a two-dimensional domain the curl of a vector $\bar{V} = (V_x, V_y)$ is actually a scalar quantity; in fact

$$\bar{\nabla} \times \bar{V} = \left(\frac{\partial V_y}{\partial x} - \frac{\partial V_x}{\partial y} \right) \bar{i}_z \quad (2.13)$$

i.e. it exhibits a single non-zero component. Moreover, through a $\frac{\pi}{2}$ rotation of \bar{V} in the clockwise direction, the following vector can be defined

$$\bar{V}^\perp = (V_y, -V_x) \quad (2.14)$$

Then, one has

$$|\bar{\nabla} \times \bar{V}| = |\bar{\nabla} \cdot \bar{V}^\perp| \quad (2.15)$$

namely, curl and divergence identify the same operator.

2.1.2 Definition of a Vector Field

A vector field \bar{V} is defined in a simply-connected domain Ω , giving its divergence and curl in Ω as well as its normal component on the boundary Γ (Helmholtz's theorem).

In a domain Ω bounded by Γ , given

$$\bar{\nabla} \cdot \bar{V} = s \text{ in } \Omega \quad (2.16)$$

$$\bar{\nabla} \times \bar{V} = \bar{c} \quad (2.17)$$

$$\bar{V} \cdot \bar{n} = h \text{ along } \Gamma \quad (2.18)$$

where \bar{n} is the outward normal versor, the vector field \bar{V} is defined in a unique way.

In fact, let us assume that both \bar{V}_1 and \bar{V}_2 fulfil the above equations. It follows

$$\bar{\nabla} \cdot \bar{V}_1 = \bar{\nabla} \cdot \bar{V}_2 = s \text{ then } \bar{\nabla} \cdot (\bar{V}_1 - \bar{V}_2) = 0 \quad (2.19)$$

$$\bar{\nabla} \times \bar{V}_1 = \bar{\nabla} \times \bar{V}_2 = \bar{c} \text{ then } \bar{\nabla} \times (\bar{V}_1 - \bar{V}_2) = 0 \quad (2.20)$$

$$\bar{V}_1 \cdot \bar{n} = \bar{V}_2 \cdot \bar{n} = h \text{ then } (\bar{V}_1 - \bar{V}_2) \cdot \bar{n} = 0 \quad (2.21)$$

For the vector $\bar{W} = \bar{V}_1 - \bar{V}_2$, from (2.20) one has

$$\bar{\nabla} \times \bar{W} = 0 \quad (2.22)$$

It is so possible to find a scalar Ψ so that, if Ω is simply connected,

$$\bar{W} = \bar{\nabla} \Psi \quad (2.23)$$

and

$$\bar{W} \cdot \bar{n} = \bar{\nabla} \Psi \cdot \bar{n} = 0 \quad (2.24)$$

Moreover, being

$$\bar{\nabla} \cdot \bar{W} = 0 \quad (2.25)$$

one has also

$$\bar{\nabla} \cdot \bar{\nabla} \Psi = 0 = \nabla^2 \Psi \quad (2.26)$$

By applying the Gauss's theorem (see A.10) to $\Psi \bar{\nabla} \Psi$ one obtains

$$\int_{\Gamma} \Psi \bar{\nabla} \Psi \cdot \bar{n} d\Gamma = \int_{\Omega} \bar{\nabla} \cdot (\Psi \bar{\nabla} \Psi) d\Omega = \int_{\Omega} (\bar{\nabla} \Psi \cdot \bar{\nabla} \Psi + \Psi \nabla^2 \Psi) d\Omega \quad (2.27)$$

Taking (2.24) and (2.26) into account, it results

$$\int_{\Omega} \bar{\nabla} \Psi \cdot \bar{\nabla} \Psi d\Omega = 0 \quad (2.28)$$

Therefore, it must be everywhere

$$\bar{\nabla} \Psi = \bar{W} = 0 \quad (2.29)$$

i.e.

$$\bar{V}_1 = \bar{V}_2 \quad (2.30)$$

So, the two vectors \bar{V}_1 and \bar{V}_2 are identical

$$\bar{V} = \bar{V}_1 = \bar{V}_2 \quad (2.31)$$

The following remarks can be put forward:

- (i) The value of s , \bar{c} and h , which are the sources of the field, cannot be chosen arbitrarily.

In fact:

- (a) \bar{c} must be divergence-free (solenoidal)

$$\bar{\nabla} \cdot (\bar{\nabla} \times \bar{V}) = \bar{\nabla} \cdot \bar{c} = 0 \quad (2.32)$$

- (b)
$$\int_{\Omega} \bar{\nabla} \cdot \bar{V} d\Omega = \int_{\Gamma} \bar{V} \cdot \bar{n} d\Omega \quad (2.33)$$

i.e.

$$\int_{\Omega} s d\Omega = \int_{\Gamma} h d\Gamma \quad (2.34)$$

- (ii) Specifying just $\bar{\nabla} \cdot \bar{V} = s$ is not enough to determine \bar{V} since also $\bar{V} + \bar{\nabla} \times \bar{W}$ fulfils (2.16)

$$\bar{\nabla} \cdot (\bar{V} + \bar{\nabla} \times \bar{W}) = \bar{\nabla} \cdot \bar{V} + \bar{\nabla} \cdot \bar{\nabla} \times \bar{W} = s \quad (2.35)$$

Conversely, \bar{V} is not determined by just $\bar{\nabla} \times \bar{V} = \bar{c}$ since $\bar{V} + \bar{\nabla}\Psi$ also obeys (2.17)

$$\bar{\nabla} \times (\bar{V} + \bar{\nabla}\Psi) = \bar{\nabla} \times \bar{V} + \bar{\nabla} \times \bar{\nabla}\Psi = \bar{c} + 0 \quad (2.36)$$

(iii) If $s = 0$, the field is called solenoidal.

(iv) If $\bar{c} = 0$, the field is called irrotational.

The problem of finding the field \bar{V} in a domain, knowing its sources and normal component on the boundary, is normally referred to as a *boundary-value problem*. As shown by the Helmholtz's theorem, this problem has, at most, a unique solution.

2.1.3 Decomposition of a Field

Every vector field \bar{V} with vanishing normal component at the boundary is the sum of a curl-free field \bar{V}_1 and a divergence-free field \bar{V}_2 , both of which with vanishing normal component at the boundary.

In fact, it is assumed that \bar{V}_1 subject to

$$\bar{\nabla} \cdot \bar{V}_1 = s \text{ in } \Omega \quad (2.37)$$

$$\bar{\nabla} \times \bar{V}_1 = 0 \quad (2.38)$$

and to

$$\bar{V}_1 \cdot \bar{n} = 0 \text{ along } \Gamma \quad (2.39)$$

is known, together with \bar{V}_2 for which

$$\bar{\nabla} \cdot \bar{V}_2 = 0 \text{ in } \Omega \quad (2.40)$$

$$\bar{\nabla} \times \bar{V}_2 = \bar{c} \quad (2.41)$$

and

$$\bar{V}_2 \cdot \bar{n} = 0 \text{ along } \Gamma \quad (2.42)$$

hold. Then, for

$$\bar{V} = \bar{V}_1 + \bar{V}_2 \quad (2.43)$$

one has

$$\bar{\nabla} \cdot \bar{V} = \bar{\nabla} \cdot (\bar{V}_1 + \bar{V}_2) = \bar{\nabla} \cdot \bar{V}_1 = s \quad (2.44)$$

$$\bar{\nabla} \times \bar{V} = \nabla \times (\bar{V}_1 + \bar{V}_2) = \bar{\nabla} \times \bar{V}_2 = \bar{c} \text{ in } \Omega \quad (2.45)$$

$$\bar{V} \cdot \bar{n} = (\bar{V}_1 + \bar{V}_2) \cdot \bar{n} = 0 \text{ along } \Gamma \quad (2.46)$$

Therefore \bar{V} in (2.43) is defined in a unique way.

It can be proven that the result holds, in general, also for other boundary conditions.

2.1.4 Scalar and Vector Potentials

Every field $\bar{\mathbf{V}}$ in an unbounded, homogeneous and simply-connected three-dimensional domain can be expressed by means of a scalar potential ϕ and a vector potential $\bar{\mathbf{A}}$.

It is assumed that

$$\bar{\mathbf{V}} = -\bar{\nabla}\phi + \bar{\nabla} \times \bar{\mathbf{A}} \quad (2.47)$$

with

$$\phi(\mathbf{r}) = \frac{1}{4\pi} \int_{\Omega} \frac{s}{r} d\Omega \quad (2.48)$$

and

$$\bar{\mathbf{A}}(\mathbf{r}) = \frac{1}{4\pi} \int_{\Omega} \frac{\bar{\mathbf{c}}}{r} d\Omega \quad (2.49)$$

where $r = |\bar{\mathbf{r}}_P - \bar{\mathbf{r}}_Q|$ is the distance between source (s or $\bar{\mathbf{c}}$) point Q and field point P . If $\Omega_Q \subset \Omega$ is the subdomain represented by all source points and $\Omega_P \subset \Omega$ is the subdomain of all field points, it is assumed that $\Omega_Q \cup \Omega_P = \Omega$ and $\Omega_Q \cap \Omega_P = 0$.

It is possible to show that $\bar{\mathbf{V}}$ fulfils

$$\bar{\nabla} \cdot \bar{\mathbf{V}} = s \quad (2.50)$$

$$\bar{\nabla} \times \bar{\mathbf{V}} = \bar{\mathbf{c}} \quad (2.51)$$

so that it is defined in unique way.

In fact, taking the divergence of (2.47) one has (see A.5 and A.8)

$$\begin{aligned} \bar{\nabla} \cdot \bar{\mathbf{V}} &= -\bar{\nabla} \cdot \bar{\nabla}\phi + \bar{\nabla} \cdot \bar{\nabla} \times \bar{\mathbf{A}} = -\bar{\nabla} \cdot \bar{\nabla}\phi = -\nabla^2\phi = \\ &= -\frac{1}{4\pi} \nabla^2 \left(\int_{\Omega} \frac{s}{r} d\Omega \right) = -\frac{1}{4\pi} \int_{\Omega} s \nabla^2 \left(\frac{1}{r} \right) d\Omega = s \end{aligned} \quad (2.52)$$

On the other hand, taking the curl of (2.47) and assuming $\bar{\nabla} \cdot \bar{\mathbf{A}} = 0$ one obtains (see A.5 and A.9)

$$\begin{aligned} \bar{\nabla} \times \bar{\mathbf{V}} &= -\bar{\nabla} \times (\bar{\nabla}\phi) + \bar{\nabla} \times \bar{\nabla} \times \bar{\mathbf{A}} = \bar{\nabla} \times \bar{\nabla} \times \bar{\mathbf{A}} = \bar{\nabla} (\bar{\nabla} \cdot \bar{\mathbf{A}}) - \bar{\nabla}^2 \bar{\mathbf{A}} = \\ &= -\frac{1}{4\pi} \int_{\Omega} \bar{\mathbf{c}} \nabla^2 \left(\frac{1}{r} \right) d\Omega = \bar{\mathbf{c}} \end{aligned} \quad (2.53)$$

It can be proven that the result is valid also for bounded domains.

2.1.5 Green's Theorem

Any two scalar and regular functions ϕ and ψ defined in a domain Ω bounded by Γ fulfil the following reciprocity relation (Green's theorem or Green's second identity).

$$\int_{\Gamma} \left(\phi \frac{\partial \psi}{\partial n} - \psi \frac{\partial \phi}{\partial n} \right) d\Gamma = \int_{\Omega} \left(\phi \nabla^2 \psi - \psi \nabla^2 \phi \right) d\Omega \quad (2.54)$$

In fact, applying the divergence theorem (see A.10) to $\phi \bar{\nabla} \psi$, one has

$$\int_{\Gamma} (\phi \bar{\nabla} \psi) \cdot \bar{n} d\Gamma = \int_{\Omega} \bar{\nabla} \cdot (\phi \bar{\nabla} \psi) d\Omega \quad (2.55)$$

and

$$\int_{\Gamma} \phi \frac{\partial \psi}{\partial n} d\Gamma = \int_{\Omega} \left(\bar{\nabla} \phi \cdot \bar{\nabla} \psi + \phi \nabla^2 \psi \right) d\Omega \quad (2.56)$$

Equation (2.56) is called Green's first identity and can be put into the form

$$\int_{\Omega} \phi \nabla^2 \psi d\Omega = \int_{\Gamma} \phi \frac{\partial \psi}{\partial n} d\Gamma - \int_{\Omega} \bar{\nabla} \phi \cdot \bar{\nabla} \psi d\Omega \quad (2.57)$$

which expresses the rule of integration by parts.

Doing the same for $\psi \bar{\nabla} \phi$, one obtains

$$\int_{\Gamma} (\psi \bar{\nabla} \phi) \cdot \bar{n} d\Gamma = \int_{\Omega} \bar{\nabla} \cdot (\psi \bar{\nabla} \phi) d\Omega \quad (2.58)$$

and

$$\int_{\Gamma} \psi \frac{\partial \phi}{\partial n} d\Gamma = \int_{\Omega} \left(\bar{\nabla} \psi \cdot \bar{\nabla} \phi + \psi \nabla^2 \phi \right) d\Omega \quad (2.59)$$

Subtracting (2.59) from (2.56) gives

$$\int_{\Gamma} \left(\phi \frac{\partial \psi}{\partial n} - \psi \frac{\partial \phi}{\partial n} \right) d\Gamma = \int_{\Omega} \left(\phi \nabla^2 \psi - \psi \nabla^2 \phi \right) d\Omega \quad (2.60)$$

2.1.6 Green's Formula

In a three-dimensional domain Ω a function ϕ can be expressed as a function of $\nabla^2 \phi$ in Ω and of ϕ and $\frac{\partial \phi}{\partial n}$ on Γ .

In fact, from (2.60), for $\psi = \frac{1}{r}$, one has (see A.5)

$$\int_{\Gamma} \left(\phi \frac{\partial \psi}{\partial n} - \psi \frac{\partial \phi}{\partial n} \right) d\Gamma = - \int_{\Omega} 4\pi \phi \delta(r) d\Omega - \int_{\Omega} \psi \nabla^2 \phi d\Omega \quad (2.61)$$

and

$$\int_{\Gamma} \phi \frac{\partial \psi}{\partial n} d\Gamma - \int_{\Gamma} \psi \frac{\partial \phi}{\partial n} d\Gamma + \int_{\Omega} \psi \nabla^2 \phi d\Omega = -4\pi \phi \quad (2.62)$$

Finally

$$\phi = \frac{1}{4\pi} \left\{ \int_{\Gamma} \psi \frac{\partial \phi}{\partial n} d\Gamma - \int_{\Gamma} \phi \frac{\partial \psi}{\partial n} d\Gamma - \int_{\Omega} \psi \nabla^2 \phi d\Omega \right\} \quad (2.63)$$

is obtained, which is the Green's formula.

In particular, for an unbounded domain, it results

$$\phi = -\frac{1}{4\pi} \int_{\Omega} \frac{1}{r} \nabla^2 \phi d\Omega \quad (2.64)$$

Comparing (2.64) with (2.48), ϕ is the scalar potential if $\nabla^2 \phi = -s$, where s is the field source.

In terms of scalar potential, the boundary-value problem becomes that of finding the potential ϕ in the domain Ω , knowing the field source s and the values of potential (Dirichlet's problem) or normal derivative of the potential (Neumann's problem) on the boundary Γ .

2.2 Electrostatic Field

In a domain Ω with boundary Γ , filled in by an insulating medium, in the presence of free electric charges distributed with density ρ (C m^{-3}) in Ω and/or electric charges distributed with density σ (C m^{-2}) along Γ , the electrostatic field is defined by field intensity \bar{E} (V m^{-1}) as well as by flux density \bar{D} (C m^{-2}). The medium is supposed to be at rest with respect to the observer of the field. The two vectors are linked by the constitutive law, which, if the medium is isotropic and linear and in the absence of permanent polarization, is

$$\bar{D} = \epsilon \bar{E} \quad (2.65)$$

The parameter ϵ is called permittivity (F m^{-1}).

2.2.1 Maxwell's Equations for Electrostatics

The electrostatic field is governed by the following equations in Ω

$$\bar{\nabla} \times \bar{E} = 0 \quad (2.66)$$

$$\bar{\nabla} \cdot \bar{D} = \rho \quad (2.67)$$

and along Γ

$$\bar{\mathbf{n}} \times \bar{\mathbf{E}} = 0 \quad (2.68)$$

if Γ is a perfect conductor (flux lines perpendicular to Γ), or

$$\bar{\mathbf{n}} \cdot \bar{\mathbf{D}} = \sigma \quad (2.69)$$

if Γ carries charge density σ (C m^{-2}), or

$$\bar{\mathbf{n}} \cdot \bar{\mathbf{D}} = 0 \quad (2.70)$$

if Γ is a perfect insulator (flux lines parallel to Γ).

In terms of just vector $\bar{\mathbf{E}}$, the equations governing the electrostatic field for a homogeneous, isotropic and linear medium become in Ω

$$\bar{\nabla} \times \bar{\mathbf{E}} = 0 \quad (2.71)$$

$$\bar{\nabla} \cdot \bar{\mathbf{E}} = \frac{\rho}{\epsilon} \quad (2.72)$$

and along Γ

$$\bar{\mathbf{n}} \times \bar{\mathbf{E}} = 0 \quad (2.73)$$

or, for Γ conducting

$$\bar{\mathbf{n}} \cdot \bar{\mathbf{E}} = \frac{\sigma}{\epsilon} \quad (2.74)$$

and, for Γ insulating

$$\bar{\mathbf{n}} \cdot \bar{\mathbf{E}} = 0 \quad (2.75)$$

respectively.

According to theorem (2.2) $\bar{\mathbf{E}}$ is uniquely defined and, because of (2.66), it is irrotational.

Moreover, if both σ and ρ are given, then according to (2.67), (2.69) and Gauss's theorem (see A.10) it must be

$$\int_{\Gamma} |\sigma| d\Gamma = \int_{\Omega} |\rho| d\Omega \quad (2.76)$$

i.e. the total charge sums up to zero; in other words, surface charge density on Γ and volume charge density in Ω are not independent.

In a two-dimensional domain, at the interface between two different media of permittivity ϵ_1 and ϵ_2 , respectively (Fig. 2.2), in the presence of free charge of density σ (C m^{-2}) at the interface, from (A.10), integrating $\bar{\mathbf{D}}$ along a closed surface including point P, the following two transmission conditions hold

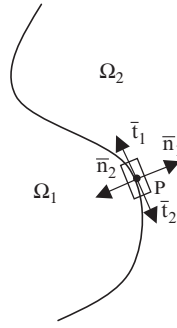


Fig. 2.2 Interface between two field regions

First of all

$$\bar{n}_1 \cdot \bar{D}_2 + \bar{n}_2 \cdot \bar{D}_1 = \bar{n}_1 \cdot \bar{D}_2 - \bar{n}_1 \cdot \bar{D}_1 = \bar{n}_1 \cdot (\bar{D}_2 - \bar{D}_1) = \sigma \quad (2.77)$$

If $\sigma = 0$, the normal component of \bar{D} is continuous.

Then, from (A.11), integrating \bar{E} along a closed rectangular line surrounding point P, one has

$$\bar{t}_1 \cdot \bar{E}_1 + \bar{t}_2 \cdot \bar{E}_2 = \bar{t}_1 \cdot \bar{E}_1 - \bar{t}_1 \cdot \bar{E}_2 = \bar{t}_1 \cdot (\bar{E}_1 - \bar{E}_2) = 0 \quad (2.78)$$

i.e. the tangential component of \bar{E} is continuous.

In the case of a non-homogeneous medium, the following remark can be put forward. After (2.65) and (2.66), considering vector identity (A.16), it turns out to be

$$\bar{\nabla} \times \varepsilon^{-1} \bar{D} = \varepsilon^{-1} \bar{\nabla} \times \bar{D} + \bar{\nabla} \varepsilon^{-1} \times \bar{D} = 0 \quad (2.79)$$

Apparently, field \bar{D} is irrotational if $\bar{\nabla} \varepsilon^{-1}$ and \bar{D} are parallel vectors; this means that lines separating layers of different ε are orthogonal to field lines of \bar{D} . If $\bar{\nabla} \varepsilon^{-1} = 0$ (homogeneous medium), then \bar{D} is always irrotational.

Conversely, in a charge-free domain, after (2.65) and (2.67), considering vector identity (A.14), one has

$$\bar{\nabla} \cdot \varepsilon \bar{E} = \varepsilon \bar{\nabla} \cdot \bar{E} + \bar{\nabla} \varepsilon \cdot \bar{E} = 0 \quad (2.80)$$

In the case of a non-homogeneous medium, field \bar{E} is solenoidal if $\bar{\nabla} \varepsilon$ and \bar{E} are orthogonal vectors; this means that lines separating layers of different ε are parallel to field lines of \bar{E} .

Finally, an extension of constitutive law (2.65) is considered. When a permanent polarization \bar{D}_0 is present in the insulating medium (electret), the constitutive law becomes

$$\bar{D} = \varepsilon \bar{E} + \bar{D}_0 \quad (2.81)$$

Then, the field equations are

$$\bar{\nabla} \times \bar{\mathbf{E}} = 0 \quad (2.82)$$

$$\bar{\nabla} \cdot (\epsilon \bar{\mathbf{E}}) = \rho - \bar{\nabla} \cdot \bar{\mathbf{D}}_0 \quad (2.83)$$

in terms of $\bar{\mathbf{E}}$, and

$$\bar{\nabla} \cdot (\epsilon \bar{\nabla} U) = -\rho + \bar{\nabla} \cdot \bar{\mathbf{D}}_0 \quad (2.84)$$

in terms of U , respectively (see (2.85)).

2.2.2 Electrostatic Potentials

- (i) If Ω is simply connected, because of (2.66) it is always possible to introduce a scalar function U (potential (V)) defined as

$$\bar{\mathbf{E}} = -\bar{\nabla} U \quad (2.85)$$

This way, the field is oriented from higher to lower values of potential. Therefore (2.67) becomes

$$\bar{\nabla} \cdot (\epsilon \bar{\nabla} U) = -\rho \quad (2.86)$$

This is the Poisson's equation governing potential U , which reduces to

$$\nabla^2 U = -\frac{\rho}{\epsilon} \quad (2.87)$$

for a homogeneous, isotropic and linear domain Ω .

In the case of $\rho = 0$, (2.87) is called Laplace's equation and the potential function U fulfilling it is said to be harmonic.

It must be remarked that, adding any constant k to U , all the equations defined above are fulfilled as well; in order to have U uniquely defined, boundary conditions must be added.

In a two-dimensional domain, along the boundary Γ with normal versor $\bar{\mathbf{n}} = (n_x, n_y)$ and tangential versor $\bar{\mathbf{t}} = (t_x, t_y) = (-n_y, n_x)$ (Fig. 2.3), the condition (2.75) in terms of field $\bar{\mathbf{E}} = (E_x, E_y)$ becomes, in terms of potential U ,

$$\bar{\mathbf{n}} \cdot \bar{\mathbf{E}} = n_x E_x + n_y E_y = -n_x \frac{\partial U}{\partial x} - n_y \frac{\partial U}{\partial y} = -\bar{\mathbf{n}} \cdot \bar{\nabla} U = -\frac{\partial U}{\partial n} = 0 \quad (2.88)$$

(homogeneous Neumann's condition).

Similarly, condition (2.73) becomes

$$\bar{\mathbf{n}} \times \bar{\mathbf{E}} = \bar{\mathbf{i}}_z (n_x E_y - n_y E_x) = -\bar{\mathbf{i}}_z \left(t_y \frac{\partial U}{\partial y} + t_x \frac{\partial U}{\partial x} \right) = -\bar{\mathbf{i}}_z \frac{\partial U}{\partial t} = 0 \quad (2.89)$$

In this case U is constant along Γ (Dirichlet's condition).

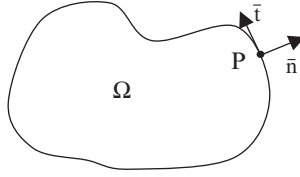


Fig. 2.3 Normal and tangential versors along the domain boundary

Lines of equal U are called equipotential lines.

A boundary-value problem is one in which (2.86) is the governing equation, subject to known boundary conditions which may be (2.88) (Neumann's problem) or (2.89) (Dirichlet's problem) or, more generally, (2.88) and (2.89) along Γ_1 and Γ_2 , respectively, with $\Gamma = \Gamma_1 \cup \Gamma_2$ and $0 = \Gamma_1 \cap \Gamma_2$.

- (ii) If $\rho = 0$ in Ω , then, along with scalar potential U , a vector potential \bar{A} (flux, stream ($C\ m^{-1}$)) can be uniquely defined, specifying its curl

$$\bar{D} = \bar{\nabla} \times \bar{A} \quad (2.90)$$

and its divergence (gauge condition)

$$\bar{\nabla} \cdot \bar{A} = 0 \quad (2.91)$$

In fact, since $\bar{\nabla} \cdot (\bar{\nabla} \times \bar{A}) = 0$ holds, (2.67) is always fulfilled, while (2.66) becomes

$$\bar{\nabla} \times \frac{1}{\epsilon} (\bar{\nabla} \times \bar{A}) = 0 \quad (2.92)$$

The latter is Laplace's vector equation governing flux \bar{A} . It has to be observed that the gradient of an harmonic function η may be added to \bar{A} , having all the above equations fulfilled. In fact, if $\bar{\nabla} \times \bar{A} = 0$ holds, then

$$\bar{A} = -\bar{\nabla}\eta \quad (2.93)$$

and, due to (2.91), it results

$$-\bar{\nabla} \cdot \bar{A} = \bar{\nabla} \cdot \bar{\nabla}\eta = \nabla^2\eta = 0 \quad (2.94)$$

In view to have \bar{A} defined uniquely, suitable boundary conditions along Γ and, if necessary, cuts in Ω must be introduced, transforming a multiply-connected domain into a simply connected one (Fig. 2.4).

For a homogeneous domain, Laplace's equation (2.92) becomes

$$\frac{1}{\epsilon} \bar{\nabla} \times (\bar{\nabla} \times \bar{A}) = 0 \quad (2.95)$$

and therefore

$$\bar{\nabla}(\bar{\nabla} \cdot \bar{A}) - \bar{\nabla}^2 \bar{A} = 0 \quad (2.96)$$

or, because of (2.91)

$$-\bar{\nabla}^2 \bar{A} = 0 \quad (2.97)$$

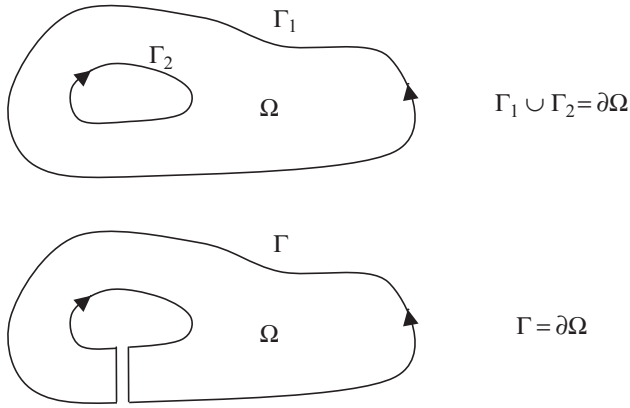


Fig. 2.4 Transforming a doubly connected domain in a simply connected one

2.2.3 Electrostatic Energy

Given an electrostatic field characterized by intensity \bar{E} and flux density \bar{D} in a linear non-dissipative medium, the specific energy (J m^{-3}) stored in the field is defined as $\frac{1}{2}\bar{E} \cdot \bar{D}$.

Taking into account (A.14), one has

$$\bar{E} \cdot \bar{D} = -\bar{\nabla}U \cdot \bar{D} = U\bar{\nabla} \cdot \bar{D} - \bar{\nabla} \cdot (U\bar{D}) \quad (2.98)$$

Then, the total energy W (J) stored in a region Ω of boundary Γ , is

$$\begin{aligned} W &= \frac{1}{2} \int_{\Omega} \bar{E} \cdot \bar{D} \, d\Omega = \frac{1}{2} \int_{\Omega} U\rho \, d\Omega - \frac{1}{2} \int_{\Omega} \bar{\nabla} \cdot (U\bar{D}) \, d\Omega = \\ &= \frac{1}{2} \int_{\Omega} U\rho \, d\Omega - \frac{1}{2} \int_{\Gamma} U\bar{D} \cdot \bar{n} \, d\Gamma \end{aligned} \quad (2.99)$$

The equation above represents an expression of the total energy as a function of potential U , source ρ in the region Ω and source $\sigma = \bar{D} \cdot \bar{n}$ on the boundary Γ .

If the medium is isotropic, the energy W (J) stored in region Ω is given by:

$$W = \frac{1}{2} \int_{\Omega} E D \, d\Omega \quad (2.100)$$

Under the same assumptions, if the constitutive relationship of the dielectric material is non-linear, the specific energy is $\int_0^D E \, dD'$ and the total energy W is

$$W = \int_{\Omega} \left(\int_0^D E \, dD' \right) d\Omega \quad (2.101)$$

In some cases it is convenient to introduce the specific co-energy $\int_0^E \mathbf{D} \, dE'$ so that the total co-energy W' is

$$W' = \int_{\Omega} \left(\int_0^E \mathbf{D} \, dE' \right) d\Omega \quad (2.102)$$

In the case of a linear medium $W = W'$ results.

2.2.4 Field of a Charged Plane in a Rectangular Domain

A conducting plane (y, z) of infinite extension with a uniform distribution σ ($C \, m^{-2}$) of charge is considered. Due to the field symmetry one has $\bar{\mathbf{D}} = (D, 0, 0)$ so that the problem can be formulated as:

$$\bar{\nabla} \cdot \bar{\mathbf{D}} = \sigma \delta(x) = \frac{\partial(\epsilon E)}{\partial x} \quad (2.103)$$

where $\delta(x)$ is the delta function (or Dirac's delta) at $x = 0$ (see Appendix). By integrating the latter equation along $x \in (-\infty, \infty)$, one has

$$\frac{\sigma}{\epsilon} = E(\infty) - E(-\infty) \quad (2.104)$$

Taking into account the field orientation with respect to the plane, the boundary condition

$$E(\infty) = -E(-\infty) \quad (2.105)$$

can be set up. Therefore one obtains

$$E(x) = \frac{\sigma}{2\epsilon} \operatorname{sgn}(x) \quad (2.106)$$

The potential is

$$U(x) = \frac{\sigma}{2\epsilon} |x| \quad (2.107)$$

2.2.5 Field of a Point Charge in a Spherical Domain

A point charge q (C), located at the origin of a system of spherical coordinates (r, ϑ, φ), is considered.

The symmetry implies $\bar{\mathbf{D}} = (D, 0, 0)$; after (A.19), the field equation is

$$\bar{\nabla} \cdot \bar{\mathbf{D}} = r^{-2} \frac{\partial(r^2 D)}{\partial r} = \frac{\partial D}{\partial r} + \frac{2}{r} D = q \delta(r), \quad r > 0 \quad (2.108)$$

where D vanishes as r approaches infinity. Treating (2.108) as a first-order differential equation in terms of r^2D , one has

$$r^2D(r) = \int_0^r q\delta(\rho)\rho^2d\rho + k \quad (2.109)$$

where k is the integration constant; then, the general solution is:

$$D(r) = r^{-2} \left(q \int_0^r \rho^2 \delta(\rho) d\rho + k \right) \quad (2.110)$$

The Dirac's δ in a spherical geometry can be approximated by

$$\delta = \lim_{\alpha \rightarrow 0} \delta_\alpha, \quad \alpha > 0 \quad (2.111)$$

with $\delta_\alpha = \frac{3}{4\pi\alpha^3}$ if $\rho \leq \alpha$ and $\delta_\alpha = 0$ elsewhere. Consequently, field D can be approximated as

$$D = \lim_{\alpha \rightarrow 0} D_\alpha \quad (2.112)$$

For $r \leq \alpha$ one has

$$D_\alpha = \frac{1}{r^2} \left(q \int_0^r \rho^2 \delta_\alpha d\rho + k_\alpha \right) = \frac{1}{r^2} \left(\frac{3q}{4\pi\alpha^3} \frac{r^3}{3} + k_\alpha \right) \quad (2.113)$$

namely

$$D_\alpha = \frac{qr}{4\pi\alpha^3} + \frac{k_\alpha}{r^2} \quad (2.114)$$

Since δ_α is a regular function near the origin, also D_α will be regular near zero; therefore $k_\alpha = 0$.

For $r \geq \alpha$ one has

$$D_\alpha = \frac{1}{r^2} \left(q \int_0^\alpha \rho^2 \delta_\alpha d\rho + k_\alpha \right) = \frac{1}{r^2} \frac{3q}{4\pi\alpha^3} \int_0^\alpha \rho^2 d\rho = \frac{1}{r^2} \frac{3q}{4\pi\alpha^3} \frac{\alpha^3}{3} = \frac{q}{4\pi r^2} \quad (2.115)$$

hence

$$D_\alpha(r) = \frac{qr}{4\pi\alpha^3}, \quad r \leq \alpha \quad (2.116)$$

and

$$D_\alpha(r) = \frac{q}{4\pi r^2}, \quad \alpha < r \quad (2.117)$$

Coulomb's law follows

$$D(r) = \lim_{\alpha \rightarrow 0} D_\alpha(r) = \frac{q}{4\pi r^2}, \quad r > \alpha \quad (2.118)$$

Finally, the potential results

$$U(r) = - \int_\infty^r \frac{q}{4\pi\epsilon\rho^2} d\rho = \frac{q}{4\pi\epsilon r}, \quad r > 0 \quad (2.119)$$

2.2.6 Field of a Dipole

A dipole consisting of a point charge $-q$ located at a distance d from a point charge $+q$ is considered (Fig. 2.5). In a system of spherical coordinates, the dipole moment is defined as $\vec{p} = q\vec{d} = -qd\vec{i}_z$, if oriented from the negative charge to the positive one.

The potential at a distance r from the centre of the dipole is the superposition of the potentials due to $-q$ and $+q$, respectively (see 2.119)

$$U = \frac{q}{4\pi\epsilon r_1} - \frac{q}{4\pi\epsilon r_2} = \frac{q}{4\pi\epsilon} \left(\frac{r_2 - r_1}{r_1 r_2} \right) \quad (2.120)$$

If $r \gg d$, then $r_1 r_2 \cong r^2$ and $r_2 - r_1 \cong d \cos \vartheta$. In fact one has

$$\begin{aligned} r_1 &= \left[r^2 + \frac{d^2}{4} - rd \cos(\pi - \vartheta) \right]^{\frac{1}{2}} = r \left[1 + \frac{d^2}{4r^2} - \frac{d}{r} \cos \vartheta \right]^{\frac{1}{2}} \cong \\ &\cong \frac{r}{2} \left[\frac{d^2}{4r^2} - \frac{d}{r} \cos \vartheta \right] \end{aligned} \quad (2.121)$$

and

$$\begin{aligned} r_2 &= \left[r^2 + \frac{d^2}{4} + rd \cos \vartheta \right]^{\frac{1}{2}} = r \left[1 + \frac{d^2}{4r^2} + \frac{d}{r} \cos \vartheta \right]^{\frac{1}{2}} \cong \\ &\cong \frac{r}{2} \left[\frac{d^2}{4r^2} + \frac{d}{r} \cos \vartheta \right] \end{aligned} \quad (2.122)$$

respectively; it follows

$$r_2 - r_1 \cong \frac{r}{2} \left[\left(\frac{d^2}{4r^2} + \frac{d}{r} \cos \vartheta \right) - \left(\frac{d^2}{4r^2} - \frac{d}{r} \cos \vartheta \right) \right] = d \cos \vartheta \quad (2.123)$$

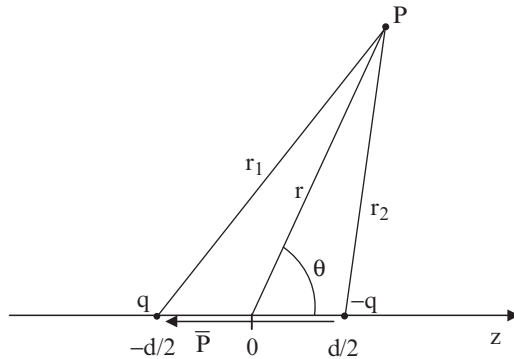


Fig. 2.5 Electric dipole

Therefore, the potential

$$U = \frac{q}{4\pi\epsilon} \frac{d\cos\vartheta}{r^2} = \frac{\bar{p} \cdot \bar{i}_r}{4\pi\epsilon r^2} \quad (2.124)$$

and the electrostatic field

$$\begin{aligned} \bar{E} &= -\bar{\nabla}U = -\left(\frac{\partial U}{\partial r}\bar{i}_r + \frac{1}{r}\frac{\partial U}{\partial\vartheta}\bar{i}_\vartheta\right) = \\ &= -\left(\frac{\partial U}{\partial r}\bar{i}_r + \frac{1}{r}\frac{\partial U}{\partial\vartheta}\bar{i}_\vartheta\right) = \frac{qd\cos\vartheta}{2\pi\epsilon r^3}\bar{i}_r + \frac{qdsin\vartheta}{4\pi\epsilon r^3}\bar{i}_\vartheta \end{aligned} \quad (2.125)$$

follow, respectively.

In particular, along the line joining the two charges the potential is given by

$$U(z) = \frac{q}{4\pi\epsilon} \frac{d}{z^2} \quad \text{for } \vartheta = 0, z \neq 0 \quad (2.126)$$

$$U(z) = -\frac{q}{4\pi\epsilon} \frac{d}{z^2} \quad \text{for } \vartheta = \pi, z \neq 0 \quad (2.127)$$

Comparing the electrostatic field (2.125) due to a dipole with that due to a single charge (monopole) (2.118), it can be realized that, while the former varies inversely with r^3 , the latter varies inversely with r^2 .

2.2.7 Field of a Line Charge in a Cylindrical Domain

Let a line charge be located at $r = 0$ and let λ be the associated uniform charge density ($C\ m^{-1}$). The line charge is infinitely extended in the z direction. In a system of cylindrical coordinates (r, φ, z) the symmetry implies $\bar{D} = (D, 0, 0)$; after (2.67) and (A.17), the field equation is

$$\bar{\nabla} \cdot \bar{D} = r^{-1} \frac{\partial(rD)}{\partial r} = \frac{\partial D}{\partial r} + r^{-1}D = \lambda\delta(r), \quad r > 0 \quad (2.128)$$

where D vanishes as r approaches infinity. Treating (2.128) as a first-order differential equation in terms of rD , one has

$$rD(r) = \int_0^r \lambda\delta(\rho)\rho d\rho + k \quad (2.129)$$

and then the general solution is

$$D(r) = \frac{1}{r} \left(\int_0^r \lambda\delta(\rho)\rho d\rho + k \right) \quad (2.130)$$

where k is the integration constant.

The Dirac's δ in a cylindrical geometry can be approximated by

$$\delta = \lim_{\alpha \rightarrow 0} \delta_\alpha, \quad \alpha > 0 \quad (2.131)$$

with $\delta_\alpha = \frac{1}{\pi\alpha^2}$ if $\rho \leq \alpha$ and $\delta_\alpha = 0$ elsewhere. Consequently, the field D can be approximated as

$$D = \lim_{\alpha \rightarrow 0} D_\alpha \quad (2.132)$$

For $r \leq \alpha$ one has

$$\begin{aligned} D_\alpha &= \frac{1}{r} \left(\int_0^r \lambda \delta_\alpha \rho d\rho + k_\alpha \right) = \frac{1}{r} \left(\frac{\lambda}{\pi\alpha^2} \int_0^r \rho d\rho + k_\alpha \right) = \\ &= \frac{1}{r} \left(\frac{\lambda}{\pi\alpha^2} \frac{r^2}{2} + k_\alpha \right) \end{aligned} \quad (2.133)$$

$$D_\alpha = \frac{\lambda r}{2\pi\alpha^2} + \frac{k_\alpha}{r} \quad (2.134)$$

Since δ_α is a regular function near the origin, also D_α will be regular near zero; therefore $k_\alpha = 0$.

For $r \geq \alpha$ one has

$$\begin{aligned} D_\alpha &= \frac{1}{r} \left(\int_0^\alpha \lambda \delta_\alpha \rho d\rho + k_\alpha \right) = \frac{1}{r} \left(\frac{\lambda}{\pi\alpha^2} \int_0^\alpha \rho d\rho \right) = \\ &= \frac{1}{r} \left(\frac{\lambda}{\pi\alpha^2} \frac{\alpha^2}{2} \right) = \frac{\lambda}{2\pi r} \end{aligned} \quad (2.135)$$

The electric field turns out to be

$$E = \frac{\lambda}{2\pi\epsilon r} \quad (2.136)$$

The potential with respect to the point $r = r_0$ is

$$U(r) = - \int_{r_0}^r \frac{\lambda}{2\pi\epsilon\rho} d\rho = \frac{\lambda}{2\pi\epsilon} \ln \frac{r_0}{r}, \quad r > 0, \quad r_0 > 0 \quad (2.137)$$

2.2.8 Field of a Surface Charge on a Sphere

If a is the radius of the sphere and σ the surface uniform charge density, from Gauss's theorem (A.10) one has

$$E = 0, \quad 0 < r < a \quad (2.138)$$

$$E = \frac{q}{4\pi\epsilon r^2}, \quad r \geq a \quad (2.139)$$

with $q = \int_\Gamma \sigma d\Gamma = 4\pi\sigma a^2$. Therefore, from (2.85) by integration one has

$$U = - \int_\infty^r \frac{q}{4\pi\epsilon\rho^2} d\rho = \frac{q}{4\pi\epsilon r}, \quad r \geq a \quad (2.140)$$

$$U = \frac{q}{4\pi\epsilon a}, \quad 0 < r < a \quad (2.141)$$

Note that U is continuous with respect to r , while E is not (Fig. 2.6).

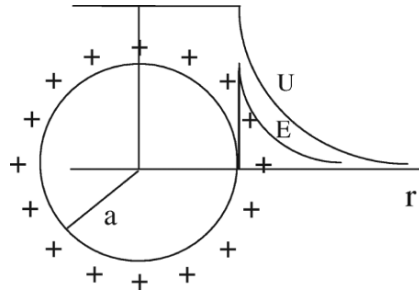


Fig. 2.6 Surface charge distribution on a sphere

Moreover for $r = a$ it results

$$E = \frac{\partial U}{\partial n} = \frac{\sigma}{\epsilon}, \quad \sigma = \epsilon \frac{\partial U}{\partial n} \quad (2.142)$$

Like the current case, the cases described in Sections 2.2.4, 2.2.5 and 2.2.7 can be solved also easily by means of the integral approach.

In fact, in the rectangular case, a parallelepiped surface with an axis orthogonal to the metallic plate can be taken as integration surface. Due to the field symmetry, the application of the Gauss's theorem gives

$$D \cdot 2S = 2\epsilon ES = \sigma S \quad (2.143)$$

where S is the area of the rectangular surface parallel to the plate. It results

$$E = \frac{\sigma}{2\epsilon} \quad (2.144)$$

In turn, in the spherical case, taking a spherical surface having radius r and centre in the point charge q , one has

$$D4\pi r^2 = \epsilon E 4\pi r^2 = q \quad (2.145)$$

and therefore

$$E = \frac{q}{4\pi\epsilon r^2} \quad (2.146)$$

$$U = \frac{q}{4\pi\epsilon r}, \quad \text{if } U \rightarrow 0 \text{ for } r \rightarrow \infty \quad (2.147)$$

Finally, in the cylindrical case, considering a cylindrical surface of radius r , height l and coaxially located with respect to the line charge distributed with density λ , one gets

$$D2\pi r l = \epsilon E 2\pi r l = \lambda l \quad (2.148)$$

whence

$$E = \frac{\lambda}{2\pi\epsilon r} \quad (2.149)$$

and

$$U = \frac{\lambda}{2\pi\epsilon} \ln \frac{r}{r_0}, \quad \text{if } U = 0 \text{ for } r = r_0 \quad (2.150)$$

2.2.9 Energy and Forces in the Electrostatic Field

In order to evaluate the mechanical effect on structures located in the field region, three methods can be applied.

Principle of Virtual Work

Given the structure, on which force \bar{F} is to be calculated, a virtual linear displacement ds in the direction of \bar{F} , supposing that the field source q is constant, mechanical work Fds and variation of internal energy dW take place so that

$$Fds + dW = 0 \quad (2.151)$$

Hence, the force acting on the structure can be evaluated as

$$F = -\frac{dW}{ds} \quad (2.152)$$

Similarly, in the case of a virtual angular displacement $d\vartheta$, the torque T with respect to the rotation axis is

$$T = -\frac{dW}{d\vartheta} \quad (2.153)$$

The system spontaneously tends to assume the configuration corresponding to the minimum energy stored.

On the other hand, if the structure has constant voltage U , one gets

$$Fdx + dW = Udq \quad (2.154)$$

$$Fdx = d(qU - W) \quad (2.155)$$

$$F = \frac{d}{dx}(qU - W) \quad (2.156)$$

where qU is the electric work done to keep U constant.

Correspondingly, the torque is

$$T = \frac{d}{d\vartheta}(qU - W) \quad (2.157)$$

The quantity $qU - W$, denoted by W' , is called complementary energy or co-energy (see (2.102)) of the system; if the latter is linear, W' and W coincide.

If U is kept constant, the system evolution is towards the geometry of maximum co-energy.

The geometric interpretation of energy and co-energy in the charge-potential plane is straightforward (Fig. 2.7).

There are two possible ways, in fact, to move the system from the initial point $(0, 0)$ to the final point (U, q) , namely:

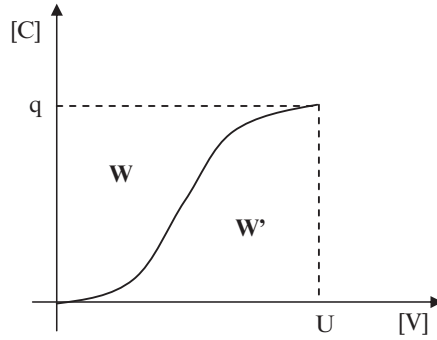


Fig. 2.7 Electrostatic energy and co-energy

- (i) From 0 to q by means of increments of free charge on the electrodes; in this case, the system is electrically insulated and the total work done is W (energy)
- (ii) From 0 to U by, by means of increments of voltage between the electrodes; in this case, the system is electrically connected to a voltage source and the total work done is W' (co-energy)

It is always $W + W' = qU$, while, if the system is linear, $W = W' = \frac{1}{2}qU$ holds.

Coulomb's Method

It is based on the definition of electric field; the force \bar{F} exerted on the free charge distributed with density ρ in the region Ω is

$$\bar{F} = \int_{\Omega} \rho \bar{E} d\Omega = \int_{\Omega} (\nabla \cdot \bar{D}) \bar{E} d\Omega \quad (2.158)$$

where \bar{E} is the external field, i.e. the field in the absence of charge. Directions of force and electric field are coincident.

Method of Maxwell's Stress Tensor

Defined a closed surface Γ enclosing the structure, then the force \bar{F} is evaluated as

$$\bar{F} = \int_{\Gamma} \bar{\bar{T}} \cdot \bar{n} d\Gamma \quad (2.159)$$

where \bar{n} is the outward normal versor.

The Maxwell's electric stress tensor $\bar{\bar{T}}$ can be represented as a matrix whose elements are specific energies related to the field; assuming a system of rectangular coordinates, in a three-dimensional domain, tensor $\bar{\bar{T}}$ is

$$\bar{\bar{T}} = \begin{bmatrix} \frac{1}{2}(E_x D_x - E_y D_y - E_z D_z) & E_x D_y & E_x D_z \\ E_y D_x & \frac{1}{2}(E_y D_y - E_x D_x - E_z D_z) & E_y D_z \\ E_z D_x & E_z D_y & \frac{1}{2}(E_z D_z - E_x D_x - E_y D_y) \end{bmatrix} \quad (2.160)$$

The integration surface must not be coincident with the boundary between materials with different values of permittivity, for tensor to be properly defined.

2.2.10 Force between the Plates of a Capacitor

Let us consider a capacitor made of a pair of parallel plates of infinite extension, which carry a surface charge density equal to σ and $-\sigma$, respectively (Fig. 2.8).

Knowing the field of a single charged plate, after the principle of superposition one gets from (2.108)

$$x < -\frac{d}{2}, \quad E = -\frac{\sigma}{2\epsilon} + \frac{\sigma}{2\epsilon} = 0, \quad U = 0 \quad (2.161)$$

$$-\frac{d}{2} < x < \frac{d}{2}, \quad E = 2\frac{\sigma}{2\epsilon} = \frac{\sigma}{\epsilon}, \quad U = -\frac{\sigma}{\epsilon} \left(x + \frac{d}{2} \right) \quad (2.162)$$

$$x > \frac{d}{2}, \quad E = \frac{\sigma}{2\epsilon} - \frac{\sigma}{2\epsilon} = 0, \quad U = -\frac{\sigma}{\epsilon} d \quad (2.163)$$

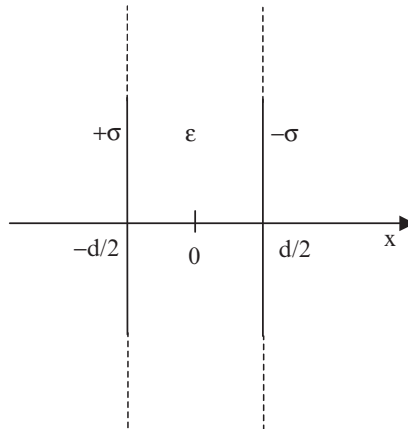


Fig. 2.8 Single-layer plane capacitor

If a capacitor with plates of finite area S is considered, the capacitance C is defined as

$$C = \frac{q}{U} = \epsilon \frac{S}{d} \quad (2.164)$$

where $q = \sigma S$ is the charge on each plate of the capacitor and $U = \frac{\sigma d}{\epsilon}$ is the voltage.

If the capacitor is subject to a constant voltage U , the co-energy is $W' = \frac{1}{2}CU^2$ and the force acting on a plate is from (2.156)

$$F = \frac{\partial W'}{\partial d} = \frac{1}{2}U^2 \frac{\partial C}{\partial d} = -\frac{1}{2}U^2 \frac{\epsilon S}{d^2} \quad (2.165)$$

If, in turn, the charge is constant, the energy is $W = \frac{q^2}{2C}$ and the force is from (2.152)

$$F = -\frac{\partial W}{\partial d} = -\frac{\sigma^2 S}{2\epsilon} = -\frac{1}{2}U^2 \frac{\epsilon S}{d^2} \quad (2.166)$$

In both cases, the negative sign denotes an attractive force.

Resorting to the Coulomb's method, supposing the charge to be constant and uniformly distributed, the field external to the plate located at $x = \frac{d}{2}$ is equal to $\frac{\sigma}{2\epsilon}$ while the charge carried by the plate itself is equal to $-\sigma S$. Therefore, the force acting on the plate of surface S results $-\frac{\sigma^2 S}{2\epsilon} = -\frac{1}{2}U^2 \frac{\epsilon S}{d^2}$; the force is attractive.

Finally, on the basis of the Maxwell's stress tensor, considering a parallelepiped surface, with an axis orthogonal to a plate and enclosing a portion S of it, one can easily obtain

$$\bar{\bar{T}} = \begin{bmatrix} \frac{1}{2}E_x D_x & 0 & 0 \\ 0 & -\frac{1}{2}E_x D_x & 0 \\ 0 & 0 & -\frac{1}{2}E_x D_x \end{bmatrix} \quad (2.167)$$

with $\bar{n} = (-1, 0, 0)$ and then

$$\left| \bar{\bar{T}} \cdot \bar{n} \right| = -\frac{1}{2}\epsilon E_x^2 \quad (2.168)$$

$$F = -\frac{1}{2}\epsilon E_x^2 S = -\frac{1}{2}U^2 \frac{\epsilon S}{d^2} \quad (2.169)$$

The force is attractive.

2.2.11 Force at the Interface between Two Dielectric Materials

Let two layers of dielectric materials characterized by permittivities ϵ_1 and ϵ_2 , respectively, and subject to an applied voltage V as shown in Fig. 2.9, be considered.

If the boundary is charge-free, voltages and field intensities in each layer are such that

$$E_1 x + E_2(h - x) = V_1 + V_2 = V \quad (2.170)$$

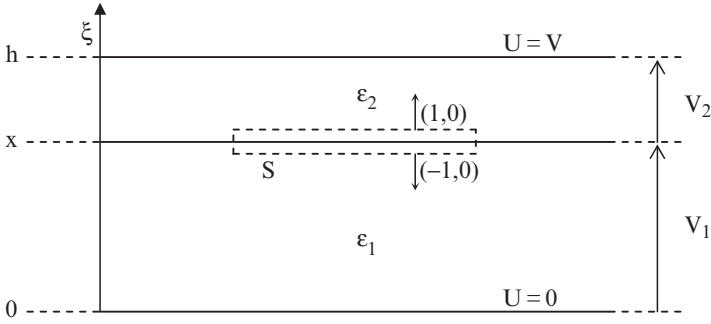


Fig. 2.9 Two-layer plane capacitor

and

$$\epsilon_1 E_1 = \epsilon_2 E_2 \quad (2.171)$$

following (2.85) in its integral form and (2.77), respectively.

Therefore, one has

$$E_1 = \frac{\epsilon_2 V}{\epsilon_1(h-x) + \epsilon_2 x}, \quad E_2 = \frac{\epsilon_1 V}{\epsilon_1(h-x) + \epsilon_2 x} \quad (2.172)$$

The co-energy of the system is

$$W'(x) = \frac{1}{2} \epsilon_1 E_1^2 S x + \frac{1}{2} \epsilon_2 E_2^2 S (h-x) = \frac{1}{2} \epsilon_1 \epsilon_2 \frac{V^2 S}{\epsilon_1(h-x) + \epsilon_2 x} \quad (2.173)$$

By means of the principle of virtual work (2.156), the force between the two layers results

$$F = \frac{\partial W'}{\partial x} = \frac{1}{2} (\epsilon_1 - \epsilon_2) \frac{\epsilon_1 \epsilon_2 V^2 S}{[\epsilon_1(h-x) + \epsilon_2 x]^2} \quad (2.174)$$

If $\epsilon_1 \neq \epsilon_2$ the dielectric with higher permittivity tends to penetrate into the other one; if $\epsilon_1 = \epsilon_2$ the force is zero.

By means of Maxwell's stress tensor, a parallelepiped surface, incorporating the inner boundary between the two dielectric materials and parallel to it, is considered as the integration surface. It results:

inside layer 1

$$\left| \overline{\overline{T}} \cdot \overline{\overline{n}} \right| = -\frac{1}{2} \epsilon_1 E_1^2 \quad (2.175)$$

$$F_1 = -\frac{1}{2} \epsilon_1 E_1^2 S = -\frac{\epsilon_1 \epsilon_2^2 V^2 S}{2 [\epsilon_1(h-x) + \epsilon_2 x]^2} \quad (2.176)$$

inside layer 2

$$\left| \overline{\mathbf{T}} \cdot \overline{\mathbf{n}} \right| = \frac{1}{2} \varepsilon_2 E_2^2 \quad (2.177)$$

$$F_2 = \frac{1}{2} \varepsilon_2 E_2^2 S = \frac{\varepsilon_1^2 \varepsilon_2 V^2 S}{2 [\varepsilon_1 (h - x) + \varepsilon_2 x]^2} \quad (2.178)$$

Therefore, the total force at the interface between layers 1 and 2 is

$$F = F_1 + F_2 = -\frac{1}{2} (\varepsilon_1 - \varepsilon_2) \frac{\varepsilon_1 \varepsilon_2 V^2 S}{[\varepsilon_1 (h - x) + \varepsilon_2 x]^2} \quad (2.179)$$

Resorting to the Coulomb's method, supposing the charge to be constant and uniformly distributed, the field $\tilde{E}(h)$ external to the plate located at $\xi = h$ is equal to

$$\tilde{E}(h) = \frac{1}{2} E_2 = \frac{\varepsilon_1 V}{2 [\varepsilon_1 (h - x) + \varepsilon_2 x]} \quad (2.180)$$

while the charge carried by the plate itself is equal to

$$q_2 = D_2 S = \varepsilon_2 E_2 S = \frac{\varepsilon_1 \varepsilon_2 V S}{\varepsilon_1 (h - x) + \varepsilon_2 x} \quad (2.181)$$

Then, the force acting on the plate of surface S at $\xi = h$ is

$$F_2 = q_2 \tilde{E}(h) = \frac{\varepsilon_1^2 \varepsilon_2 V^2 S}{2 [\varepsilon_1 (h - x) + \varepsilon_2 x]^2} \quad (2.182)$$

Conversely, the field $\tilde{E}(0)$ external to the plate located at $\xi = 0$ is equal to

$$\tilde{E}(0) = \frac{1}{2} E_1 = \frac{\varepsilon_2 V}{2 [\varepsilon_1 (h - x) + \varepsilon_2 x]} \quad (2.183)$$

while the charge carried by the plate itself is equal to

$$q_1 = -D_1 S = -\varepsilon_1 E_1 S = -\frac{\varepsilon_1 \varepsilon_2 V S}{\varepsilon_1 (h - x) + \varepsilon_2 x} \quad (2.184)$$

Then, the force acting on the plate of surface S at $\xi = 0$ is

$$F_1 = q_1 \tilde{E}(0) = -\frac{\varepsilon_1 \varepsilon_2^2 V^2 S}{2 [\varepsilon_1 (h - x) + \varepsilon_2 x]^2} \quad (2.185)$$

Finally, the total force acting on the surface at $\xi = x$ between the two dielectric layers is

$$F = \frac{1}{2} (\varepsilon_1 - \varepsilon_2) \frac{\varepsilon_1 \varepsilon_2 V^2 S}{[\varepsilon_1 (h - x) + \varepsilon_2 x]^2} \quad (2.186)$$

2.3 Magnetostatic Field

In a domain Ω with boundary Γ , containing permanent magnets i.e. aggregates of magnetic dipoles or, from now on, steady electric current distributed with density $\bar{\mathbf{J}}$ (A m^{-2}), a magnetostatic field is set up; it is defined by field intensity $\bar{\mathbf{H}}$ (A m^{-1}) as well as flux density $\bar{\mathbf{B}}$ ($\text{Wb m}^{-2} = \text{T}$). In general, the link between $\bar{\mathbf{H}}$ and $\bar{\mathbf{B}}$, i.e. the constitutive law of the medium, is complicated. Neglecting hysteresis, the law is single-valued and can be expressed, for an isotropic medium in the absence of permanent magnetization, by

$$\bar{\mathbf{B}} = \mu \bar{\mathbf{H}} \quad (2.187)$$

where μ is called permeability (H m^{-1}) and, in the most general case, is a function of $|\bar{\mathbf{H}}|$; the inverse of μ is called reluctivity ν . The medium is supposed to be at rest with respect to the observer of the field.

2.3.1 Maxwell's Equations for Magnetostatics

The equations governing the magnetic field are in Ω

$$\bar{\nabla} \cdot \bar{\mathbf{B}} = 0 \quad (2.188)$$

$$\bar{\nabla} \times \bar{\mathbf{H}} = \bar{\mathbf{J}} \quad (2.189)$$

and along Γ

$$\bar{\mathbf{n}} \cdot \bar{\mathbf{B}} = 0 \quad (2.190)$$

if Γ is a flux line (flux lines parallel to Γ), or

$$\bar{\mathbf{n}} \times \bar{\mathbf{B}} = \mu \bar{\mathbf{J}}_S \quad (2.191)$$

if current of surface density $\bar{\mathbf{J}}_S$ (A m^{-1}) is present, or

$$\bar{\mathbf{n}} \times \bar{\mathbf{H}} = 0 \quad (2.192)$$

if flux lines are perpendicular to Γ .

For an isotropic and linear medium, in terms of $\bar{\mathbf{B}}$, the equations become in Ω

$$\bar{\nabla} \cdot \bar{\mathbf{B}} = 0; \quad \bar{\nabla} \times \bar{\mathbf{B}} = \mu \bar{\mathbf{J}} \quad (2.193)$$

with, along Γ

$$\bar{\mathbf{n}} \cdot \bar{\mathbf{B}} = 0 \quad (2.194)$$

or

$$\bar{\mathbf{n}} \times \bar{\mathbf{B}} = \mu \bar{\mathbf{J}}_S \quad (2.195)$$

or

$$\bar{\mathbf{n}} \times \bar{\mathbf{H}} = 0 \quad (2.196)$$

The equations written above unambiguously define the magnetostatic field which, because of (2.188), is solenoidal.

If both $\bar{\mathbf{J}}_S$ and $\bar{\mathbf{J}}$ are given, then it must be

$$\int_{\Gamma} |\bar{\mathbf{J}}_s| d\Gamma = \int_{\Omega} |\bar{\mathbf{J}}| d\Omega \quad (2.197)$$

i.e. the total current sums up to zero: therefore, densities \mathbf{J}_S and \mathbf{J} cannot be independent.

In a non-homogeneous domain at the interface between two media of permeability μ_1 and μ_2 (Fig. 2.2), from (2.188) it holds

$$\bar{\mathbf{n}}_1 \cdot (\bar{\mathbf{B}}_2 - \bar{\mathbf{B}}_1) = 0 \quad (2.198)$$

so that the normal component of $\bar{\mathbf{B}}$ is continuous.

If there is a current of density $\bar{\mathbf{J}}_S$ (A m^{-1}), then from (2.189)

$$\bar{\mathbf{t}}_1 \cdot (\bar{\mathbf{H}}_1 - \bar{\mathbf{H}}_2) = \bar{\mathbf{J}}_s \quad (2.199)$$

If $\bar{\mathbf{J}}_s = 0$, the tangential component of $\bar{\mathbf{H}}$ is continuous. Equations (2.198) and (2.199) are called transmission conditions.

In the case of a non-homogeneous medium, the following remark can be put forward. After (2.187) and (2.188), considering vector identity (A.14), one has

$$\bar{\nabla} \cdot \mu \bar{\mathbf{H}} = \mu \bar{\nabla} \cdot \bar{\mathbf{H}} + \bar{\nabla} \mu \cdot \bar{\mathbf{H}} = 0 \quad (2.200)$$

In the case of a non-homogeneous medium, field $\bar{\mathbf{H}}$ is solenoidal if $\bar{\nabla} \mu$ and $\bar{\mathbf{H}}$ are orthogonal vectors; this implies that lines separating layers of different μ are parallel to field lines of $\bar{\mathbf{H}}$.

Conversely, after (2.187) and (2.189), considering vector identity (A.16), it turns out that

$$\bar{\nabla} \times \mu^{-1} \bar{\mathbf{B}} = \mu^{-1} \bar{\nabla} \times \bar{\mathbf{B}} + \bar{\nabla} \mu^{-1} \times \bar{\mathbf{B}} = \bar{\mathbf{J}} \quad (2.201)$$

It appears that, in a current-free medium (i.e. $\bar{\mathbf{J}} = 0$), field $\bar{\mathbf{B}}$ is irrotational if $\bar{\nabla} \mu^{-1}$ and $\bar{\mathbf{B}}$ are parallel vectors; this implies that lines separating layers of different μ are orthogonal to field lines of $\bar{\mathbf{B}}$. If $\bar{\nabla} \mu^{-1} = 0$ and $\bar{\mathbf{J}} = 0$ (homogeneous current-free medium), then $\bar{\mathbf{B}}$ is always irrotational.

Finally, an extension of constitutive law (2.187) is considered.

In the presence of a permanent magnetization $\bar{\mathbf{B}}_0$ in the magnetic material (permanent magnet) the constitutive law is

$$\bar{\mathbf{B}} = \mu \bar{\mathbf{H}} + \bar{\mathbf{B}}_0 \quad (2.202)$$

In this case the field equations are

$$\bar{\nabla} \cdot \bar{\mathbf{B}} = 0 \quad (2.203)$$

$$\bar{\nabla} \times \bar{\mathbf{B}} = \mu \bar{\mathbf{J}} + \bar{\nabla} \times \bar{\mathbf{B}}_0 \quad (2.204)$$

In particular, the field inside a permanent magnet is described by (2.204) with $\bar{\mathbf{J}} = 0$; it follows that the magnet can be modelled by an equivalent distribution of current given by $\bar{\mathbf{J}}_{\text{eq}} = \mu^{-1} \bar{\nabla} \times \bar{\mathbf{B}}_0$.

2.3.2 Magnetostatic Potentials

- (i) From (2.188), since, for any vector $\bar{\mathbf{A}}$, $\bar{\nabla} \cdot (\bar{\nabla} \times \bar{\mathbf{A}}) = 0$ holds (see A.8), it is possible to define a vector function $\bar{\mathbf{A}}$ (Wb m^{-1}) called vector potential by means of

$$\bar{\nabla} \times \bar{\mathbf{A}} = \bar{\mathbf{B}} \quad (2.205)$$

and the gauge condition

$$\bar{\nabla} \cdot \bar{\mathbf{A}} = 0 \quad (2.206)$$

This way (2.188) is fulfilled, while (2.189) becomes

$$\bar{\nabla} \times \frac{1}{\mu} (\bar{\nabla} \times \bar{\mathbf{A}}) = \bar{\mathbf{J}} \quad (2.207)$$

For a homogeneous domain, after (A.12) and (2.206) it turns out to be

$$\bar{\nabla}^2 \bar{\mathbf{A}} = -\mu \bar{\mathbf{J}} \quad (2.208)$$

This is the (Poisson's) vector equation governing $\bar{\mathbf{A}}$. In a system of rectangular coordinates it corresponds to the following scalar equations

$$\begin{aligned} \left(\bar{\nabla}^2 \bar{\mathbf{A}} \right)_x &= \frac{\partial^2 A_x}{\partial x^2} + \frac{\partial^2 A_x}{\partial y^2} + \frac{\partial^2 A_x}{\partial z^2} = -\mu J_x \\ \left(\bar{\nabla}^2 \bar{\mathbf{A}} \right)_y &= -\mu J_y \\ \left(\bar{\nabla}^2 \bar{\mathbf{A}} \right)_z &= -\mu J_z \end{aligned} \quad (2.209)$$

In general, the gradient of an harmonic function may be added to $\bar{\mathbf{A}}$, having all the equations satisfied. Of course, suitable boundary conditions on Γ must be added in order to define the field in a unique way.

In particular, after (2.208) and (2.204), the potential inside a permanent magnet is given by $\bar{\nabla}^2 \bar{\mathbf{A}} = -\bar{\nabla} \times \bar{\mathbf{B}}_0$.

- (ii) In a two-dimensional domain, vectors $\bar{\mathbf{J}}$ and so $\bar{\mathbf{A}}$ have only one non-zero component; hence, vector potential can be treated as a scalar quantity. Since $B_x = \frac{\partial A}{\partial y}$ and $B_y = -\frac{\partial A}{\partial x}$, the boundary conditions (2.194) and (2.196), in terms of $\bar{\mathbf{B}} = (B_x, B_y)$ along the boundary Γ with normal versor $\bar{\mathbf{n}} = (n_x, n_y)$ and tangential versor $\bar{\mathbf{t}} = (t_x, t_y) = (n_y, -n_x)$, become, in terms of A ,

$$\begin{aligned}\bar{\mathbf{n}} \cdot \bar{\mathbf{B}} &= n_x B_x + n_y B_y = n_x \frac{\partial A}{\partial y} - n_y \frac{\partial A}{\partial x} \\ &= -t_y \frac{\partial A}{\partial y} - t_x \frac{\partial A}{\partial x} = -\bar{\mathbf{t}} \cdot \bar{\nabla} A = -\frac{\partial A}{\partial \bar{\mathbf{t}}} = 0\end{aligned}\quad (2.210)$$

i.e. $A = \text{const.}$ along Γ and

$$\begin{aligned}\bar{\mathbf{n}} \times \bar{\mathbf{B}} &= (n_x B_y - n_y B_x) \bar{\mathbf{i}}_z = \left(-n_x \frac{\partial A}{\partial x} - n_y \frac{\partial A}{\partial y} \right) \bar{\mathbf{i}}_z \\ &= -(\bar{\mathbf{n}} \cdot \bar{\nabla} A) \bar{\mathbf{i}}_z = -\frac{\partial A}{\partial \bar{\mathbf{n}}} \bar{\mathbf{i}}_z = 0\end{aligned}\quad (2.211)$$

i.e. $\frac{\partial A}{\partial \bar{\mathbf{n}}} = 0$ along Γ , respectively.

- (iii) If $\bar{\mathbf{J}} = 0$ in Ω and Ω is simply connected, then, along with $\bar{\mathbf{A}}$, the field $\bar{\mathbf{H}}$ can be described by a scalar function φ (potential, (A)) defined as

$$\bar{\mathbf{H}} = -\bar{\nabla} \varphi \quad (2.212)$$

In fact, (2.189) is automatically satisfied, while from (2.188) we obtain in Ω

$$\bar{\nabla} \cdot \mu \bar{\nabla} \varphi = 0 \quad (2.213)$$

The latter is the Laplace's equation governing magnetic scalar potential φ with suitable boundary conditions.

The condition of simply connected domain can be obtained by suitable cuts, if necessary. If this condition is not fulfilled, nevertheless φ can be still defined, apart from multiples of a constant.

- (iv) When in (2.187) permeability μ depends on $|\bar{\mathbf{H}}|$, one has $|\bar{\mathbf{B}}| = \mu(|\bar{\mathbf{H}}|) |\bar{\mathbf{H}}|$ and for the solution of (2.208) one should resort to an iterative procedure. According to the Newton-Raphson method, the residual $r(A)$ of each governing equations (2.209) is developed in Taylor's series, truncating the development at the first order

$$r(A_k) = r(A_{k-1}) + \left(\frac{dr}{dA} \Big|_{A=A_{k-1}} \right) (A_k - A_{k-1}) + o(A_k) \quad (2.214)$$

If a prediction of the solution A_{k-1} at the $(k - 1)$ th iteration is available, the subsequent prediction A_k at the k th iteration is given by (2.214) imposing $r(A_k) = 0$. It results

$$A_k = A_{k-1} - \left[\frac{dr}{dA} \Big|_{A=A_{k-1}} \right]^{-1} r(A_{k-1}) \quad (2.215)$$

Then, μ and so $|\bar{\mathbf{H}}|$ are updated by means of the new estimation of A and the problem is solved again. The procedure stops when the error between two successive solutions is less than the prescribed threshold. It is necessary to know an initial prediction A_0 and the value of the derivative $\frac{dr}{dA}$ at each iteration; under these assumptions, it can be proven that the procedure converges quadratically.

2.3.3 Magnetostatic Energy

Given a magnetostatic field characterized by intensity $\bar{\mathbf{H}}$ and flux density $\bar{\mathbf{B}}$ in a linear medium, the specific energy (J m^{-3}) of the field is defined as $\frac{1}{2} \bar{\mathbf{H}} \cdot \bar{\mathbf{B}}$; if the medium is isotropic, the energy $W(J)$ stored in an unbounded region Ω is given by

$$W = \frac{1}{2} \int_{\Omega} \mathbf{H} \mathbf{B} \, d\Omega \quad (2.216)$$

If the constitutive relationship of the magnetic material is non-linear, the specific energy is $\int_0^{\mathbf{B}} \mathbf{H} d\mathbf{B}'$ and so that total energy is

$$W = \int_{\Omega} \left(\int_0^{\mathbf{B}} \mathbf{H} d\mathbf{B}' \right) d\Omega \quad (2.217)$$

In some cases it is convenient to introduce the specific co-energy $\int_0^{\mathbf{H}} \mathbf{B} d\mathbf{H}'$ so that the total co-energy is

$$W' = \int_{\Omega} \left(\int_0^{\mathbf{H}} \mathbf{B} d\mathbf{H}' \right) d\Omega \quad (2.218)$$

In the case of linear medium $W = W'$ results.

In the linear case, taking into account the following identity (see A.13)

$$\bar{\mathbf{H}} \cdot \bar{\mathbf{B}} = \bar{\mathbf{H}} \cdot (\bar{\nabla} \times \bar{\mathbf{A}}) = \bar{\mathbf{A}} \cdot (\bar{\nabla} \times \bar{\mathbf{H}}) - \bar{\nabla} \cdot (\bar{\mathbf{H}} \times \bar{\mathbf{A}}) = \bar{\mathbf{A}} \cdot \bar{\mathbf{J}} - \bar{\nabla} \cdot (\bar{\mathbf{H}} \times \bar{\mathbf{A}}) \quad (2.219)$$

and (2.189), the total energy stored in a region Ω of boundary Γ is

$$W = \frac{1}{2} \int_{\Omega} \bar{\mathbf{H}} \cdot \bar{\mathbf{B}} \, d\Omega = \frac{1}{2} \int_{\Omega} \bar{\mathbf{A}} \cdot \bar{\mathbf{J}} \, d\Omega - \frac{1}{2} \int_{\Gamma} (\bar{\mathbf{H}} \times \bar{\mathbf{A}}) \cdot \bar{\mathbf{n}} \, d\Gamma \quad (2.220)$$

The equation above reduces to $W = \frac{1}{2} \int_{\Omega} \bar{\mathbf{A}} \cdot \bar{\mathbf{J}} \, d\Omega$, if either $\bar{\mathbf{A}} \times \bar{\mathbf{n}} = 0$ or $\bar{\mathbf{H}} \times \bar{\mathbf{n}} = 0$ along Γ .

2.3.4 Field of a Line Current in a Three-Dimensional Domain: Differential Approach

A current I (A), concentrated at $r = 0$ and directed along the z axis in a system of cylindrical coordinates (r, φ, z) , is considered (Fig. 2.10).

The symmetry implies $\vec{H} = (0, H, 0)$ and the field equation is from (2.189):

$$\vec{\nabla} \times \vec{H} = \frac{1}{r} \frac{\partial r H}{\partial r} = \frac{\partial H}{\partial r} + \frac{1}{r} H = I \delta(r), \quad r > 0 \quad (2.221)$$

where H vanishes as r approaches infinity. The general solution (see Section 2.2.7) is:

$$H(r) = \frac{1}{r} \left(I \int_0^r \rho \delta(\rho) d\rho + k \right) \quad (2.222)$$

The Dirac's δ in a cylindrical geometry can be approximated by:

$$\delta = \lim_{\alpha \rightarrow 0} \delta_\alpha, \quad \alpha > 0 \quad (2.223)$$

with $\delta_\alpha = \frac{1}{\pi\alpha^2}$, $r \leq \alpha$ and $\delta_\alpha = 0$ elsewhere. Consequently, the field H can be approximated as

$$H = \lim_{\alpha \rightarrow 0} H_\alpha \quad (2.224)$$

For $r \leq \alpha$ one has

$$H_\alpha = \frac{1}{r} \left(I \int_0^r \rho \delta_\alpha d\rho + k_\alpha \right) = \frac{1}{r} \left(\frac{I}{\pi\alpha^2} \frac{r^2}{2} + k_\alpha \right) = \frac{I r}{2\pi\alpha^2} + \frac{k_\alpha}{r} \quad (2.225)$$

Since δ_α is a regular function near the origin, also H_n will be regular near zero; therefore $k_\alpha = 0$.

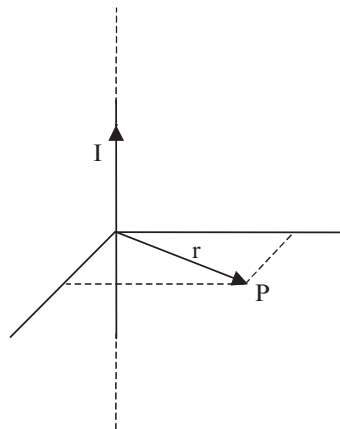


Fig. 2.10 Line current

For $r \geq \alpha$ one has

$$\begin{aligned} H_\alpha &= \frac{1}{r} \left(I \int_0^\alpha \rho \delta_\alpha d\rho + k_\alpha \right) = \frac{1}{r} \left(\frac{I}{\pi\alpha^2} \int_0^\alpha \rho d\rho \right) = \\ &= \frac{1}{r} \left(\frac{I}{\pi\alpha^2} \frac{\alpha^2}{2} \right) = \frac{I}{2\pi r}, \quad r > 0 \end{aligned} \quad (2.226)$$

The Biot-Savart's law follows:

$$H(r) = \lim_{\alpha \rightarrow 0} H_\alpha(r) = \frac{I}{2\pi r}, \quad r > 0 \quad (2.227)$$

Alternatively, the Stokes's theorem can be applied to (2.189), giving $\oint_\lambda \bar{H} \cdot \bar{t} d\lambda = I$, if λ is a closed line linking the conductor once. Thanks to the field geometry, λ can be taken as a circular line centred at $r = 0$; hence, (2.227) results.

From (2.227) and (2.205) the vector potential results:

$$\bar{A} = \frac{I}{2\pi v} \ln \bar{r}_z, \quad r > 0 \quad (2.228)$$

2.3.5 Energy and Forces in the Magnetostatic Field

Principle of Virtual Work

Given a structure in the field region, on which force \bar{F} is to be calculated, a virtual linear displacement ds in the direction of \bar{F} , supposing that the magnetic system is supplied by a constant current I creating a linkage flux Φ , the sum of mechanical work Fds and variation of magnetic energy dW is equal to the input energy $Id\Phi$ so that

$$\begin{aligned} Fds + dW &= Id\Phi \\ Fds &= d(I\Phi - W) \\ F &= \frac{d}{ds}(I\Phi - W) \end{aligned} \quad (2.229)$$

In the case of an angular displacement $d\vartheta$, the torque T with respect to the rotation axis is

$$T = \frac{d}{d\vartheta}(I\Phi - W) \quad (2.230)$$

The quantity $I\Phi - W$, denoted by W' , is the complementary energy or co-energy of the system.

On the other hand, if the magnetic system is isolated, mechanical work Fds and variation of magnetic energy dW take place so that

$$Fds + dW = 0 \quad (2.231)$$

Hence the force can be evaluated as

$$\mathbf{F} = -\frac{dW}{ds} \quad (2.232)$$

while the torque is

$$\mathbf{T} = -\frac{dW}{d\vartheta} \quad (2.233)$$

If the system is linear, W' and W coincide.

Lorentz's Method

It is based on the definition of flux density; the force $\bar{\mathbf{F}}$ exerted on current distributed with density $\bar{\mathbf{J}}$ in the region Ω is

$$\bar{\mathbf{F}} = \int_{\Omega} \bar{\mathbf{J}} \times \bar{\mathbf{B}} d\Omega \quad (2.234)$$

where $\bar{\mathbf{B}}$ is the external field, i.e. the flux density in the absence of current. Directions of force, flux density and current density are mutually orthogonal.

Method of Maxwell's Stress Tensor

Defined a closed surface Γ enclosing the structure, then force $\bar{\mathbf{F}}$ on it is evaluated as

$$\bar{\mathbf{F}} = \int_{\Omega} \bar{\nabla} \cdot \bar{\bar{\mathbf{T}}} d\Omega = \int_{\Gamma} \bar{\bar{\mathbf{T}}} \cdot \bar{\mathbf{n}} d\Gamma \quad (2.235)$$

where $\bar{\mathbf{n}}$ is the outward normal vector.

The Maxwell's magnetic stress tensors $\bar{\bar{\mathbf{T}}}$, assuming a system of rectangular coordinates, in a three-dimensional domain can be represented in matrix form as

$$\bar{\bar{\mathbf{T}}} = \begin{bmatrix} \frac{1}{2}(H_x B_x - H_y B_y - H_z B_z) & H_x B_y & H_x B_z \\ H_y B_x & \frac{1}{2}(H_y B_y - H_x B_x - H_z B_z) & H_y B_z \\ H_z B_x & H_z B_y & \frac{1}{2}(H_z B_z - H_x B_x - H_y B_y) \end{bmatrix} \quad (2.236)$$

In order the tensor be uniquely defined, surface Γ should not be coincident with the interface between materials having different permeability.

Remarks

There is a link between Lorentz's and Maxwell's approach to force calculation. In fact, using (2.187), (2.189) and (2.234), the force density $\bar{\mathbf{f}}$ (Nm^{-3}) takes the expression

$$\bar{\mathbf{f}} = \bar{\mathbf{J}} \times \bar{\mathbf{B}} = (\bar{\nabla} \times \mathbf{v}\bar{\mathbf{B}}) \times \bar{\mathbf{B}} \quad (2.237)$$

In particular, the x-directed component is

$$f_x = vB_z \frac{\partial B_x}{\partial z} - vB_z \frac{\partial B_z}{\partial x} - vB_y \frac{\partial B_y}{\partial x} + vB_y \frac{\partial B_x}{\partial y} \quad (2.238)$$

After adding and subtracting the term $\frac{v}{2} \frac{\partial B_x^2}{\partial x}$ one has

$$\begin{aligned} f_x &= \frac{v}{2} \frac{\partial B_x^2}{\partial x} + vB_z \frac{\partial B_x}{\partial z} + vB_y \frac{\partial B_x}{\partial y} + \\ &\quad - \frac{v}{2} \frac{\partial}{\partial x} (B_x^2 + B_y^2 + B_z^2) \end{aligned} \quad (2.239)$$

It follows

$$\begin{aligned} f_x &= \frac{v}{2} \frac{\partial B_x^2}{\partial x} + v \frac{\partial (B_x B_z)}{\partial z} - vB_x \frac{\partial B_z}{\partial z} + v \frac{\partial (B_x B_y)}{\partial y} + \\ &\quad - vB_x \frac{\partial B_y}{\partial y} - vB_x \frac{\partial B_x}{\partial x} - \frac{v}{2} \frac{\partial}{\partial x} (B_y^2 + B_z^2) \end{aligned} \quad (2.240)$$

$$f_x = v \left[\frac{\partial}{\partial x} \left(B_x^2 - \frac{1}{2} |\bar{\mathbf{B}}|^2 \right) + \frac{\partial (B_x B_y)}{\partial y} + \frac{\partial (B_x B_z)}{\partial z} - B_x \bar{\nabla} \cdot \bar{\mathbf{B}} \right] \quad (2.241)$$

Due to (2.188) the last term of (2.241) is zero; then, if vector

$$\begin{aligned} \bar{\mathbf{v}}_1 &= v \left(B_x^2 - \frac{1}{2} |\bar{\mathbf{B}}|^2, B_x B_y, B_x B_z \right) = \\ &= \left(\frac{1}{2} (H_x B_x - H_y B_y - H_z B_z), H_x B_y, H_x B_z \right) \end{aligned} \quad (2.242)$$

is defined, f_x can be viewed as its divergence, apart from a constant k which can be set to zero, namely

$$f_x = \bar{\nabla} \cdot \bar{\mathbf{v}}_1 \quad (2.243)$$

A similar result holds for force density components f_y and f_z ; one has

$$\bar{\mathbf{v}}_2 = \left(H_y B_x, \frac{1}{2} (H_y B_y - H_x B_x - H_z B_z), H_y B_z \right) \quad (2.244)$$

such that

$$f_y = \bar{\nabla} \cdot \bar{\mathbf{v}}_2 \quad (2.245)$$

and

$$\bar{\mathbf{v}}_3 = \left(H_z B_x, H_z B_y, \frac{1}{2} (H_z B_z - H_x B_x - H_y B_y) \right) \quad (2.246)$$

such that

$$f_z = \bar{\nabla} \cdot \bar{\mathbf{v}}_3 \quad (2.247)$$

respectively. Therefore, according to (2.235), the force $\bar{\mathbf{F}}(\mathbf{N})$ can be written as the integral of the divergence of tensor $\bar{\bar{\mathbf{T}}}$ represented by matrix (2.236), in which the row entries are the components of vectors $\bar{\mathbf{v}}_k$, $k = 1, 3$.

2.3.6 Force on an Electromagnet

Let us consider an electromagnet with a movable part (Fig. 2.11).

The iron core is supposed to have infinite permeability. The air gaps in the x direction are supposed to be much smaller than the air gap t in the y direction.

The circulation of the magnetic field H , along a line linking the excitation current NI and crossing the air gap t in the normal direction, reduces to

$$NI = Ht \quad (2.248)$$

Therefore at the air gap

$$H = \frac{NI}{t} \quad (2.249)$$

while in the iron part $H = 0$. Following (2.218), the co-energy stored in the air gap is given by

$$W' = \frac{1}{2}\mu_0 H^2 S t = \frac{\mu_0 (NI)^2 S}{2t} \quad (2.250)$$

where S is the cross-section of the central limb and μ_0 is the air permeability.

If NI is constant, according to (2.229), the force acting on the movable part is

$$F_t = \frac{\partial W'}{\partial t} = -\frac{\mu_0 S}{2} \left(\frac{NI}{t} \right)^2 \quad (2.251)$$

The force is negative, i.e. opposite to the direction of increasing t ; therefore, it is attractive, regardless of the sign of I .

In order to apply the method of Maxwell's stress tensor, an integration surface Γ enclosing the movable part is considered having \bar{n} as its outward normal versor.

Taking into account the field distribution, one actually has:

$$\bar{\bar{T}} = \begin{bmatrix} -\frac{1}{2}H_y B_y & 0 \\ 0 & \frac{1}{2}H_y B_y \end{bmatrix} \quad (2.252)$$

$$\bar{F} = \int_{\Gamma} \bar{\bar{T}} \cdot \bar{n} d\Gamma = \left(0, \frac{1}{2}H_y B_y S \right) \quad (2.253)$$

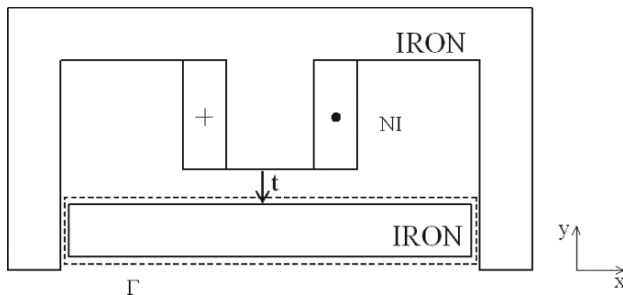


Fig. 2.11 Model of the electromagnet

Therefore it results:

$$F_y = \frac{1}{2} \mu_0 H_y^2 S = \frac{1}{2} \mu_0 S \left(\frac{NI}{t} \right)^2 \quad (2.254)$$

The force is attractive, because variables t and y are oriented in opposite directions.

2.3.7 Test Problems

Throughout the book, the problem of the computation of the magnetic field in some test cases is considered. The first case is that of the air-gap of a single-side slotted electrical machine. The model of one half of the field region is shown in Fig. 2.12. The slot accommodates a concentrated or distributed current, whereas the surrounded iron is assumed of infinite permeability.

In terms of vector potential, the following boundary conditions for the field region are set up: fixed values of A along a flux line ($A = 0$) and vanishing normal derivative at the symmetry line ($\frac{\partial A}{\partial n} = 0$).

Other test cases are presented in Fig. 2.13.

They correspond to a single slot produced in an iron core with one side facing the air-gap (magnetically open slot: case a) and to a slot fully embedded in an iron core (magnetically closed slot: case b). The relevant boundary conditions can be approximately set up as shown.

These test problems proposed might represent a benchmark because they deal with a simple, clear and meaningful example; in electrical engineering, in fact, a broad class of devices includes a magnetic pole formed by a current-carrying slot.

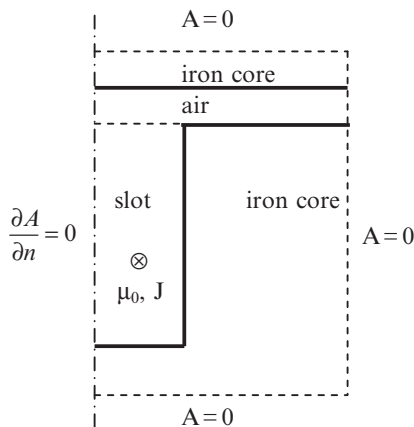


Fig. 2.12 Single-side slotted electrical machine: one half of the field region

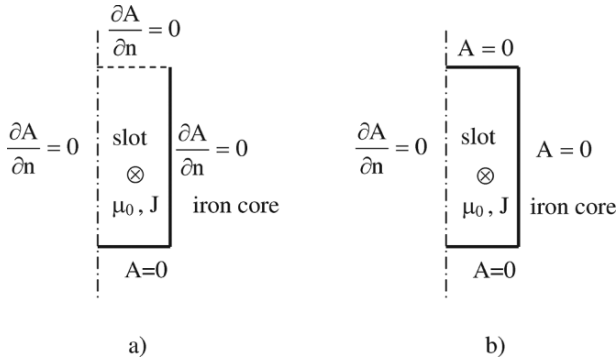


Fig. 2.13 Single slot: one half of the field region

2.4 Steady Conduction Field

In a domain Ω , composed of a conducting material, having boundary Γ , when Γ or a part of it is kept at a non-zero potential constant with time, a steady conduction field is set up, defined by field intensity \vec{E} (V m^{-1}) and current density \vec{J} (A m^{-2}). These two vectors are linked by the constitutive relation which, if the medium is linear and isotropic, is

$$\vec{J} = \sigma \vec{E} \tag{2.255}$$

The parameter σ qualifying the medium is called conductivity ($\Omega^{-1} \text{m}^{-1}$).

2.4.1 Maxwell's Equations for Conduction Field

The field is governed by the following Maxwell's equations in Ω

$$\vec{\nabla} \times \vec{E} = 0 \tag{2.256}$$

$$\vec{\nabla} \cdot \vec{J} = 0 \tag{2.257}$$

and along Γ

$$\vec{n} \cdot \vec{J} = J_0 \tag{2.258}$$

if Γ is a perfectly conducting boundary and J_0 is the current density impressed along it, or

$$\vec{n} \cdot \vec{J} = 0 \tag{2.259}$$

if Γ is a perfectly insulating boundary.

In terms of $\bar{\mathbf{E}}$ the above equations for a homogeneous medium become in Ω

$$\bar{\nabla} \times \bar{\mathbf{E}} = 0 \quad (2.260)$$

$$\bar{\nabla} \cdot \bar{\mathbf{E}} = 0 \quad (2.261)$$

and along Γ

$$\bar{\mathbf{n}} \cdot \bar{\mathbf{E}} = E_0 \quad (2.262)$$

if E_0 is the conduction field impressed along the boundary, or

$$\bar{\mathbf{n}} \cdot \bar{\mathbf{E}} = 0 \quad (2.263)$$

In the case of a non-homogeneous medium, the following remark can be put forward.

After (2.255) and (2.256), considering vector identity (A.16), it results

$$\bar{\nabla} \times \sigma^{-1} \bar{\mathbf{J}} = \sigma^{-1} \bar{\nabla} \times \bar{\mathbf{J}} + \bar{\nabla} \sigma^{-1} \times \bar{\mathbf{J}} = 0 \quad (2.264)$$

If $\bar{\nabla} \sigma^{-1} = 0$ (homogeneous medium), then $\bar{\mathbf{J}}$ is always irrotational. More generally, for $\bar{\mathbf{J}}$ to be irrotational, $\bar{\nabla} \sigma^{-1}$ and $\bar{\mathbf{J}}$ should be parallel vectors; this means that lines separating layers of different σ are orthogonal to field lines of $\bar{\mathbf{J}}$. If this condition applies, $\bar{\mathbf{J}}$ is both irrotational and solenoidal.

Conversely, after (2.261) and (A.14), one has

$$\bar{\nabla} \cdot \bar{\mathbf{E}} = \bar{\nabla} \cdot \sigma^{-1} \bar{\mathbf{J}} = \sigma^{-1} \bar{\nabla} \cdot \bar{\mathbf{J}} + \bar{\nabla} \sigma^{-1} \cdot \bar{\mathbf{J}} = 0 \quad (2.265)$$

Due to (2.257), it results

$$\bar{\nabla} \sigma^{-1} \cdot \bar{\mathbf{J}} = 0 \quad (2.266)$$

i.e. field $\bar{\mathbf{E}}$ is solenoidal if $\bar{\nabla} \sigma^{-1}$ and $\bar{\mathbf{J}}$ are orthogonal vectors; this means that lines separating layers of different σ are parallel to field lines of $\bar{\mathbf{J}}$. If this condition applies, $\bar{\mathbf{E}}$ is both irrotational and solenoidal.

2.4.2 Potentials

If Ω is simply connected, starting from (2.256) the field can be defined by a scalar function U (potential (V)) as

$$\bar{\mathbf{E}} = -\bar{\nabla} U \quad (2.267)$$

Starting from (2.257), substitution of (2.267) in it, taking into account (2.255), gives

$$\bar{\nabla} \cdot (\sigma \bar{\nabla} U) = 0 \quad (2.268)$$

In rectangular coordinates (2.268) becomes

$$\frac{\partial}{\partial x} \left(\sigma \frac{\partial U}{\partial x} \right) + \frac{\partial}{\partial y} \left(\sigma \frac{\partial U}{\partial y} \right) + \frac{\partial}{\partial z} \left(\sigma \frac{\partial U}{\partial z} \right) = 0 \quad (2.269)$$

In the case of a homogeneous domain (2.268) reduces to

$$\nabla^2 U = 0 \quad (2.270)$$

which is Laplace's equation governing potential U .

Any constant may be added to U , keeping all the equations valid.

In particular, in a two-dimensional domain, using rectangular coordinates, the field intensity $\bar{E} = (E_x, E_y)$ defined by (2.267) has components

$$E_x = -\frac{\partial U}{\partial x}, \quad E_y = -\frac{\partial U}{\partial y} \quad (2.271)$$

Conversely, starting from (2.257), according to (A.8), it is possible to introduce a vector function \bar{A} (flux ($A \text{ m}^{-1}$)) defined as

$$\bar{J} = \bar{\nabla} \times \bar{A} \quad (2.272)$$

In a two-dimensional domain, by virtue of the definition of curl as well of that of field intensity $\bar{J} = (J_x, J_y)$, similarly to what discussed in Section 2.3.2, \bar{A} turns out to be a single-component vector perpendicular to the domain, namely $\bar{A} = (0, 0, A)$. Therefore the components of \bar{J} result

$$J_x = \frac{\partial A}{\partial y}, \quad J_y = -\frac{\partial A}{\partial x} \quad (2.273)$$

Substituting (2.272) into (2.256), after multiplication by σ and taking into account (2.255), one obtains

$$\bar{\nabla} \times \frac{1}{\sigma} \bar{\nabla} \times \bar{A} = 0 \quad (2.274)$$

In a two-dimensional domain this, in turn, becomes

$$\frac{\partial}{\partial x} \left(\frac{1}{\sigma} \frac{\partial A}{\partial x} \right) + \frac{\partial}{\partial y} \left(\frac{1}{\sigma} \frac{\partial A}{\partial y} \right) = 0 \quad (2.275)$$

In the case of homogeneous domain (2.275) reduces to

$$\nabla^2 A = 0 \quad (2.276)$$

which is Laplace's equation governing flux A .

The gradient of an harmonic function, having all the equations satisfied as well, may be added to \bar{A} ; by imposing the gauge condition

$$\bar{\nabla} \cdot \bar{A} = 0 \quad (2.277)$$

\bar{A} is unambiguously defined. In a two-dimensional domain the latter condition is automatically fulfilled.

Comparing (2.271) and (2.273) one has

$$\frac{\partial A}{\partial y} = -\sigma \frac{\partial U}{\partial x}; \quad \frac{\partial A}{\partial x} = \sigma \frac{\partial U}{\partial y} \quad (2.278)$$

The latter represent the relationships of orthogonality between contour lines of the two potentials.

Boundary conditions (2.262) and (2.263) become $U = \text{const}$ and $\frac{\partial U}{\partial n} = 0$, respectively; in turn, (2.262) and (2.263) become $\frac{\partial A}{\partial n} = 0$ and $A = \text{const}$.

2.4.3 Power Loss

Given a conduction field characterized by intensity \bar{E} and current density \bar{J} , the specific power (W m^{-3}) transferred from the field to movables charges is defined as $\bar{E} \cdot \bar{J} = \sigma E^2$ and, therefore, the power loss (W) in domain Ω is given by:

$$P = \int_{\Omega} \sigma E^2 d\Omega \quad (2.279)$$

2.4.4 Analytic Functions of Complex Variable

In a two-dimensional domain, A and σU (or U and $\frac{A}{\sigma}$) may be considered as the real and imaginary components (conjugate functions), respectively, of a complex function

$$\bar{F}(\bar{z}) = A + j\sigma U \quad \text{or} \quad \bar{G}(\bar{z}) = U + j\frac{A}{\sigma} \quad (2.280)$$

with $\bar{z} = x + jy$, $j \equiv \sqrt{-1}$, for which (2.278) represent the Cauchy-Riemann equations, i.e. $\bar{\nabla}(\sigma U) \cdot \bar{\nabla}A = 0$.

2.4.5 Field of a Cylindrical Conductor

Let a cylindrical homogenous conductor of radii R_1 and R_2 , carrying current I for unit length in the radial direction, be considered (Fig. 2.14).

From (2.270), according to (A.18), one has

$$\nabla^2 U = \frac{d^2 U}{dr^2} + r^{-1} \frac{dU}{dr} = r^{-1} \frac{d}{dr} \left(r \frac{dU}{dr} \right) = 0, \quad r > 0 \quad (2.281)$$

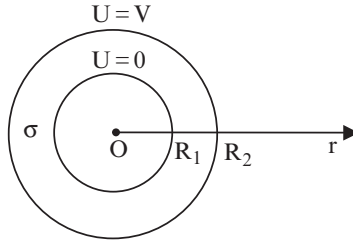


Fig. 2.14 Cross-section of a cylindrical conductor

and therefore

$$U = k \ln r + h \quad (2.282)$$

The application of boundary conditions

$$r = R_1, \quad U = 0; \quad r = R_2, \quad U = V \quad (2.283)$$

gives

$$U = V \frac{\ln r - \ln R_1}{\ln R_2 - \ln R_1}, \quad R_1 \leq r \leq R_2 \quad (2.284)$$

In the formulation in terms of flux A , after making a radial cut at $\vartheta = 0$ in order to have a simply connected domain, the boundary conditions are

$$\vartheta = 0, \quad A = 0; \quad \vartheta = 2\pi, \quad A = I \quad (2.285)$$

$$r = R_1, \quad \frac{\partial A}{\partial n} = 0; \quad r = R_2, \quad \frac{\partial A}{\partial n} = 0 \quad (2.286)$$

From (2.276), one gets

$$r^{-2} \frac{d^2 A}{d\vartheta^2} = 0, \quad r > 0 \quad (2.287)$$

and therefore

$$A = k' \vartheta + h' \quad (2.288)$$

By the application of boundary conditions, it results

$$A = \frac{I}{2\pi} \vartheta, \quad 0 \leq \vartheta \leq 2\pi \quad (2.289)$$

The following complex function may be set up

$$\bar{F}(r, \vartheta) = A(\vartheta) + j\sigma U(r) \quad (2.290)$$

The Cauchy-Riemann equations reduce to

$$J = \frac{I}{2\pi r} = -\sigma \frac{V}{\ln R_2 - \ln R_1} \frac{1}{r} = \sigma E \quad (2.291)$$

i.e. the constitutive relationship of the material.

Chapter 3

Analytical Methods for Solving Boundary-Value Problems

3.1 Method of Green's Function

The potential of a unit source s , located in Q at a distance r from the field point P in an unbounded homogeneous domain Ω , is called Green's function and is given the symbol G' .

Let $\Omega_Q \subset \Omega$ be the subdomain represented by all source points and let $\Omega_P \subset \Omega$ be the subdomain of all field points, such that $\Omega_Q \cup \Omega_P = \Omega$ and $\Omega_Q \cap \Omega_P = 0$.

In a three-dimensional unbounded domain, after (2.48) for $s = \delta(\bar{r}_Q)$ one has

$$G'(\bar{r}_P, \bar{r}_Q) = \frac{1}{4\pi |\bar{r}_P - \bar{r}_Q|} = \frac{1}{4\pi r} \quad (3.1)$$

where $r = |\bar{r}_P - \bar{r}_Q|$ is the distance between source and field point (see Appendix, Fig. A1).

From (2.48) the potential fulfilling Poisson's equation $\nabla^2\phi = -s$ is

$$\phi(\bar{r}_P) = \int_{\Omega} G'(\bar{r}_P, \bar{r}_Q) s(\bar{r}_Q) d\Omega \quad (3.2)$$

Therefore, knowing G' and s , by means of (3.2) it is possible to calculate ϕ . The Green's function G' is called the fundamental solution of the Poisson's equation.

For a bounded domain with boundary Γ the modified Green's function G is the potential due to a unit source plus that, g , due to the unit source distributed along the boundary

$$G(\bar{r}_P, \bar{r}_Q) = \frac{1}{4\pi |\bar{r}_P - \bar{r}_Q|} + g(\bar{r}_P, \bar{r}_Q) \quad (3.3)$$

Knowing g , and so G , and substituting ψ with $4\pi G$ in the Green's formula (2.63), it is possible to calculate ϕ .

By definition, the Green's function is symmetrical, i.e. it is the same, exchanging the source and the field point $G'(\bar{r}_P, \bar{r}_Q) = G'(\bar{r}_Q, \bar{r}_P)$.

Following the same procedure, in a two-dimensional unbounded domain Ω the Green's function G' results

$$G'(\bar{r}_P, \bar{r}_Q) = \frac{1}{2\pi} \ln |\bar{r}_P - \bar{r}_Q| \quad (3.4)$$

3.1.1 Green's Formula for Electrostatics

In a homogeneous three-dimensional domain Ω with boundary $\Gamma = \Gamma_1 \cup \Gamma_2$ and permittivity ε , from (2.63) taking $\phi = u$ and $\nabla^2 \phi = \nabla^2 u = -\frac{\rho}{\varepsilon}$ and substituting ψ with $4\pi G$, one has

$$u(\bar{x}) = \int_{\Omega} G(\bar{x}, \bar{y}) \frac{\rho(\bar{y})}{\varepsilon} d\Omega + \int_{\Gamma_1} G(\bar{x}, \bar{y}) \frac{\partial u(\bar{y})}{\partial \mathbf{n}} d\Gamma + \int_{\Gamma_2} u(\bar{y}) \frac{\partial G(\bar{x}, \bar{y})}{\partial \mathbf{n}} d\Gamma \quad (3.5)$$

where $\bar{\mathbf{n}}$ is the normal versor of Γ while the space vectors $\bar{x} \equiv \bar{r}_P$ and $\bar{y} \equiv \bar{r}_Q$ identify field and source point, respectively.

Formula (3.5) is the Green's formula for electrostatics. Using it to determine u , the actual problem is to know the modified Green's function G related to the given field domain Ω .

3.1.2 Green's Functions for Boundary-Value Problems

The particular case of Ω , denoted by $B(0, R)$, representing the region within a sphere ($n = 3$) or a circle ($n = 2$) is considered. The modified Green's function, related to the domain and to Poisson's equation

$$-\nabla^2 u = f \quad (3.6)$$

subject to Dirichlet's or Neumann's conditions, is to be found.

To this end, let the compound function v – called Kelvin's transformation of u – be considered. It is defined by the formula

$$v(\bar{x}) = |\bar{x}|^{n-2} R^{-n+2} u(\bar{a}(\bar{x})), \quad n = 2, 3 \quad (3.7)$$

where the transform $\bar{a}(\bar{y})$, given by the formula

$$\bar{a}(\bar{y}) = R^2 |\bar{y}|^{-2} \bar{y}, \quad \bar{y} \in \mathbb{R}^n \setminus \{0\} \quad (3.8)$$

leaves the boundary $\partial B(0, R)$ invariant. In fact, for $y = R$ it results

$$\bar{a}(\bar{y}) = \bar{y}, \quad v(\bar{x}) = |\bar{x}|^{n-2} R^{-n+2} u(\bar{x}) \quad (3.9)$$

The equation satisfied by u is now found; for this task, the radial symmetry is exploited.

In the case $n = 3$ (sphere), using spherical coordinates (r, φ, ϑ) , setting

$$\tilde{u}(r, \varphi, \vartheta) = u(r \cos \varphi \sin \vartheta, r \sin \varphi \sin \vartheta, r \cos \vartheta) \quad (3.10)$$

with $r \in (0, R)$; $\varphi \in (0, 2\pi)$, $\vartheta \in (0, \pi)$, and

$$\begin{aligned} \tilde{v}(r, \varphi, \vartheta) &= Rr^{-1}u\left(R^2r^{-1} \cos \varphi \sin \vartheta, R^2r^{-1} \sin \varphi \sin \vartheta, R^2r^{-1} \cos \vartheta\right) = \\ &= Rr^{-1}\tilde{u}\left(R^2r^{-1}, \varphi, \vartheta\right) \end{aligned} \quad (3.11)$$

with $r \in (R, +\infty)$; $\varphi \in (0, 2\pi)$, $\vartheta \in (0, \pi)$, developing the Laplacian in spherical coordinates (see A.20)

$$\nabla^2 = \frac{1}{r^2}D_r(r^2D_r) + \frac{1}{r^2}D_\vartheta^2 + \frac{\cot(\vartheta)}{r^2}D_\vartheta + \frac{1}{r^2 \sin^2 \vartheta}D_\varphi^2 \quad (3.12)$$

where $D_r \equiv \frac{\partial}{\partial r}$, $D_\varphi \equiv \frac{\partial}{\partial \varphi}$, $D_\vartheta \equiv \frac{\partial}{\partial \vartheta}$, the following relations hold

$$\begin{aligned} r^2D_r\tilde{v}(r, \varphi, \vartheta) &= -R\tilde{u}\left(R^2r^{-1}, \varphi, \vartheta\right) + \\ &\quad - R^3r^{-1}D_r\tilde{u}\left(R^2r^{-1}, \varphi, \vartheta\right) \end{aligned} \quad (3.13)$$

$$\begin{aligned} r^{-2}D_r\left(r^2D_r\tilde{v}\right)(r, \varphi, \vartheta) &= 2R^3r^{-4}D_r\tilde{u}\left(R^2r^{-1}, \varphi, \vartheta\right) + \\ &\quad + R^5r^{-5}D_r^2\tilde{u}\left(R^2r^{-1}, \varphi, \vartheta\right) \end{aligned} \quad (3.14)$$

$$D_\vartheta^j\tilde{v}(r, \varphi, \vartheta) = Rr^{-1}D_\vartheta^j\tilde{u}\left(R^2r^{-1}, \varphi, \vartheta\right), \quad j = 1, 2 \quad (3.15)$$

$$D_\varphi^j\tilde{v}(r, \varphi, \vartheta) = Rr^{-1}D_\varphi^j\tilde{u}\left(R^2r^{-1}, \varphi, \vartheta\right), \quad j = 1, 2 \quad (3.16)$$

Consequently, it can be deduced

$$\begin{aligned} \nabla^2\tilde{v}(r, \varphi, \vartheta) &= R^5r^{-5}\left[D_r^2\tilde{u}\left(R^2r^{-1}, \varphi, \vartheta\right) + 2R^{-2}rD_r\tilde{u}\left(R^2r^{-1}, \varphi, \vartheta\right) + \right. \\ &\quad \left. + \left(Rr^{-2}\right)^{-2}D_\vartheta^2\tilde{u}\left(R^2r^{-1}, \varphi, \vartheta\right)\right] + \\ &\quad + R^5r^{-5}\left[\cot \vartheta \left(Rr^{-2}\right)^{-2}D_\vartheta\tilde{u}\left(R^2r^{-1}, \varphi, \vartheta\right) + \right. \\ &\quad \left. + \frac{1}{\sin^2 \vartheta} \left(Rr^{-2}\right)^{-2}D_\varphi^2\tilde{u}\left(R^2r^{-1}, \varphi, \vartheta\right)\right] = \\ &= R^5r^{-5}\nabla^2\tilde{u}\left(R^2r^{-1}, \varphi, \vartheta\right) = \\ &= -R^5r^{-5}\tilde{f}\left(R^2r^{-1}, \varphi, \vartheta\right) \end{aligned} \quad (3.17)$$

with $r \in (R, +\infty)$, $\varphi \in (0, 2\pi)$, $\vartheta \in (0, \pi)$.

If ω represents the region outside the sphere $B(0, R)$, (3.17) proves that function v satisfies the Dirichlet's boundary-value problem

$$\nabla^2 v(\bar{x}) = \hat{f}(\bar{x}), \quad \text{in } \omega = \left\{ \bar{x} \in \mathbb{R}^3 : |\bar{x}| > R \right\} \quad (3.18)$$

$$v(x) = g(\bar{x}), \quad \text{on } \partial\omega = \left\{ \bar{x} \in \mathbb{R}^3 : |\bar{x}| = R \right\} \quad (3.19)$$

with

$$\hat{f}(\bar{x}) = -R^5 |\bar{x}|^{-5} f(R^2 |\bar{x}|^{-2} \bar{x}), \quad \bar{x} \in \omega \quad (3.20)$$

and $g(\bar{x})$ given function of the boundary.

The case $n = 2$ (circular domain) is now considered. As in the three-dimensional case, the functions

$$\tilde{u}(r, \varphi) = u(r \cos \varphi, r \sin \varphi) \quad (3.21)$$

with $r \in (0, R)$, $\varphi \in (0, 2\pi)$, and

$$\tilde{v}(r, \varphi) = u\left(R^2 r^{-1} \cos \varphi, R^2 r^{-1} \sin \varphi\right) = \tilde{u}\left(R^2 r^{-1}, \varphi\right) \quad (3.22)$$

with $r \in (R, +\infty)$, $\varphi \in (0, 2\pi)$, are introduced. Developing the Laplacian in polar coordinates (see A.18), one has

$$\nabla^2 = D_r^2 + \frac{1}{r} D_r + \frac{1}{r^2} D_\varphi^2 \quad (3.23)$$

Accordingly, the following relations hold

$$D_r \tilde{v}(r, \varphi) = -R^2 r^{-2} D_r \tilde{u}\left(R^2 r^{-1}, \varphi\right) \quad (3.24)$$

$$D_r^2 \tilde{v}(r, \varphi) = R^4 r^{-4} D_r^2 \tilde{u}\left(R^2 r^{-1}, \varphi\right) + 2R^2 r^{-3} D_r \tilde{u}\left(R^2 r^{-1}, \varphi\right) \quad (3.25)$$

$$D_\varphi^j \tilde{v}(r, \varphi) = D_\varphi^j \tilde{u}\left(R^2 r^{-1}, \varphi\right), \quad j = 1, 2 \quad (3.26)$$

Consequently, it results

$$\begin{aligned} \nabla^2 \tilde{v}(r, \varphi) &= R^4 r^{-4} \left[D_r^2 \tilde{u}\left(R^2 r^{-1}, \varphi\right) + \left(R^2 r^{-1}\right)^2 D_r \tilde{u}\left(R^2 r^{-1}, \varphi\right) + \right. \\ &\quad \left. + \left(R r^{-2}\right)^{-2} D_\varphi^2 \tilde{u}\left(R^2 r^{-1}, \varphi\right) \right] = \\ &= R^4 r^{-4} \nabla^2 u\left(R^2 r^{-1}, \varphi\right) = R^4 r^{-4} \tilde{f}\left(R^2 r^{-1}, \varphi\right), \quad r \in (R, +\infty) \end{aligned} \quad (3.27)$$

Therefore, it has been shown that function v fulfils the Dirichlet's boundary-value problem

$$\nabla^2 v(\bar{x}) = \hat{f}(\bar{x}), \text{ in } \omega = \left\{ \bar{x} \in \mathbb{R}^2 : |\bar{x}| > R \right\} \quad (3.28)$$

$$v(\bar{x}) = g(\bar{x}), \text{ on } \partial\omega = \left\{ \bar{x} \in \mathbb{R}^2 : |\bar{x}| = R \right\} \quad (3.29)$$

with

$$\hat{f}(x) = R^4 |x|^{-4} f\left(R^2 |x|^{-1} x\right), \quad x \in \omega \quad (3.30)$$

and $g(\bar{x})$ given function of the boundary.

It is now possible to determine the Green's function G_D related to the Dirichlet's condition when $n = 2$ and $n = 3$. It is given by the formula

$$G_D(\bar{x}, \bar{y}) = G'(\bar{x} - \bar{y}) - G'\left(R^{-1} |\bar{y}| (\bar{x} - \bar{a}(\bar{y}))\right), \quad \bar{x}, \bar{y} \in B(0, R) \quad (3.31)$$

where

$$\bar{a}(\bar{y}) = R^2 |\bar{y}|^{-2} \bar{y}, \quad \bar{y} \in \mathbb{R}^n \setminus \{0\}, \quad n = 2, 3 \quad (3.32)$$

and G' stands for the fundamental solution of the Laplacian operator, i.e.

$$G'(\bar{x}) = (2\pi)^{-1} \ln |\bar{x}|, \text{ if } n = 2 \quad (3.33)$$

and

$$G'(\bar{x}) = (4\pi)^{-1} |\bar{x}|^{-1}, \text{ if } n = 3 \quad (3.34)$$

assuming that the unit source is located at $y = 0$.

It is necessary to show that

$$G_D(\bar{x}, \bar{y}) = 0, \quad \bar{x} \in \partial B(0, R), \quad \bar{y} \in B(0, R) \quad (3.35)$$

To this purpose, the identity

$$|\bar{x} - \bar{y}|^2 = |\bar{x}|^2 + |\bar{y}|^2 - 2\bar{x} \cdot \bar{y} \quad (3.36)$$

holding for any pair of vectors $\bar{x}, \bar{y} \in \mathbb{R}^n$, is used. In particular, for any $\bar{x} \in \partial B(0, R)$, i.e. $|\bar{x}| = R$, and for any $\bar{y} \in B(0, R)$ it turns out to be

$$\begin{aligned} R^{-2} |\bar{y}|^2 |\bar{x} - \bar{a}(\bar{y})|^2 &= R^{-2} |\bar{y}|^2 \left[|\bar{x}|^2 + |\bar{a}(\bar{y})|^2 - 2\bar{x} \cdot \bar{a}(\bar{y}) \right] = \\ &= R^{-2} |\bar{y}|^2 \left[R^2 + R^4 |\bar{y}|^{-2} - 2R^2 |\bar{y}|^{-2} \bar{x} \cdot \bar{y} \right] = \\ &= |\bar{y}|^2 + R^2 - 2\bar{x} \cdot \bar{y} = |\bar{y}|^2 + |\bar{x}|^2 - 2\bar{x} \cdot \bar{y} = |\bar{x} - \bar{y}|^2 \end{aligned} \quad (3.37)$$

implying that (3.36) holds.

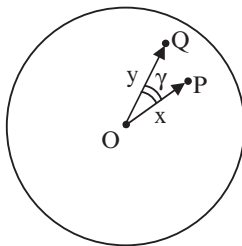


Fig. 3.1 Inner spherical domain Ω

Now, the Green's function related to a sphere $B(0, R)$ when $n = 3$ can be determined. It is given by the formula:

$$G_D(\bar{x}, \bar{y}) = \frac{1}{4\pi(r^2 - 2r\rho\bar{u}_x \cdot \bar{u}_y + \rho^2)^{\frac{1}{2}}} + \frac{R}{4\pi(r^2\rho^2 - 2rR^2\rho\bar{u}_x \cdot \bar{u}_y + R^4)^{\frac{1}{2}}} \quad (3.38)$$

where $\bar{x} = r\bar{u}_x$ and $\bar{y} = \rho\bar{u}_y$. In other words, r and ρ are the Euclidean norms of vectors \bar{x} and \bar{y} , respectively, while \bar{u}_x and \bar{u}_y are the unit vectors in the directions of \bar{x} and \bar{y} , respectively. The situation is represented in Fig. 3.1, where $\gamma = \cos^{-1}(\bar{u}_x \cdot \bar{u}_y)$

Comparing (3.3) and (3.38), it follows

$$g(\bar{x}, \bar{y}) = -\frac{R}{4\pi(r^2\rho^2 - 2rR^2\rho\bar{u}_x \cdot \bar{u}_y + R^4)^{\frac{1}{2}}} \quad (3.39)$$

Moreover, from (3.38), the following relation can be deduced:

$$\begin{aligned} D_{n(\bar{y})}G_D(\bar{x}, \bar{y}) &= D_\rho[G_D(r\bar{u}_x, \rho\bar{u}_y)] \\ &= \frac{\rho - r\bar{u}_x \cdot \bar{u}_y}{4\pi(r^2 - 2r\rho\bar{u}_x \cdot \bar{u}_y + \rho^2)^{\frac{3}{2}}} + \\ &\quad + \frac{R(r^2\rho - rR^2\bar{u}_x \cdot \bar{u}_y)}{4\pi(r^2\rho^2 - 2rR^2\rho\bar{u}_x \cdot \bar{u}_y + R^4)^{\frac{3}{2}}}, \quad \bar{x}, \bar{y} \in B(0, R) \end{aligned} \quad (3.40)$$

where the operator $D_{n(\bar{y})}$ stands for the normal derivative along the direction of vector \bar{y} ; in particular, the relation

$$\begin{aligned} D_\rho[G_D(r\bar{u}_x, R\bar{u}_y)] &= -\frac{R - r\bar{u}_x \cdot \bar{u}_y}{4\pi(r^2 - 2rR\bar{u}_x \cdot \bar{u}_y + R^2)^{\frac{3}{2}}} + \\ &\quad + \frac{r(r - R\bar{u}_x \cdot \bar{u}_y)}{4R\pi(r^2 - 2rR\bar{u}_x \cdot \bar{u}_y + R^2)^{\frac{3}{2}}} = \\ &= \frac{r^2 - R^2}{4R\pi(r^2 - 2rR\bar{u}_x \cdot \bar{u}_y + R^2)^{\frac{3}{2}}} \end{aligned} \quad (3.41)$$

with $\bar{x} \in B(0, R)$, $\bar{y} \in \partial B(0, R)$, can be obtained. Consequently, the following representation holds:

$$D_{n(\bar{y})}G_D(x, y) = \frac{|\bar{x}|^2 - R^2}{4R\pi |\bar{x} - \bar{y}|^3}, \quad \bar{x} \in \partial B(0, R), \quad \bar{y} \in B(0, R) \quad (3.42)$$

Therefore, it can be concluded that the solution to the Dirichlet's problem in $\Omega = B(0, R)$

$$-\nabla^2 u(\bar{x}) = f(\bar{x}) \quad (3.43)$$

with $u(\bar{x}) = g(\bar{x})$ on $\Gamma = \partial B(0, R)$, according to (3.5) is given by the formula

$$u(\bar{x}) = \int_{\Omega} G_D(\bar{x}, \bar{y})f(\bar{y}) d\Omega - \int_{\Gamma} g(\bar{y})D_{n(\bar{y})}G_D(\bar{x}, \bar{y}) d\Gamma \quad (3.44)$$

where the functions G_D and $D_{n(\bar{y})}G_D$ have been explicitly computed.

In the case $n = 2$, the Green's function is given by the formula

$$G_D(\bar{x}, \bar{y}) = \frac{1}{4\pi} \left\{ \ln(\rho) - \ln(R) + \ln(r^2 - 2r\rho\bar{u}_x \cdot \bar{u}_y + \rho^2) - \log(r^2\rho^2 - 2rR^2\rho\bar{u}_x \cdot \bar{u}_y + R^4) \right\} \quad (3.45)$$

Then, one gets

$$\begin{aligned} 2\pi D_{n(\bar{y})}G_D(\bar{x}, \bar{y}) &= 2\pi D_{\rho} [G_D(r\bar{u}_x, \rho\bar{u}_y)] = \\ &= \frac{1}{\rho} + \frac{\rho - r\bar{u}_x \cdot \bar{u}_y}{r^2 - 2r\rho\bar{u}_x \cdot \bar{u}_y + \rho^2} - \frac{r^2\rho - R^2r\bar{u}_x \cdot \bar{u}_y}{r^2\rho^2 - 2rR^2\rho\bar{u}_x \cdot \bar{u}_y + R^4} \end{aligned} \quad (3.46)$$

and

$$\begin{aligned} 2\pi D_{n(\bar{y})}G_D(\bar{x}, R\bar{u}_y) &= \frac{1}{R} + \frac{R - r\bar{u}_x \cdot \bar{u}_y}{r^2 - 2Rr\bar{u}_x \cdot \bar{u}_y + R^2} - \frac{r^2 - Rr\bar{u}_x \cdot \bar{u}_y}{R(r^2 - 2Rr\bar{u}_x \cdot \bar{u}_y + R^2)} = \\ &= \frac{1}{R} + \frac{R^2 - r^2}{R(r^2 - 2Rr\bar{u}_x \cdot \bar{u}_y + R^2)} \end{aligned} \quad (3.47)$$

In turn, this gives

$$D_{n(\bar{y})}G_D(\bar{x}, \bar{y}) = \frac{1}{2\pi R} + \frac{R^2 - r^2}{2\pi R(r^2 - 2Rr\bar{u}_x \cdot \bar{u}_y + R^2)} \quad (3.48)$$

with $\bar{x} \in B(0, R)$, $\bar{y} \in \partial B(0, R)$.

Therefore, it can be concluded that, according to (3.5), the solution to the Dirichlet's problem

$$-\nabla^2 u(\bar{x}) = f(\bar{x}) \text{ in } \Omega = B(0, R), \quad u(\bar{x}) = g(\bar{x}) \text{ on } \Gamma = \partial B(0, R) \quad (3.49)$$

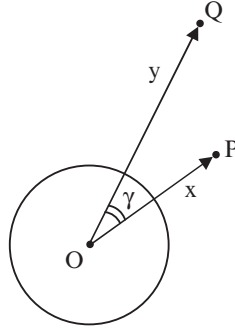


Fig. 3.2 Outer spherical domain ω

is given by the formula

$$u(\bar{x}) = \int_{\Omega} G_D(\bar{x}, \bar{y}) f(\bar{y}) d\Omega - \int_{\Gamma} g(\bar{y}) D_n(\bar{y}) G_D(\bar{x}, \bar{y}) d\Gamma \quad (3.50)$$

Finally the solution to the Dirichlet's problem for the domain ω and its boundary $\partial\omega$ outside the domain Ω can now be obtained (Fig. 3.2).

Using (3.43) and (3.20) the representation for the solution v to the problem (3.18)–(3.19) can be deduced from the solution u to the Dirichlet's problem for the sphere, where $B(0, R) = \Omega$ and $B(0, R)^c = \omega$:

$$-\nabla^2 u(\bar{x}) = f(\bar{x}) \text{ in } B(0, R), \quad u(\bar{x}) = g(\bar{x}) \text{ on } \partial B(0, R) \quad (3.51)$$

where f is defined through the equation

$$\hat{f}(\bar{x}) = -R^5 |\bar{x}|^{-5} f(R^2 |\bar{x}|^{-2} \bar{x}), \quad \bar{x} \in \omega \quad (3.52)$$

The solution to the equation $R^2 |\bar{x}|^{-2} \bar{x} = \bar{y}$, $\bar{x} \neq \{0\}$ is $\bar{x} = R^2 |\bar{y}|^{-2} \bar{y}$. Indeed, if a solution \bar{x} exists, then $|\bar{x}| = R^2 |\bar{y}|^{-1}$, so that $\bar{x} = R^{-2} |\bar{x}|^2 \bar{y} = R^2 |\bar{y}|^{-2} \bar{y}$. Of course, it is easy to check that $\bar{x} = R^2 |\bar{y}|^{-2} \bar{y}$ solves the given equation. In other words, the inverse transform coincides with the transform itself. Consequently, it is easy to verify that f can be expressed in terms of \hat{f} by the formula

$$f(\bar{y}) = -R^5 |\bar{y}|^{-5} \hat{f}(R^2 |\bar{y}|^{-2} \bar{y}), \quad \bar{y} \in \omega \quad (3.53)$$

Then u can be expressed as follows

$$\begin{aligned} u(\bar{x}) &= R^5 \int_{B(0,R)} G_D(\bar{x}, \bar{y}) |\bar{y}|^{-5} \hat{f}(R^2 |\bar{y}|^{-2} \bar{y}) d\omega(\bar{y}) + \\ &+ \int_{\partial B(0,R)} g(\bar{y}) D_n(\bar{y}) G_D(\bar{x}, \bar{y}) d\sigma(\bar{y}) = \\ &= u_1(\bar{x}) + \int_{\partial B(0,R)} g(\bar{y}) D_n(\bar{y}) G_D(\bar{x}, \bar{y}) d\sigma(\bar{y}) \end{aligned} \quad (3.54)$$

A change of variable in the volume integral defining u_1 is convenient. To this purpose, the Jacobian $J(\bar{\eta})$ of the transformation $\bar{y} = R^2 |\bar{\eta}|^{-2} \bar{\eta}$ is to be computed. Assuming

$$y_k = R^2 |\bar{\eta}|^{-2} \eta_k, \quad D_{\eta_j} y_k = -2R^2 |\bar{\eta}|^{-4} \eta_j \eta_k + R^2 |\bar{\eta}|^{-2} \delta_{j,k} \quad (3.55)$$

with $j, k = 1, \dots, n$, $n = 2, 3$, where $\delta_{j,k} = (-1)^{j+k}$ is the Kronecker's index, it turns out to be

$$J(\bar{\eta}) = 2R^2 |\bar{\eta}|^{-10} \quad (3.56)$$

whence the formula

$$\begin{aligned} u_1(\bar{x}) &= \frac{1}{2} R^5 \int_{B(0,R)} G_D(\bar{x}, \bar{y}) |\bar{y}|^{-5} \hat{f} \left(R^2 |\bar{y}|^{-2} \bar{y} \right) d\omega(\bar{y}) = \\ &= R^{-5} \int_{B(0,R)^c} G_D \left(\bar{x}, R^2 |\bar{\eta}|^{-2} \bar{\eta} \right) |\bar{\eta}|^5 \hat{f}(\bar{\eta}) d\omega(\bar{\eta}) \end{aligned} \quad (3.57)$$

is obtained. Since the solution v to the problem (3.28) and (3.29) is related to u by the formula $v(\bar{\xi}) = u \left(R^2 |\bar{\xi}|^{-2} \bar{\xi} \right)$, from (3.57) the desired representation

$$\begin{aligned} v(\bar{\xi}) &= \frac{1}{2} R^{-5} \int_{B(0,R)^c} G_D \left(R^2 |\bar{\xi}|^{-2} \bar{\xi}, R^2 |\bar{\eta}|^{-2} \bar{\eta} \right) |\bar{\eta}|^5 \hat{f}(\bar{\eta}) d\omega(\bar{\eta}) + \\ &+ \int_{\partial B(0,R)} g(\bar{\eta}) D_{n(\bar{\eta})} G_D \left(R^2 |\bar{\xi}|^{-2} \bar{\xi}, \bar{\eta} \right) d\sigma(\bar{\eta}) \end{aligned} \quad (3.58)$$

is derived.

Finally, in the two-dimensional case one has

$$f(\bar{y}) = R^4 |\bar{y}|^{-4} \hat{f} \left(R^2 |\bar{y}|^{-1} \bar{y} \right), \quad \bar{y} \in B(0, R) \quad (3.59)$$

and

$$J(\bar{\eta}) = R^2 |\bar{\eta}|^{-4} \quad (3.60)$$

It follows

$$\begin{aligned} u_1(\bar{x}) &= R^2 \int_{B(0,R)} G_D(\bar{x}, \bar{y}) |\bar{y}|^{-4} \hat{f} \left(R^2 |\bar{y}|^{-2} \bar{y} \right) d\omega(\bar{y}) = \\ &= R^{-4} \int_{B(0,R)^c} G_D \left(\bar{x}, R^2 |\bar{\eta}|^{-2} \bar{\eta} \right) |\bar{\eta}|^4 \hat{f}(\bar{\eta}) d\omega(\bar{\eta}) \end{aligned} \quad (3.61)$$

and

$$\begin{aligned} v(\bar{\xi}) &= R^{-4} \int_{B(0,R)^c} G_D \left(R^2 |\bar{\xi}|^{-2} \bar{\xi}, R^2 |\bar{\eta}|^{-2} \bar{\eta} \right) |\bar{\eta}|^4 \hat{f}(\bar{\eta}) d\omega(\bar{\eta}) + \\ &+ \int_{\partial B(0,R)} g(\bar{\eta}) D_{n(\bar{\eta})} G_D \left(R^2 |\bar{\xi}|^{-2} \bar{\xi}, \bar{\eta} \right) d\sigma(\bar{\eta}) \end{aligned} \quad (3.62)$$

respectively.

3.1.3 Field of a Point Charge Surrounded by a Spherical Surface at Known Potential

The source charge $+q$ gives rise to an induced charge $-q$ on the sphere; in addition to it, the free charge on the sphere, originating the potential $U = k$, is $q' = 4\pi\epsilon Rk$ (see 2.119).

From Gauss's theorem the field turns out to be

$$E(r) = \frac{q}{4\pi\epsilon r^2}, \quad 0 < r < R; \quad E(r) = \frac{Rk}{r^2}, \quad r > R \quad (3.63)$$

Independently, the problem can be solved using the method of Green's function. When $f(\bar{y}) = \frac{q}{\epsilon}\delta(\bar{y})$ and $|\bar{x}| < R$, from (3.44) with $g(\bar{y}) = k$, it turns out to be

$$U(\bar{x}) = \int_{\Omega} \frac{q}{\epsilon} G_D(\bar{x}, \bar{y}) \delta(\bar{y}) d\Omega - \int_{\Gamma} k D_{n(\bar{y})} G_D(\bar{x}, \bar{y}) d\Gamma \quad (3.64)$$

After (3.38) and (3.41) one has

$$\int_{\Omega} \frac{q}{\epsilon} G_D(\bar{x}, \bar{y}) \delta(\bar{y}) d\Omega = \frac{q}{\epsilon} G_D(\bar{x}, 0) = \frac{q}{\epsilon} \left(\frac{1}{4\pi r} - \frac{1}{4\pi R} \right), \quad r < R \quad (3.65)$$

and

$$\int_{\Gamma} k D_{n(\bar{y})} G_D(\bar{x}, \bar{y}) d\Gamma = k \int_{\Gamma} \frac{|\bar{x}|^2 - R^2}{4\pi R |\bar{x} - R\bar{u}_y|^3} d\Gamma = -k \quad (3.66)$$

respectively.

It can be verified that $U(r) = k$ solves the particular case of $q = 0$, for which

$$\nabla^2 U(r) = D_r^2 U(r) + \frac{2}{r} D_r U(r) = 0, \quad U(R) = k \quad (3.67)$$

holds.

The potential is given by

$$U(r) = \frac{q}{\epsilon} \left(\frac{1}{4\pi r} - \frac{1}{4\pi R} \right) + k, \quad 0 < r < R \quad (3.68)$$

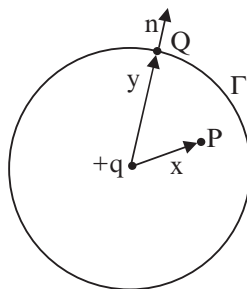


Fig. 3.3 Point charge surrounded by a sphere at potential k

whence (3.63) follows.

In turn, when $R < |\bar{x}|$, from (3.58) with $\hat{f}(\bar{\eta}) = 0$ and $g(\bar{\eta}) = k$ one has

$$v(\bar{\xi}) = \int_{\Gamma} k D_n(\bar{\eta}) G_D \left(R^2 |\bar{\xi}|^{-2} \bar{\xi}, \bar{\eta} \right) d\Gamma = \frac{Rk}{r}, \quad r > R \quad (3.69)$$

Again, it can be verified that $u(r)$ solves the particular case of $q = 0$, for which

$$\nabla^2 U(r) = D_r^2 U(r) + \frac{2}{r} D_r U(r) = 0, \quad U(R) = k, \quad U(\infty) = 0 \quad (3.70)$$

holds.

Potential and field are represented in Figs. 3.4 and 3.5, respectively.

At $r = R$, U is continuous for any k , while E is not if $k \neq \frac{q}{4\pi\epsilon R}$. The particular cases of a grounded sphere and a supplied sphere follow, when $k = 0$ with $q \neq 0$ and $k \neq 0$ with $q = 0$, respectively.

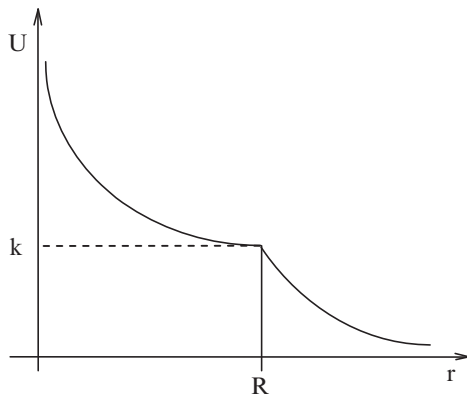


Fig. 3.4 Potential vs position

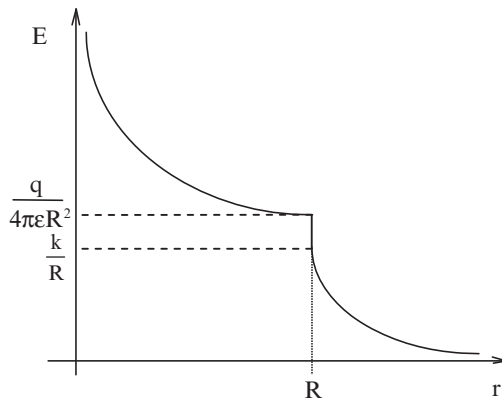


Fig. 3.5 Field vs position ($q > 4\pi\epsilon Rk$)

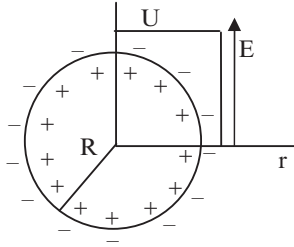


Fig. 3.6 Surface dipole distribution on a sphere

3.1.4 Field of a Surface Dipole Distributed on a Sphere of Radius R

Let a double-layer distribution of charge be considered, characterized by a uniform dipole density $\bar{\tau} = \frac{q}{4\pi R} \bar{i}_r$ (Fig. 3.6). According to (2.124), the potential of a single dipole of moment \bar{p} is given by $\frac{\bar{p} \cdot \bar{i}_r}{4\pi\epsilon r^2}$, $r \neq 0$; summing elementary contributions, the potential due to the surface dipole distribution is

$$U(r) = \int_{\Gamma} \frac{\bar{\tau} \cdot \bar{i}_r}{4\pi\epsilon r^2} d\Gamma = \frac{\tau}{4\pi\epsilon R^2} \int_{\Gamma} d\Gamma = \frac{\tau}{\epsilon} = \frac{q}{4\pi\epsilon R}, \quad 0 < r < R \quad (3.71)$$

The latter holds when the field point P is within the sphere; when P crosses the sphere, the solid angle subtended by the surface has a discontinuity equal to 4π . Consequently, the potential has a discontinuity equal to $\frac{\tau}{\epsilon}$ determining $U(r) = 0$, $r > R$.

Remarks

The following remark can be put forward. Denoting by $\sigma = \epsilon \frac{\partial U}{\partial n}$ the charge density ($C m^{-2}$) on Γ and with $\tau = \epsilon U$ the dipole density ($C m^{-1}$), see Section 2.2.6) on Γ , respectively, Green's formula (3.5) can be also expressed as

$$U(\bar{x}, \bar{y}) = \int_{\Omega} \frac{\rho(\bar{y})}{\epsilon} G(\bar{x}, \bar{y}) d\Omega + \int_{\Gamma_1} \frac{\sigma(\bar{y})}{\epsilon} G(\bar{x}, \bar{y}) d\Gamma + \int_{\Gamma_2} \frac{\tau(\bar{y})}{\epsilon} \frac{\partial G(\bar{x}, \bar{y})}{\partial n} d\Gamma \quad (3.72)$$

Hence, the electrostatic potential U in a domain Ω bounded by Γ is known, knowing G' and ρ in the domain, σ and τ on the boundary. The three terms are called volume term, single-layer term and double-layer term, respectively.

In the case of the surface dipole distributed on a sphere, using (3.72) with $\rho = 0$, $\sigma = 0$ and taking $G = \frac{1}{4\pi r}$ and $U = \frac{\tau}{\epsilon}$, the potential results

$$\begin{aligned}
 U(r) &= - \int_{\Gamma} \frac{\tau}{\varepsilon} \frac{\partial G}{\partial n} d\Gamma = \int_{\Gamma} \frac{\tau}{\varepsilon} \frac{1}{4\pi r^2} d\Gamma = \\
 &= \frac{q}{4\pi\varepsilon R} \frac{1}{4\pi R^2} \int_{\Gamma} d\Gamma = \frac{q}{4\pi\varepsilon R}, \quad 0 < r < R
 \end{aligned} \tag{3.73}$$

with $U(r) = 0$, $r > R$.

It can be noted that, at $r = R$, both U and E are not continuous (Fig. 3.6); in particular, the field is singular and can be expressed as $\vec{E}(r) = \frac{q}{4\pi\varepsilon R} \delta(r - R) \vec{i}_r$.

As a final example, let a surface distribution of charges and dipoles be identified, such that the field external to the sphere of radius R is zero, while the inner field is that due to a point charge $+q$ located at the centre.

To this end, forcing a uniform charge distribution of density $\sigma = -\frac{q}{4\pi R^2}$ on the sphere, the relevant potential is $U_{\sigma}(r) = -\frac{q}{4\pi\varepsilon R}$, $0 < r < R$ and $U_{\sigma}(r) = -\frac{q}{4\pi\varepsilon r}$, $R < r$.

Then, adding a surface dipole distribution of density $\tau = \frac{q}{4\pi R}$ the contributions $U_{\tau}(r) = \frac{q}{4\pi\varepsilon R}$, $0 < r < R$ and $U_{\tau}(r) = 0$, $R < r$ to the potential originate.

Since the potential due to the point charge is $U_0(r) = \frac{q}{4\pi\varepsilon r}$, $r \neq 0$, summing the three terms above, one obtains $U(r) = \frac{q}{4\pi\varepsilon r}$, $0 < r < R$ and $U(r) = 0$, $R < r$.

3.1.5 Green's Formula for Two-Dimensional Magnetostatics

The formula of vector potential A corresponding to (3.5) is

$$A = \int_{\Omega} G \mu J d\Omega + \int_{\Gamma_1} G \frac{\partial A}{\partial n} d\Gamma - \int_{\Gamma_2} A \frac{\partial G}{\partial n} d\Gamma \tag{3.74}$$

where $\Gamma = \Gamma_1 \cup \Gamma_2 = \partial\Omega$ and $\Gamma_1 \cap \Gamma_2 = \emptyset$; in the latter G' is the modified Green's function and μ is the permeability ($H m^{-1}$) of the material.

3.1.6 Field of a Line Current in a Three-Dimensional Domain: Integral Approach

Let a straight conductor, placed in an unbounded three-dimensional domain and carrying direct current of density J , be considered. Assuming cylindrical coordinates, from (3.74) it follows

$$\vec{A} = A \vec{i}_z, \quad \vec{J} = J \vec{i}_z, \quad A = \frac{\mu}{4\pi} \int_{\Omega} \frac{J}{|\vec{r}|} d\Omega \tag{3.75}$$

where \vec{r} is the distance between the fixed field point P and the source point Q (Fig. 3.7) oriented from Q to P and Ω is the conductor volume.

Moving from potential to field, at point P one has

$$\vec{B} = \vec{\nabla}_P \times \vec{A} = \frac{\mu}{4\pi} \int_{\Omega} \vec{\nabla}_P \times \frac{\vec{J}}{|\vec{r}|} d\Omega \tag{3.76}$$

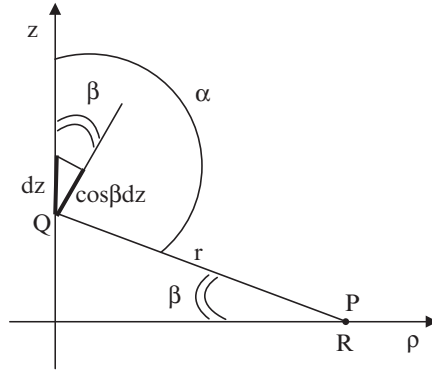


Fig. 3.7 Line current

where the operator $\bar{\nabla}_P$ acts on the coordinates of point P. The following identity holds

$$\bar{\nabla}_P \times \frac{\bar{J}}{|\bar{r}|} = \frac{1}{|\bar{r}|} \bar{\nabla}_P \times \bar{J} - \bar{J} \times \bar{\nabla}_P \frac{1}{|\bar{r}|} \quad (3.77)$$

Since \bar{J} depends on the coordinates of point Q and not on those of point P, it follows that $\bar{\nabla}_P \times \bar{J} = 0$; then, according to (A.3), it comes out that

$$-\bar{J} \times \bar{\nabla}_P \frac{1}{|\bar{r}|} = \frac{\bar{J} \times \bar{r}}{|\bar{r}|^3} \quad (3.78)$$

and therefore

$$\bar{B} = \frac{\mu}{4\pi} \int_{\Omega} \frac{\bar{J} \times \bar{r}}{|\bar{r}|^3} d\Omega \quad (3.79)$$

which is called Laplace's law of the elementary action.

Since the conductor is cylindrical and the current density is uniform, $J d\Omega = I dz$ and the volume integral becomes a line integral

$$\bar{B} = \frac{\mu}{4\pi} \int_{-\infty}^{+\infty} \frac{\bar{i}_z \times \bar{r}}{|\bar{r}|^3} dz = \frac{\mu I}{4\pi} \int_{-\infty}^{+\infty} \frac{\bar{i}_y |\bar{r}| \sin \alpha}{|\bar{r}|^3} dz = \bar{i}_y \frac{\mu I}{4\pi} \int_{-\infty}^{+\infty} \frac{\sin \alpha}{|\bar{r}|^2} dz \quad (3.80)$$

Substituting $r \cos \beta = R$ and $\cos \beta dz = r d\beta$, since $\sin \alpha = \cos \beta$, finally it results

$$\bar{B} = \bar{i}_y \frac{\mu I}{4\pi R} \int_{-\frac{\pi}{2}}^{+\frac{\pi}{2}} \cos \beta d\beta = \bar{i}_y \frac{\mu I}{2\pi R} \quad (3.81)$$

and

$$\bar{H} = \bar{i}_y \frac{I}{2\pi R} \quad (3.82)$$

coincident with (2.227) when $\beta = 0$, so that $r \equiv R$.

3.1.7 Field of a Current-Carrying Conductor of Rectangular Cross-Section

In a two-dimensional unbounded domain, which is supposed to be homogeneous and free of ferromagnetic material, after (3.4) the Green's function for a cylindrical conductor carrying a constant current I is given by

$$A(r) = \frac{\mu_0 I}{2\pi} \ln r, \quad r > 0 \tag{3.83}$$

Let a conductor of rectangular cross-section, having width $2a$ and height $2b$ and carrying a constant current distributed with uniform density J , be considered (Fig. 3.8). At the gravity centre of the conductor cross-section the origin of a rectangular system of coordinates is placed.

After integrating the elementary contributions, the potential of the rectangular conductor is given by

$$\begin{aligned} A(x, y) &= \frac{\mu_0 J}{2\pi} \int_{-a}^a \int_{-b}^b \ln [r(x, y, x', y')] dy' dx' = \\ &= \frac{\mu_0 J}{4\pi} \int_{-a}^a \int_{-b}^b \ln [(x - x')^2 + (y - y')^2] dy' dx' \end{aligned} \tag{3.84}$$

where (x', y') and (x, y) are source point Q and field point P , respectively. It turns out to be

$$\begin{aligned} A(x, y) &= \frac{\mu_0 J}{4\pi} \left\{ (a - x)(b - y) \ln [(a - x)^2 + (b - y)^2] + \right. \\ &\quad + (a + x)(b - y) \ln [(a + x)^2 + (b - y)^2] + \\ &\quad + (a - x)(b + y) \ln [(a - x)^2 + (b + y)^2] + \\ &\quad \left. + (a + x)(b + y) \ln [(a + x)^2 + (b + y)^2] + \right\} \end{aligned}$$

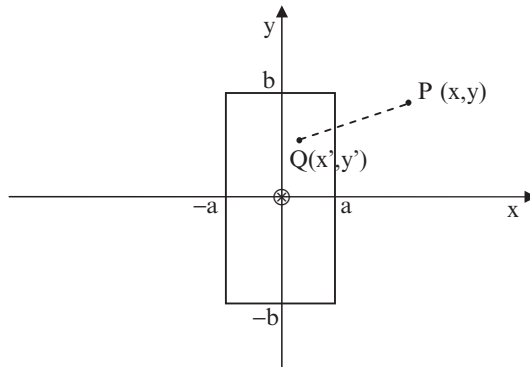


Fig. 3.8 Conductor of rectangular cross-section

$$\begin{aligned}
& + (a - x)^2 \left(\operatorname{arctg} \frac{b - y}{a - x} + \operatorname{arctg} \frac{b + y}{a - x} \right) + \\
& + (a + x)^2 \left(\operatorname{arctg} \frac{b - y}{a + x} + \operatorname{arctg} \frac{b + y}{a + x} \right) + \\
& + (b - y)^2 \left(\operatorname{arctg} \frac{a - x}{b - y} + \operatorname{arctg} \frac{a + x}{b - y} \right) + \\
& + (b + y)^2 \left(\operatorname{arctg} \frac{a - x}{b + y} + \operatorname{arctg} \frac{a + x}{b + y} \right) \} \quad (3.85)
\end{aligned}$$

for $x \neq \pm a$, $y \neq \pm b$. If the assumption $b \ll a$ holds, the model of the current sheet follows. It turns out to be

$$\begin{aligned}
A(x, y) &= \frac{\mu_0 J}{4\pi} \int_{-a}^a \ln \left[(x - x')^2 + y^2 \right] dx' = \\
&= \frac{\mu_0 J}{4\pi} \left\{ (a + x) \ln \left[(a + x)^2 + y^2 \right] + (a - x) \ln \left[(a - x)^2 + y^2 \right] + \right. \\
&\quad \left. + 2y \left(\operatorname{arctg} \frac{a + x}{y} + \operatorname{arctg} \frac{a - x}{y} \right) - 4a \right\}, \quad y \neq 0 \quad (3.86)
\end{aligned}$$

where J is the line current density ($A \text{ m}^{-1}$). After (3.85) or (3.86), from (2.205) the components of induction field can be obtained.

3.2 Method of Images

Field problems characterized by concentrated sources in non-homogeneous domains with simple boundaries can be solved by the method of images.

Electrostatic images

Let a dielectric half-space Ω of permittivity ε with a point charge q at a distance h from a conducting half-space be considered. The field in the dielectric region Ω is uniquely specified by the charge q and the boundary condition of the region, where $\vec{E} \cdot \vec{i} = 0$ holds. Comparing this field with that produced in an unbounded dielectric domain of permittivity ε by two point charges q and $-q$ at a distance $2h$, one can conclude that in the dielectric region Ω the fields are the same. Therefore in this region the field is equal to that produced by charge q and its image $-q$ placed at distance $2h$ in a homogeneous domain of permittivity ε (Fig. 3.9).

Therefore, according to (2.118) the electric field is expressed by

$$\vec{E} = \frac{1}{4\pi\varepsilon} q \frac{1}{x^2 + (y - h)^2} \vec{i}_{r_1} - \frac{1}{4\pi\varepsilon} q \frac{1}{x^2 + (y + h)^2} \vec{i}_{r_2}, \quad y > 0 \quad (3.87)$$

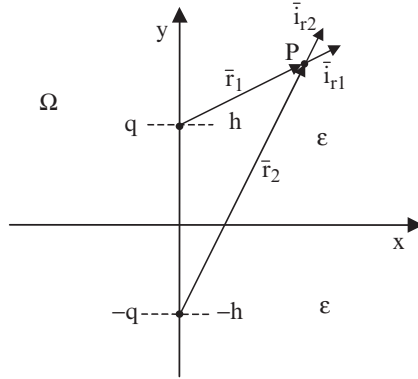


Fig. 3.9 Point charge near the boundary with a conducting half space: source and image charge

where the radial unit vectors are defined as follows

$$\bar{i}_{r_1} = \left(\frac{x}{\sqrt{x^2 + (y - h)^2}}, \frac{y - h}{\sqrt{x^2 + (y - h)^2}} \right), \quad y > 0 \quad (3.88)$$

$$\bar{i}_{r_2} = \left(\frac{x}{\sqrt{x^2 + (y + h)^2}}, \frac{y + h}{\sqrt{x^2 + (y + h)^2}} \right), \quad y > 0 \quad (3.89)$$

In turn, the electric field for $y < 0$ is given by $\bar{E} = 0$.

Field lines are plotted in Fig. 3.10.

More generally, let a dielectric medium of permittivity ϵ_1 be considered, filling the upper half-space where a point charge q is located; at a distance h from the charge, let another dielectric medium of permittivity ϵ_2 fill the lower half-space (Fig. 3.11).

In this case, the field in the upper half-space is equivalent to that produced in a homogeneous region of permittivity ϵ_1 by both source charge q and image charge $q' = -\alpha q$ with $0 \leq \alpha < 1$, placed at a distance $2h$ from q .

In an analogous way, the field in the lower half-space is equivalent to that produced by a second image charge $q'' = \beta q$ with $0 \leq \beta < 1$, placed instead of q in a homogeneous region of permittivity ϵ_2 .

In fact, at the interface $y = 0$, the transmission conditions for tangential component of electric field and normal component of induction (2.78) and (2.77) imply

$$E_x - \alpha E_x = \beta E_x, \quad y = 0^+ \quad (3.90)$$

$$\epsilon_1 E_y + \epsilon_1 \alpha E_y = \epsilon_2 \beta E_y, \quad y = 0^- \quad (3.91)$$

respectively. It is easily found that

$$\alpha = \frac{\epsilon_2 - \epsilon_1}{\epsilon_1 + \epsilon_2}; \quad \beta = \frac{2\epsilon_1}{\epsilon_1 + \epsilon_2} \quad (3.92)$$

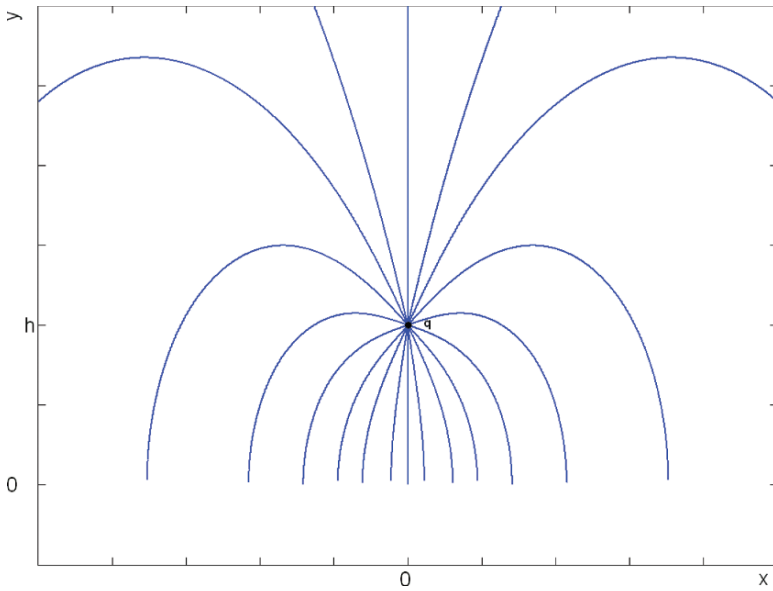


Fig. 3.10 Electrostatic images: field lines for $y > 0$

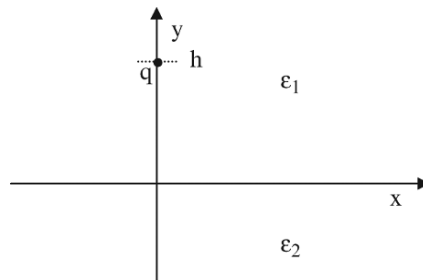


Fig. 3.11 Point charge near the boundary of two dielectric half-spaces

Therefore, the electric field for $y > 0$ is expressed by

$$\bar{\mathbf{E}} = \frac{1}{4\pi\epsilon_1} q \frac{1}{x^2 + (y-h)^2} \bar{\mathbf{i}}_{r1} - \frac{1}{4\pi\epsilon_1} \frac{\epsilon_2 - \epsilon_1}{\epsilon_1 + \epsilon_2} q \frac{1}{x^2 + (y+h)^2} \bar{\mathbf{i}}_{r2} \quad (3.93)$$

$$\bar{\mathbf{i}}_{r1} = \left(\frac{x}{\sqrt{x^2 + (y-h)^2}}, \frac{y-h}{\sqrt{x^2 + (y-h)^2}} \right) \quad (3.94)$$

$$\bar{\mathbf{i}}_{r2} = \left(\frac{x}{\sqrt{x^2 + (y+h)^2}}, \frac{y+h}{\sqrt{x^2 + (y+h)^2}} \right) \quad (3.95)$$

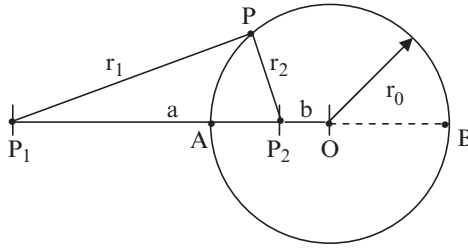


Fig. 3.12 Image of a charge with respect to a grounded sphere

In turn, the electric field for $y < 0$ is given by

$$\vec{E} = \frac{1}{4\pi\epsilon_2} \frac{2\epsilon_1}{\epsilon_1 + \epsilon_2} q \frac{1}{x^2 + (y - h)^2} \vec{i}_{r_1} \quad (3.96)$$

Now, let a point charge q_1 be located at point P_1 externally to a conducting sphere, of radius r_0 and centre O , having potential $U = 0$; the distance between P_1 and the centre of the sphere is d .

The field distribution does not change if the spherical surface is replaced by an equivalent point-charge q_2 , located at a suitable point P_2 , such that the sphere represents its zero-potential surface; in that case q_2 is called the image charge of q_1 with respect to the sphere. The problem is that of identifying: (i) distance a between P_1 and P_2 ; (ii) displacement b of P_2 with respect to the sphere centre O ; (iii) value q_2 of the image charge, knowing the value q_1 of source charge and the distance $d = a + b$ (Fig. 3.12).

From (2.119) the potential at point P is

$$U = \frac{1}{4\pi\epsilon_0} \left(\frac{q_1}{r_1} + \frac{q_2}{r_2} \right) \quad (3.97)$$

where r_1 and r_2 are the distances of P from P_1 and P_2 , respectively.

All points of the domain for which $U = 0$ should fulfil

$$\frac{q_1}{r_1} + \frac{q_2}{r_2} = 0 \quad (3.98)$$

or

$$\frac{r_1}{r_2} = -\frac{q_1}{q_2} = k \quad (3.99)$$

In a two-dimensional domain they belong to a circle surrounding the point P_2 where the image charge should be located. Equation (3.99) for points A and B gives

$$\frac{a + b - r_0}{r_0 - b} = \frac{a + b + r_0}{r_0 + b} = k \quad (3.100)$$

The last two equations yield

$$k = \frac{d}{r_0} \quad (3.101)$$

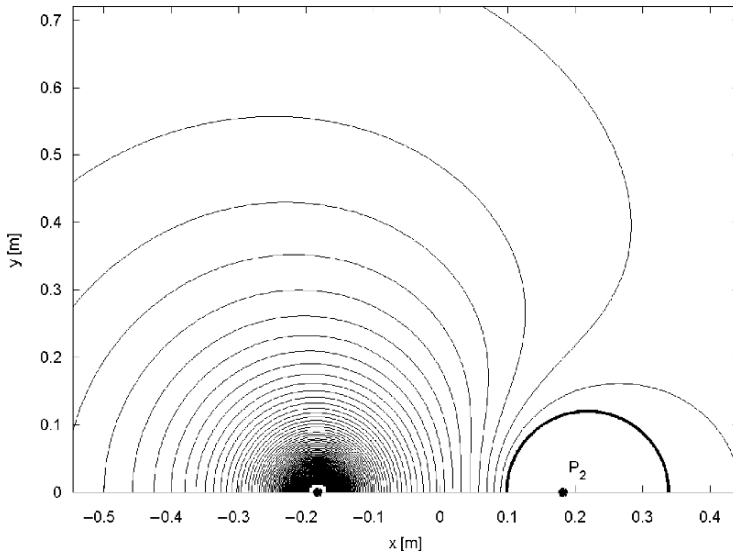


Fig. 3.13 Contour plot of potential for two unlike charges of different magnitude

$$a = \frac{d^2 - r_0^2}{d} \quad (3.102)$$

$$b = \frac{r_0^2}{d} \quad (3.103)$$

$$q_2 = -\frac{q_1}{k} \quad (3.104)$$

It should be noted that source and image charge are unlike and have different magnitude.

Assuming $q_1 = 4 \mu\text{C}$, $d = 40 \text{ cm}$, $r_0 = 12 \text{ cm}$, one has $\frac{1}{k} = 0.3$, $q_2 = -1.2 \mu\text{C}$, $a = 36.4 \text{ cm}$ and $b = 3.6 \text{ cm}$; the corresponding potential lines are shown in Fig. 3.13.

Finally, if the potential of the sphere is $U = U_0 \neq 0$, the problem can be solved as above with the addition of a second image charge $q_3 = 4\pi\epsilon_0 r_0 U_0$ placed at the centre of the sphere.

Magnetostatic images

A magnetic region Ω of permeability μ with a line current I , located at a distance h from a half-space of infinite permeability and parallel to the space itself, is considered.

The field in the magnetic region Ω is uniquely specified by the current I and the boundary condition, where $\vec{H} \cdot \vec{t} = 0$ holds. Comparing this field with that produced in an unbounded magnetic domain by two line currents of equal magnitude and equal sign at a distance $2h$, one can conclude that in the magnetic region the fields are the same. Therefore in this region the field is equal to that of current I and its image I at distance $2h$ placed in a homogeneous domain of permeability μ (Fig. 3.14).

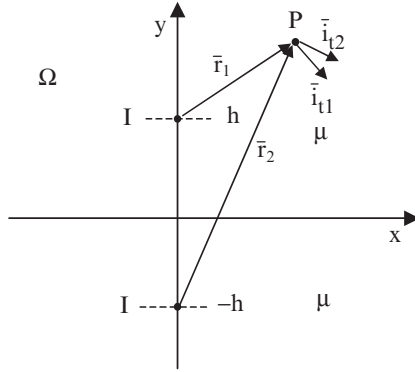


Fig. 3.14 Source and image currents

Therefore, the flux density for $y > 0$ is expressed by

$$\bar{B} = \frac{\mu}{2\pi} I \frac{1}{\sqrt{x^2 + (y - h)^2}} \bar{i}_{t1} + \frac{\mu}{2\pi} I \frac{1}{\sqrt{x^2 + (y + h)^2}} \bar{i}_{t2} \quad (3.105)$$

where the tangential unit vectors are defined as follows

$$\bar{i}_{t1} = \left(-\frac{y - h}{\sqrt{x^2 + (y - h)^2}}, \frac{x}{\sqrt{x^2 + (y - h)^2}} \right) \quad (3.106)$$

$$\bar{i}_{t2} = \left(-\frac{y + h}{\sqrt{x^2 + (y + h)^2}}, \frac{x}{\sqrt{x^2 + (y + h)^2}} \right) \quad (3.107)$$

In turn, the flux density for $y < 0$ is given by $\bar{B} = 0$.

Field lines for $y > 0$ are plotted in Fig. 3.15.

More generally, let a line current I , placed in a half-space of permeability μ_1 at a distance h from the boundary of a half-space of permeability μ_2 , be considered (Fig. 3.16).

In analogy to the electrostatic case, the magnetic field in the upper half-space is equivalent to that produced, in a homogeneous region of permeability μ_1 , by both source current I and image current $I' = \alpha I$ with $0 \leq \alpha < 1$ placed at a distance $2h$ from I .

In a similar way, the field in the lower half-space is equivalent to that produced by a second image current $I'' = \beta I$ with $0 \leq \beta < 1$ placed instead of I in a homogeneous region of permeability μ_2 .

The transmission conditions for tangential component of magnetic field and normal component of induction at $y = 0$ imply

$$H_x - \alpha H_x = \beta H_x, \quad y = 0^+ \quad (3.108)$$

$$\mu_1 H_y + \mu_1 \alpha H_y = \mu_2 \beta H_y, \quad y = 0^- \quad (3.109)$$

$$0 \leq \alpha < 1 \quad 0 \leq \beta < 1 \quad (3.110)$$

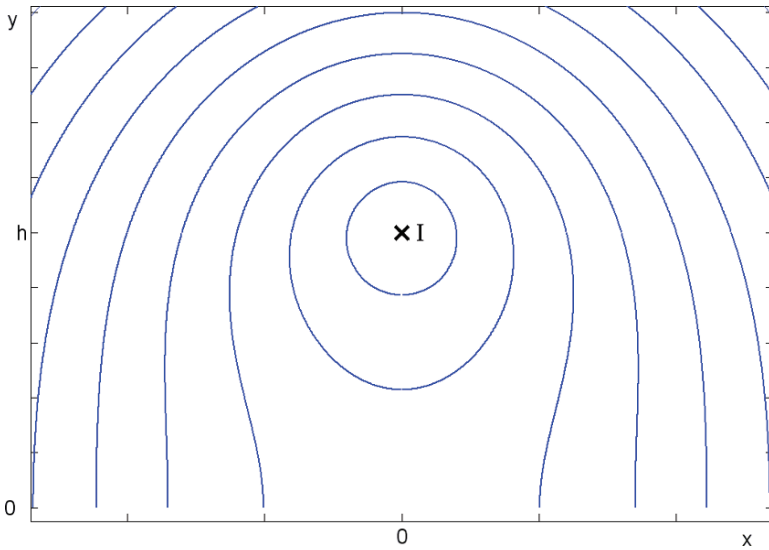


Fig. 3.15 Magnetostatic images: vector plot for $y > 0$

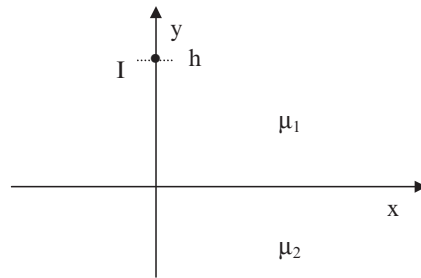


Fig. 3.16 Line current near the boundary of two magnetic half-spaces

respectively. It is easily found that

$$\alpha = \frac{\mu_2 - \mu_1}{\mu_1 + \mu_2}; \quad \beta = \frac{2\mu_1}{\mu_1 + \mu_2} \quad (3.111)$$

Therefore, the flux density for $y > 0$ is expressed by

$$\vec{B} = \frac{\mu_1 I}{2\pi} \frac{1}{\sqrt{x^2 + (y-h)^2}} \vec{i}_{t1} + \frac{\mu_1 \mu_2 - \mu_1}{2\pi \mu_1 + \mu_2} I \frac{1}{\sqrt{x^2 + (y+h)^2}} \vec{i}_{t2} \quad (3.112)$$

$$\vec{i}_{t1} = \left(-\frac{y-h}{\sqrt{x^2 + (y-h)^2}}, \frac{x}{\sqrt{x^2 + (y-h)^2}} \right) \quad (3.113)$$

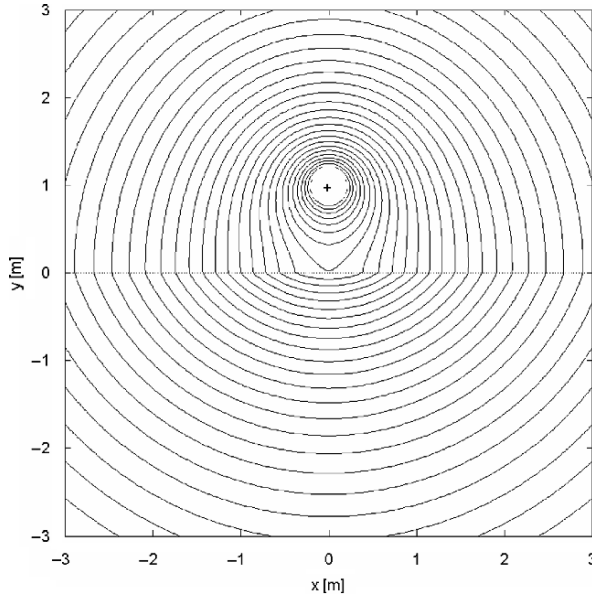


Fig. 3.17 Line current: field of source and image current ($\mu_2 = 20\mu_1$)

$$\vec{i}_{t2} = \left(-\frac{y+h}{\sqrt{x^2+(y+h)^2}}, \frac{x}{\sqrt{x^2+(y+h)^2}} \right) \quad (3.114)$$

In turn, the flux density for $y < 0$ is given by

$$\vec{B} = \frac{\mu_2}{2\pi} \frac{2\mu_1}{\mu_1 + \mu_2} I \frac{1}{\sqrt{x^2+(y-h)^2}} \vec{i}_{t1} \quad (3.115)$$

In Fig. 3.17 the contour plot of flux lines is reported in the case $\mu_2 = 20\mu_1$.

3.2.1 Magnetic Field of a Line Current in a Slot

Let the test case shown in Fig. 2.13b be considered. A rectangular slot, having width a and height b is surrounded by ferromagnetic material of infinite permeability (closed slot). A constant line current I is concentrated at the gravity centre of the slot where the origin of a system of rectangular coordinates is placed (Fig. 3.18). Due to the presence of ferromagnetic material, the following boundary conditions hold:

$$B_x = 0 \quad \text{for} \quad y = \left(+\frac{b}{2}\right)^- \quad \text{and} \quad y = \left(-\frac{b}{2}\right)^+ \quad (3.116)$$

$$B_y = 0 \quad \text{for} \quad x = \left(+\frac{a}{2}\right)^- \quad \text{and} \quad x = \left(-\frac{a}{2}\right)^+ \quad (3.117)$$

for an observer located in the slot (flux lines orthogonal to the air/iron boundary).

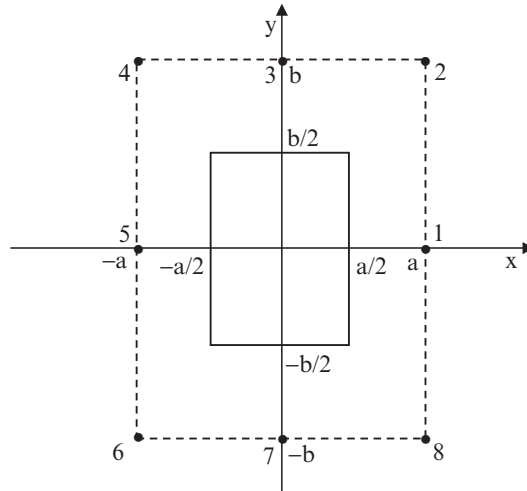


Fig. 3.18 Closed slot and images

Table 3.1 Location of images for the closed slot (single images)

Image k	x_k	y_k
1	a	0
2	a	b
3	0	b
4	-a	b
5	-a	0
6	-a	-b
7	0	-b
8	a	-b

If images due to multiple reflections in x and y directions are neglected, then eight equivalent currents $I_k = I, k = 1, 8$ approximate the effect of the slot boundary; they have to be placed symmetrically according to Table 3.1.

The closed slot is characterized by a double air/iron boundary in both x and y directions: in principle, the images form an infinite series, because each image current gives rise to a new reflection with respect to the boundaries. A better approximation of the field in the slot is obtained if a second layer of images is taken into account; then, twenty-four sources are originated, according to Table 3.2.

The total field is thus given by the superposition of the fields due to source current and like image currents, all of them being located in an unbounded domain of permeability μ_0 , namely

$$\bar{B} = \frac{\mu_0 I}{2\pi\sqrt{x^2 + y^2}} \bar{i}_t + \sum_k \frac{\mu_0 I_k}{2\pi\sqrt{(x - x_k)^2 + (y - y_k)^2}} \bar{i}_{t,k} \tag{3.118}$$

$$-\frac{a}{2} \leq x \leq \frac{a}{2}, \quad -\frac{b}{2} \leq y \leq \frac{b}{2}, \quad x \neq x_k, \quad y \neq y_k$$

Table 3.2 Location of images for the closed slot (double images)

Image k	x_k	y_k
1	a	0
2	a	b
3	0	b
4	-a	b
5	-a	0
6	-a	-b
7	0	-b
8	a	-b
9	2a	0
10	2a	b
11	2a	2b
12	a	2b
13	0	2b
14	-a	2b
15	-2a	2b
16	-2a	b
17	-2a	0
18	-2a	-b
19	-2a	-2b
20	-a	-2b
21	0	-2b
22	a	-2b
23	2a	-2b
24	2a	-b

with

$$\bar{i}_t = \left(-\frac{y}{\sqrt{x^2 + y^2}}, \frac{x}{\sqrt{x^2 + y^2}} \right) \quad (3.119)$$

and

$$\bar{i}_{t,k} = \left(-\frac{y-y_k}{\sqrt{(x-x_k)^2 + (y-y_k)^2}}, \frac{x-x_k}{\sqrt{(x-x_k)^2 + (y-y_k)^2}} \right) \quad (3.120)$$

where (x_k, y_k) are the coordinates of k th image, while the summation index is $k = 1, \dots, 8$ and $k = 1, \dots, 24$ when single and double images are considered, respectively.

The case of a magnetically open slot, the height of which is assumed to be much greater than its width a , accommodating a conductor of height b , can be easily treated; boundary conditions become

$$B_x = 0, \quad y = \left(-\frac{b}{2} \right)^+ \quad (3.121)$$

$$B_y = 0, \quad x = \left(-\frac{a}{2} \right)^+, \left(\frac{a}{2} \right)^- \quad (3.122)$$

Again, the field is given by (3.118)–(3.120), this time taking the summation index $k = \{1, 5, 6, 7, 8\}$ and $k = \{1, 5, 6, 7, 8, 9, 17, 18, 19, 20, 21, 22, 23, 24\}$ when single and double images are considered, respectively.

The following remark can be put forward. Expanding the field in terms of current images is equivalent to set a particular solution fulfilling the given boundary conditions. The fact that boundary conditions (3.116) and (3.117) are not fully satisfied is due to the truncation of multiple images.

3.2.2 Magnetic Field of a Line AC Current over a Conducting Half-Space

The case of an AC line current located in a magnetic region of permeability μ at a distance h from a conducting half-space of infinite conductivity is here discussed (Fig. 3.19). The effect of induced currents in the conducting space gives rise to a flux barrier, i.e. the conducting plane can be treated as a space of zero permeability located at a distance h from the current; therefore, the field for $y > 0$ can be expressed as

$$\begin{aligned} \bar{\mathbf{B}} = & \frac{\mu}{2\pi} I \frac{1}{\sqrt{x^2 + (y-h)^2}} \bar{\mathbf{i}}_{t1} + \\ & - \frac{\mu}{2\pi} I \frac{1}{\sqrt{x^2 + (y+h)^2}} \bar{\mathbf{i}}_{t2}, \quad y > 0, y \neq h \end{aligned} \quad (3.123)$$

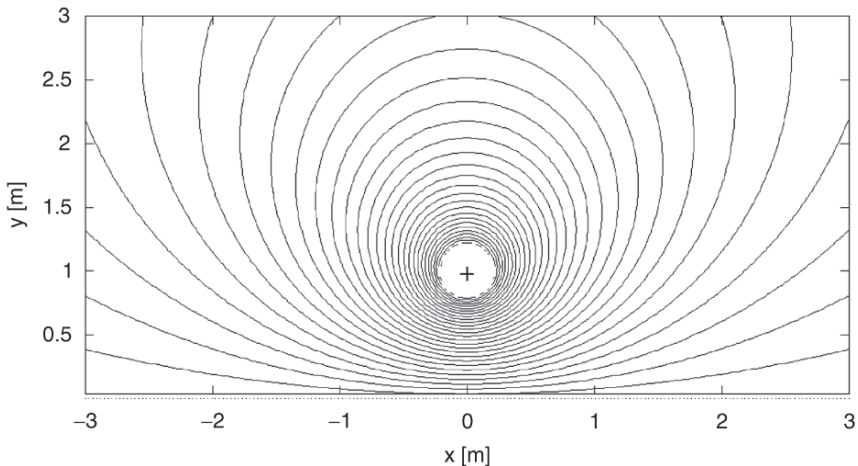


Fig. 3.19 AC line current near a conducting half-space of infinite permeability: field lines

with

$$\bar{i}_{t1} = \left(-\frac{y-h}{\sqrt{x^2+(y-h)^2}}, \frac{x}{\sqrt{x^2+(y-h)^2}} \right) \quad (3.124)$$

and

$$\bar{i}_{t2} = \left(-\frac{y+h}{\sqrt{x^2+(y+h)^2}}, \frac{x}{\sqrt{x^2+(y+h)^2}} \right) \quad (3.125)$$

In other words, the field for $y > 0$, is given by the superposition of source current I and image current $-I$ located at a distance $2h$ in an unbounded homogeneous region of permeability μ ; the boundary between magnetic and conducting regions is a flux line.

3.3 Method of Separation of Variables

In a two-dimensional homogeneous domain Ω , with constant permeability μ and no current, using rectangular coordinates, Laplace's equation of magnetic vector potential A is from (2.208)

$$\frac{\partial^2 A}{\partial x^2} + \frac{\partial^2 A}{\partial y^2} = 0 \quad (3.126)$$

If the domain boundaries lay along constant x or constant y lines, then the following solution can be tried

$$A(x, y) = X(x)Y(y) \quad (3.127)$$

where X and Y depend on x only and y only, respectively. Consequently, substituting (3.127) into (3.126), it turns out to be

$$Y \frac{d^2 X}{dx^2} + X \frac{d^2 Y}{dy^2} = 0, \quad \frac{1}{X} \frac{d^2 X}{dx^2} + \frac{1}{Y} \frac{d^2 Y}{dy^2} = 0 \quad (3.128)$$

if $X(x) \neq 0$ for any x and $Y(y) \neq 0$ for any y .

The only way (3.128) are true is that separately

$$\frac{1}{X} \frac{d^2 X}{dx^2} = -k^2 \quad (3.129)$$

$$\frac{1}{Y} \frac{d^2 Y}{dy^2} = k^2 \quad (3.130)$$

where $k^2 \neq 0$ is called the separation constant; it is assumed that both $X(x)$ and $Y(y)$ are non-constant functions.

Then, the partial differential equations (3.128) reduce to a pair of ordinary differential equations

$$\frac{d^2X}{dx^2} + k^2X = 0 \quad (3.131)$$

$$\frac{d^2Y}{dy^2} - k^2Y = 0 \quad (3.132)$$

For $k^2 \neq 0$, the two general solutions are given by

$$X(x) = \alpha_k \sin(|k|x) + \beta_k \cos(|k|x) \quad (3.133)$$

$$Y(y) = \gamma_k \text{sh}(|k|y) + \delta_k \text{ch}(|k|y) \quad (3.134)$$

If $k^2 = 0$, it results

$$X(x) = \alpha_0 + \alpha_1 x, \quad Y(y) = \beta_0 + \beta_1 y \quad (3.135)$$

The most general solution of (3.126) is then given by

$$\begin{aligned} A(x, y) = & c_1 + c_2 x + c_3 y + c_4 xy + \\ & + \sum_{n=1}^{\infty} [\alpha_n \sin(n|k|x) + \beta_n \cos(n|k|x)] [\gamma_n \text{sh}(n|k|y) + \delta_n \text{ch}(n|k|y)] \end{aligned} \quad (3.136)$$

In principle, the separation constant and all unknown coefficients can be determined by imposing the boundary conditions. The actual problem is to fit the latter; although there is an infinite number of solutions to Laplace's equation, it is often impossible to identify analytically the right set of constants fulfilling field conditions along the boundary.

In the case of a current source in the field domain, the Poisson's equation holds

$$\frac{\partial^2 A}{\partial x^2} + \frac{\partial^2 A}{\partial y^2} = -\mu J \quad (3.137)$$

and a particular solution should be added to the general one in order to take the source term J into account. In that case, boundary conditions are then imposed on the whole solution.

Finally, the following remark can be put forward. If the case

$$\frac{d^2X}{dx^2} - h^2X = 0 \quad (3.138)$$

$$\frac{d^2Y}{dy^2} + h^2Y = 0 \quad (3.139)$$

with $h^2 \neq 0$ is considered, the behaviour of $X(x)$ and $Y(y)$ is found to be symmetrical with respect to the corresponding solutions of the case (3.131)–(3.132).

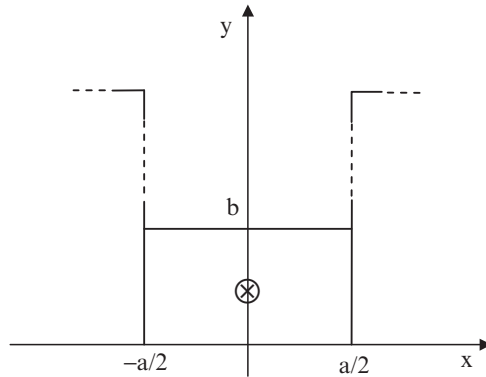


Fig. 3.20 Conductor in the slot

3.3.1 Magnetic Field of a Current Uniformly Distributed in a Slot

Let the test problem shown in Fig. 2.13a be considered; the height of the slot (Fig. 3.20) is assumed to be much greater than its width a .

A conductor of rectangular cross section, having width a and height b , is located at the bottom of the slot. The conductor carries a constant current I , supposed to be uniformly distributed inside the cross section. Due to the presence of ferromagnetic material of infinite permeability, the following boundary conditions hold

$$A = 0, \quad \text{for } y = 0^+ \quad (3.140)$$

$$\frac{\partial A}{\partial x} = 0, \quad \text{for } x = \left(+\frac{a}{2}\right)^- \quad \text{and} \quad x = \left(-\frac{a}{2}\right)^+ \quad (3.141)$$

Because of symmetry, the potential should be an even function of x ; taking this into account, after (3.136) the general solution to the Laplace's equation in a rectangular domain can be expressed as

$$A_L = \sum_{n=1}^{\infty} c_n \text{sh}(nky) \cos(nkx) \quad (3.142)$$

with k and c_n to be determined. A particular solution A_P to Poisson's equation, after integrating twice the right-hand side of (3.137) with respect to y , is

$$A_P(y) = -\frac{1}{2}\mu J y^2 \quad \text{with } J = \frac{I}{ab} \quad (3.143)$$

Consequently, the solution for the potential is

$$A = A_P + A_L = -\frac{1}{2}\mu J y^2 + \sum_{n=1}^{\infty} c_n \text{sh}(nky) \cos(nkx) \quad (3.144)$$

with $-\frac{a}{2} \leq x \leq \frac{a}{2}$, $0 \leq y \leq b$.

In the region $y > b$, $J = 0$ and the field tends to be uniform such that $(B_x, B_y) = (B_0, 0)$ at least for $y \gg b$; accordingly, a suitable expression of the potential in this region is

$$\tilde{A}_L = \alpha + \beta y + \sum_{n=1}^{\infty} \gamma_n e^{-nky} \cos(nkx), \quad -\frac{a}{2} < x < \frac{a}{2}, \quad b \leq y \quad (3.145)$$

with α , β , γ_n to be determined.

Boundary conditions are now imposed. It follows

$$\frac{\partial A}{\partial x} = - \sum_{n=1}^{\infty} nk c_n \operatorname{sh}(nky) \sin(nkx) \quad (3.146)$$

and

$$\left. \frac{\partial A}{\partial x} \right|_{x=\pm \frac{a}{2}} = \mu \sum_{n=1}^{\infty} nk c_n \operatorname{sh}(nky) \sin\left(nk \frac{a}{2}\right) = 0 \quad (3.147)$$

which is true if $k = \frac{2\pi}{a}$, $c_n \neq 0$.

Moreover $A(x, 0) = 0$ is automatically fulfilled.

Finally, the asymptotic boundary condition states

$$\lim_{y \rightarrow \infty} B_x = B_0 \quad (3.148)$$

$$\lim_{y \rightarrow \infty} B_y = 0 \quad (3.149)$$

From (3.145), for $y > b$ and $-\frac{a}{2} < x < \frac{a}{2}$, one has

$$B_x = \frac{\partial \tilde{A}_L}{\partial y} = \beta - \sum_{n=1}^{\infty} nk \gamma_n e^{-nky} \cos(nkx) \quad (3.150)$$

and, because of (3.148), it results $\beta = B_0$.

In turn, one has

$$B_y = - \frac{\partial \tilde{A}_L}{\partial x} = \sum_{n=1}^{\infty} nk \gamma_n e^{-nky} \sin(nkx) \quad (3.151)$$

and (3.149) is always fulfilled, for $y \gg b$ and $-\frac{a}{2} < x < \frac{a}{2}$.

At $y = b$, the continuity of potential requires $A_L + A_P = \tilde{A}_L$ i.e.

$$-\frac{1}{2} \mu J b^2 + \sum_{n=1}^{\infty} c_n \operatorname{sh}(nkb) \cos(nkx) = \alpha + B_0 b + \sum_{n=1}^{\infty} \gamma_n e^{-nkb} \cos(nkx) \quad (3.152)$$

Moreover, the continuity of field components B_x and B_y requires

$$-\mu Jb + \sum_{n=1}^{\infty} nkc_n \operatorname{ch}(nkb) \cos(nkx) = B_0 - \sum_{n=1}^{\infty} nk\gamma_n e^{-nkb} \cos(nkx) \quad (3.153)$$

and

$$\sum_{n=1}^{\infty} nkc_n \operatorname{sh}(nkb) \sin(nkx) = \sum_{n=1}^{\infty} nk\gamma_n e^{-nkb} \sin(nkx) \quad (3.154)$$

respectively.

It follows

$$B_0 = -\mu Jb \quad (3.155)$$

$$\alpha = \frac{1}{2} \mu Jb^2 \quad (3.156)$$

$$\gamma_n = -c_n e^{nkb} \operatorname{ch}(nkb) = c_n e^{nkb} \operatorname{sh}(nkb) \quad (3.157)$$

One has $\gamma_n = c_n = 0$ if $nkb \neq 0$.

Therefore, one obtains

$$A = -\frac{1}{2} \mu Jy^2, \quad 0 \leq y \leq b \quad (3.158)$$

$$A = \mu Jb \left(\frac{b}{2} - y \right), \quad b \leq y \quad (3.159)$$

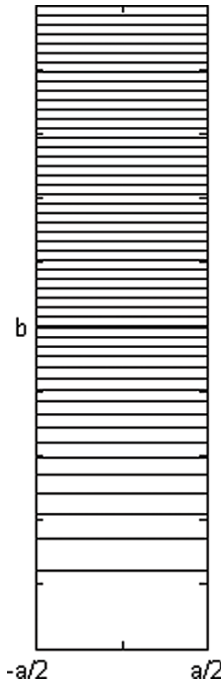


Fig. 3.21 Conductor in the slot: plot of flux lines

Correspondingly, the field components are

$$B_x = -\mu Jy, \quad 0 \leq y \leq b \quad (3.160)$$

$$B_x = -\mu Jb, \quad b \leq y \quad (3.161)$$

and $B_y = 0$ everywhere. Fig. 3.21 shows the plot of flux lines.

Chapter 4

Numerical Methods for Solving Boundary-Value Problems

4.1 Variational Formulation in Two-Dimensional Magnetostatics

Let the following magnetostatic boundary-value problem be considered

$$-\bar{\nabla} \cdot (\mu^{-1} \bar{\nabla} A) = J \text{ in } \Omega \quad (4.1)$$

$$A = 0 \text{ along } \Gamma_D \quad (4.2)$$

$$\frac{\partial A}{\partial n} = 0 \text{ along } \Gamma_N \quad (4.3)$$

where $\Gamma_D \cup \Gamma_N = \Gamma$ is the boundary of the two-dimensional simply-connected domain Ω , while A and μ are vector potential and magnetic permeability, respectively. Assuming rectangular coordinates, one has $\bar{A} = A\bar{i}_z$ and $\bar{J} = J\bar{i}_z$, whereas in cylindrical coordinates $\bar{A} = A\bar{i}_\varphi$ and $\bar{J} = J\bar{i}_\varphi$.

It is assumed that J and the second derivative of A are continuous in Ω so that the integral of both sides of (4.1) exists.

A way to approximate the solution to (4.1)–(4.3) is to relax the differential formulation of the boundary-value problem (weak formulation); to this end, the average of both sides of (4.1), weighted by a suitable test function, is considered. Accordingly, if u is a test function which is continuous up to its second derivative, from (4.1) one has

$$u(\bar{\nabla} \cdot (\mu^{-1} \bar{\nabla} A) + J) = 0 \quad (4.4)$$

and, by integrating over the domain, one gets

$$\int_{\Omega} u \bar{\nabla} \cdot (\mu^{-1} \bar{\nabla} A) d\Omega + \int_{\Omega} Ju d\Omega = 0 \quad (4.5)$$

Due to vector identity (A.14), taking $\varphi = u$ and $\bar{\nabla} = \mu^{-1} \bar{\nabla} A$, it follows

$$\int_{\Omega} \bar{\nabla} \cdot (u\mu^{-1} \bar{\nabla} A) d\Omega - \int_{\Omega} \bar{\nabla} u \cdot \mu^{-1} \bar{\nabla} A d\Omega + \int_{\Omega} Ju d\Omega = 0 \quad (4.6)$$

By applying Gauss's theorem one obtains

$$\begin{aligned} & \int_{\Gamma} u \mu^{-1} \bar{\nabla} A \cdot \bar{n} \, d\Gamma - \int_{\Omega} \bar{\nabla} u \cdot \mu^{-1} \bar{\nabla} A \, d\Omega + \int_{\Omega} J u \, d\Omega = \\ & = \int_{\Gamma_D} u \mu^{-1} \bar{\nabla} A \cdot \bar{n} \, d\Gamma + \int_{\Gamma_N} u \mu^{-1} \frac{\partial A}{\partial n} \, d\Gamma + \\ & - \int_{\Omega} \bar{\nabla} u \cdot \mu^{-1} \bar{\nabla} A \, d\Omega + \int_{\Omega} J u \, d\Omega = 0 \end{aligned} \quad (4.7)$$

Due to boundary conditions (4.2) and (4.3) the first two terms are zero; therefore, it results

$$- \int_{\Omega} \bar{\nabla} u \cdot \mu^{-1} \bar{\nabla} A \, d\Omega + \int_{\Omega} J u \, d\Omega = 0 \quad (4.8)$$

which is the variational equation associated to the differential equation (4.1).

Now, taking $u = \delta A$ where δA is the elementary variation of A , (4.8) becomes

$$- \int_{\Omega} \delta \bar{\nabla} A \cdot \mu^{-1} \bar{\nabla} A \, d\Omega + \int_{\Omega} J \delta A \, d\Omega = 0 \quad (4.9)$$

or, equivalently

$$\delta \left[\int_{\Omega} \left(\frac{1}{2\mu} \bar{\nabla} A \cdot \bar{\nabla} A - J A \right) d\Omega \right] = 0 \quad (4.10)$$

which states the necessary condition for A to be a steady point of the functional

$$\chi(A) = \int_{\Omega} \frac{1}{2\mu} \bar{\nabla} A \cdot \bar{\nabla} A \, d\Omega - \int_{\Omega} J A \, d\Omega \quad (4.11)$$

In other words, if A is a solution of differential equation (4.1) subject to (4.2) and (4.3), then A is a solution also of variational equation (4.10) and is such to give origin to a steady point of functional (4.11).

Conversely, having defined the energy functional of the simply connected domain Ω as

$$\chi = \int_{\Omega} \frac{1}{2\mu} \bar{\nabla} A \cdot \bar{\nabla} A \, d\Omega - \int_{\Omega} J A \, d\Omega \quad (4.12)$$

or, thanks to (2.15)

$$\chi = \int_{\Omega} \frac{1}{2\mu} \bar{\mathbf{B}} \cdot \bar{\mathbf{B}} \, d\Omega - \int_{\Omega} J A \, d\Omega \quad (4.13)$$

where

$$\bar{\mathbf{B}} = \left(\frac{\partial A}{\partial y}, -\frac{\partial A}{\partial x}, 0 \right) = (\bar{\nabla} A)^{\perp} \quad (4.14)$$

(see Section 2.3.2), equation (4.1) follows.

In fact, let the first-order variation $\delta\chi$ of functional χ , which represents minus the co-energy of the domain Ω for given current density (see Section 2.3.5), be considered. It results

$$\begin{aligned}\delta\chi &= \int_{\Omega} \frac{1}{2\mu} \delta(\bar{\nabla}A \cdot \bar{\nabla}A) d\Omega - \int_{\Omega} J\delta A d\Omega = \\ &= \int_{\Omega} \left[\frac{1}{2\mu} \bar{\nabla}(\delta A) \cdot \bar{\nabla}A + \frac{1}{2\mu} \bar{\nabla}A \cdot \bar{\nabla}(\delta A) \right] d\Omega - \int_{\Omega} J\delta A d\Omega = \quad (4.15) \\ &= \int_{\Omega} \mu^{-1} \bar{\nabla}A \cdot \bar{\nabla}(\delta A) d\Omega - \int_{\Omega} J\delta A d\Omega\end{aligned}$$

Due to (A.14) with $\varphi = \delta A$ and $\bar{\nabla} = \mu^{-1} \bar{\nabla}A$ one has

$$\delta\chi = \int_{\Omega} \bar{\nabla} \cdot (\delta A \mu^{-1} \bar{\nabla}A) d\Omega - \int_{\Omega} \delta A \bar{\nabla} \cdot (\mu^{-1} \bar{\nabla}A) d\Omega - \int_{\Omega} J\delta A d\Omega \quad (4.16)$$

Then, applying Gauss's theorem, it follows

$$\begin{aligned}\delta\chi &= \int_{\Gamma} \delta A \mu^{-1} \bar{\nabla}A \cdot \bar{n} d\Gamma - \int_{\Omega} \delta A (\bar{\nabla} \cdot \mu^{-1} \bar{\nabla}A + J) d\Omega = \\ &= \int_{\Gamma_D} \mu^{-1} \delta A \bar{\nabla}A \cdot \bar{n} d\Gamma + \int_{\Gamma_N} \mu^{-1} \delta A \frac{\partial A}{\partial n} d\Gamma - \int_{\Omega} \delta A (\bar{\nabla} \cdot \mu^{-1} \bar{\nabla}A + J) d\Omega\end{aligned} \quad (4.17)$$

If A fulfils (4.2) and (4.3), one has

$$\delta\chi = - \int_{\Omega} \delta A (\bar{\nabla} \cdot \mu^{-1} \bar{\nabla}A + J) d\Omega \quad (4.18)$$

Since the co-energy has a steady point when $\delta\chi = 0$, the Poisson's equation

$$\bar{\nabla} \cdot \mu^{-1} \bar{\nabla}A + J = 0 \quad (4.19)$$

is verified; (4.19) is called the Euler's equation associated to functional (4.12)

As a result, the equivalence between the search of a solution to Poisson's equation and the search of a steady point of an energy functional has been proven. The two approaches are known as Ritz's method and Galerkin's method, respectively.

According to the latter, a numerical procedure approximating the minimization of the energy functional is developed.

The following remarks are applicable:

- (i) Dirichlet's condition (4.2) is an essential boundary condition, because the value of A must be forced at least in a point of the boundary.
- (ii) Homogeneous Neumann's condition (4.3) is a natural boundary condition, because it is already taken into account both in (4.7) and (4.17).

4.2 Finite Elements for Two-Dimensional Magnetostatics

4.2.1 Discretization of Energy Functional

Let the following continuous problem be considered: find the steady point of $\chi(A)$, $A = \text{const.}$ along Γ_D , $\frac{\partial A}{\partial n} = 0$ along Γ_N , where

$$\chi(A) = \int_{\Omega} \frac{1}{2\mu} \left[\left(\frac{\partial A}{\partial x} \right)^2 + \left(\frac{\partial A}{\partial y} \right)^2 \right] d\Omega - \int_{\Omega} JA \, d\Omega \quad (4.20)$$

is the energy functional associated to a simply-connected domain Ω in which rectangular coordinates are assumed. In (4.20) it is supposed that A is continuous up to its first derivative, while J is assumed to be a continuous function.

Let Ω be discretized by means of a grid of triangular elements subject to the following constraints (Fig. 4.1):

- Two adjacent elements do not overlap
- No vertex of a triangle belongs to the edge of an adjacent triangle

The following discretization of problem (4.20) is introduced: find the steady point of $\chi(A)$ for the net of triangles of the grid, upon the condition that the restriction of potential A to an element of the given grid is represented by a linear polynomial and $A = \text{const.}$ along Γ_D , $\frac{\partial A}{\partial n} = 0$ along Γ_N . As a consequence, in the whole domain the potential A is approximated by a piecewise-linear function.

Given a numbering of grid nodes ($i = 1, 2, \dots, n$), the piecewise-linear functions

$$\begin{aligned} \psi_i(x, y) &= 1 \text{ at node } i = 1, n \\ \psi_j(x, y) &= 0 \text{ at all the other nodes } j = 1, n, j \neq i \end{aligned} \quad (4.21)$$

are called global shape functions (Fig. 4.2). A can be written as

$$A(x, y) = \sum_{i=1}^n \psi_i(x, y) A_i \quad (4.22)$$

where A_i is the unknown value of $A(x, y)$ at i th node and $A(x, y)$ varies linearly.

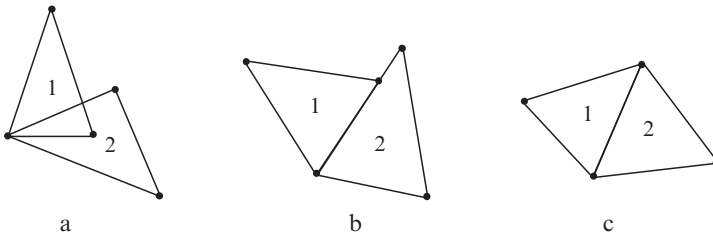


Fig. 4.1 Examples of incorrectly (a, b) and correctly (c) shaped triangles

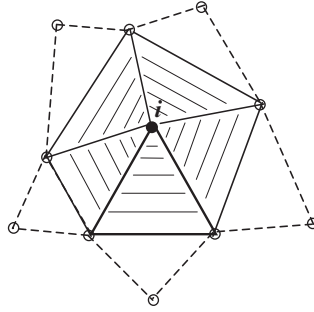


Fig. 4.2 Detail of a grid: representation of the global shape function associated to i th node. Shaded triangles show the linear variation of the function

After substituting (4.22) in (4.20) one obtains

$$\begin{aligned} \chi(A_1, A_2, \dots, A_n) = & \int_{\Omega} \frac{1}{2\mu} \left[\left(\sum_{i=1}^n A_i \frac{\partial \psi_i}{\partial x} \right)^2 + \left(\sum_{i=1}^n A_i \frac{\partial \psi_i}{\partial y} \right)^2 \right] d\Omega + \\ & - \int_{\Omega} J \sum_{i=1}^n A_i \psi_i d\Omega \end{aligned} \quad (4.23)$$

that represents the discrete version of (4.20).

In (4.23) the terms dependent on just A_i can be separated from those independent of A_i . Explicitly, one gets

$$\begin{aligned} \chi(A_1, A_2, \dots, A_n) = & A_i^2 \int_{\Omega} \frac{1}{2\mu} \left[\left(\frac{\partial \psi_i}{\partial x} \right)^2 + \left(\frac{\partial \psi_i}{\partial y} \right)^2 \right] d\Omega + \\ & + 2A_i \sum_{\substack{j=1 \\ j \neq i}}^n A_j \int_{\Omega} \frac{1}{2\mu} \left(\frac{\partial \psi_i}{\partial x} \frac{\partial \psi_j}{\partial x} + \frac{\partial \psi_i}{\partial y} \frac{\partial \psi_j}{\partial y} \right) d\Omega + \\ & - A_i \int_{\Omega} J \psi_i d\Omega - \sum_{\substack{k=1 \\ k \neq i}}^n A_k \int_{\Omega} J \psi_k d\Omega \end{aligned} \quad (4.24)$$

In order $A = (A_1, A_2, \dots, A_n)$ to make functional (4.23) steady, it must be

$$\frac{\partial \chi}{\partial A_i} = 0, \quad i = 1, 2, \dots, n \quad (4.25)$$

From (4.24) and (4.25) one obtains

$$\begin{aligned}
 & A_i \int_{\Omega} \mu^{-1} \left[\left(\frac{\partial \psi_i}{\partial x} \right)^2 + \left(\frac{\partial \psi_i}{\partial y} \right)^2 \right] d\Omega + \\
 & + \sum_{\substack{j=1 \\ j \neq i}}^n A_j \int_{\Omega} \mu^{-1} \left(\frac{\partial \psi_i}{\partial x} \frac{\partial \psi_j}{\partial x} + \frac{\partial \psi_i}{\partial y} \frac{\partial \psi_j}{\partial y} \right) d\Omega + \\
 & - \int_{\Omega} J \psi_i d\Omega = 0, \quad i = 1, 2, \dots, n
 \end{aligned} \tag{4.26}$$

It should be noted that (4.26) represents a linear system of n equations in n unknowns A_i . If the system is expressed in matrix form, the entries of the coefficient matrix $H(n, n)$ become

$$h_{ij} = \int_{\Omega} \frac{1}{\mu} \left(\frac{\partial \psi_i}{\partial x} \frac{\partial \psi_j}{\partial x} + \frac{\partial \psi_i}{\partial y} \frac{\partial \psi_j}{\partial y} \right) d\Omega, \quad i, j = 1, 2, \dots, n \tag{4.27}$$

while the entries of the source vector $d(n, 1)$ are

$$d_i = \int_{\Omega} J \psi_i d\Omega, \quad i = 1, 2, \dots, n \tag{4.28}$$

Then, system (4.26) can be written in matrix form as

$$H A = d \tag{4.29}$$

where $H(n, n)$ is the reluctance ($H^{-1} \text{ m}$) matrix, while $A(n, 1)$ and $d(n, 1)$ are nodal potential (Wb m^{-1}) and nodal current (A) vectors, respectively.

It is easy to realize that in (4.27) functions ψ_i, ψ_j can be interchanged, i.e. matrix H is symmetric. The problem of finding a steady point of functional (4.23) is then reduced to the solution of a linear system governed by matrix H and source term d .

It should be noted that system (4.29) is singular; in order its solution to be unique, it is necessary to fix the value of potential A of all n_D nodes where (4.2) holds; at least one node located along boundary Γ must be constrained.

4.2.2 Local Shape Functions in Rectangular Coordinates

Referring to a triangle of the grid, the following local shape functions

$$\begin{aligned}
 \psi_k(x, y) &= 1 \quad \text{at node } k = 1, 2, 3 \text{ anticlockwise} \\
 \psi_k(x, y) &= 0 \quad \text{at the other two nodes}
 \end{aligned} \tag{4.30}$$

with linear variation with respect to (x, y) can be introduced; they represent the restriction of (4.21) to node k of the triangle.

Referring to a triangle of vertices $V_1 = (x_1, y_1)$, $V_2 = (x_2, y_2)$, $V_3 = (x_3, y_3)$, the following functions

$$\begin{aligned}\psi_1(x, y) &= \frac{1}{2S} [(x_2y_3 - x_3y_2) + x(y_2 - y_3) + y(x_3 - x_2)] \\ \psi_2(x, y) &= \frac{1}{2S} [(x_3y_1 - x_1y_3) + x(y_3 - y_1) + y(x_1 - x_3)] \\ \psi_3(x, y) &= \frac{1}{2S} [(x_1y_2 - x_2y_1) + x(y_1 - y_2) + y(x_2 - x_1)]\end{aligned}\quad (4.31)$$

where

$$S = \frac{1}{2} \begin{vmatrix} 1 & x_1 & y_1 \\ 1 & x_2 & y_2 \\ 1 & x_3 & y_3 \end{vmatrix}\quad (4.32)$$

is the area of the triangle considered, are linear in both x and y . They fulfil conditions (4.30) and are the local shape functions. A geometric interpretation of (4.31) is given in Fig. 4.3.

Considering an inner point $V(x, y)$, the ratio

$$\frac{s}{h} = \frac{S_1}{S_1 + S_2 + S_3} = \frac{S_1}{S}\quad (4.33)$$

is called area coordinate ξ_1 referred to vertex 1; in general, area coordinates are defined as

$$\xi_k = \frac{S_k}{S}, \quad k = 1, 2, 3\quad (4.34)$$

The following properties hold

$$0 \leq \xi_k \leq 1, \quad \sum_{k=1}^3 \xi_k = 1, \quad k = 1, 2, 3\quad (4.35)$$

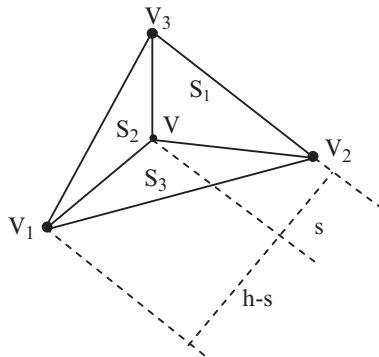


Fig. 4.3 Geometric interpretation of local shape functions

It can be proven that

$$\psi_k = \xi_k, \quad k = 1, 2, 3 \quad (4.36)$$

In fact, S_k is obtained by substituting vector $[1 \ x \ y]$ in the k th row of area matrix determinant (4.32); considering (4.34) and (4.31), (4.36) immediately follows.

Consequently, the restriction of potential $A(x, y)$ to the given triangle is

$$A(x, y) = \sum_{k=1}^3 \psi_k(x, y) A_k = [\psi_1(x, y) \ \psi_2(x, y) \ \psi_3(x, y)] \begin{bmatrix} A_1 \\ A_2 \\ A_3 \end{bmatrix} \quad (4.37)$$

where A_1, A_2, A_3 are the nodal values of potential in the triangle itself.

4.2.3 Coefficient Matrix and Source Vector

If (4.27) is applied to all the triangular elements composing the grid, the entry h_{ij} is the sum of the contributions of each element e

$$h_{ij} = \sum_e \int_e \mu^{-1} \left(\frac{\partial \psi_i}{\partial x} \frac{\partial \psi_j}{\partial x} + \frac{\partial \psi_i}{\partial y} \frac{\partial \psi_j}{\partial y} \right) dx \, dy, \quad i, j = 1, 2, \dots, n \quad (4.38)$$

where ψ_i, ψ_j are the global shape functions.

However, it is easily seen that the contribution of a triangle e to the integral in (4.38) is zero if either the i th or the j th node does not belong to triangle e itself. As a consequence, the majority of terms forming the integral is zero and the matrix is sparse.

In this respect, it is convenient to define the local coefficient matrix $H_e(3, 3)$ associated to a single triangle e having area S_e with entries

$$h_{k\lambda} = \int_e \mu^{-1} \left(\frac{\partial \psi_k}{\partial x} \frac{\partial \psi_\lambda}{\partial x} + \frac{\partial \psi_k}{\partial y} \frac{\partial \psi_\lambda}{\partial y} \right) dx \, dy, \quad k, \lambda = 1, 2, 3 \quad (4.39)$$

where ψ_k, ψ_λ are local shape functions.

From (4.31), by a cyclic permutation of indices, it results

$$\begin{aligned} \frac{\partial \psi_k}{\partial x} &= \frac{y_{k+1} - y_{k+2}}{2S_e} \equiv \frac{a_k}{2S_e} \\ \frac{\partial \psi_k}{\partial y} &= \frac{x_{k+2} - x_{k+1}}{2S_e} \equiv \frac{b_k}{2S_e} \end{aligned} \quad (4.40)$$

with $k = 1, 2, 3$ and $x_4 = x_1, x_5 = x_2, y_4 = y_1, y_5 = y_2$. The entries of the local coefficient matrix (4.39) are then given by

$$h_{k\lambda} = \int_e \left(\frac{a_k a_\lambda + b_k b_\lambda}{4\mu S_e^2} \right) dx \, dy = \frac{a_k a_\lambda + b_k b_\lambda}{4\mu S_e}, \quad k, \lambda = 1, 2, 3 \quad (4.41)$$

In practice, the entries of the global matrix are assembled starting from entries of local matrices, for the correspondence between local and global numbering of nodes is unique. The assembling rules will be clarified later on by means of an example.

In a similar way, it is possible to construct (4.28) by assembling local contributions; in fact

$$d_i = \int_{\Omega} J \psi_i d\Omega = \sum_e \int_e J \psi_k dx dy, \quad i = 1, 2, \dots, n, \quad k = 1, 2, 3 \quad (4.42)$$

The local source vector d_e associated to a single triangle e has entry

$$d_k = \int_e J \psi_k dx dy, \quad k = 1, 2, 3 \quad (4.43)$$

In particular, if current density J is assumed to be constant in the element considered, each local source term is equal to $\frac{JS_e}{3}$.

4.2.4 From Potential to Field

Assuming that the magnetic potential $A(x, y)$ is approximated by a linear polynomial on each element of the grid, if A_1, A_2, A_3 are the values of potential in vertices $V_1 = (x_1, y_1), V_2 = (x_2, y_2), V_3 = (x_3, y_3)$ of triangle e , respectively, the induction field $\vec{B} = (B_x, B_y, B_z)$ is approximated on each element by

$$\vec{B} = \left(\frac{\partial A}{\partial y}, -\frac{\partial A}{\partial x}, 0 \right) \quad (4.44)$$

From (4.32) and (4.37) it results

$$\begin{aligned} \begin{bmatrix} B_x \\ B_y \end{bmatrix} &= \frac{1}{2S_e} \begin{bmatrix} x_3 - x_2 & x_1 - x_3 & x_2 - x_1 \\ y_3 - y_2 & y_1 - y_3 & y_2 - y_1 \end{bmatrix} \begin{bmatrix} A_1 \\ A_2 \\ A_3 \end{bmatrix} = \\ &= \frac{1}{2S_e} \begin{bmatrix} b_1 & b_2 & b_3 \\ -a_1 & -a_2 & -a_3 \end{bmatrix} \begin{bmatrix} A_1 \\ A_2 \\ A_3 \end{bmatrix} \end{aligned} \quad (4.45)$$

Apparently, matrix

$$\frac{1}{2S_e} \begin{bmatrix} b_1 & b_2 & b_3 \\ -a_1 & -a_2 & -a_3 \end{bmatrix} \quad (4.46)$$

approximates the curl operator.

The following remark can be put forward. At the interface between two triangles, having an edge in common, both normal component B_n of induction field and tangential component of magnetic field $H_t = \mu^{-1}B_t$ are not continuous. In other words, field components are approximated by means of piecewise constant functions all over the domain.

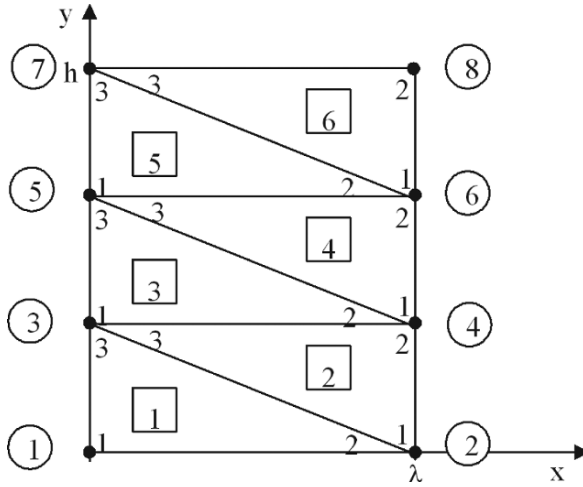


Fig. 4.4 Grid discretizing a half-slot

4.2.5 Magnetic Field in a Slot Solved by the Finite Element Method

Let the test problem shown in Fig. 2.13a be considered. The rectangular domain corresponding to half a slot is discretized by means of six triangular elements numbered, for instance, as shown in Fig. 4.4. The n nodes are numbered from 1 to 8 arbitrarily within the grid and from 1 to 3 (anticlockwise) inside each triangle.

According to (4.41), the coefficient matrix associated to a triangle e having vertices $V_1 = (x_1, y_1)$, $V_2 = (x_2, y_2)$ and $V_3 = (x_3, y_3)$ results

$$H_e = \frac{1}{4\mu S} \begin{bmatrix} (y_2 - y_3)^2 + (x_3 - x_2)^2 & (y_2 - y_3)(y_3 - y_1) + (x_3 - x_2)(x_1 - x_3) & (y_2 - y_3)(y_1 - y_2) + (x_3 - x_2)(x_2 - x_1) \\ & (y_3 - y_1)^2 + (x_1 - x_3)^2 & (y_3 - y_1)(y_1 - y_2) + (x_1 - x_3)(x_2 - x_1) \\ \text{symmetric} & & (y_1 - y_2)^2 + (x_2 - x_1)^2 \end{bmatrix} \quad (4.47)$$

where μ and S are magnetic permeability and area of the triangle, respectively.

For element 1, given height h and half-width λ of the slot, one has $V_1 = (0, 0)$, $V_2 = (\lambda, 0)$, $V_3 = (0, \frac{h}{3})$ and the local coefficient matrix is:

$$H_1 = \frac{1}{4\mu S} \begin{bmatrix} \frac{h^2}{9} + \lambda^2 & -\frac{h^2}{9} & -\lambda^2 \\ & \frac{h^2}{9} & 0 \\ \text{symm.} & & \lambda^2 \end{bmatrix} \quad (4.48)$$

Analogously, for element 2, one has $V_1 = (\lambda, 0)$, $V_2 = (\lambda, \frac{h}{3})$, $V_3 = (0, \frac{h}{3})$ and the local coefficient matrix is:

$$H_2 = \frac{1}{4\mu S} \begin{bmatrix} \lambda^2 & -\lambda^2 & 0 \\ & \frac{h^2}{9} + \lambda^2 & -\frac{h^2}{9} \\ \text{symm.} & & \frac{h^2}{9} \end{bmatrix} \quad (4.49)$$

From Fig. 4.4 it can be noted that elements 3 and 5 correspond to element 1 and keep the same local numbering of nodes as in element 1. The same happens for elements 4 and 6 with respect to element 2. Therefore, it results: $H_3 = H_1$ and $H_5 = H_1$; $H_4 = H_2$ and $H_6 = H_2$.

Supposing current density J is uniform, local source terms are all equal to $\frac{JS}{3}$ in each triangle and

$$d_e = \frac{JS}{3} \begin{bmatrix} 1 \\ 1 \\ 1 \end{bmatrix} \quad (4.50)$$

In general, the global coefficient matrix H can be assembled node by node according to the following rule:

- Diagonal terms h_{ii} are obtained as the sum of the corresponding terms of local matrices of all triangles having i th node in common
- Off-diagonal terms h_{ij} are obtained by summing the corresponding terms of local matrices of the two triangles sharing the edge between i th node and j th node

For instance, global node 1 belongs to element 1 only, corresponding to local node 1; therefore $H(1, 1) = H_1(1, 1)$. Moreover, global node 2 is in common between elements 1 and 2 for which it corresponds to local nodes 2 and 1, respectively; therefore $H(2, 2) = H_1(2, 2) + H_2(1, 1)$. Going on, global node 3 is in common among elements 1, 2, 3 where it corresponds to local nodes 3, 3, 1 respectively; therefore $H(3, 3) = H_1(3, 3) + H_2(3, 3) + H_3(1, 1)$.

Passing to off-diagonal terms, for the sake of an example, the edge joining global node 3 to global node 4 is in common between elements 2 and 3; moreover, global node 4 corresponds to local node 2 in both elements 2 and 3; therefore one has $H(3, 4) = H_2(2, 3) + H_3(1, 2) = H(4, 3)$.

By iterating the assembling algorithm on all global nodes, finally it results:

$$H = \frac{1}{4\mu S} \begin{bmatrix} \frac{h^2}{9} + \lambda^2 & -\frac{h^2}{9} & -\lambda^2 & 0 & 0 & 0 & 0 & 0 \\ & \frac{h^2}{9} + \lambda^2 & 0 & -\lambda^2 & 0 & 0 & 0 & 0 \\ & & 2\frac{h^2}{9} + 2\lambda^2 & -2\frac{h^2}{9} & -\lambda^2 & 0 & 0 & 0 \\ & & & 2\frac{h^2}{9} + 2\lambda^2 & 0 & -\lambda^2 & 0 & 0 \\ & & & & 2\frac{h^2}{9} + 2\lambda^2 & -2\frac{h^2}{9} & -\lambda^2 & 0 \\ & & & & & 2\frac{h^2}{9} + 2\lambda^2 & 0 & -\lambda^2 \\ & & & & & & \frac{h^2}{9} + \lambda^2 & -\frac{h^2}{9} \\ \text{symmetric} & & & & & & & \frac{h^2}{9} + \lambda^2 \end{bmatrix} \quad (4.51)$$

It can be noted that H is sparse and has a bandwidth that depends on the global numbering of the grid nodes; moreover, it exhibits diagonal-dominance, in fact $H(i, i) \geq \sum_{j=i+1}^n |H(i, j)|$, $i = 1, n - 1$. By assembling local contributions node by node, the source vector $d(n, 1)$ is obtained:

$$d = \frac{JS}{3} [1 \ 2 \ 3 \ 3 \ 3 \ 2 \ 1]^T \tag{4.52}$$

In this way, the solving system (4.29) results.

In order matrix $H(n, n)$ to be non-singular, the boundary condition of Dirichlet's type should be imposed in at least one node. In the test problem: $A_1 = A_2 = 0$. In order to fulfil $A_1 = 0$, the first row and the first column of H are cancelled, while to fulfil $A_2 = 0$ the second row and the second column of H are cancelled, so obtaining a matrix $H'(n - 2, n - 2)$ that is non-singular. Correspondingly, the first and the second terms of source vector are cancelled, obtaining a vector $d'(n - 2, 1)$. Finally, the reduced algebraic system comes out

$$H'A' = d' \tag{4.53}$$

with

$$H' = \frac{1}{4\mu S} \begin{bmatrix} 2\frac{h^2}{9} + 2\lambda^2 & -2\frac{h^2}{9} & -\lambda^2 & 0 & 0 & 0 \\ & 2\frac{h^2}{9} + 2\lambda^2 & 0 & -\lambda^2 & 0 & 0 \\ & & 2\frac{h^2}{9} + 2\lambda^2 & -2\frac{h^2}{9} & -\lambda^2 & 0 \\ & & & 2\frac{h^2}{9} + 2\lambda^2 & 0 & -\lambda^2 \\ & \text{symmetric} & & & \frac{h^2}{9} + \lambda^2 & -\frac{h^2}{9} \\ & & & & & \frac{h^2}{9} + \lambda^2 \end{bmatrix} \tag{4.54}$$

and

$$d' = \frac{JS}{3} [3 \ 3 \ 3 \ 3 \ 2 \ 1]^T \tag{4.55}$$

It should be noted that matrix H' is better conditioned than matrix H owing to the specification of boundary condition of the Dirichlet's kind.

More generally, when the potential A_k to be imposed in the k th node is different from zero, one should proceed as follows:

- Set $H(k, j) = 0$, $j = 1, n, j \neq k$
- Set $H(i, k) = 0$, $i = 1, n, i \neq k$
- Leave $H(k, k)$ unaltered
- Replace d_k with $H(k, k)A_k$
- Replace d_i with $d_i - H(i, k)A_k$, $i = 1, n, i \neq k$.

The sizes of matrix H and vector d remain unchanged.

A few physical remarks are worth being considered. The elements of system matrix, measured in $[H^{-1}m]$, depend on geometry and material property. In turn, the

source term J_S , measured in [A], can be regarded as the current attributed to element e while $\frac{J_S}{3}$ represents the nodal current.

From the numerical viewpoint, the following data are assumed: $h = 6 \text{ cm}$, $\lambda = 1 \text{ cm}$, $\mu = 1.25610^{-6} \text{ H m}^{-1}$, $J = 10^5 \text{ A m}^{-2}$.

All triangles have surface area $S = 1 \text{ cm}^2$. Considering these data, the condition number of H is $4.5594 \cdot 10^{16}$, while that of H' is 120. Matrix H' is definite positive; therefore, the solution of the linear system is unique. The solution of the reduced system (4.54)–(4.55) is

$$\begin{bmatrix} A_3 \\ A_4 \\ A_5 \\ A_6 \\ A_7 \\ A_8 \end{bmatrix} = 10^{-3} \begin{bmatrix} 0.1256 \\ 0.1256 \\ 0.2010 \\ 0.2009 \\ 0.2270 \\ 0.2251 \end{bmatrix} \left(\frac{\text{Wb}}{\text{m}} \right) \quad (4.56)$$

Calculation of the induction field

Knowing node potentials, the components of induction field (Wb m^{-2}) can be obtained applying (4.45) element by element. To this end, the correspondence between local and global numbering of nodes, shown in Table 4.1, should be taken into account.

Element 1

$$\begin{aligned} \begin{bmatrix} B_x \\ B_y \end{bmatrix} &= \frac{1}{2S} \begin{bmatrix} -\lambda & 0 & \lambda \\ \frac{h}{3} & -\frac{h}{3} & 0 \end{bmatrix} \begin{bmatrix} A_1 \\ A_2 \\ A_3 \end{bmatrix} = 10^{-3} \begin{bmatrix} -50 & 0 & 50 \\ 100 & -100 & 0 \end{bmatrix} \begin{bmatrix} 0 \\ 0 \\ 0.1256 \end{bmatrix} \\ &= 10^{-3} \begin{bmatrix} 6.2801 \\ 0 \end{bmatrix} \end{aligned}$$

Element 2

$$\begin{bmatrix} B_x \\ B_y \end{bmatrix} = \frac{1}{2S} \begin{bmatrix} -\lambda & \lambda & 0 \\ 0 & -\frac{h}{3} & \frac{h}{3} \end{bmatrix} \begin{bmatrix} A_2 \\ A_4 \\ A_3 \end{bmatrix} = 10^{-3} \begin{bmatrix} -50 & 50 & 0 \\ 0 & -100 & 100 \end{bmatrix} \begin{bmatrix} 0 \\ 0.1256 \\ 0.1256 \end{bmatrix}$$

Table 4.1 Correspondence between local and global nodes

Element	Local nodes	Global nodes
1	1, 2, 3	1, 2, 3
2	1, 2, 3	2, 4, 3
3	1, 2, 3	3, 4, 5
4	1, 2, 3	4, 6, 5
5	1, 2, 3	5, 6, 7
6	1, 2, 3	6, 8, 7

$$= 10^{-3} \begin{bmatrix} 6.2799 \\ 0 \end{bmatrix}$$

Element 3

$$\begin{bmatrix} B_x \\ B_y \end{bmatrix} = \frac{1}{2S} \begin{bmatrix} -\lambda & 0 & \lambda \\ \frac{h}{3} & -\frac{h}{3} & 0 \end{bmatrix} \begin{bmatrix} A_3 \\ A_4 \\ A_5 \end{bmatrix} = 10^{-3} \begin{bmatrix} -50 & 0 & 50 \\ 100 & -100 & 0 \end{bmatrix} \begin{bmatrix} 0.1256 \\ 0.1256 \\ 0.2010 \end{bmatrix} \\ = 10^{-3} \begin{bmatrix} 3.7705 \\ 0 \end{bmatrix}$$

Element 4

$$\begin{bmatrix} B_x \\ B_y \end{bmatrix} = \frac{1}{2S} \begin{bmatrix} -\lambda & \lambda & 0 \\ 0 & -\frac{h}{3} & \frac{h}{3} \end{bmatrix} \begin{bmatrix} A_4 \\ A_6 \\ A_5 \end{bmatrix} = 10^{-3} \begin{bmatrix} -50 & 50 & 0 \\ 0 & -100 & 100 \end{bmatrix} \begin{bmatrix} 0.1256 \\ 0.2009 \\ 0.2010 \end{bmatrix} \\ = 10^{-3} \begin{bmatrix} 3.7655 \\ 1.043410^{-2} \end{bmatrix}$$

Element 5

$$\begin{bmatrix} B_x \\ B_y \end{bmatrix} = \frac{1}{2S} \begin{bmatrix} -\lambda & 0 & \lambda \\ \frac{h}{3} & -\frac{h}{3} & 0 \end{bmatrix} \begin{bmatrix} A_5 \\ A_6 \\ A_7 \end{bmatrix} = 10^{-3} \begin{bmatrix} -50 & 0 & 50 \\ 100 & -100 & 0 \end{bmatrix} \begin{bmatrix} 0.2010 \\ 0.2009 \\ 0.2270 \end{bmatrix} \\ = 10^{-3} \begin{bmatrix} 1.3002 \\ 1.043410^{-2} \end{bmatrix}$$

Element 6

$$\begin{bmatrix} B_x \\ B_y \end{bmatrix} = \frac{1}{2S} \begin{bmatrix} -\lambda & \lambda & 0 \\ 0 & -\frac{h}{3} & \frac{h}{3} \end{bmatrix} \begin{bmatrix} A_6 \\ A_8 \\ A_7 \end{bmatrix} = 10^{-3} \begin{bmatrix} -50 & 50 & 0 \\ 0 & -100 & 100 \end{bmatrix} \begin{bmatrix} 0.2009 \\ 0.2251 \\ 0.2270 \end{bmatrix} \\ = 10^{-3} \begin{bmatrix} 1.2118 \\ 1.872310^{-1} \end{bmatrix}$$

Finally, it results

$$\begin{bmatrix} B_{1x} \\ B_{2x} \\ B_{3x} \\ B_{4x} \\ B_{5x} \\ B_{6x} \end{bmatrix} = 10^{-3} \begin{bmatrix} 6.2801 \\ 6.2799 \\ 3.7705 \\ 3.7655 \\ 1.3002 \\ 1.2118 \end{bmatrix}; \quad \begin{bmatrix} B_{1y} \\ B_{2y} \\ B_{3y} \\ B_{4y} \\ B_{5y} \\ B_{6y} \end{bmatrix} = 10^{-6} \begin{bmatrix} 0 \\ 0 \\ 0 \\ 10.434 \\ 10.434 \\ 187.23 \end{bmatrix} \quad (4.57)$$

It should be remarked that in odd elements the value of B_y depends on $A_1 - A_2$ and symmetry implies $A_1 = A_2$ (indexes 1 and 2 refer to the local numbering); in an analogous way, in even elements the value of B_y depends on $-A_2 + A_3$ and symmetry implies $A_2 = A_3$ (indexes 2 and 3 refer to the local numbering). Residuals of B_y are due to approximation error in computing potentials.

Table 4.2 Distribution of nodal error (Fig. 4.4)

Node	3	4	5	6	7	8
Y coordinate	0.02		0.04		0.06	
E_i	-2.3076 10^{-5}	2.3076 10^{-5}	-2.5961 10^{-4}	2.5961 10^{-4}	-4.1409 10^{-3}	4.1409 10^{-3}

Error analysis

The test problem has an exact analytical solution, namely

$$A = \mu J \left(hy - \frac{1}{2}y^2 \right) \quad (4.58)$$

$$(B_x, B_y) = (\mu J (h - y), 0) \quad (4.59)$$

such that $A = 0$ at $y = 0$ and $0 < y < h$.

As far as potential is concerned, the local error

$$E_i = 1 - \frac{A(i)}{A_i}, \quad i = 3, 8 \quad (4.60)$$

can be defined, where $A(i)$ and A_i are approximated and exact values of potential at the i th node, respectively. The distribution of error is reported in Table 4.2.

It can be noted that the local error increases with the distance from constrained nodes 1, 2; moreover, the potential is overestimated at the left-boundary nodes ($x = 0$) and underestimated at the right-boundary nodes ($x = \lambda$).

In order to test the effect of grid on accuracy, the following norms are introduced

$$\|f\|_2 = \sqrt{\sum_{i=3}^{n_p} [f(i)]^2} \quad (4.61)$$

and

$$\|f\|_\infty = \max_{i=3, n_p} \{f(i)\} \quad (4.62)$$

with $n_p = 8$ grid nodes.

In terms of the residual it results

$$f(i) = \left| 1 - \frac{A_g(i)}{A_i} \right| \quad (4.63)$$

where A_g is the approximated value of potential computed using grid g while A_i is the exact one.

Having fixed the size of the slot, the test problem can be solved using grids with an increasing number of triangular elements.

Table 4.3 Error norms

No. of elements	6	30	46	330	1210
$\ f\ _2$	$0.286 \cdot 10^{-2}$	$0.160 \cdot 10^{-2}$	$0.441 \cdot 10^{-3}$	$0.233 \cdot 10^{-3}$	$0.140 \cdot 10^{-3}$
$\ f\ _\infty$	$0.414 \cdot 10^{-2}$	$0.200 \cdot 10^{-2}$	$0.504 \cdot 10^{-3}$	$0.252 \cdot 10^{-3}$	$0.168 \cdot 10^{-3}$

Table 4.4 Error on elements (coarsest grid)

Element	1	2	3	4	5	6
E_e	0.0624784	-0.0714038	0.0994116	-0.1242645	0.2236068	-0.4472136

The results obtained using different grids give rise to the error norms reported in Table 4.3; the latter decrease monotonically with the number of elements. In particular, $\|f\|_2$ and $\|f\|_\infty$ give a measurement of average and maximum error, respectively.

In turn, the error in terms of x component of induction field can be defined, in each element, as follows

$$E_e = 1 - \frac{B_e}{B} \quad (4.64)$$

where B_e and B are approximated and exact value of the x component of the induction field, respectively; the exact value is that referred to the gravity centre of the element. In Table 4.4 the distribution of error is reported, referring to the coarsest grid composed of six elements.

Again, it can be noted that the error increases as long as the distance from constrained nodes increases.

Finally, Fig. 4.5 shows the plot of flux lines. The results have been obtained using a grid composed of 736 triangles with linear variation of potential.

Remarks on the topology of the grid

From Table 4.2 it can be remarked that the approximated values of potential in the left boundary nodes are greater than the values of corresponding right boundary nodes. This discrepancy can be attributed to the grid asymmetry. In fact, let a new grid be considered, as the mirror-image with respect to the previous one; it is shown in Fig. 4.6.

The coefficient matrices of elements 1 and 2 are

$$H_1 = \frac{1}{4\mu S} \begin{bmatrix} \frac{h^2}{9} & -\frac{h^2}{9} & 0 \\ \text{symm.} & \frac{h^2}{9} + \lambda^2 & -\lambda^2 \\ & & \lambda^2 \end{bmatrix} \quad (4.65)$$

$$H_2 = \frac{1}{4\mu S} \begin{bmatrix} \lambda^2 & 0 & -\lambda^2 \\ \text{symm.} & \frac{h^2}{9} & -\frac{h^2}{9} \\ & & \frac{h^2}{9} + \lambda^2 \end{bmatrix} \quad (4.66)$$

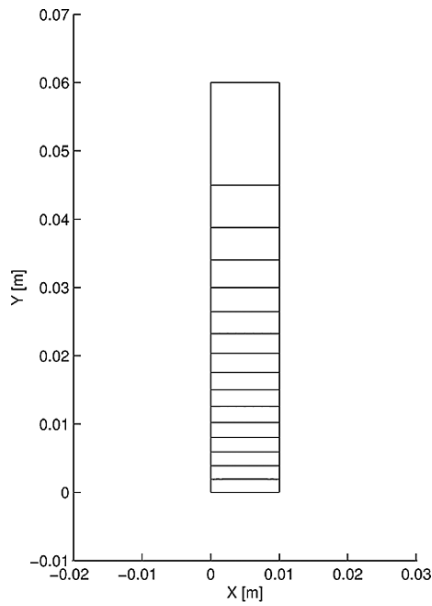


Fig. 4.5 Open slot: plot of flux lines

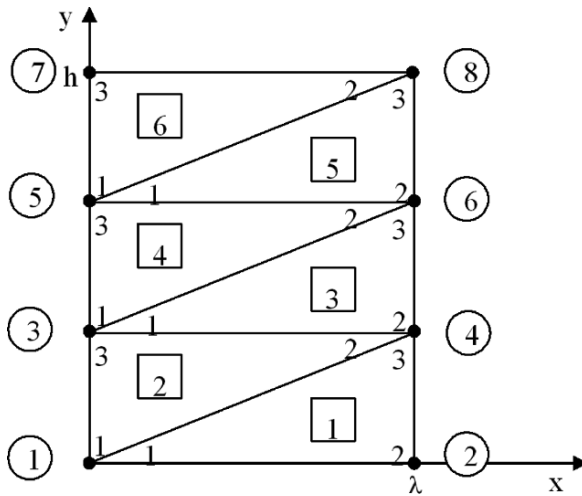


Fig. 4.6 Right-oriented grid discretizing half a slot

respectively. Keeping the same local numbering of nodes, one has $H_3 = H_1$ and $H_5 = H_1$; $H_4 = H_2$ and $H_6 = H_2$. In turn, local source terms are equal in all the elements

$$d_1 = d_2 = d_3 = d_4 = d_5 = d_6 = \frac{1}{3}JS \quad (4.67)$$

By assembling local coefficient matrices and source vectors the system

$$H^* A^* = d^* \tag{4.68}$$

with

$$d^* = \frac{JS}{3} (2, 1, 3, 3, 3, 3, 1, 2)^T \tag{4.69}$$

results. It can be remarked that H^* is the same as H in the previous case (4.51); in turn, d^* has first and second elements exchanged with respect to d , next-to-the-last and last elements exchanged as well, the other four components being unmodified.

After imposing boundary conditions in nodes 1 and 2 and introducing numerical data, the non-singular system

$$310^5 \begin{bmatrix} 1.9904 & -1.5924 & -0.1990 & 0 & 0 & 0 & & \\ & 1.9904 & 0 & -0.1990 & 0 & 0 & & \\ & & 1.9904 & -1.5924 & -0.1990 & 0 & & \\ & & & 1.9904 & 0 & -0.1990 & & \\ & \text{symmetric} & & & 0.9952 & -0.7962 & & \\ & & & & & 0.9952 & & \end{bmatrix} \begin{bmatrix} A_3 \\ A_4 \\ A_5 \\ A_6 \\ A_7 \\ A_8 \end{bmatrix} = \begin{bmatrix} 3 \\ 3 \\ 3 \\ 3 \\ 1 \\ 2 \end{bmatrix} \tag{4.70}$$

is obtained, the solution of which is

$$\begin{bmatrix} A_3 \\ A_4 \\ A_5 \\ A_6 \\ A_7 \\ A_8 \end{bmatrix} = 10^{-3} \begin{bmatrix} 0.1255 \\ 0.1256 \\ 0.2009 \\ 0.2010 \\ 0.2251 \\ 0.2270 \end{bmatrix} \left(\frac{Wb}{m} \right) \tag{4.71}$$

The mirror-like aspect of the grid gives rise to the exchange of two pairs of components of the source vector.

As shown in Table 4.5, this exchange has the final effect of making the potentials at right-boundary nodes overestimated with respect to the corresponding potentials at left-boundary nodes.

Table 4.5 Distribution of nodal error (Fig. 4.6)

Node	3	4	5	6	7	8
Y coordinate	0.02		0.04		0.06	
E_i	$3076 \cdot 10^{-5}$	$-2.3076 \cdot 10^{-5}$	$2.5961 \cdot 10^{-4}$	$-2.5961 \cdot 10^{-4}$	$4.1409 \cdot 10^{-3}$	$-4.1409 \cdot 10^{-3}$

4.3 Finite Elements for Three-Dimensional Magnetostatics

4.3.1 Surface and Solid Modelling

Generally, the three-dimensional model of an object can be built by means of either of two techniques: surface modelling and solid modelling, respectively.

According to the former, given a rectangular reference system, the orthogonal projection of the given object onto one of the three coordinate planes (Oxy , Oyz , Oxz) defines the base plane, which is then extruded to form volumes. Subsequently, the finite-element mesh is generated in two steps: first, a surface mesh is created in the base plane, using triangles or quadrilateral elements; next, the volume mesh follows, based on tetrahedrons or prisms, if the surface mesh is composed of triangles, or on hexahedral elements, otherwise.

In turn, solid modelling uses three-dimensional elementary volumes and Boolean operations to build the model of the object. This technique allows generating an object through operations such as transformations and combinations. Basic elements are parallelepipeds, cylinders, discs, spheres, cones, pyramids and toroids; they can be generated at any point and then combined. Using Boolean operators, basic elements can also be merged, intersected or subtracted to model complex geometries. Finally, the finite-element mesh is generated, based on either tetrahedra or hexahedra or prismatic elements.

4.3.2 Local Shape Functions in Rectangular Coordinates

The extension of the results of Section 4.2 to the three-dimensional case can be easily obtained.

Let the domain Ω be discretised by means of a grid of tetrahedral elements, such that:

- Two adjacent elements do not overlap
- No vertex of a tetrahedron belongs to either the face or the edge of an adjacent tetrahedron

Moreover, let the magnetic potential be approximated by means of a linear polynomial within the element.

For the sake of simplicity, only the case of a source-free simply-connected field region is considered; consequently, the scalar magnetic potential $\phi(x, y, z)$ can be used (see 2.212).

Referring to a tetrahedron of vertices $v_i = (x_i, y_i, z_i)$ $i = 1, 4$, the following functions

$$\psi_i(x, y, z) = \frac{\det(C_i)}{\det(C)}, \quad i = 1, 4 \quad (4.72)$$

can be defined, where

$$\det(C) = \begin{vmatrix} 1 & x_1 & y_1 & z_1 \\ 1 & x_2 & y_2 & z_2 \\ 1 & x_3 & y_3 & z_3 \\ 1 & x_4 & y_4 & z_4 \end{vmatrix} = 6V \tag{4.73}$$

In (4.73) V is the volume of the given tetrahedron, $\det(C)$ is constant while

$$\begin{aligned} \det(C_1) &= \begin{vmatrix} 1 & x & y & z \\ 1 & x_2 & y_2 & z_2 \\ 1 & x_3 & y_3 & z_3 \\ 1 & x_4 & y_4 & z_4 \end{vmatrix}, & \det(C_2) &= \begin{vmatrix} 1 & x_1 & y_1 & z_1 \\ 1 & x & y & z \\ 1 & x_3 & y_3 & z_3 \\ 1 & x_4 & y_4 & z_4 \end{vmatrix} \\ \det(C_3) &= \begin{vmatrix} 1 & x_1 & y_1 & z_1 \\ 1 & x_2 & y_2 & z_2 \\ 1 & x & y & z \\ 1 & x_4 & y_4 & z_4 \end{vmatrix}, & \det(C_4) &= \begin{vmatrix} 1 & x_1 & y_1 & z_1 \\ 1 & x_2 & y_2 & z_2 \\ 1 & x_3 & y_3 & z_3 \\ 1 & x & y & z \end{vmatrix} \end{aligned} \tag{4.74}$$

are linear functions of the coordinates (x, y, z) of a point P inside the tetrahedron.

A straightforward geometric interpretation in terms of volume coordinates is possible (Fig. 4.7); in fact, the denominator of (4.72) is proportional to the volume of the given tetrahedron, while the numerator is proportional to the volume of another tetrahedron, included into the given one and having the i th vertex coincident with point $P(x, y, z)$.

It is easy to prove that $0 \leq \psi_k \leq 1$, $k = 1, 4$ and $\sum_{k=1}^4 \psi_k(x, y, z) = 1$. Consequently, (4.72) can be assumed as the local shape functions.

In turn, the restriction of potential $\phi(x, y, z)$ to the tetrahedron is

$$\begin{aligned} \phi(x, y, z) &= \sum_{k=1}^4 \psi_k(x, y, z) \phi_k \\ &= [\psi_1(x, y, z) \ \psi_2(x, y, z) \ \psi_3(x, y, z) \ \psi_4(x, y, z)] \begin{bmatrix} \phi_1 \\ \phi_2 \\ \phi_3 \\ \phi_4 \end{bmatrix} \end{aligned} \tag{4.75}$$

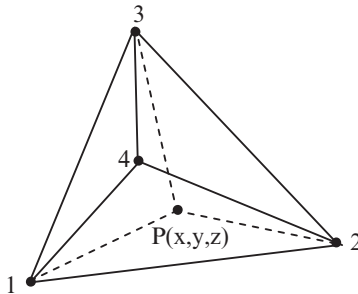


Fig. 4.7 Geometric interpretation of 3D local shape functions

where $(\phi_1, \phi_2, \phi_3, \phi_4)$ are the nodal values of the potential at the vertices $V_i = (x_i, y_i, z_i)$, $i = 1, 4$ of tetrahedron.

The coefficient matrix and source vector are formed and assembled like in Sections 4.2.3 and 4.2.5, respectively.

A similar procedure applies when passing from the potential to the induction field $\bar{B} = (B_x, B_y, B_z)$ which is approximated on each element by

$$\bar{B} = -\mu \left(\frac{\partial \phi}{\partial x}, \frac{\partial \phi}{\partial y}, \frac{\partial \phi}{\partial z} \right) \quad (4.76)$$

From (4.72) and (4.75) it follows

$$\begin{bmatrix} B_x \\ B_y \\ B_z \end{bmatrix} = -\mu \begin{bmatrix} \frac{\partial \psi_1}{\partial x} & \frac{\partial \psi_2}{\partial x} & \frac{\partial \psi_3}{\partial x} & \frac{\partial \psi_4}{\partial x} \\ \frac{\partial \psi_1}{\partial y} & \frac{\partial \psi_2}{\partial y} & \frac{\partial \psi_3}{\partial y} & \frac{\partial \psi_4}{\partial y} \\ \frac{\partial \psi_1}{\partial z} & \frac{\partial \psi_2}{\partial z} & \frac{\partial \psi_3}{\partial z} & \frac{\partial \psi_4}{\partial z} \end{bmatrix} \begin{bmatrix} \phi_1 \\ \phi_2 \\ \phi_3 \\ \phi_4 \end{bmatrix} \quad (4.77)$$

where μ is the element permeability.

Since (4.72) are linear in (x, y, z) , each entry in the gradient matrix above is constant; therefore, the induction field in the domain Ω is approximated by means of a piecewise-constant function.

4.3.3 Comparison of 2D and 3D Simulations of an Electromagnet

Let the electromagnet discussed in Section 2.3.6 be considered again. The magnetic field is here computed by means of the finite-element method, based on both two-dimensional and three-dimensional models.

In Fig. 4.8 the two-dimensional mesh of the electromagnet is represented, for an air-gap $t = 1$ mm wide; the mesh is composed of 4,500 triangles, approximately. The resulting vector plot of the induction field is represented in Fig. 4.9; the air-gap

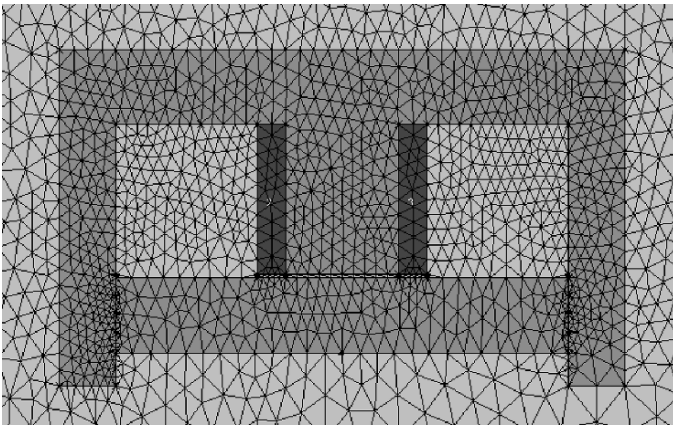


Fig. 4.8 2D finite-element mesh of the electromagnet ($t = 1$ mm)

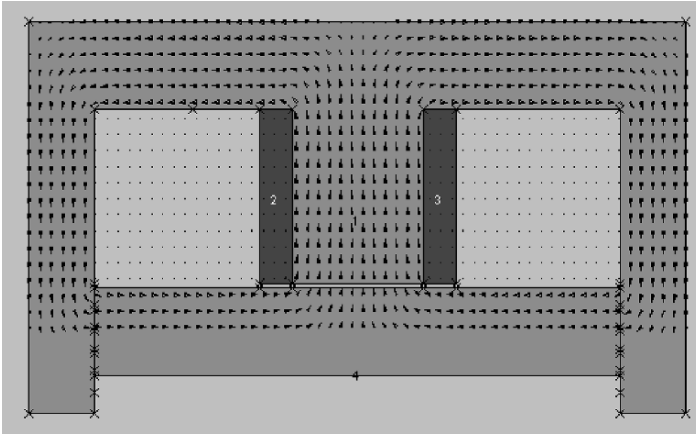


Fig. 4.9 Vector plot of magnetic induction ($t = 1$ mm)

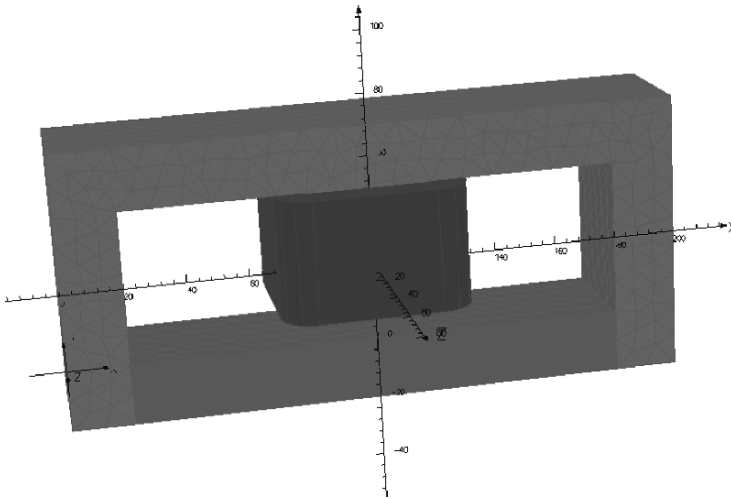


Fig. 4.10 3D finite-element mesh of the electromagnet ($t = 10$ mm)

width is comparable with the linear size of the central limb and a consequent leakage field can be noted.

Using the solid modelling technique, the model shown in Fig. 4.10 is obtained. From this model a three-dimensional mesh composed of about 250,000 tetrahedra has been generated. The depth of the magnetic core, in particular, has been taken equal to the square root of the cross-section of the central limb (30 mm).

The corresponding plot of computed vectors is shown in Fig. 4.11.

The force acting on the movable part of the electromagnet is computed too, by means of the Maxwell's stress tensor. A surface embedding the movable core is taken as the integration surface. The two models can be compared: in Fig. 4.12 the forces vs air-gap curves are shown for both two- and three-dimensional models.

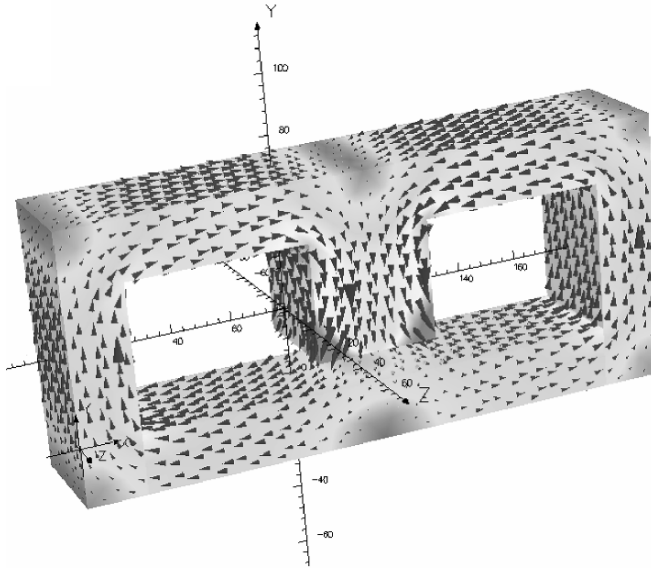


Fig. 4.11 Vector plot of magnetic induction ($t = 10$ mm, winding not shown)

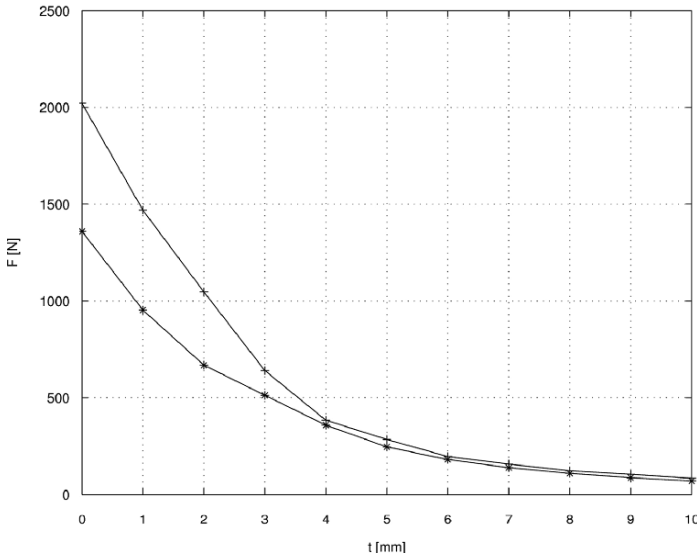


Fig. 4.12 Force vs air-gap curve (+2D, *3D)

The discrepancy between the two curves can be attributed to the leakage field in the z direction, that is neglected in the two-dimensional analysis. In principle, the three-dimensional analysis gives a more accurate prediction of the force. On the other hand, the remarkable increase of the number of elements, and so the computational cost, when passing from two to three dimensions, must be noted as well.

Chapter 5

Time-Varying Electromagnetic Field

5.1 Maxwell's Equations in Differential Form

In general, the presence of a charge distributed with density ρ (C m^{-3}) and of an impressed current density \bar{J}_0 (A m^{-2}) variable with time gives origin to the electromagnetic field described by the following time-dependent vectors:

- \bar{D} electric displacement (C m^{-2})
- \bar{E} electric field intensity (V m^{-1})
- \bar{B} magnetic induction (T)
- \bar{H} magnetic field intensity (A m^{-1})
- \bar{J} current density (A m^{-2})

As far as the origin of current density is concerned, the following remark can be put forward. In a solid or liquid medium the *conduction current* density is a function of \bar{E}

$$\bar{J} = \bar{J}(\bar{E}) \quad (5.1)$$

For a linear medium the above function becomes

$$\bar{J} = \sigma \bar{E} \quad (5.2)$$

Another kind of current is originated by the movement of free ions and electrons (e.g. in gases or vacuum). This *convection current* density is expressed by the formula

$$\bar{J} = \rho_+ \mathbf{u}_+ + \rho_- \mathbf{u}_- \quad (5.3)$$

where ρ_+ and ρ_- are positive and negative charge densities, respectively, while \mathbf{u}_+ and \mathbf{u}_- are the relevant velocities of positive and negative free charges.

Finally, the *displacement current* density is defined as

$$\bar{J} = \frac{\partial \bar{D}}{\partial t} \quad (5.4)$$

Considering the principle of charge conservation in any point of the domain, the following equation always holds (charge continuity equation)

$$\nabla \cdot \bar{\mathbf{J}} + \frac{\partial \rho}{\partial t} = 0 \quad (5.5)$$

The coupled electric and magnetic fields influence a charge q (C) by exerting a mechanical force $\bar{\mathbf{F}}$ (N) on it (Lorentz's equation)

$$\bar{\mathbf{F}} = q(\bar{\mathbf{E}} + \bar{\mathbf{u}} \times \bar{\mathbf{B}}) \quad (5.6)$$

where $\bar{\mathbf{u}}$ is the velocity of the charge with respect to the magnetic field. In particular, the term $q\bar{\mathbf{E}}$ modifies the value of velocity, while the term $q\bar{\mathbf{u}} \times \bar{\mathbf{B}}$ modifies also the direction of velocity.

In a simply-connected domain Ω with boundary Γ filled in by a linear medium characterized by permittivity ϵ , permeability μ and conductivity σ , the time-varying electromagnetic field is described by the following equations:

$$\nabla \times \bar{\mathbf{E}} = -\frac{\partial \bar{\mathbf{B}}}{\partial t} \quad \text{Faraday's equation} \quad (5.7)$$

$$\nabla \cdot \bar{\mathbf{D}} = \rho \quad \text{Gauss's electric equation} \quad (5.8)$$

$$\nabla \times \bar{\mathbf{H}} = \bar{\mathbf{J}} + \frac{\partial \bar{\mathbf{D}}}{\partial t} \quad \text{Ampère's equation} \quad (5.9)$$

$$\nabla \cdot \bar{\mathbf{B}} = 0 \quad \text{Gauss's magnetic equation} \quad (5.10)$$

In a three-dimensional domain, the above equations represent a set of eight scalar equations to which constitutive relations (2.65), (2.187), (2.255) must be added.

In total, fifteen scalar unknowns (i.e. field components) have to be determined, subject to suitable boundary conditions.

The system of eight plus nine equations can be solved since there are two relations among the unknowns which are automatically satisfied. In fact, taking the divergence of (5.9) and the time derivative of (5.8), continuity equation (5.5) follows. Similarly, taking the divergence of (5.7) and the time derivative of (5.10), one obtains an identity.

It should be remarked that in (5.9), in general,

$$\bar{\mathbf{J}} = \bar{\mathbf{J}}_0 + \sigma \bar{\mathbf{E}} + \mu \sigma \bar{\mathbf{u}} \times \bar{\mathbf{H}} \quad (5.11)$$

where $\bar{\mathbf{J}}_0$ is the term impressed by an external source, while the last term of the right-hand side takes into account the current density due to motional effect, if any.

In steady conditions all vectors are independent of time. Therefore, the two equations governing the electric field, namely (5.7) and (5.8), are decoupled with respect to the two equations governing the magnetic field, namely (5.9) and (5.10) (see Section 2.2 and Section 2.3).

5.2 Poynting's Vector

Let Maxwell's equations (5.7) and (5.9) be considered. By means of a vector identity (see A.13) one obtains

$$\bar{\nabla} \cdot (\bar{\mathbf{E}} \times \bar{\mathbf{H}}) = \bar{\mathbf{H}} \cdot (\bar{\nabla} \times \bar{\mathbf{E}}) - \bar{\mathbf{E}} \cdot (\bar{\nabla} \times \bar{\mathbf{H}}) = -\bar{\mathbf{H}} \cdot \frac{\partial \bar{\mathbf{B}}}{\partial t} - \bar{\mathbf{E}} \cdot \frac{\partial \bar{\mathbf{D}}}{\partial t} - \bar{\mathbf{E}} \cdot \bar{\mathbf{J}} \quad (5.12)$$

Referring to the specific energy in the electric and magnetic case and under the assumption of linear constitutive relationships, one has

$$\begin{aligned} \frac{1}{2} \frac{\partial}{\partial t} (\bar{\mathbf{H}} \cdot \bar{\mathbf{B}} + \bar{\mathbf{E}} \cdot \bar{\mathbf{D}}) &= \frac{1}{2} \left(\bar{\mathbf{H}} \cdot \frac{\partial \bar{\mathbf{B}}}{\partial t} + \bar{\mathbf{B}} \cdot \frac{\partial \bar{\mathbf{H}}}{\partial t} \right) + \frac{1}{2} \left(\bar{\mathbf{E}} \cdot \frac{\partial \bar{\mathbf{D}}}{\partial t} + \bar{\mathbf{D}} \cdot \frac{\partial \bar{\mathbf{E}}}{\partial t} \right) = \\ &= \bar{\mathbf{H}} \cdot \frac{\partial \bar{\mathbf{B}}}{\partial t} + \bar{\mathbf{E}} \cdot \frac{\partial \bar{\mathbf{D}}}{\partial t} \end{aligned} \quad (5.13)$$

Integrating (5.12) over Ω and using Gauss's theorem (see A.10), it results

$$\int_{\Gamma} (\bar{\mathbf{E}} \times \bar{\mathbf{H}}) \cdot \bar{\mathbf{n}} d\Gamma = -\frac{\partial}{\partial t} \int_{\Omega} \left(\frac{\bar{\mathbf{H}} \cdot \bar{\mathbf{B}}}{2} + \frac{\bar{\mathbf{E}} \cdot \bar{\mathbf{D}}}{2} \right) d\Omega - \int_{\Omega} \bar{\mathbf{E}} \cdot \bar{\mathbf{J}} d\Omega \quad (5.14)$$

Vector

$$\bar{\mathbf{S}} = \bar{\mathbf{E}} \times \bar{\mathbf{H}} \quad (5.15)$$

is called Poynting's vector (W m^{-2}).

According to (5.14), its flux out of a closed surface Γ is equal to (minus) the sum of the power of the electromagnetic field inside the domain Ω and the power transferred to the current (Poynting's theorem).

5.3 Maxwell's Equations in the Frequency Domain

The most important case of time-varying electromagnetic fields occurs when field sources, namely charge and current densities, vary with sinusoidal law. A given vector

$$\begin{aligned} \bar{\mathbf{V}}(x, y, z, t) &= [V_{0x}(x, y, z) \cos(\omega t - \varphi), V_{0y}(x, y, z) \cos(\omega t - \varphi), \\ &\quad V_{0z}(x, y, z) \cos(\omega t - \varphi)] = \\ &= \bar{\mathbf{V}}_0 \cos(\omega t - \varphi) \end{aligned} \quad (5.16)$$

can be expressed as

$$\begin{aligned} \bar{\mathbf{V}}(x, y, z, t) &= [V_{0x}(x, y, z) \text{Re} \{ e^{j(\omega t - \varphi)} \}, V_{0y}(x, y, z) \text{Re} \{ e^{j(\omega t - \varphi)} \}, \\ &\quad V_{0z}(x, y, z) \text{Re} \{ e^{j(\omega t - \varphi)} \}] = \end{aligned}$$

$$= \bar{V}_0 \operatorname{Re} \left\{ e^{j(\omega t - \varphi)} \right\} \quad (5.17)$$

The algebraic quantity $\bar{V} = \bar{V}_0 e^{-j\varphi}$ (phasor) represents the vector $\bar{V}(x, y, z, t)$ in a unique way; moreover, in the frequency domain, since $\frac{d}{dt} \cos(\omega t) = \omega \cos(\omega t + \frac{\pi}{2})$, the differential operator $\frac{\partial}{\partial t}$ is transformed into the complex operator $j\omega$.

Consequently, Maxwell's equation (5.7), (5.8), (5.9) and (5.10) are transformed as follows:

$$\bar{\nabla} \times \bar{E} = -j\omega \bar{B} \quad (5.18)$$

$$\bar{\nabla} \cdot \bar{B} = 0 \quad (5.19)$$

$$\bar{\nabla} \times \bar{H} = \bar{J} + j\omega \bar{D} \quad (5.20)$$

$$\bar{\nabla} \cdot \bar{D} = \rho \quad (5.21)$$

The latter equations are referred to as Helmholtz's equations and are valid at sinusoidal steady state for frequency $f = \frac{\omega}{2\pi}$ (field equations in the frequency domain).

It should be remarked that field quantities in the latter equations are the phasors corresponding to the associated time functions; by definition, the amplitude of the phasor is the maximum value of the corresponding time function.

Considering the constitutive equations, in a non-conducting region free of spatial charges ($\rho = 0$) and impressed currents, from vector identity (A.12), taking into account (5.21) one has

$$\bar{\nabla} \times \bar{\nabla} \times \bar{E} = \bar{\nabla} (\bar{\nabla} \cdot \bar{E}) - \bar{\nabla}^2 \bar{E} = -\bar{\nabla}^2 \bar{E} \quad (5.22)$$

From (5.18) and (5.20), if μ is a constant and $\sigma = 0$, $J_0 = 0$, it follows

$$\begin{aligned} \bar{\nabla} \times \bar{\nabla} \times \bar{E} &= \bar{\nabla} \times (-j\omega \bar{B}) = -j\omega \bar{\nabla} \times \bar{B} = \\ &= -j\omega \mu \bar{\nabla} \times \bar{H} = -j\omega \mu (j\omega \bar{D}) = \omega^2 \mu \varepsilon \bar{E} \end{aligned} \quad (5.23)$$

Comparing (5.22) and (5.23), Helmholtz's equation of electric field results

$$\bar{\nabla}^2 \bar{E} = -\omega^2 \mu \varepsilon \bar{E} = k^2 \bar{E} \quad (5.24)$$

with $k = j\omega \sqrt{\mu \varepsilon}$.

If the same procedure is applied to field \bar{H} , one obtains

$$\bar{\nabla}^2 \bar{H} = -\omega^2 \mu \varepsilon \bar{H} = k^2 \bar{H} \quad (5.25)$$

At sinusoidal steady state, the Poynting's vector (phasor) resulting from the time average of (5.15), considering the root-mean-square value of each vector, is

$$\bar{S} = \frac{\bar{E} \times \bar{H}^*}{2} \quad (5.26)$$

where the star denotes the conjugate phasor.

Referring to a volume Ω with boundary Γ , (5.14) takes the form

$$\int_{\Gamma} \left(\frac{\bar{E} \times \bar{H}^*}{2} \right) \cdot \bar{n} \, d\Gamma = -2j\omega \int_{\Omega} \left(\frac{\bar{H} \cdot \bar{B}^*}{4} + \frac{\bar{E} \cdot \bar{D}^*}{4} \right) d\Omega - \int_{\Omega} \frac{\bar{E} \cdot \bar{J}^*}{2} d\Omega \quad (5.27)$$

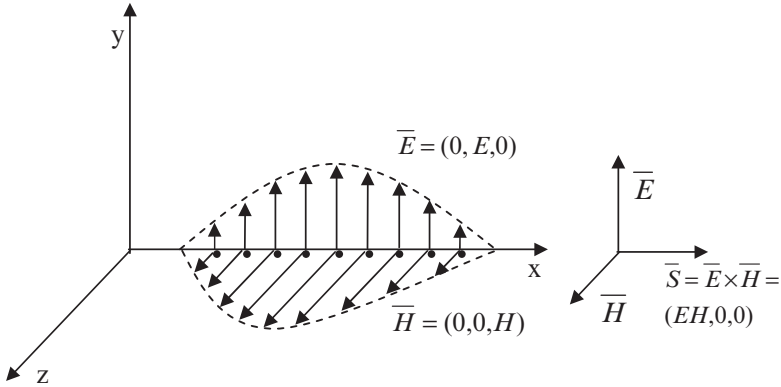


Fig. 5.1 Travelling plane electromagnetic wave

5.4 Plane Waves in an Infinite Domain

Let a simply-connected unbounded domain, filled in by a perfectly insulating medium ($\rho = 0, \sigma = 0$), be considered. For the sake of simplicity, let a time-harmonic electric field $E_0 \cos \omega t$ have only a non-zero component in the y -direction and vary only in the x direction (Fig. 5.1).

The Helmholtz's equation (5.24) reduces to

$$\frac{\partial^2 \bar{E}}{\partial x^2} = -\omega^2 \mu \epsilon \bar{E} \tag{5.28}$$

It can be easily proven that the complex function

$$\bar{E} = \bar{E}_0 e^{j\omega \sqrt{\mu \epsilon} \left(x - \frac{1}{\sqrt{\mu \epsilon}} t\right)} \tag{5.29}$$

with \bar{E}_0 phasor of the given electric field, is a solution of (5.28).

In the time domain it results

$$E(x, t) = E_0 \cos \left[\frac{\omega}{u} (x - ut) \right] \tag{5.30}$$

with $u = \frac{1}{\sqrt{\mu \epsilon}}$ (ms^{-1}). It can be verified that also

$$E(x, t) = E_0 \cos \left[\frac{\omega}{u} (x + ut) \right] \tag{5.31}$$

once transformed in its complex form $\bar{E} = \bar{E}_0 e^{j\omega \sqrt{\mu \epsilon} \left(x + \frac{1}{\sqrt{\mu \epsilon}} t\right)}$ is a solution of (5.28).

From the physical standpoint, (5.30) and (5.31) represent harmonic waves travelling with velocity u in positive and negative x -direction, respectively.

Owing to (5.18) a time-harmonic field \bar{B} is associated to \bar{E} .

In the frequency domain it results

$$\bar{\mathbf{B}} = \left(0, 0, \frac{1}{j\omega} \frac{\partial \bar{\mathbf{E}}}{\partial x} \right) = (0, 0, \sqrt{\mu\epsilon} \bar{\mathbf{E}}) \quad (5.32)$$

In the time domain one obtains:

$$\mathbf{B}(x, t) = \frac{E_0}{u} \cos \left[\frac{\omega}{u} (x \pm ut) \right] \quad (5.33)$$

From (5.30), (5.31) and (5.32), it results that the couple of vectors $(\bar{\mathbf{E}}, \bar{\mathbf{B}})$ defined above is a plane wave; $\bar{\mathbf{E}}$ and $\bar{\mathbf{B}}$ are orthogonal vectors; the ratio of electric field intensity to induction field intensity is equal to the velocity u of propagation in the dielectric medium.

Moreover, the Poynting's vector $\bar{\mathbf{S}}$ in the time domain results

$$\bar{\mathbf{S}} = \bar{\mathbf{E}} \times \bar{\mathbf{H}} = \frac{E_0^2}{u\mu} \left[1 + \cos \left(\frac{2\omega}{u} (x \pm ut) \right) \right] \bar{\mathbf{i}}_x \quad (5.34)$$

Therefore, the direction of propagation of the plane wave is orthogonal to both electric and magnetic field (transverse electromagnetic wave, TEM).

5.5 Wave and Diffusion Equations in Terms of Vectors $\bar{\mathbf{E}}$ and $\bar{\mathbf{H}}$

Considering the constitutive relations (2.65), (2.187), (2.255), Maxwell's equations (5.7)–(5.10) become, in terms of fields $\bar{\mathbf{E}}$ and $\bar{\mathbf{H}}$,

$$\bar{\nabla} \times \bar{\mathbf{E}} = -\mu \frac{\partial \bar{\mathbf{H}}}{\partial t} \quad (5.35)$$

$$\bar{\nabla} \times \bar{\mathbf{H}} = \bar{\mathbf{J}}_0 + \sigma \bar{\mathbf{E}} + \epsilon \frac{\partial \bar{\mathbf{E}}}{\partial t} \quad (5.36)$$

$$\bar{\nabla} \cdot \bar{\mathbf{E}} = \frac{\rho}{\epsilon} \quad (5.37)$$

$$\bar{\nabla} \cdot \bar{\mathbf{H}} = 0 \quad (5.38)$$

where $\bar{\mathbf{J}}_0$ is the impressed current density.

From (5.35) one has

$$\bar{\nabla} \times \bar{\nabla} \times \bar{\mathbf{E}} = -\frac{\partial}{\partial t} (\bar{\nabla} \times \mu \bar{\mathbf{H}}) \quad (5.39)$$

Since (see A.12)

$$\bar{\nabla} \times \bar{\nabla} \times \bar{\mathbf{E}} = \bar{\nabla} (\bar{\nabla} \cdot \bar{\mathbf{E}}) - \bar{\nabla}^2 \bar{\mathbf{E}} \quad (5.40)$$

taking into account that, in the absence of free charges (i.e. $\rho = 0$), if ϵ is a constant $\bar{\nabla} \cdot \bar{E} = \bar{\nabla} \cdot \frac{\bar{D}}{\epsilon} = 0$, one obtains

$$-\bar{\nabla}^2 \bar{E} = -\frac{\partial}{\partial t} (\bar{\nabla} \times \mu \bar{H}) \quad (5.41)$$

Then, for a homogeneous medium from (5.41) and (5.36) it results

$$\bar{\nabla}^2 \bar{E} = \mu \epsilon \frac{\partial^2 \bar{E}}{\partial t^2} + \mu \sigma \frac{\partial \bar{E}}{\partial t} + \mu \frac{\partial \bar{J}_0}{\partial t} \quad (5.42)$$

namely, the equation governing electric field \bar{E} ; if $\frac{\partial \bar{J}_0}{\partial t} = 0$, the homogeneous wave equation is obtained.

Similarly, it can be proven that for field H the following equation holds

$$\bar{\nabla}^2 \bar{H} = \mu \epsilon \frac{\partial^2 \bar{H}}{\partial t^2} + \mu \sigma \frac{\partial \bar{H}}{\partial t} - \bar{\nabla} \times \bar{J}_0 \quad (5.43)$$

If in (5.36) the displacement current density $\epsilon \frac{\partial \bar{E}}{\partial t}$ can be neglected, then equations (5.42) and (5.43) become

$$\bar{\nabla}^2 \bar{E} = \mu \sigma \frac{\partial \bar{E}}{\partial t} + \mu \frac{\partial \bar{J}_0}{\partial t} \quad (5.44)$$

and

$$\bar{\nabla}^2 \bar{H} = \mu \sigma \frac{\partial \bar{H}}{\partial t} - \bar{\nabla} \times \bar{J}_0 \quad (5.45)$$

respectively; they are the differential equations governing the electromagnetic field under quasi-static conditions (diffusion equations).

In turn, by taking the divergence of both sides of (5.36) and considering (A.8), the equation of charge relaxation follows

$$\bar{\nabla} \cdot \left(\sigma \bar{E} + \epsilon \frac{\partial \bar{E}}{\partial t} \right) = -\bar{\nabla} \cdot \bar{J}_0 \quad (5.46)$$

where the driving term is due to the impressed current density. It can be remarked that (5.46) states the current density balance in a dissipative dielectric medium, characterised by both conductivity σ and permittivity ϵ . In the frequency domain, (5.46) transforms as

$$\bar{\nabla} \cdot [(\sigma + j\omega\epsilon) \bar{E}] = -\bar{\nabla} \cdot \bar{J}_0 \quad (5.47)$$

where the complex conductivity $\sigma + j\omega\epsilon$ appears; in (5.47) \bar{E} and \bar{J}_0 are the phasors corresponding to the associated time functions.

5.6 Wave and Diffusion Equations in Terms of Scalar and Vector Potentials

In a simply connected domain Ω filled in by a linear and homogeneous medium, the magnetic vector potential \bar{A} (Wb m^{-1}) is defined by the equation (see 2.205)

$$\bar{B} = \bar{\nabla} \times \bar{A} \quad (5.48)$$

associated to a suitable gauge condition to be specified later on.

By means of (5.7) one has

$$\bar{\nabla} \times \left(\bar{E} + \frac{\partial \bar{A}}{\partial t} \right) = 0 \quad (5.49)$$

This means that the vector in brackets can be expressed as the gradient of a scalar potential φ (V)

$$\bar{E} + \frac{\partial \bar{A}}{\partial t} = -\bar{\nabla} \varphi \quad (5.50)$$

Hence

$$\bar{E} = -\bar{\nabla} \varphi - \frac{\partial \bar{A}}{\partial t} \quad (5.51)$$

Substituting (5.51) into (5.36) one obtains

$$\bar{\nabla} \times \bar{H} = \bar{J}_0 - \sigma \bar{\nabla} \varphi - \sigma \frac{\partial \bar{A}}{\partial t} - \varepsilon \frac{\partial}{\partial t} \bar{\nabla} \varphi - \varepsilon \frac{\partial^2 \bar{A}}{\partial t^2} \quad (5.52)$$

From (5.48) one has

$$\bar{\nabla} \times \bar{H} = \bar{\nabla} \times \mu^{-1} \bar{\nabla} \times \bar{A} \quad (5.53)$$

and

$$\bar{\nabla} \times \bar{\nabla} \times \bar{A} + \mu \varepsilon \bar{\nabla} \frac{\partial \varphi}{\partial t} + \mu \varepsilon \frac{\partial^2 \bar{A}}{\partial t^2} = \mu \left(\bar{J}_0 - \sigma \bar{\nabla} \varphi - \sigma \frac{\partial \bar{A}}{\partial t} \right) \quad (5.54)$$

In the case of a current-free and charge-free ideal dielectric region ($\bar{J}_0 = 0$, $\rho = 0$ and $\sigma = 0$) it results

$$\bar{\nabla} \times \bar{\nabla} \times \bar{A} + \mu \varepsilon \bar{\nabla} \frac{\partial \varphi}{\partial t} + \mu \varepsilon \frac{\partial^2 \bar{A}}{\partial t^2} = 0 \quad (5.55)$$

On the other hand, substituting (5.50) into (5.37) gives

$$-\nabla^2 \varphi - \frac{\partial}{\partial t} (\bar{\nabla} \cdot \bar{A}) = 0 \quad (5.56)$$

Equations (5.54) and (5.56) represent the link between the two potentials.

Taking into account that (see A.12)

$$\bar{\nabla} \times \bar{\nabla} \times \bar{\mathbf{A}} = -\bar{\nabla}^2 \bar{\mathbf{A}} + \bar{\nabla} (\bar{\nabla} \cdot \bar{\mathbf{A}}) \quad (5.57)$$

and by substituting this expression into (5.55) one has

$$-\bar{\nabla}^2 \bar{\mathbf{A}} + \bar{\nabla} (\bar{\nabla} \cdot \bar{\mathbf{A}}) + \mu\epsilon \bar{\nabla} \frac{\partial \varphi}{\partial t} + \mu\epsilon \frac{\partial^2 \bar{\mathbf{A}}}{\partial t^2} = 0 \quad (5.58)$$

or

$$-\bar{\nabla}^2 \bar{\mathbf{A}} + \bar{\nabla} \left(\bar{\nabla} \cdot \bar{\mathbf{A}} + \mu\epsilon \frac{\partial \varphi}{\partial t} \right) + \mu\epsilon \frac{\partial^2 \bar{\mathbf{A}}}{\partial t^2} = 0 \quad (5.59)$$

If the Lorentz's gauge

$$\bar{\nabla} \cdot \bar{\mathbf{A}} + \mu\epsilon \frac{\partial \varphi}{\partial t} = 0 \quad (5.60)$$

is imposed, then from (5.59) one obtains

$$-\bar{\nabla}^2 \bar{\mathbf{A}} + \mu\epsilon \frac{\partial^2 \bar{\mathbf{A}}}{\partial t^2} = 0 \quad (5.61)$$

which is the wave equation for the magnetic vector potential $\bar{\mathbf{A}}$, subject to boundary and initial conditions. After determining $\bar{\mathbf{A}}$, following (5.60), φ is given by

$$\varphi(t) = \varphi_0 - \frac{1}{\mu\epsilon} \int_0^t \bar{\nabla} \cdot \bar{\mathbf{A}}(t') dt' \quad (5.62)$$

with φ_0 to be determined.

Alternatively, imposing gauge (5.60) to equation (5.56), the wave equation for the electric scalar potential is obtained

$$-\nabla^2 \varphi + \mu\epsilon \frac{\partial^2 \varphi}{\partial t^2} = 0 \quad (5.63)$$

After determining φ , $\bar{\mathbf{A}}$ can be recovered.

In the case current \mathbf{J}_0 and charge ρ are present, (5.61) and (5.63) become

$$-\bar{\nabla}^2 \bar{\mathbf{A}} + \mu\epsilon \frac{\partial^2 \bar{\mathbf{A}}}{\partial t^2} = \mu \mathbf{J}_0 \quad (5.64)$$

$$-\nabla^2 \varphi + \mu\epsilon \frac{\partial^2 \varphi}{\partial t^2} = \frac{\rho}{\epsilon} \quad (5.65)$$

respectively.

In a three-dimensional unbounded domain Ω , their particular solutions are (see 2.48 and 2.49)

$$\bar{A} = \int_{\Omega} \frac{\mu \bar{J}'_0}{4\pi r} d\Omega \quad (5.66)$$

$$\varphi = \int_{\Omega} \frac{\rho'}{4\pi \epsilon r} d\Omega \quad (5.67)$$

where the values \bar{J}'_0 and ρ' are taken at an earlier time $t' = t - r\sqrt{\mu\epsilon}$ with respect to the time t at which \bar{A} and φ are observed. The latter two potentials are therefore called retarded potentials. Additionally, it can be noted that \bar{A} depends only on \bar{J}_0 and φ depends only on ρ . This dependence is, except for the correspondence of time, the same as in magnetostatics and electrostatics, respectively.

In the case of a conductor ($\rho = 0$, $\sigma \neq 0$), by imposing the following gauge

$$\bar{\nabla} \cdot \bar{A} + \mu\epsilon \frac{\partial \varphi}{\partial t} + \mu\sigma\varphi = 0 \quad (5.68)$$

from (5.54) and (5.57) it follows

$$-\bar{\nabla}^2 \bar{A} + \bar{\nabla} \left(\bar{\nabla} \cdot \bar{A} + \mu\epsilon \frac{\partial \varphi}{\partial t} + \mu\sigma\varphi \right) + \mu\epsilon \frac{\partial^2 \bar{A}}{\partial t^2} + \mu\sigma \frac{\partial \bar{A}}{\partial t} = \mu \bar{J}_0 \quad (5.69)$$

or

$$-\bar{\nabla}^2 \bar{A} + \mu\epsilon \frac{\partial^2 \bar{A}}{\partial t^2} + \mu\sigma \frac{\partial \bar{A}}{\partial t} = \mu \bar{J}_0 \quad (5.70)$$

After determining \bar{A} and so $\bar{\nabla} \cdot \bar{A}$, φ can be recovered from (5.68).

5.7 Electromagnetic Field Radiated by an Oscillating Dipole

Let a point charge $q(t) = q \sin(\omega t)$ oscillate with angular frequency ω along an element $d\lambda$ of line λ in a three-dimensional domain, so that the resulting current is $i = \omega q \cos \omega t$. If line λ is coincident with the z axis, in the frequency domain the phasor of the elementary vector potential (see 5.66) can be expressed as

$$d\bar{A} = \frac{\mu_0 \bar{I}}{4\pi r} e^{-j\frac{\omega r}{c}} d\lambda \bar{i}_z \quad (5.71)$$

where \bar{I} is the phasor of current i , r is the distance between field point and source point, $c = \frac{1}{\sqrt{\epsilon_0 \mu_0}}$ is the velocity of the electromagnetic wave in free space and the operator $e^{-j\frac{\omega r}{c}}$ accounts for the phase delay of $d\bar{A}$ with respect to \bar{I} .

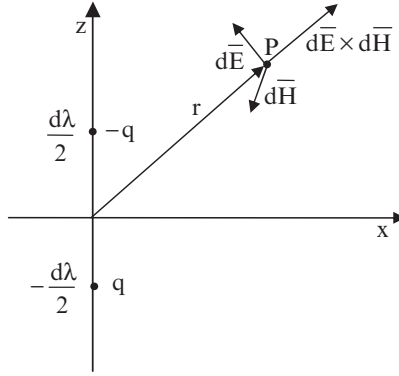


Fig. 5.2 Field radiated at point P by an oscillating dipole

Assuming spherical coordinates with origin at the gravity centre of the dipole (Fig. 5.2), the components of vector potential are

$$\begin{aligned} d\bar{A}_r &= d\bar{A} \cos \vartheta \\ d\bar{A}_\vartheta &= -d\bar{A} \sin \vartheta \\ d\bar{A}_\varphi &= 0 \end{aligned} \tag{5.72}$$

Since $\mu_0 \bar{H} = \bar{\nabla} \times \bar{A}$, the components of the elementary magnetic field in the frequency domain are (see A.21–A.23)

$$\begin{aligned} d\bar{H}_r &= d\bar{H}_\vartheta = 0 \\ d\bar{H}_\varphi &= \frac{\bar{I} \sin \vartheta d\lambda}{4\pi r^2} \left(1 + j \frac{\omega r}{c} \right) e^{-j \frac{\omega r}{c}} \end{aligned} \tag{5.73}$$

Thanks to (5.73), it can be noted that lines of magnetic fields are circular and are located on planes normal to the direction of z axis.

According to the Lorentz's gauge (5.60), the phasor of the elementary scalar potential associated to vector potential is

$$d\varphi = j \frac{c^2}{\omega} \bar{\nabla} \cdot (d\bar{A}) \tag{5.74}$$

Considering (5.51) and (5.74), the relationship between potentials and electric field

$$d\bar{E} = -j\omega d\bar{A} - \bar{\nabla} d\varphi \tag{5.75}$$

becomes

$$d\bar{E} = -j\omega d\bar{A} - j \frac{c^2}{\omega} \bar{\nabla} (\bar{\nabla} \cdot d\bar{A}) \tag{5.76}$$

After (5.72), (A.19) and (A.24), the components of the elementary electric field follow in phasor form

$$\begin{aligned} d\bar{E}_r &= -j \frac{2\bar{I} \cos \vartheta d\lambda}{4\pi\epsilon_0 r^3 \omega} \left(1 + j \frac{\omega r}{c}\right) e^{-j \frac{\omega r}{c}} \\ d\bar{E}_\vartheta &= -j \frac{\bar{I} \sin \vartheta d\lambda}{4\pi\epsilon_0 r^3 \omega} \left[1 + j \frac{\omega r}{c} - \left(\frac{\omega r}{c}\right)^2\right] e^{-j \frac{\omega r}{c}} \\ d\bar{E}_\phi &= 0 \end{aligned} \quad (5.77)$$

The situation is represented in Fig. 5.2.

It is interesting to consider the approximated expressions of field components near the oscillating dipole and far from it, respectively.

Under the approximation $\frac{\omega r}{c} \ll 1$ of near field, the field components become in phasor form

$$d\bar{H}_\phi = \frac{\bar{I} \sin \vartheta d\lambda}{4\pi r^2} \quad (5.78)$$

$$d\bar{E}_r = -j \frac{2\bar{I} \cos \vartheta d\lambda}{4\pi\epsilon_0 r^3 \omega} \quad (5.79)$$

$$d\bar{E}_\vartheta = -j \frac{\bar{I} \sin \vartheta d\lambda}{4\pi\epsilon_0 r^3 \omega} \quad (5.80)$$

It can be noted that the magnetic field scales as $\frac{1}{r^2}$ following the Laplace's law of the elementary action valid for a steady current (see 3.79); in turn, the electric field scales as $\frac{1}{r^3}$ according to the static field of a dipole (see Section 2.2.6).

Conversely, under the approximation $\frac{\omega r}{c} \gg 1$ of far field, the field components become

$$d\bar{H}_\phi = j \frac{\bar{I} \sin \vartheta d\lambda}{4\pi c} \left(\frac{\omega}{r}\right) e^{-j \frac{\omega r}{c}} \quad (5.81)$$

$$d\bar{E}_\vartheta = j \frac{\bar{I} \sin \vartheta d\lambda}{4\pi\epsilon_0 c^2} \left(\frac{\omega}{r}\right) e^{-j \frac{\omega r}{c}} \quad (5.82)$$

The component $d\bar{E}_r$ can be neglected with respect to $d\bar{E}_\vartheta$, apart from points in which $|\sin \vartheta| \ll 1$. It is important to note that electric and magnetic fields are orthogonal, in phase and tangent to the sphere of radius r ; consequently, the Poynting's vector has a radial direction only and the corresponding phasor results

$$d\bar{S} = \frac{d\bar{E}_\vartheta \times d\bar{H}_\phi^*}{2} = \frac{I^2 \sin^2 \vartheta (d\lambda)^2}{16\pi^2 \epsilon_0 c^3} \left(\frac{\omega}{r}\right)^2 \bar{i}_r \quad (5.83)$$

where I is the root-mean-square value of current.

It comes out that the power radiated by the dipole is maximum for $\vartheta = \frac{\pi}{2}$ (equatorial plane) and zero for $\vartheta = 0$ (z axis); furthermore, the average power flowing through a spherical surface is independent of its radius. Finally, the amplitude of fields depends on $\frac{\omega}{r}$; therefore, to make a long-distance transmission, it is necessary to increase the source frequency.

5.8 Diffusion Equation in Terms of Dual Potentials

Let a linear homogeneous isotropic medium, characterized by conductivity σ , permeability μ and permittivity ϵ be considered, where an impressed current \bar{J}_0 is present, the time variations of which are small, i.e., if time harmonic variations occur, the angular frequency is much lower than $\frac{\sigma}{\epsilon}$. Then, displacement current density $\frac{\partial \bar{D}}{\partial t}$ may be neglected with respect to impressed \bar{J}_0 and induced $\sigma \bar{E}$ current densities (quasi-static approximation). In this case, Maxwell's equations reduce to

$$\bar{\nabla} \times \bar{E} = -\frac{\partial \bar{B}}{\partial t} \quad (5.84)$$

$$\bar{\nabla} \cdot \bar{D} = 0 \quad (5.85)$$

$$\bar{\nabla} \times \bar{H} = \bar{J} = \bar{J}_0 + \sigma \bar{E} \quad (5.86)$$

$$\bar{\nabla} \cdot \bar{B} = 0 \quad (5.87)$$

along with the constitutive relations (5.2) and (2.187).

Given appropriate boundary and initial conditions, vectors \bar{H} (or \bar{B}) and \bar{E} (or \bar{D}) are uniquely defined.

This is a special case of Section 5.1 and is particularly important in low-frequency applications (eddy current problem).

The electromagnetic field can be also described in terms of potentials in two different ways.

According to the $\bar{A} - \phi$ method (see Section 5.6) a magnetic vector potential \bar{A} (Wb m^{-1}) is introduced by (5.48); moreover, an electric scalar potential ϕ (V) is defined according to (5.50).

In order to specify \bar{A} uniquely, a further condition must be introduced: this may be the Coulomb's gauge (2.206) or the Lorentz's gauge (5.60).

This way \bar{E} and \bar{H} can be expressed by means of two potentials (see Section 2.1.4), namely \bar{A} and ϕ .

From (5.86) taking into account (5.48) and (5.51) one has

$$\bar{\nabla} \times \mu^{-1} \bar{\nabla} \times \bar{A} = \bar{J}_0 - \sigma \frac{\partial \bar{A}}{\partial t} - \sigma \bar{\nabla} \phi \quad (5.88)$$

From (5.5), taking into account (5.51), it follows

$$\bar{\nabla} \cdot \left(\bar{J}_0 - \sigma \frac{\partial \bar{A}}{\partial t} - \sigma \bar{\nabla} \phi \right) = 0 \quad (5.89)$$

Equations (5.88) and (5.89) with appropriate boundary and initial conditions solve the electromagnetic problem in terms of \bar{A} and ϕ . In a region where $\sigma = 0$ (eddy-current free) the latter reduce to the classical equations of magnetostatics (see Section 2.3.1). On the other hand, (5.88) is a special case of (5.54).

Moreover, imposing the gauge $\bar{\nabla} \cdot \bar{A} + \mu\sigma\phi = 0$, from (5.88) one obtains

$$-\bar{\nabla}^2 \bar{A} + \mu\sigma \frac{\partial \bar{A}}{\partial t} = \mu \bar{J}_0 \quad (5.90)$$

that represents the diffusion equation in terms of vector potential; it is an approximation of equation (5.70) in the quasi-static state. After determining \bar{A} , scalar potential $\phi = -(\mu\sigma)^{-1} \bar{\nabla} \cdot \bar{A}$ can be recovered.

Alternatively, following the $\bar{T} - \Omega$ method, in regions free of impressed current ($J_0 = 0$) an electric vector potential T ($A \text{ m}^{-1}$) can be defined as

$$\bar{\nabla} \times \bar{T} = \bar{J} \quad (5.91)$$

Comparing (5.91) and (5.86) it turns out that \bar{H} and \bar{T} , which have the same curl, must differ by the gradient of a function $\Omega(A)$ (magnetic scalar potential)

$$\bar{H} = \bar{T} - \bar{\nabla} \Omega \quad (5.92)$$

The electric and magnetic vectors, \bar{J} and \bar{H} , have been so expressed in terms of two potentials.

In order to define \bar{T} uniquely, a gauge must be introduced.

The equation governing the electromagnetic field can be now expressed in terms of \bar{T} and Ω . In fact, from (5.86) taking the curl of both members and taking into account (5.84) and (5.92), one has

$$\bar{\nabla} \times \left(\sigma^{-1} \bar{\nabla} \times \bar{T} \right) = \bar{\nabla} \times \sigma^{-1} \bar{J}_0 - \frac{\partial}{\partial t} \mu (\bar{T} - \bar{\nabla} \Omega) \quad (5.93)$$

and from (5.87)

$$\bar{\nabla} \cdot \mu (\bar{T} - \bar{\nabla} \Omega) = 0 \quad (5.94)$$

In regions where $\sigma = 0$ one has $\bar{J} = 0$ and therefore, from (5.91), $\bar{\nabla} \times \bar{T} = 0$.

Moreover, imposing the gauge $\bar{\nabla} \cdot \bar{T} = \mu\sigma \frac{\partial \Omega}{\partial t}$, from (5.93) and (5.94) one obtains two independent equations for T and Ω , namely

$$\bar{\nabla}^2 \bar{T} - \mu\sigma \frac{\partial \bar{T}}{\partial t} = -\bar{\nabla} \times \bar{J}_0 \quad (5.95)$$

and

$$\nabla^2 \Omega - \mu\sigma \frac{\partial \Omega}{\partial t} = 0 \quad (5.96)$$

subject to appropriate boundary conditions. They are

$$\bar{n} \times \bar{T} = 0, \quad \Omega = 0 \quad (5.97)$$

or

$$\bar{n} \cdot \bar{T} = 0, \quad \frac{\partial \Omega}{\partial n} = 0 \quad (5.98)$$

if the boundary is normal to a flux line (i.e. $\bar{n} \times \bar{B} = 0$) or it is parallel to a flux line (i.e. $\bar{n} \cdot \bar{B} = 0$), respectively.

After determining \bar{T} , Ω is given by

$$\Omega(t) = \Omega_0 + (\mu\sigma)^{-1} \int_0^t \bar{\nabla} \cdot \bar{T}(t') dt' \tag{5.99}$$

with Ω_0 to be determined.

5.9 Weak Eddy Current in a Conducting Plane under AC Conditions

Let a conducting plane of thickness b and infinite extension, as shown in Fig. 5.3, be considered.

A time-varying magnetic field $\bar{H} = (H, 0, 0)$, with $H = H_0 \sin \omega t$, is impressed to the conductor characterized by conductivity σ .

Thanks to symmetry, all variables depend merely on y coordinate. From (5.35), $\bar{\nabla} \times \bar{E}$ turns out to be directed along the x axis and to depend merely on the z component of \bar{E} . It follows that the electric field \bar{E} induced within the conductor is $\bar{E} = (0, 0, E)$; the same holds for induced current density $\bar{J} = (0, 0, J)$. Therefore

$$\bar{\nabla} \times \bar{E} = \left(\frac{\partial E}{\partial y}, 0, 0 \right) \tag{5.100}$$

From (5.35), neglecting the magnetic field created by $\bar{J} = \sigma \bar{E}$, one has

$$\frac{\partial E}{\partial y} = -\mu_0 \frac{\partial H}{\partial t} \tag{5.101}$$

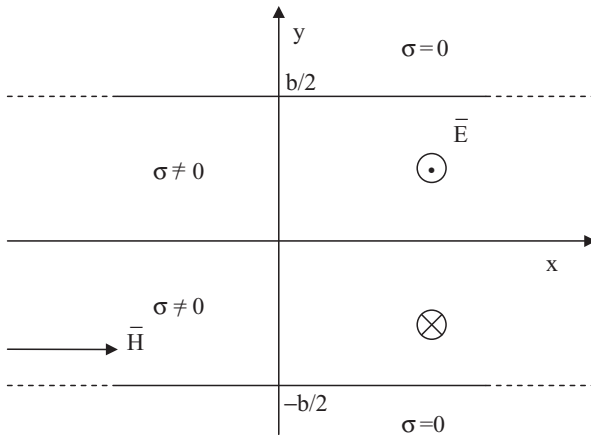


Fig. 5.3 Conducting plane in a magnetic field

or

$$\frac{\partial E}{\partial y} = -\omega\mu_0 H_0 \cos \omega t \quad (5.102)$$

Therefore:

$$E(y, t) = E(y) \cos \omega t \quad (5.103)$$

$$E(y) = -\omega\mu_0 H_0 y + k \quad (5.104)$$

with k to be determined.

Following (5.86) with $\bar{J}_0 = 0$ (solenoidality of the specific current $\sigma\bar{E}$), the boundary condition is

$$E\left(-\frac{b}{2}\right) = -E\left(\frac{b}{2}\right) \quad (5.105)$$

It follows

$$\frac{1}{2}\omega\mu_0 H_0 b + k = \frac{1}{2}\omega\mu_0 H_0 b - k \quad (5.106)$$

Therefore, it results that $k = 0$ and

$$E(y, t) = -\omega\mu_0 H_0 y \cos \omega t \quad (5.107)$$

In terms of eddy current density one has

$$\bar{J}(y, t) = -\sigma\omega\mu_0 H_0 y \cos \omega t \bar{i}_z, \quad -\frac{b}{2} < y < \frac{b}{2} \quad (5.108)$$

and $\bar{J}(y, t) = 0$ elsewhere.

By assuming $b = 2$ cm, $H_0 = 10^4$ A m⁻¹, $\sigma = 5.93 \cdot 10^7$ Ω⁻¹m⁻¹, $f = 50$ Hz, the amplitude of induced electric field is shown in Fig. 5.4.

5.10 Strong Eddy Current in a Conducting Plane under AC Conditions

Unlike the previous example, if the magnetic field due to the induced current dominates over the impressed field within the conductor, then the governing equations become

$$\bar{\nabla} \times \bar{E} = -\mu_0 \frac{\partial \bar{H}}{\partial t} \quad (5.109)$$

$$\bar{\nabla} \times \bar{H} = \sigma \bar{E} \quad (5.110)$$

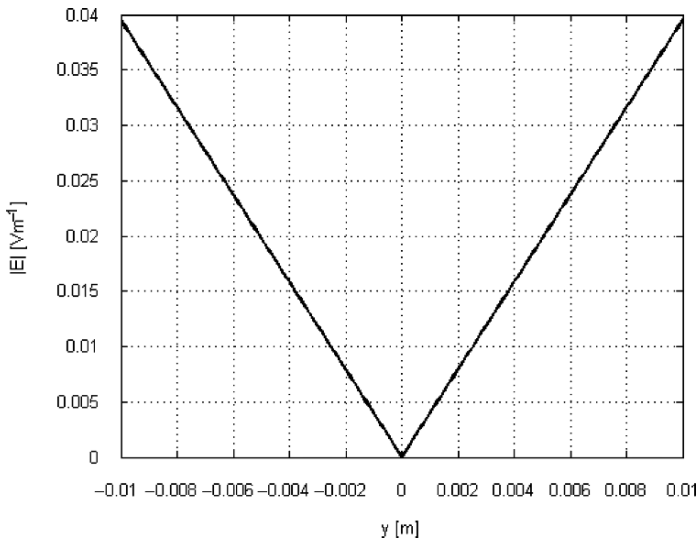


Fig. 5.4 Induced electric field in the conductor cross-section (weak reaction)

Thanks to symmetry

$$\bar{\nabla} \times \bar{E} = \left(\frac{\partial E}{\partial y}, 0, 0 \right); \quad \bar{\nabla} \times \bar{H} = \left(0, 0, -\frac{\partial H}{\partial y} \right) \quad (5.111)$$

From (5.109) one has

$$\frac{\partial E}{\partial y} = -\mu_0 \frac{\partial H}{\partial t} \quad (5.112)$$

and from (5.110)

$$-\frac{\partial H}{\partial y} = \sigma E \quad (5.113)$$

so that differentiating the latter with respect to y and substituting into the former yields

$$\frac{1}{\sigma} \frac{\partial^2 H}{\partial y^2} = \mu_0 \frac{\partial H}{\partial t} \quad (5.114)$$

Likewise, after differentiating (5.112) with respect to y and (5.113) with respect to t , one has

$$\frac{\partial^2 E}{\partial y^2} = -\mu_0 \frac{\partial}{\partial y} \frac{\partial H}{\partial t} \quad \text{and} \quad -\frac{\partial}{\partial t} \frac{\partial H}{\partial y} = \sigma \frac{\partial E}{\partial t} \quad (5.115)$$

respectively. Therefore

$$\mu_0^{-1} \frac{\partial^2 \mathbf{E}}{\partial y^2} = \sigma \frac{\partial \mathbf{E}}{\partial t} \quad (5.116)$$

results.

It is assumed that both \mathbf{H} and \mathbf{E} are time-harmonic functions

$$\begin{aligned} \mathbf{H}(y, t) &= H(y) \cos(\omega t + \varphi_H) \\ \mathbf{E}(y, t) &= E(y) \cos(\omega t + \varphi_E) \end{aligned} \quad (5.117)$$

or

$$\begin{aligned} \mathbf{H}(y, t) &= \Re \left\{ H(y) e^{j\varphi_H} e^{j\omega t} \right\} = \Re \left\{ \bar{H} e^{j\omega t} \right\} \\ \mathbf{E}(y, t) &= \Re \left\{ E(y) e^{j\varphi_E} e^{j\omega t} \right\} = \Re \left\{ \bar{E} e^{j\omega t} \right\} \end{aligned} \quad (5.118)$$

Combining (5.118) with (5.114) gives

$$\frac{1}{\sigma} \frac{\partial^2 \bar{H}}{\partial y^2} = \mu_0 j \omega \bar{H} \quad \text{and} \quad \frac{\partial^2 \bar{H}}{\partial y^2} - j \omega \sigma \mu_0 \bar{H} = 0 \quad (5.119)$$

where \bar{H} now denotes the phasor corresponding to $\mathbf{H}(y, t)$.

Similarly

$$\mu_0^{-1} \frac{\partial^2 \bar{E}}{\partial y^2} = \sigma j \omega \bar{E} \quad \text{and} \quad \frac{\partial^2 \bar{E}}{\partial y^2} - j \omega \sigma \mu_0 \bar{E} = 0 \quad (5.120)$$

holds.

Let quantities

$$\alpha^2 = j \omega \sigma \mu_0; \quad k = \sqrt{\frac{\omega \sigma \mu_0}{2}} \text{ (m}^{-1}\text{);} \quad \delta = \frac{1}{k} \text{ (m)} \quad (5.121)$$

be defined, where δ is called penetration depth or skin depth. It results $(1 + j)^2 k^2 = \alpha^2 = (1 + j)^2 \delta^{-2}$. The general solution to the equation

$$\frac{\partial^2 \bar{H}}{\partial y^2} - \alpha^2 \bar{H} = 0 \quad (5.122)$$

is

$$\bar{H} = C_1 e^{\alpha y} + C_2 e^{-\alpha y} \quad (5.123)$$

The application of the boundary conditions

$$y = \pm \frac{b}{2}; \quad \bar{H} = \bar{H}_0 \quad (5.124)$$

gives

$$\begin{aligned}\bar{H}_0 &= C_1 e^{-\alpha \frac{b}{2}} + C_2 e^{+\alpha \frac{b}{2}} \\ \bar{H}_0 &= C_1 e^{+\alpha \frac{b}{2}} + C_2 e^{-\alpha \frac{b}{2}}\end{aligned}\quad (5.125)$$

This implies

$$\begin{aligned}e^{-\alpha \frac{b}{2}}(C_1 - C_2) &= e^{+\alpha \frac{b}{2}}(C_1 - C_2) \\ C_1 &= C_2\end{aligned}\quad (5.126)$$

and

$$\begin{aligned}\bar{H}_0 &= C_1 (e^{-\alpha \frac{b}{2}} + e^{+\alpha \frac{b}{2}}) = C_1 2\text{ch}\left(\alpha \frac{b}{2}\right) \\ C_1 = C_2 &= \frac{\bar{H}_0}{2\text{ch}\left(\alpha \frac{b}{2}\right)}\end{aligned}\quad (5.127)$$

Finally, from (5.123) it follows

$$\bar{H} = \bar{H}_0 \frac{e^{\alpha y} + e^{-\alpha y}}{2\text{ch}\left(\alpha \frac{b}{2}\right)} = \bar{H}_0 \frac{\text{ch}(\alpha y)}{\text{ch}\left(\alpha \frac{b}{2}\right)}\quad (5.128)$$

Because of (5.113), one has

$$\bar{J} = -\frac{\partial \bar{H}}{\partial y} = -\alpha \bar{H}_0 \frac{\text{sh}(\alpha y)}{\text{ch}\left(\alpha \frac{b}{2}\right)}\quad (5.129)$$

Returning to the time domain, the amplitude of time-varying field H inside the conductor is given by the norm of (5.128). Using the identity $|\text{ch}(u + jv)| = \sqrt{\cos^2 u + \text{sh}^2 v}$ with u and v real numbers, after (5.121) and (5.128) it follows

$$|\bar{H}(y)| = |\bar{H}_0| \frac{\sqrt{\cos^2 \frac{y}{\delta} + \text{sh}^2 \frac{y}{\delta}}}{\sqrt{\cos^2 \frac{b}{2\delta} + \text{sh}^2 \frac{b}{2\delta}}}; \quad -\frac{b}{2} < y < \frac{b}{2}\quad (5.130)$$

while $|\bar{H}(y)| = |\bar{H}_0|$ elsewhere.

By assuming $b = 2 \text{ cm}$, $H_0 = 10^4 \text{ A m}^{-1}$, $\sigma = 5.93 \cdot 10^7 \Omega^{-1} \text{ m}^{-1}$, $f = 10^3 \text{ Hz}$, the distribution of magnetic field shown in Fig. 5.5 is obtained. When frequency f decreases, the magnetic field tends to become constant and equal to H_0 .

In turn, after (5.129) the amplitude J of the eddy current density is given by:

$$|\bar{J}(y)| = \beta \frac{|\bar{H}_0|}{\delta} \sqrt{\cos^2 \frac{y}{\delta} \text{sh}^2 \frac{y}{\delta} + \sin^2 \frac{y}{\delta} \text{ch}^2 \frac{y}{\delta}} = \beta \frac{|\bar{H}_0|}{\delta} \sqrt{\sin^2 \frac{y}{\delta} + \text{sh}^2 \frac{y}{\delta}}\quad (5.131)$$

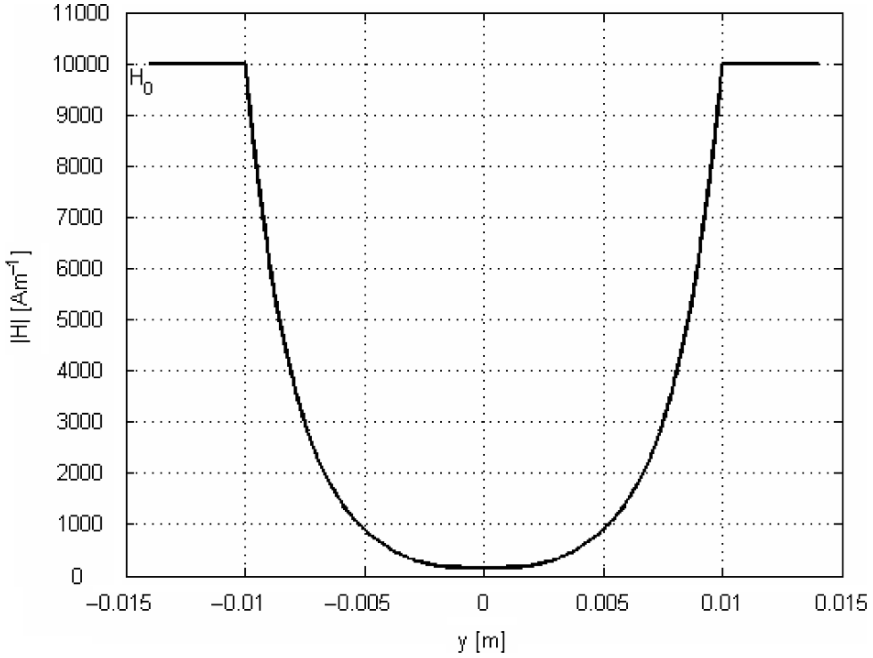


Fig. 5.5 Magnetic field in the conductor cross section

with $\beta^{-1} = \frac{1}{\sqrt{2}}\sqrt{\cos^2 \frac{b}{2\delta} + \text{sh}^2 \frac{b}{2\delta}}$, $\delta = \sqrt{\frac{2}{\omega\sigma\mu_0}}$, $-\frac{b}{2} < y < \frac{b}{2}$ and $J(y) = 0$ elsewhere.

The maximum value J_m of the induced current density is

$$J_m = J\left(-\frac{b}{2}\right) = J\left(\frac{b}{2}\right) = \sqrt{2} \frac{|\bar{H}_0|}{\delta} \sqrt{\frac{\sin^2 \frac{b}{2\delta} + \text{sh}^2 \frac{b}{2\delta}}{\cos^2 \frac{b}{2\delta} + \text{sh}^2 \frac{b}{2\delta}}} \tag{5.132}$$

By assuming the previous data, the distribution of electric field $E(y) = \sigma^{-1}J(y)$ shown in Fig. 5.6 is obtained. When frequency f decreases, the maximum value of electric field decreases and its distribution tends to become linear. In turn, when f increases, the magnetic field decreases in the limits

$$|\bar{H}| \rightarrow 0, \quad -\frac{b}{2} < y < \frac{b}{2} \tag{5.133}$$

and

$$|\bar{H}| \rightarrow |\bar{H}_0|, \quad y = \pm \frac{b}{2} \tag{5.134}$$

when f tends to infinity.

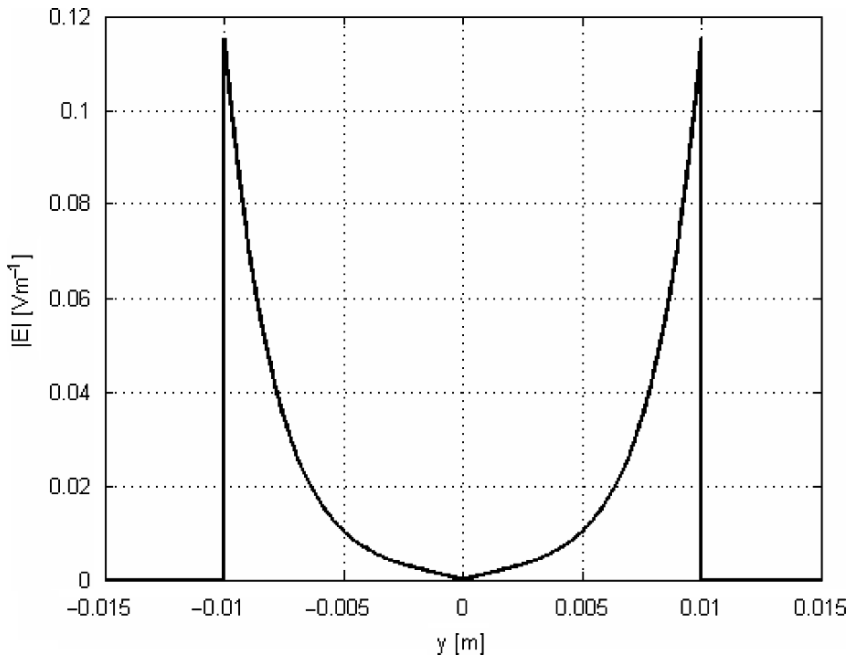


Fig. 5.6 Induced electric field in the conductor cross section (strong reaction)

Resorting to the definition of power loss given in Section 2.4.3, the surface power density P (W m^{-2}) dissipated in the conductor is

$$\begin{aligned}
 P &= \frac{1}{2} \int_{-\frac{b}{2}}^{\frac{b}{2}} \frac{1}{\sigma} |\bar{J}(y)|^2 dy = \frac{H_0^2}{\sigma \delta^2 \left(\cos^2 \frac{b}{2\delta} + \text{sh}^2 \frac{b}{2\delta} \right)} \int_{-\frac{b}{2}}^{\frac{b}{2}} \left(\sin^2 \frac{y}{\delta} + \text{sh}^2 \frac{y}{\delta} \right) dy = \\
 &= \frac{H_0^2}{2\sigma \delta} \frac{\text{sh} \frac{b}{\delta} - \sin \frac{b}{\delta}}{\cos^2 \frac{b}{2\delta} + \text{sh}^2 \frac{b}{2\delta}} = \frac{H_0^2}{2\sigma \delta} \frac{\text{sh} \frac{b}{\delta} - \sin \frac{b}{\delta}}{\frac{\cos \frac{b}{\delta} + 1}{2} + \frac{(e^{\frac{b}{2\delta}} - e^{-\frac{b}{2\delta}})^2}{4}} = \\
 &= \frac{H_0^2}{\sigma \delta} \frac{\text{sh} \frac{b}{\delta} - \sin \frac{b}{\delta}}{\cos \frac{b}{\delta} + \text{ch} \frac{b}{\delta}} = H_0^2 \sqrt{\frac{\omega \mu_0}{2\sigma}} \frac{\text{sh} kb - \sin kb}{\text{ch} kb + \cos kb} \quad (5.135)
 \end{aligned}$$

where $k = \delta^{-1}$.

Alternatively, in the frequency domain, since \bar{E} and \bar{H} are orthogonal vectors, the phasor of the Poynting's vector (5.26) is

$$\bar{S} = \frac{\bar{E} \bar{H}^*}{2} = -\frac{\alpha H_0^2}{2\sigma} \frac{\text{sh}(\alpha y) \text{ch}^*(\alpha y)}{\left| \text{ch} \left(\frac{\alpha b}{2} \right) \right|^2} \quad (5.136)$$

It results

$$\text{sh}(\alpha y)\text{ch}^*(\alpha y) = \frac{\text{sh}(2ky) + j \sin(2ky)}{2} \quad (5.137)$$

where the star denotes the complex conjugate and

$$\left| \text{ch} \left(\frac{\alpha b}{2} \right) \right|^2 = \text{sh}^2 \left(\frac{kb}{2} \right) + \cos^2 \left(\frac{kb}{2} \right) \quad (5.138)$$

respectively. After substitution, it comes out

$$\bar{S} = -\frac{kH_0^2 [\text{sh}(2ky) - \sin(2ky)] + j [\text{sh}(2ky) + \sin(2ky)]}{4\sigma \text{sh}^2 \left(\frac{kb}{2} \right) + \cos^2 \left(\frac{kb}{2} \right)} \quad (5.139)$$

Therefore, the total power dissipated per unit section of the conductor is

$$\begin{aligned} P &= \text{Re} \left\{ \bar{S} \left(-\frac{b}{2} \right) \right\} - \text{Re} \left\{ \bar{S} \left(\frac{b}{2} \right) \right\} = \frac{k |\bar{H}_0|^2}{2\sigma} \frac{\text{sh} kb - \sin kb}{\text{sh}^2 \frac{kb}{2} + \cos^2 \frac{kb}{2}} \\ &= |\bar{H}_0|^2 \sqrt{\frac{\omega \mu_0}{2\sigma}} \frac{\text{sh} kb - \sin kb}{\text{ch} kb + \cos kb} \end{aligned} \quad (5.140)$$

coincident with (5.135).

5.11 Eddy Current in a Cylindrical Conductor under Step Excitation Current

The problem is that of searching for the current density distribution $J(r, t)$ in a conductor of infinite length and circular cross-section of radius R carrying current $i(t)$ defined as a step function: $i(t) = 0$ when $t < 0$ and $i(t) = I$ when $t \geq 0$.

According to (5.2) and (5.44), assuming cylindrical coordinates, the following equation holds

$$\frac{\partial^2 J}{\partial r^2} + \frac{1}{r} \frac{\partial J}{\partial r} - \mu \sigma \frac{\partial J}{\partial t} = 0, \quad 0 \leq r \leq R \quad (5.141)$$

subject to the boundary condition

$$\frac{\partial J}{\partial r} = 0, \quad r = 0 \quad (5.142)$$

the integral condition

$$2\pi \int_0^R J(r, t) r \, dr = I \quad (5.143)$$

and the initial condition

$$J(r, 0^+) = \frac{I}{2\pi R} \delta^-(r - R) \quad (5.144)$$

where $\delta^-(r - R) = \lim_{r_0 \rightarrow R^-} \delta(r - r_0)$. At $t = 0^+$ a step of current is applied; in the frequency domain, it corresponds to a vanishing penetration depth (see Section 5.10); accordingly, current I is concentrated at $r = R$. The laminar current density $J_S = J(r, 0^+)$ determines the magnetic field \bar{H} such that $\bar{n} \times \bar{H} = \bar{J}_S$.

The solution to (5.141) can be obtained by means of the separation of variables

$$J(r, t) = J_m + \sum_{k=1}^{\infty} R_k(r) T_k(t), \quad 0 \leq r \leq R \quad (5.145)$$

Substituting (5.145) into (5.141) gives

$$\sum_{k=1}^{\infty} \frac{d^2 R_k}{dr^2} T_k + \frac{1}{r} \sum_{k=1}^{\infty} \frac{dR_k}{dr} T_k - \mu_0 \sigma \sum_{k=1}^{\infty} R_k \frac{dT_k}{dt} = 0 \quad (5.146)$$

Let one assume that for any $k \geq 1$

$$R_k'' T_k + \frac{1}{r} R_k' T_k - \mu_0 \sigma R_k T_k' = 0 \quad (5.147)$$

where $R_k'' \equiv \frac{d^2 R_k}{dr^2}$, $R_k' \equiv \frac{dR_k}{dr}$ and $T_k' \equiv \frac{dT_k}{dt}$ respectively.

After dividing each term of (5.147) by $R_k T_k$, it results

$$\frac{R_k''}{R_k} + \frac{1}{r} \frac{R_k'}{R_k} - \mu_0 \sigma \frac{T_k'}{T_k} = 0 \quad (5.148)$$

The latter transforms into the following pair of ordinary differential equations (see Section 3.3)

$$\mu_0 \sigma \frac{T_k'}{T_k} \equiv -\lambda_k^2 \quad (5.149)$$

$$\frac{R_k''}{R_k} + \frac{1}{r} \frac{R_k'}{R_k} \equiv -\lambda_k^2 \quad (5.150)$$

namely

$$T_k' + \frac{\lambda_k^2}{\mu_0 \sigma} T_k = 0 \quad (5.151)$$

$$R_k'' + \frac{1}{r} R_k' + \lambda_k^2 R_k = 0 \quad (5.152)$$

where $\lambda_k^2 \neq 0$ is the separation constant.

The solution to (5.151) is of the type

$$T_k(t) = \alpha_k e^{-\frac{\lambda_k^2 t}{\mu_0 \sigma}} \quad (5.153)$$

where α_k is a coefficient to be determined.

In turn, from (5.152) it results

$$R_k(r) = \beta_k J_0(\lambda_k r) + \gamma_k Y_0(\lambda_k r) \quad (5.154)$$

where β_k and γ_k are coefficients to be determined, while $J_0(\lambda_k r)$ and $Y_0(\lambda_k r)$ are the zero-order Bessel's functions of first and second kind, respectively. It is to be noted that $J_0(\lambda_k r)$ and $Y_0(\lambda_k r)$ tend to 1 and to minus infinity, respectively, when r approaches zero. Since at $r = 0$ current density should take a finite value at any time, constant γ_k must be zero. Therefore, it results

$$J(r, t) = J_m + \sum_{k=1}^{\infty} c_k J_0(\lambda_k r) e^{-\frac{\lambda_k^2 t}{\mu_0 \sigma}}, \quad 0 \leq r \leq R \quad (5.155)$$

where constants J_m , $c_k \equiv \alpha_k \beta_k$ and λ_k are to be determined by imposing boundary and initial conditions.

If R is very large and so the term $\frac{1}{r} \frac{\partial J}{\partial r}$ in (5.141) is neglected, a closed form of (5.155) can be determined in a straightforward way. In fact, under this assumption (5.152) and (5.154) become

$$R_k'' + \lambda_k^2 R_k = 0 \quad (5.156)$$

and

$$R_k(r) = a_k \cos(\lambda_k r) + b_k \sin(\lambda_k r) \quad (5.157)$$

respectively, where a_k and b_k are coefficients to be determined. As a consequence, (5.145) becomes

$$J(r, t) = J_m + \sum_{k=1}^{\infty} e^{-\frac{\lambda_k^2 t}{\mu_0 \sigma}} [a_k \cos(\lambda_k r) + b_k \sin(\lambda_k r)] \quad (5.158)$$

From (5.142) it follows that:

$$\lambda_k b_k e^{-\frac{\lambda_k^2 t}{\mu_0 \sigma}} = 0 \quad (5.159)$$

Therefore, $b_k = 0$. In turn, from (5.143) and (5.158) it results

$$J_m \pi R^2 + \sum_{k=1}^{\infty} \frac{2\pi}{\lambda_k^2} d_k e^{-\frac{\lambda_k^2 t}{\mu_0 \sigma}} [\lambda_k R \sin(\lambda_k R) + \cos(\lambda_k R) - 1] = I \quad (5.160)$$

where $d_k \equiv a_k$; (5.160) is fulfilled if $J_m = \frac{I}{\pi R^2}$, which represents the impressed current density when $t \rightarrow \infty$, and if either $d_k = 0$, $k \geq 1$ or

$$[\lambda_k R \sin(\lambda_k R) + \cos(\lambda_k R) - 1] = 0, \quad k \geq 1 \quad (5.161)$$

Two solutions to (5.161) exist, namely $\lambda_k = \frac{2k\pi}{R}$ with $k \geq 1$ integer number and $\{\gamma_k\}$ such that $\lambda_k < \gamma_k < \lambda_{k+1}$ with $k \geq 1$ integer number.

Accordingly, a particular solution is

$$J(r, 0^+) = \frac{I}{2\pi R} \delta^-(r - R) \quad (5.162)$$

and

$$J(r, t) = \frac{I}{\pi R^2} + \sum_{k=1}^{\infty} d_k e^{-\frac{4k^2\pi^2 t}{\mu_0\sigma R^2}} \cos\left(2k\pi \frac{r}{R}\right) \quad (5.163)$$

where coefficient d_k is determined for $r = 0$ by means of (5.144); this implies

$$\sum_{k=1}^{\infty} d_k = -\frac{I}{\pi R^2}, \quad r \in [0, R) \quad (5.164)$$

Considering the k th contribution to (5.163), it can be noted that the current carried by the round conductor is distributed sinusoidally in space and diffuses exponentially with a time constant $\tau_k = \frac{\mu_0\sigma R^2}{4k^2\pi^2}$. At time t the penetration depth can be defined as $\delta_k = 2\pi\sqrt{\frac{t}{\mu_0\sigma}}$ and the minimum value of current density is located on the axis of the conductor; $t = 0^+$ is the critical instant, when a laminar current density J_S is originated at $r = R$ such that $\int_{\Gamma} J_S d\Gamma = \int_{\Omega} J_m d\Omega$ fulfilling condition (5.143).

In the insulating medium surrounding the conductor, the current density is zero, while the induced electric field $\vec{E} = E\vec{i}_z$ fulfils the equation

$$\frac{\partial E}{\partial r} = \frac{\mu_0 I}{2\pi r} \delta(t), \quad r > R \quad (5.165)$$

By integrating the latter with respect to r , the finite variation ΔE of the field between any position $r > R$ and the boundary $r = R$ of the conductor results

$$\Delta E = E(r) - E(R) = \frac{\mu_0 I}{2\pi} \ln \frac{r}{R} \delta(t), \quad r \geq R \quad (5.166)$$

The field is impulsive, i.e. $E = 0$, $t \neq 0$.

5.12 Electromagnetic Field Equations in Different Reference Frames

In free space, let us consider an inertial frame of reference $O = (x, y, z)$ in which the observer perceives an electric field of intensity \vec{E} and a magnetic field of induction \vec{B} at time t .

Let a second frame of reference $O' = (x', y', z')$ move at a constant velocity $\bar{u} = (u, 0, 0)$ with respect to O at time t' .

Lorentz's transformation of coordinates, in which any observer measures the same velocity c of light in the free space, i.e. defines the same wave equation, can be obtained in the following way. Let time t and time t' be initialised so that at $t = t' = 0$ the axes of the two frames are coincident, namely $x' = x$, $y' = y$, $z' = z$. Owing to symmetry, it can be stated that O' moves at a velocity u with respect to O and, conversely, O moves at a speed $-u$ with respect to O' . This implies

$$x' = \gamma(x - ut) \quad (5.167)$$

$$x = \gamma(x' + ut') \quad (5.168)$$

where γ is a dimensionless coefficient to be determined. To this end, let a light flash, originated at the origin of both systems at $t = t' = 0$, be considered. The light travels as a spherical wave in both frames with the same speed c ; therefore, the equation of the wavefront is

$$x^2 + y^2 + z^2 = c^2t^2 \quad (5.169)$$

in frame O and

$$x'^2 + y'^2 + z'^2 = c^2t'^2 \quad (5.170)$$

in frame O' . Since $y' = y$ and $z' = z$, it follows

$$x^2 - c^2t^2 = x'^2 - c^2t'^2 \quad (5.171)$$

and then

$$t'^2 = \frac{x'^2}{c^2} - \frac{x^2}{c^2} + t^2 \quad (5.172)$$

Replacing x' by means of (5.167) one obtains

$$t'^2 = \frac{\gamma^2 - 1}{c^2}x^2 - 2\frac{\gamma^2 u}{c^2}xt + \left(\frac{\gamma^2 u^2}{c^2} + 1\right)t^2 \quad (5.173)$$

Independently, taking t' from (5.168) and using (5.167) one has

$$t'^2 = \left(\frac{1 - \gamma^2}{\gamma u}\right)^2 x^2 - 2\frac{\gamma^2 - 1}{u}xt + \gamma^2 t^2 \quad (5.174)$$

By equating the corresponding coefficients of (5.173) and (5.174), it results

$$\gamma = \frac{1}{\sqrt{1 - \frac{u^2}{c^2}}} \quad (5.175)$$

and then

$$t' = \frac{t - \frac{u}{c^2}x}{\sqrt{1 - \frac{u^2}{c^2}}} \quad (5.176)$$

Finally, the Lorentz's transformation from O to O' results

$$x' = \gamma(x - ut); \quad y' = y; \quad z' = z; \quad t' = \gamma\left(t - \frac{u}{c^2}x\right) \quad (5.177)$$

The inverse transformation can be obtained by changing the sign of velocity u, namely

$$x = \gamma(x' + ut'); \quad y = y'; \quad z = z'; \quad t = \gamma\left(t' + \frac{u}{c^2}x'\right) \quad (5.178)$$

Galilean transformation, on the contrary, is:

$$x' = x - ut; \quad y' = y; \quad z' = z; \quad t' = t \quad (5.179)$$

and

$$x = x' + ut'; \quad y = y'; \quad z = z'; \quad t = t' \quad (5.180)$$

Using Lorentz's transformation, Maxwell's equations remain the same, if electric field intensity \bar{E} transforms as follows:

$$E'_x = E_x; \quad E'_y = \gamma(E_y - uB_z); \quad E'_z = \gamma(E_z + uB_y) \quad (5.181)$$

If $u \ll c$, then $\gamma \cong 1$ and

$$E'_x = E_x; \quad E'_y = E_y - uB_z; \quad E'_z = E_z + uB_y \quad (5.182)$$

For vector \bar{B} , the transformation is

$$B'_x = B_x; \quad B'_y = \gamma(B_y + u\mu_0\epsilon_0E_z); \quad B'_z = \gamma(B_z - u\mu_0\epsilon_0E_y) \quad (5.183)$$

If $u \ll c$, then

$$B'_x = B_x; \quad B'_y = B_y + u\mu_0\epsilon_0E_z; \quad B'_z = B_z - u\mu_0\epsilon_0E_y \quad (5.184)$$

For the sake of some examples, let us first focus on a point charge q moving at a constant velocity \bar{u} with $u \ll c$ in free space with respect to a fixed frame (Fig. 5.7).

If the observer moves together with the charge, he/she just observes

$$\begin{aligned} \bar{E}' &= \frac{q}{4\pi\epsilon_0 r'^2} \bar{i}_r \\ \bar{B}' &= 0 \end{aligned} \quad (5.185)$$

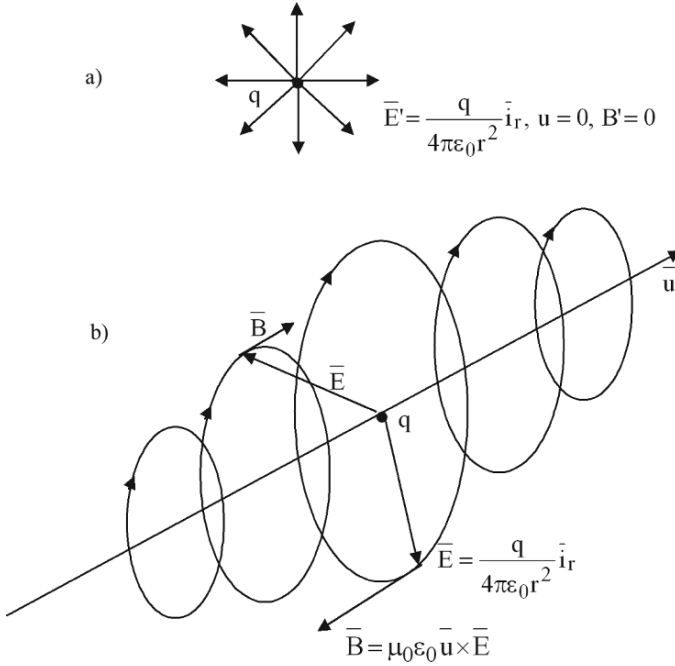


Fig. 5.7 Fields of a moving charge in different frames: (a) moving observer; (b) fixed observer

where r is the radial coordinate. An observer in the fixed frame sees

$$\begin{aligned} \bar{E} &= \bar{E}' \\ \bar{B} &= \mu_0 \epsilon_0 \bar{u} \times \bar{E} \end{aligned} \tag{5.186}$$

Therefore, it is reasonable to state that magnetism is a relativistic aspect of electricity; in other words, a magnetic field is given, if a relative motion between charge and observer is established.

In particular, (5.186) gives the field of a single travelling charge; the induction field can be expressed as

$$\bar{B} = \frac{\mu_0}{4\pi} \frac{q\bar{u} \times \bar{i}_r}{r^2} \tag{5.187}$$

If $n d\Omega$ travelling charges of value q are available in the elementary volume $d\Omega$, the elementary field is

$$d\bar{B} = \frac{\mu_0}{4\pi} \frac{nq\bar{u} \times \bar{i}_r}{r^2} d\Omega = \frac{\mu_0}{4\pi} \frac{\bar{J} \times \bar{i}_r}{r^2} d\Omega \tag{5.188}$$

where $\bar{J} = nq\bar{u}$ is the current density. If the direction of \bar{u} , and so \bar{J} , is coincident with the z axis, then (5.188) corresponds to (3.79) and by integration the Biot-Savart law follows (see 3.81).

As a second example, let a rectangular coil placed in a uniform induction field \bar{B} orthogonal to it be considered (Fig. 5.8). It is assumed that one of the four sides of

the coil is movable with a constant velocity \bar{u} with $u \ll c$. While an observer at rest with respect to a fixed frame measures the magnetic field of induction \bar{B} and no electric field, a second observer, located on the movable side, observes an electric field \bar{E} parallel to the movable side, the magnitude of which is $E = uB$.

5.12.1 A Relativistic Example: Steady Motion and Magnetic Diffusion

Let a pair of plane and parallel electrodes be considered; they are supposed to have infinite extension in the x direction, along which a finite portion of width w is taken into account. The length of the electrodes in the z direction is finite and equal to λ while the distance between them is equal to d (Fig. 5.9). An external circuit forces a constant current I through a conductive strip, filling the region between the two electrodes, such that current lines are normal to the electrodes; assuming $d \ll \lambda$, end effects in the current distribution are neglected.

Current lines when the strip speed is zero are also shown.

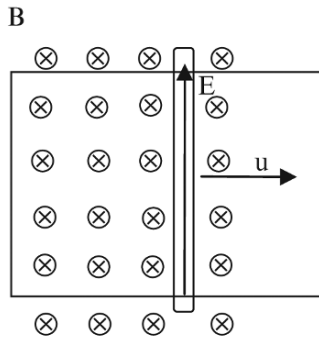


Fig. 5.8 Rectangular coil with a movable side in an induction field

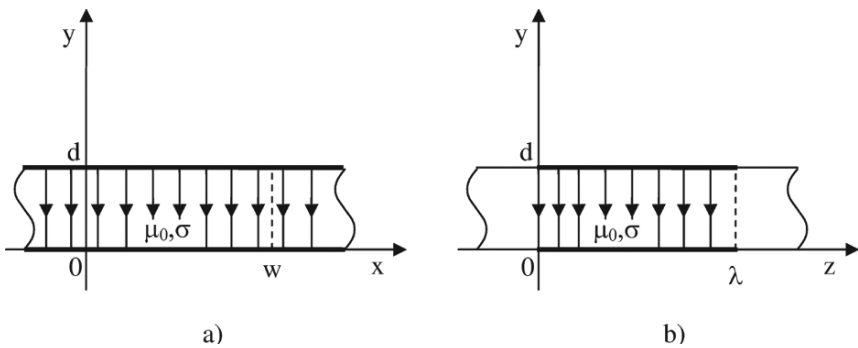


Fig. 5.9 Parallel electrodes with a conducting strip: (a) $x - y$ cross-section, (b) $z - y$ cross-section

The strip of infinite extension, which exhibits conductivity σ and permeability μ_0 , is free to slide at a constant speed $\bar{u} = u\bar{i}_z$. After (5.45) and (5.11) the induction field in the strip is governed by the following equation

$$\mu_0\sigma\frac{\partial\bar{B}}{\partial t} - \nabla^2\bar{B} = \mu_0\sigma\bar{\nabla} \times (\bar{u} \times \bar{B}) \quad (5.189)$$

subject to appropriate boundary and initial conditions; thanks to the assumptions made on the geometry of the electrodes, $\bar{J} = (0, J, 0)$ and $\bar{B} = (B, 0, 0)$. The problem can be tackled in either of two ways.

Steady State in the Fixed Frame

This viewpoint implies that

- the observer is at rest with respect to the electrodes
- the strip slides at a speed \bar{u} with respect to the observer
- the field is steady, i.e. $\frac{\partial\bar{B}}{\partial t} = 0$

The governing equation (5.189) reduces to

$$\frac{\partial^2 B}{\partial z^2} = \mu_0\sigma u \frac{\partial B}{\partial z} \quad (5.190)$$

As far as the boundary conditions are concerned, the following remark can be put forward. At $z = \lambda$, the Ampère's law gives $-H(0)w + H(\lambda)w = I$. Assuming that the field is zero at $z = 0$, it turns out to be

$$B(0) = 0, \quad B(\lambda) = \frac{\mu_0 I}{w} \quad (5.191)$$

Consequently, the solution to (5.190) is

$$B(z) = \sum_{i=1}^2 k_i e^{\lambda_i z} \quad (5.192)$$

with λ_i such that $\lambda_i^2 - \mu_0\sigma u\lambda_i = 0$, giving $\lambda_1 = 0$ and $\lambda_2 = \mu_0\sigma u$, respectively. Applying boundary conditions (5.191), it follows

$$k_1 + k_2 = 0, \quad k_1 + k_2 e^{\mu_0\sigma u\lambda} = \frac{\mu_0 I}{w} \quad (5.193)$$

namely

$$k_1 = \frac{\mu_0 I}{w} \frac{1}{1 - e^{\mu_0\sigma u\lambda}}, \quad k_2 = -k_1 \quad (5.194)$$

Therefore, it results

$$\mathbf{B}(z) = \frac{\mu_0 \mathbf{I}}{w} \frac{1 - e^{\mu_0 \sigma u z}}{1 - e^{\mu_0 \sigma u \lambda}}, \quad u \neq 0, \quad 0 < z < \lambda \quad (5.195)$$

The distribution of flux lines is non-linear with z .

The associated current density $\bar{\mathbf{J}} = \mu_0^{-1} \nabla \times \bar{\mathbf{B}}$ is

$$\mathbf{J}(z) = \mu_0^{-1} \frac{\partial \mathbf{B}}{\partial z} = \frac{\mu_0 \mathbf{I}}{w} \frac{\sigma u e^{\mu_0 \sigma u z}}{e^{\mu_0 \sigma u \lambda} - 1}, \quad u \neq 0, \quad 0 \leq z \leq \lambda \quad (5.196)$$

which is non-uniform with z .

In the case $u = 0$ (strip at rest), after (5.195) and (5.196) it follows

$$\mathbf{B}(z) = \frac{\mu_0 \mathbf{I}}{w} \lim_{u \rightarrow 0} \frac{\mu_0 \sigma z e^{\mu_0 \sigma u z}}{\mu_0 \sigma \lambda e^{\mu_0 \sigma u \lambda}} = \frac{\mu_0 \mathbf{I}}{w} \frac{z}{\lambda} \quad (5.197)$$

and

$$\mathbf{J}(z) = \frac{\mu_0 \mathbf{I}}{w} \lim_{u \rightarrow 0} \frac{\sigma e^{\mu_0 \sigma u z} + \mu_0 \sigma^2 u z e^{\mu_0 \sigma u z}}{\mu_0 \sigma \lambda e^{\mu_0 \sigma u \lambda}} = \frac{\mathbf{I}}{w \lambda} \quad (5.198)$$

The distribution of flux lines is linear with z , while the current density is uniform.

Transient State in the Moving Frame

This viewpoint implies that the observer travels at the same speed as the field; therefore, in (5.189) $u = 0$. In order to have a non-uniform field in the strip equal to (5.195), an appropriate value of the time derivative of \mathbf{B} should be prescribed; this way, a problem of transient magnetic diffusion is set up. In particular, comparing (5.189) with $u = 0$ and (5.190), it turns out to be

$$\mu_0 \sigma \frac{\partial \mathbf{B}}{\partial t} - u \frac{\partial^2 \mathbf{B}}{\partial z^2} = 0 \quad (5.199)$$

with

$$\frac{\partial \mathbf{B}}{\partial t} = u \frac{\partial \mathbf{B}}{\partial z} = \frac{\mu_0^2 \mathbf{I}}{w} \frac{\sigma u^2 z e^{\mu_0 \sigma u z}}{e^{\mu_0 \sigma u \lambda} - 1} \quad (5.200)$$

It can be noted that the time derivative varies with coordinates and is constant in time. Accordingly, the initial condition is

$$\mathbf{B}(z) = \frac{\mu_0 \mathbf{I}}{w} \frac{z}{\lambda}, \quad t = 0 \quad (5.201)$$

Boundary conditions are the same as in the previous case.

5.12.2 Galileian and Lorentzian Transformations in Electromagnetism

It can be shown that equations of electromagnetism are invariant with respect to the Lorentzian transformation, not to the Galileian transformation. In particular, referring to the one-dimensional wave equation (see Section 5.6), it can be proven that if $\phi(x, t)$ fulfils the equation

$$\frac{\partial^2 \phi}{\partial x^2} - \frac{1}{c^2} \frac{\partial^2 \phi}{\partial t^2} = 0 \quad (5.202)$$

then $\phi(x', t')$ fulfils the equation

$$\frac{\partial^2 \phi}{\partial x'^2} - \frac{1}{c^2} \frac{\partial^2 \phi}{\partial t'^2} = 0 \quad (5.203)$$

where (x, t) is related to (x', t') through (5.177), in which u is now called v .

In fact, using the chain derivation rule with respect to x' , one has

$$\begin{aligned} \frac{\partial \phi}{\partial x'} &= \frac{\partial \phi}{\partial x} \frac{\partial x}{\partial x'} + \frac{\partial \phi}{\partial t} \frac{\partial t}{\partial x'} = \frac{\partial \phi}{\partial x} \left(1 - \frac{v^2}{c^2}\right)^{-\frac{1}{2}} + \\ &+ \frac{\partial \phi}{\partial t} \frac{v}{c^2} \left(1 - \frac{v^2}{c^2}\right)^{-\frac{1}{2}} \end{aligned} \quad (5.204)$$

at the first order, and

$$\begin{aligned} \frac{\partial^2 \phi}{\partial x'^2} &= \frac{\partial^2 \phi}{\partial x^2} \left(1 - \frac{v^2}{c^2}\right)^{-1} + \frac{\partial^2 \phi}{\partial x \partial t} \frac{v}{c^2} \left(1 - \frac{v^2}{c^2}\right)^{-\frac{1}{2}} \frac{\partial x}{\partial x'} + \\ &+ \frac{\partial^2 \phi}{\partial t \partial x} \left(1 - \frac{v^2}{c^2}\right)^{-\frac{1}{2}} \frac{\partial t}{\partial x'} + \frac{\partial^2 \phi}{\partial t^2} \frac{v^2}{c^4} \left(1 - \frac{v^2}{c^2}\right)^{-1} \end{aligned} \quad (5.205)$$

at the second order. Since $\frac{\partial^2}{\partial x \partial t} = \frac{\partial^2}{\partial t \partial x}$, it follows that

$$\begin{aligned} \frac{\partial^2 \phi}{\partial x'^2} &= \frac{\partial^2 \phi}{\partial x^2} \left(1 - \frac{v^2}{c^2}\right)^{-1} + 2 \frac{\partial^2 \phi}{\partial x \partial t} \frac{v}{c^2} \left(1 - \frac{v^2}{c^2}\right)^{-\frac{1}{2}} \frac{\partial x}{\partial x'} + \\ &+ \frac{\partial^2 \phi}{\partial t^2} \frac{v^2}{c^4} \left(1 - \frac{v^2}{c^2}\right)^{-1} \end{aligned} \quad (5.206)$$

In turn, by deriving with respect to t' , one obtains

$$\begin{aligned} \frac{\partial \phi}{\partial t'} &= \frac{\partial \phi}{\partial x} \frac{\partial x}{\partial t'} + \frac{\partial \phi}{\partial t} \frac{\partial t}{\partial t'} = \frac{\partial \phi}{\partial x} v \left(1 - \frac{v^2}{c^2}\right)^{-\frac{1}{2}} + \\ &+ \frac{\partial \phi}{\partial t} \left(1 - \frac{v^2}{c^2}\right)^{-\frac{1}{2}} \end{aligned} \quad (5.207)$$

at the first order, and

$$\begin{aligned} \frac{\partial^2 \phi}{\partial t'^2} &= \frac{\partial^2 \phi}{\partial x^2} v \left(1 - \frac{v^2}{c^2}\right)^{-\frac{1}{2}} \frac{\partial x}{\partial t'} + \frac{\partial^2 \phi}{\partial x \partial t} \left(1 - \frac{v^2}{c^2}\right)^{-\frac{1}{2}} \frac{\partial x}{\partial t'} + \\ &+ \frac{\partial^2 \phi}{\partial t \partial x} v \left(1 - \frac{v^2}{c^2}\right)^{-\frac{1}{2}} \frac{\partial t}{\partial t'} + \frac{\partial^2 \phi}{\partial t^2} \left(1 - \frac{v^2}{c^2}\right)^{-\frac{1}{2}} \frac{\partial t}{\partial t'} \end{aligned} \quad (5.208)$$

at the second order. It follows that

$$\begin{aligned} \frac{\partial^2 \phi}{\partial t'^2} &= \frac{\partial^2 \phi}{\partial x^2} v^2 \left(1 - \frac{v^2}{c^2}\right)^{-1} + 2 \frac{\partial^2 \phi}{\partial x \partial t} v \left(1 - \frac{v^2}{c^2}\right)^{-1} + \\ &+ \frac{\partial^2 \phi}{\partial t^2} \left(1 - \frac{v^2}{c^2}\right)^{-1} \end{aligned} \quad (5.209)$$

As a result, it turns out to be

$$\frac{\partial^2 \phi}{\partial x'^2} - \frac{1}{c^2} \frac{\partial^2 \phi}{\partial t'^2} = \frac{\partial^2 \phi}{\partial x^2} - \frac{1}{c^2} \frac{\partial^2 \phi}{\partial t^2} \quad (5.210)$$

Conversely, using Galileian transformations (5.179) one has

$$\begin{aligned} \frac{\partial^2 \phi}{\partial x'^2} - \frac{1}{c^2} \frac{\partial^2 \phi}{\partial t'^2} &= \frac{\partial^2 \phi}{\partial x^2} \frac{1 - \frac{v^2}{c^2}}{1 - \frac{v^2}{c^2}} + 2 \frac{\partial^2 \phi}{\partial x \partial t} \frac{\frac{v}{c^2} - \frac{v}{c^2}}{1 - \frac{v^2}{c^2}} + \\ &+ \frac{\partial^2 \phi}{\partial t^2} \frac{\frac{v^2}{c^4} - \frac{1}{c^2}}{1 - \frac{v^2}{c^2}} - \frac{1}{c^2} \frac{\partial^2 \phi}{\partial t^2} \frac{1 - \frac{v^2}{c^2}}{1 - \frac{v^2}{c^2}} \end{aligned} \quad (5.211)$$

It follows that

$$\frac{\partial^2 \phi}{\partial x'^2} = \frac{\partial^2 \phi}{\partial x^2} \quad (5.212)$$

and

$$\frac{\partial^2 \phi}{\partial t'^2} = v^2 \frac{\partial^2 \phi}{\partial x^2} + 2v \frac{\partial^2 \phi}{\partial x \partial t} + \frac{\partial^2 \phi}{\partial t^2} \quad (5.213)$$

One obtains

$$\begin{aligned} \frac{\partial^2 \phi}{\partial x'^2} - \frac{1}{c^2} \frac{\partial^2 \phi}{\partial t'^2} &= \frac{\partial^2 \phi}{\partial x^2} - \frac{v^2}{c^2} \frac{\partial^2 \phi}{\partial x^2} - 2 \frac{v}{c^2} \frac{\partial^2 \phi}{\partial x \partial t} - \frac{1}{c^2} \frac{\partial^2 \phi}{\partial t^2} = \\ &= \left(1 - \frac{v^2}{c^2}\right) \frac{\partial^2 \phi}{\partial x^2} - 2 \frac{v}{c^2} \frac{\partial^2 \phi}{\partial x \partial t} - \frac{1}{c^2} \frac{\partial^2 \phi}{\partial t^2} \end{aligned} \quad (5.214)$$

Finally, it results

$$\frac{\partial^2 \phi}{\partial x'^2} - \frac{1}{c^2} \frac{\partial^2 \phi}{\partial t'^2} \neq \frac{\partial^2 \phi}{\partial x^2} - \frac{1}{c^2} \frac{\partial^2 \phi}{\partial t^2} \quad (5.215)$$

Chapter 6

Inverse Problems

6.1 Direct and Inverse Problems

Typically, direct (or forward) problems are defined as those where, given the input or the cause of a phenomenon or a process, the purpose is that of finding the output or the effect.

Inverse problems, conversely, are those where, given the measured or expected output or effect, one wants to determine the input or the cause; inverse problems are also those where, given the input and the corresponding output, one tries to understand their interconnection.

The two types of problems, when applied to the same phenomenon or process, represent the two logical ways of conceiving it: from input to output or the other way round. The latter way is central for design applications. This is why students of engineering, in particular, are invited to get familiar with inverse problems, after making experience with direct problems.

In applied electricity and magnetism, inverse problems may appear in two forms:

- (i) Given measured data, which may be affected by noise or error, in a field region, to identify, or recover, the relevant field sources or material properties or boundary conditions of the region (identification or parameter-estimation problems)
- (ii) Given desired fields in a device, or given the device performance based on them, to determine, or to design, sources or materials or shape of the device, producing the specified performance (synthesis or design problems)

6.2 Well-Posed and Ill-Posed Problems

From the mathematical viewpoint, following the Hadamard's definition, well-posed problems (or, properly, correctly-posed problems) are those for which

- (i) a solution always exists;
- (ii) there is only one solution;
- (iii) a small change of data leads to a small change in the solution.

The last property implies that the solution depends continuously upon the data, which often are measured quantities and therefore are affected by noise or error.

Ill-posed problems, instead, are those for which

- (i) a solution may not exist;
- (ii) there may be more than one solution;
- (iii) a small change of data may lead to a big change in the solution.

The Hadamard's example of an ill-posed problem is the so called Cauchy's problem. For Laplace's equation in two dimensions it reads:

solve

$$\frac{\partial^2 u}{\partial x^2} - \frac{\partial^2 u}{\partial y^2} = 0, \quad -\infty < x < \infty, \quad y > 0 \quad (6.1)$$

subject to boundary conditions

$$u(x, 0) = f(x) \quad \text{and} \quad \frac{\partial u}{\partial y}(x, 0) = g(x) \quad (6.2)$$

where f and g are given functions. For wave equation in one dimension it reads:

solve

$$\frac{\partial^2 u}{\partial x^2} - \frac{\partial^2 u}{\partial t^2} = 0, \quad t > 0 \quad (6.3)$$

subject to boundary condition

$$u(x, 0) = f(x) \quad (6.4)$$

and initial condition

$$\frac{\partial u}{\partial t}(x, 0) = g(x) \quad (6.5)$$

It can be proved that a small change in boundary/initial conditions produces a big change in the solution.

In a similar way, another ill-posed problem can be set up. To this end, let the magnetic field of a current uniformly distributed in a slot be considered (see Section 3.3.1). The governing equation in terms of vector potential is

$$\frac{\partial^2 A}{\partial x^2} + \frac{\partial^2 A}{\partial y^2} = -\mu_0 J, \quad -\frac{a}{2} < x < \frac{a}{2}, \quad y > 0 \quad (6.6)$$

The solution to the homogeneous equation, subject to boundary conditions

$$A\left(-\frac{a}{2}, y\right) = A\left(\frac{a}{2}, y\right) = 0, \quad y > 0 \quad (6.7)$$

$$\frac{\partial A}{\partial y}(x, 0) = \mu_0 J \frac{a}{2\pi} \sin\left(\frac{2\pi x}{a}\right), \quad -\frac{a}{2} < x < \frac{a}{2} \tag{6.8}$$

is

$$A(x, y) = \mu_0 J \left(\frac{a}{2\pi}\right)^2 \sin\left(\frac{2\pi x}{a}\right) \operatorname{sh}\left(\frac{2\pi y}{a}\right) \tag{6.9}$$

with $-\frac{a}{2} < x < \frac{a}{2}$, $y > 0$.

The homogeneous solution (6.9) is unstable with respect to a small variation of parameter a ; in fact, the derivative of A with respect to a gives

$$\begin{aligned} \frac{1}{\mu_0 J} \frac{\partial A}{\partial a} &= \frac{a}{2\pi^2} \sin\left(\frac{2\pi x}{a}\right) \operatorname{sh}\left(\frac{2\pi y}{a}\right) + \\ &- \frac{1}{2\pi} \left[x \cos\left(\frac{2\pi x}{a}\right) \operatorname{sh}\left(\frac{2\pi y}{a}\right) + y \sin\left(\frac{2\pi x}{a}\right) \operatorname{ch}\left(\frac{2\pi y}{a}\right) \right] \end{aligned} \tag{6.10}$$

It turns out to be

$$\begin{aligned} \left| \frac{\partial A}{\partial a} \right| &\leq \frac{a}{2\pi^2} \left| \operatorname{sh}\left(\frac{2\pi y}{a}\right) \right| + \frac{|x|}{2\pi} \left| \operatorname{sh}\left(\frac{2\pi y}{a}\right) \right| + \frac{|y|}{2\pi} \operatorname{ch}\left(\frac{2\pi y}{a}\right) \\ &\approx e^{\frac{2\pi y}{a}} \pm e^{-\frac{2\pi y}{a}} \end{aligned} \tag{6.11}$$

i.e. a perturbation of the parameter a is magnified exponentially.

6.3 Fredholm’s Integral Equation of the First Kind

In field theory, using an integral approach (Green’s function, Biot-Savart law, etc.), one frequently encounters an equation of the type:

$$g(x) = \int_{\Omega} H(x, y) f(y) dy, \quad x \in \Omega, \quad y \in \Omega \tag{6.12}$$

where Ω is the domain. This is called Fredholm’s equation of the first kind.

When g is given, f is the unknown and H is the so-called known kernel, the problem of finding f is an inverse problem. Normally, kernel H is assumed to be bounded, i.e. a constant $M > 0$ exists such that $|H(x, y)| \leq M$, and symmetrical, i.e. $H(x, y) = H(y, x)$. It can be shown that f does not depend continuously upon the given function g . Therefore, the problem is an ill-posed problem.

6.4 Case Study: Synthesis of the Source Producing a Magnetic Field in Two Dimensions

The problem is that of identifying the density $J(x')$ with $-\frac{a}{2} \leq x' \leq \frac{a}{2}$ of the current flowing along a linear conductor in air, such that the induction produced in a controlled subregion Ω_0 defined by $\alpha_1 \leq x \leq \alpha_2$ and $\beta_1 \leq y \leq \beta_2$ (Fig. 6.1) is

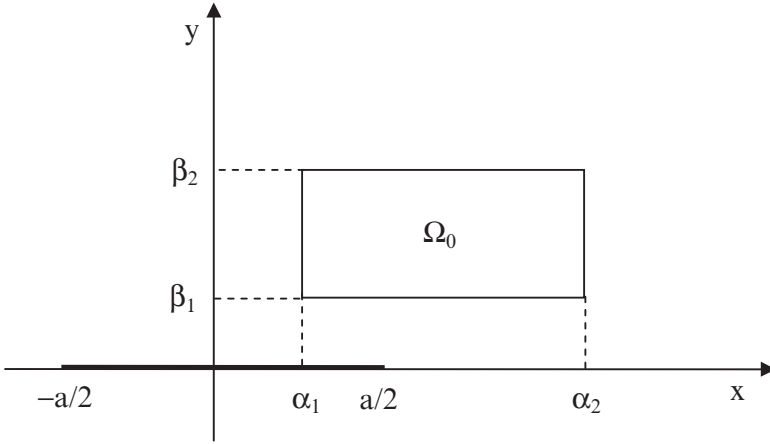


Fig. 6.1 Linear conductor producing a prescribed field in Ω_0

equal to a prescribed value. From Section 3.1.7, one has that the vector potential, parallel to J , has amplitude given by

$$A(x, y) = \frac{\mu_0}{4\pi} \int_{-a/2}^{a/2} \ln \left[(x - x')^2 + y^2 \right] J(x') dx' \tag{6.13}$$

where the kernel is equal to the Green’s function in an unbounded two-dimensional domain.

If induction $\bar{B} = (B_x, B_y)$ is given in the controlled subregion, one can get the corresponding potential A by integrating the relationships $B_x = \frac{\partial A}{\partial y}$ and $B_y = -\frac{\partial A}{\partial x}$.

Therefore, (6.13) becomes a Fredholm’s equation of the first kind. The solution can be arranged by a numerical technique.

6.5 Under- and Over-Determined Systems of Equations

In general, the numerical solution of problems, including field problems, usually leads to a system of equations of the type:

$$Ax = b \tag{6.14}$$

where A is a rectangular $m \times n$ matrix, x is the unknown n -vector and b the known m -vector.

If $m < n$, the system is called under-determined. If, on the contrary, $m > n$, the system is called over-determined.

Finally, if $m = n$, the matrix A is square. In this case, if $\det(A) \neq 0$, then A is non singular; therefore A^{-1} exists and the corresponding system of equations has a unique solution for any b .

The effect of a small perturbation of b on x is represented by the condition number of A :

$$\text{cond}(A) \equiv \|A\| \|A^{-1}\| = \frac{\lambda_{\max}}{\lambda_{\min}} \geq 1 \quad (6.15)$$

where λ_{\max} and λ_{\min} are the maximum and minimum eigenvalues of matrix A , respectively. If $\text{cond}(A)$ is large, then the matrix is called ill-conditioned and the solution may be perturbed substantially by even a small change of b . An example of condition number calculation was already reported in Section 4.2.5 for the stiffness matrix resulting from a finite-element scheme.

For the inversion of a square non-singular matrix there are various methods, the most popular of which is the Gauss's factorisation of matrix $A = LU$ into the product of a lower triangular matrix L by an upper triangular matrix U .

If A is rectangular, theoretically the inverse of A does not exist and the system of equations has no solution or infinite solutions. However, if $m > n$ and the rank of A is equal to n (i.e. the n columns of A are linearly independent), a pseudo-inverse of A can be looked for in terms of a related least-squares problem.

6.6 Least-Squares Solution

If A is a $m \times n$ matrix ($m > n$) of rank n and b is a given m -vector, then a solution to (6.14) can be found by minimizing a norm, for instance the Euclidean or two-norm, of the residual $Ax - b$; this corresponds to solving the least-squares problem

$$\min_x \|Ax - b\|_2 \quad (6.16)$$

In order to carry out the solution of (6.14), a number of numerical techniques can be adopted.

A possible way is to solve the normal equations associated to (6.14), which are defined as

$$A^T A x = A^T b \quad (6.17)$$

where $A^T A$ is a square $n \times n$ matrix. It can be proven that the vector

$$x^* = (A^T A)^{-1} A^T b \quad (6.18)$$

fulfils the condition

$$\|Ax^* - b\|_2 \leq \|Ax - b\|_2 \quad (6.19)$$

for each n -vector x and so x^* is the least-squares solution to (6.14).

In principle, if A has full column rank, $A^T A$ is positive definite; however, from the numerical viewpoint, this assumption might fail for a twofold reason

- the magnification of ill-conditioning when passing from A to $A^T A$;
- the round-off errors.

Therefore, the use of normal equations is not recommended because it might lead to instability.

A more effective approach is given e.g. by the Singular Value Decomposition (SVD) method; basically, it consists of decomposing the matrix A , which is assumed to be full column rank ($m > n$), into the product of three matrices, i.e. a $m \times m$ orthogonal matrix U , a $m \times n$ block diagonal matrix S , a $n \times n$ orthogonal matrix V , such that $A = USV^T$. In particular, it results

$$S = \begin{bmatrix} \Sigma & 0 \\ 0 & 0 \end{bmatrix} \quad (6.20)$$

with $\Sigma = \text{diag}(\sigma_1, \dots, \sigma_n)$.

The diagonal entries of Σ are the singular values of A . The solution to the least-squares problem is then given by

$$x^* = VS^{-1}U^Tb \quad (6.21)$$

with

$$S^{-1} = \begin{bmatrix} \Sigma^{-1} & 0 \\ 0 & 0 \end{bmatrix} \quad (6.22)$$

and $\Sigma^{-1} = \text{diag}(\sigma_1^{-1}, \dots, \sigma_n^{-1})$.

Matrix $VS^{-1}U^T$ is called also pseudo-inverse of A .

For the sake of an example, let the case

$$A = \begin{bmatrix} 1 & 1 \\ 1 & 1 \\ 0 & 10^{-4} \end{bmatrix}, \quad b = \begin{bmatrix} 1 \\ 1 \\ 1 \end{bmatrix} \quad (6.23)$$

be considered. Apparently, bad scaling is the source of ill conditioning of A .

The normal-equation matrix and known vector are

$$A^T A = \begin{bmatrix} 2 & 2 \\ 2 & 2 + 10^{-8} \end{bmatrix}, \quad A^T b = \begin{bmatrix} 2 \\ 2 + 10^{-4} \end{bmatrix} \quad (6.24)$$

with $\text{cond}(A^T A) = 8 \cdot 10^8$; the corresponding solution is

$$x^* = 10^4 \begin{bmatrix} -0.9998 \\ 0.9999 \end{bmatrix} \quad (6.25)$$

In turn, the SVD decomposition gives

$$U = \begin{bmatrix} -0.7071 & 2.510^{-5} & 0.7071 \\ -0.7071 & 2.510^{-5} & -0.7071 \\ -3.5310^{-5} & -0.9999 & 0 \end{bmatrix} \quad S = \begin{bmatrix} 2 & 0 \\ 0 & 7.07110^{-5} \\ 0 & 0 \end{bmatrix} \\ V = \begin{bmatrix} -0.7071 & 0.7071 \\ -0.7071 & -0.7071 \end{bmatrix} \quad (6.26)$$

with solution

$$x^* = 10^4 \begin{bmatrix} -0.9999 \\ 1 \end{bmatrix} \quad (6.27)$$

The two solutions are practically coincident.

6.7 Classification of Inverse Problems

The formulation of inverse problems in electricity and magnetism implies to associate a routine for field computation (direct problem) to a routine for the solution of the inverse problem.

There are many ways to classify inverse problems. A classification can be based on the approach for field computation (integral or differential, analytical or numerical). Another classification can be made, according to the formulation of the inverse problem and to the relevant mathematical method employed for the solution.

When the given data come from measurements and the parameters governing field equations, including field source, are to be found, one has identification problems.

Otherwise, when the given data are arbitrarily taken and the field source or specifications of the field region (boundary conditions, material properties, etc.) are required, the problem is called a synthesis problem.

In engineering applications often the goal is to design the geometry of a device or to select suitable materials and source so that a prescribed performance of the device, depending on the field, is obtained. This kind of problem is commonly defined as optimal shape design problem.

The ultimate goal of engineering problems is to perform an Automated Optimal Design (AOD); in this case, the solution is obtained automatically in terms of the required or best performance.

Chapter 7

Optimization

7.1 Solution of Inverse Problems by the Minimization of a Functional

The n unknowns x of an inverse problem are normally called design variables. In general, they are real values, although in some cases they are integer, belonging to a feasible region Ω . In multivariate problems, $n > 1$.

The design variables may be geometric coordinates of the field region or values of sources or parameters characterizing the region or whatever.

The solution of the inverse problem is generally performed by means of the optimization (minimization) of a suitable function $f(x)$ called objective function or cost function or design criterion

$$\text{given } x_0 \in \Omega, \quad \text{find } \inf_x f(x), \quad x \in \Omega \quad (7.1)$$

where x_0 is the initial guess; properly speaking, (7.1) is a problem of unconstrained optimization. Normally, it is assumed that f is bounded in Ω .

Function f may represent some performance depending on the field or simply the discrepancy between computed and known field values (error functional), that is the residual $\|Ax - b\|$ in (6.16).

When it is required to maximize an objective function, it must be considered that

$$\sup_x f(x) = \inf_x [-f(x)] \quad (7.2)$$

In general, the objective function f , which depends on the field, is not known analytically. Consequently, the classical conditions of optimality (i.e. null gradient and positive-definite Hessian matrix) cannot be applied a priori, because the objective function is known only numerically as a set of values at sample points. Moreover, in general, f is neither convex nor differentiable or smooth. Therefore, it is not guaranteed to get solutions; in particular, f might exhibit some local minima in addition to the global one. Any way, a solution to (7.1) can be obtained just numerically and the procedure may be troublesome and time-consuming.

As said before, the numerical solution of inverse problems in electricity and magnetism requires, as a rule, a routine for calculating the field, which is integrated with a routine minimizing the objective function.

Usually, the device or system to be optimized is represented by a finite-element model in two or three dimensions. The main flow of the computation is driven by the minimization routine, which in the simplest way is carried out step by step. Starting from x_0 , an iterative procedure updates the current design point x_k as

$$x_{k+1} = x_k + \lambda s_k \quad (7.3)$$

where λ is a scalar and s_k is the current search direction within the feasible region. Given x_{k+1} , the routine of field analysis generates a new finite-element grid, the field simulation is restarted and the evaluation of $f(x)$ is so updated.

At the end of computation, the result could represent either a local minimum or simply a point which is better than the initial one because f has decreased; in the latter case, a mere improvement (and not the optimization) of f has been achieved. In general, the optimization trajectory may converge to different local minima, depending on the initial point, and the global optimum cannot be deduced from the local behaviour of the objective function.

7.2 Constrained Optimization

In a more advanced formulation, the objective function should fulfil constraints, which may be expressed as inequalities, equalities and bilateral bounds. Formally, the problem can be stated as follows

$$\text{given } x_0 \in \Omega, \quad \text{find } \inf_x f(x), \quad x \in \Omega \quad (7.4)$$

subject to

$$\begin{aligned} g_j(x) &\leq 0 & j &= 1, \dots, n_i \\ h_j(x) &= 0 & j &= n_i + 1, \dots, n_c \\ \lambda_k &\leq x \leq u_k & k &= 1, \dots, n_b \end{aligned} \quad (7.5)$$

Constraints and bounds set the limits of the feasible region Ω . A simple technique to manage constraints is to transform the constrained problem into an unconstrained one, by adding a penalty term to the objective function, when the design variables violate the constraints. This way, a sequence of unconstrained problems is solved, which is assumed to converge to the solution of the constrained problem.

A cost-effective and accurate solution to the optimization problem depends on the number of design variables and constraints, as well as on the properties of objective function and constraints.

7.3 Multiobjective Optimization

In some cases many objective functions are prescribed simultaneously. Problems of this kind belong to the category of multi-objective or multi-criteria optimization. Several design problems in electricity and magnetism are characterized by a vector of n_f objective functions in mutual conflict, for which the most general solution is represented by the Pareto front of non-dominated solutions, i.e. those for which the decrease of a function is not possible without the simultaneous increase of at least one of the other functions. Non-dominated solutions are called also non-inferior or efficient solutions.

Formally, considering n_v variables, a multiobjective optimization problem can be cast as follows

$$\text{given } x_0 \in \Omega, \text{ find } \inf_x F(x), \quad x \in \Omega \quad (7.6)$$

subject to (7.5).

In (7.6), $F(x) = \{f_1(x), \dots, f_{n_f}(x)\} \subset \mathbb{R}^{n_f}$ is the objective vector, assuming $n_f \geq 2$. Therefore, F defines a transformation from the design space \mathbb{R}^{n_v} to the corresponding objective space \mathbb{R}^{n_f} . It is assumed that the objectives are bounded and conflicting, namely

$$\text{there exists } x_i^* \text{ such that } f_i(x_i^*) = \inf f_i(x), \quad i = 1, \dots, n_f \quad (7.7)$$

and $x_i^* \neq x_j^*$, $i \neq j$, $j = 1, \dots, n_f$.

In general, the utopia solution

$$U = \{U_i\} = \{\inf f_i(x)\}, \quad i = 1, \dots, n_f \quad (7.8)$$

minimizing all f_i does not exist and non-dominated solutions $\tilde{x} \in \Omega$ are accepted.

In this respect, given two feasible solutions $x_a \in \Omega$ and $x_b \in \Omega$, x_a is said to dominate x_b if $f_i(x_a) \leq f_i(x_b)$, $i = 1, \dots, n_f$ and $f_i(x_a) < f_i(x_b)$ for at least a value of index $i = 1, \dots, n_f$. Now, let $P \subset \Omega$ be a set of non-dominated solutions \tilde{x}_a ; if, for any $\tilde{x}_a \in P$, there is no $x_b \in \Omega$ dominating \tilde{x}_a , then P represents the Pareto set and the corresponding image $F(P)$ is the Pareto front; the latter is called also trade-off curve.

Traditionally, the multiobjective problem is reduced to a single-objective one by introducing a preference function $\psi(x)$, e.g. the weighted sum of $f_i(x)$:

$$\psi(x) = \sum_{i=1}^{n_f} c_i f_i(x), \quad 0 < c_i < 1, \quad \sum_{i=1}^{n_f} c_i = 1 \quad (7.9)$$

The numerical identification of the whole Pareto front can be pursued as shown later.

7.4 Gradient-Free and Gradient-Based Methods

Several algorithms for both unconstrained and constrained optimization are available; basically, they can be sorted into two broad classes, i.e. gradient-free and gradient-based methods; in the former case, the information about the derivative is not used while in the latter case it is.

Methods that use only function evaluations (zero-order methods) fall under the first class; they are suitable for problems characterized by non-linearity and discontinuities of the objective function. The computational efficiency is low, due to repeated calls to the objective function.

In turn, first-order gradient-based methods basically follow the direction of the steepest descent; they are more efficient than the zero-order ones. When regular objective functions are dealt with. The simplest way to approximate the gradient of the objective function relies on finite differences; e.g. if $g_i(x_i) \equiv \frac{\partial f}{\partial x_i}$ is the i th component of the gradient, a forward difference gives

$$g_i(x_i) \cong \frac{f(x_i + h) - f(x_i)}{h}, \quad i = 1, \dots, n \quad (7.10)$$

where h is the incremental step. However, it should be noted that the approximation of the gradient is expensive and represents also an additional source of numerical ill conditioning (round-off errors in the computation of both objective functions and finite differences).

Higher-order methods, like Newton's method, are rarely used because they are suitable only when the Hessian matrix can be easily computed.

7.5 Deterministic vs Non-Deterministic Search

Regardless of the order, all the aforementioned methods are local in a sense, because they are able to identify the closest minimum to the starting point, which is a local one, unless f is convex. For this reason they are said to perform a deterministic search.

To cope with these difficulties, non-deterministic minimization algorithms, which are derivative-free and perform a stochastic search, have been developed.

Non-deterministic methods offer remarkable advantages over methods that use only local information to improve the current solution. In fact, they are robust, reliable and suitable for non-convex, non-smooth and discontinuous functions, also with discrete-valued variables. In particular, they give a chance to approximate the global minimum of the objective function, regardless of the starting point. Another advantage is that they exhibit an inherent parallelism. The drawbacks are the huge computational effort and the slow convergence.

Since they have a heuristic background, it has to be pointed out that for non-deterministic methods convergence is proven just in numerical terms and not on theoretical basis, contrary to what happens for their deterministic counterpart.

In the non-deterministic category, the most popular methods are: simulated annealing, evolution strategies, genetic algorithms. More recently, a class of nature-inspired methods has been developed, among which: ant colony, particle swarm, artificial immune systems.

7.6 A Deterministic Algorithm of Lowest Order: Simplex Method

The simplex method is based on the comparison among the cost function values at the $n + 1$ vertices of a polytope (simplex), where n is equal to the dimension of the search space. In the case of $n = 2$ ($n = 3$), the polytope is a triangle (a tetrahedron).

The algorithm begins with $n + 1$ points, which form the starting polytope, and the calculation of the associated objective function values. At each iteration a new polytope is set up by generating a new point to replace the worst vertex of the old polytope, i.e. the vertex corresponding to the highest value of objective function. Specifically, the worst vertex is replaced by its reflection with respect to the remaining n vertices. If the objective function evaluated at the new point is higher than at the worst vertex, then the new point is rejected and the vertex with the second worst value is reflected.

When it happens that a vertex belongs to the polytope for a number of iterations which exceeds the given one, then the polytope is updated by contraction. The whole procedure is iterated until the diameter of the simplex is less than the specified tolerance.

7.7 A Non-Deterministic Algorithm of Lowest Order: Evolution Strategy

Evolution strategy mimics the survival of the fittest individual that is observed in nature. An algorithm of the lowest order (i.e. a single parent generates a single offspring) is here shortly presented (Fig. 7.1). The search in the design space begins in a region of radius d_0 (standard deviation) centered at the initial point m_0 (mean value); m_0 is externally provided, while d_0 is internally calculated on the basis of the bounds boxing the variation of the design variables.

Setting $m = m_0$ and $d = d_0$ at the initial iteration, the *generation* of the design vector $x = m + ud$ then proceeds, resorting to a stochastic sample $u \in (0, 1)$; generally, u is a normally distributed sample. It is verified that x fulfils bounds and constraints (i.e. that x is feasible), otherwise a new design vector is generated until it falls inside the feasible region.

The associated objective function $f(x)$ is then evaluated and the test $f(x) < f(m)$ is performed; if the test is successful, m is replaced by x (the so-called *mutation* or *selection* process), otherwise m is retained.

The next step is concerned with the size of the search region that will be used for the successive iteration. The underlying rationale is that, when a point better than the current one is found, the radius of the search region is increased around the new point to search for further improvements; if no improvement is found, the radius of the search region is gradually decreased up to convergence (*annealing* process).

In this respect, the evolutionary algorithm substantially differs from a deterministic one, in which the search region would be narrowed around the better point in order

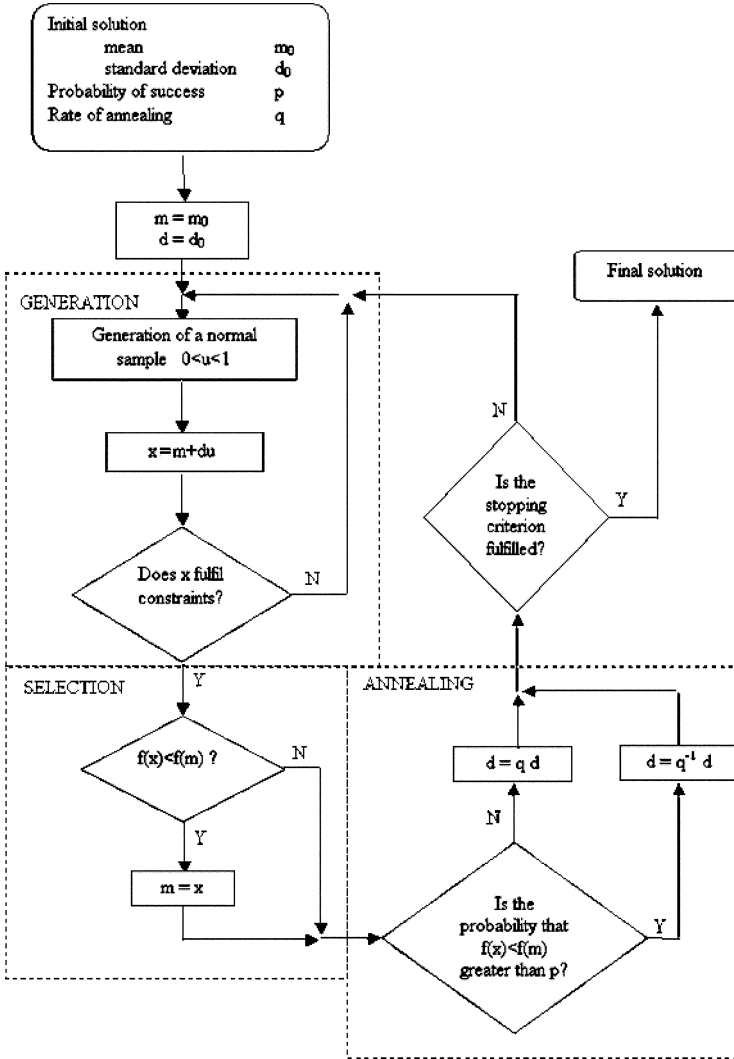


Fig. 7.1 Flow-chart of the evolutionary minimization algorithm

to converge towards the corresponding nearest minimum. The drawback, in the latter case, is that this minimum might be a local one. On the contrary, the evolutionary algorithm, if successful in finding a better point, covers a larger region of search in order to see if there might be another good candidate in the neighborhood, and then does the opposite when this is not possible. This way, there is a non-zero probability of finding the region where the global optimum of the objective function is located.

The *annealing* process is ruled by the history of the k previous iterations, used to establish a trend: if at least a fraction p of the last k iterations were successful (an

iteration is successful if x is feasible and improves the objective function), then the trend is said to be positive, while it is negative otherwise. If the trend is positive, the radius d of the search region is set to $q^{-1}d$; otherwise, it is set to qd . In particular, during the first k iterations, d remains unchanged.

The procedure stops when the prescribed accuracy $|\frac{d}{d_0}|$ is achieved. Quantities p and q are named probability of success and rate of annealing, respectively and represent the “tuning knobs” of the algorithm; heuristic values for k , p and q are 50, 0.2 and 0.8–0.9, respectively.

7.8 Numerical Case Studies

A few case studies are here presented.

The solution of the direct problem relies on a finite-element analysis of the field, while the inverse problem is solved by optimizing a suitable objective function subject to constraints.

All case studies refer to the computational domain shown in Fig. 7.2, which in Section 2.3.7 has been assumed as a test problem to simulate the so-called slot of electrical machine.

The direct problem is formulated as follows

find the magnetic potential $A(x_1, x_2)$ such that in $\Omega = \bigcup_{i=1}^4 \Omega_i$

$$-\bar{\nabla} \cdot (\mu^{-1} \bar{\nabla} A) = J \chi_{\Omega_1} \tag{7.11}$$

where J is constant and χ_{Ω_1} is the characteristic function of Ω_1 (i.e. the current density is uniform in the winding and zero elsewhere); (7.11) is subject to boundary conditions

$$A(x_1, 0) = 0 \tag{7.12}$$

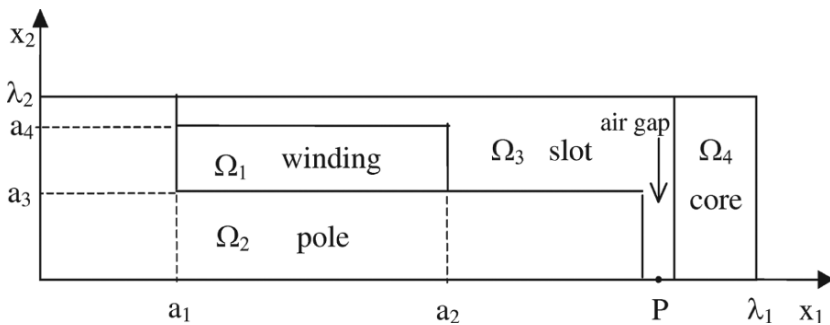


Fig. 7.2 Single-side slotted electrical machine: field domain

and along $\partial\Omega \setminus \{x_2 = 0\}$

$$\frac{\partial A}{\partial \mathbf{n}} = 0 \tag{7.13}$$

The problem might be either linear or non-linear, depending on the constitutive relationship assumed for the ferromagnetic material.

Some cases of solution to problem (7.11)–(7.13) are shown in the following.

7.8.1 Identification of the B–H Curve of the Iron Region of a Magnetic Pole

The problem reads

given the geometry of the pole and the current density in the winding, find the constitutive relationship $\mathbf{B} = \mathbf{B}(\mathbf{H})$ of the ferromagnetic region $\Omega_2 \cup \Omega_4$, such that the x_1 -directed component of induction is prescribed along the line $x_1 = x_1(\mathbf{P})$, $0 \leq x_2 \leq \lambda_2$ passing through point P (Fig. 7.2).

The following analytical model for the iron reluctivity is assumed:

$$\nu \left(|\overline{\mathbf{B}}|^2 \right) = \nu_0 \frac{1 + \gamma |\overline{\mathbf{B}}|^{2\alpha}}{\mu_{\max} + \mu_{\min} \gamma |\overline{\mathbf{B}}|^{2\alpha}}, \quad 2\alpha > 1, \quad \gamma > 0 \tag{7.14}$$

where ν_0 is the reluctivity of the free space, while μ_{\max} and μ_{\min} are maximum and minimum values of relative permeability, respectively. Fig. 7.3 shows a typical B–H curve of an iron lamination; it corresponds to

$$(\alpha, \gamma) = (5, 5 \cdot 10^{-2}) \text{ and } (\mu_{\max}, \mu_{\min}) = (5 \cdot 10^3, 2 \cdot 10^2).$$

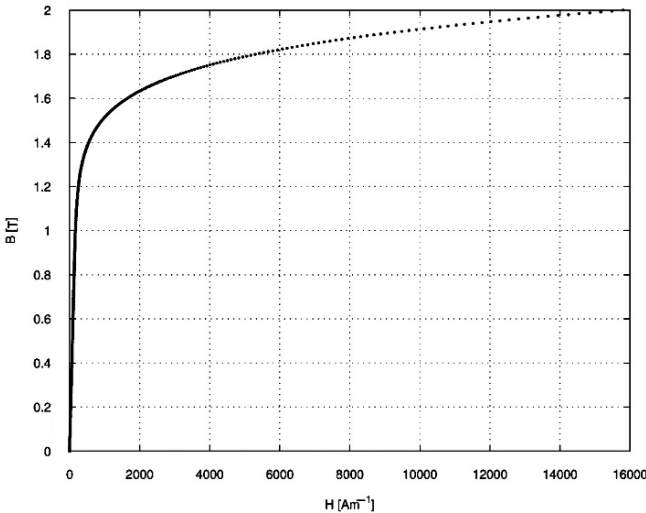


Fig. 7.3 A typical B–H curve of iron lamination

From the theoretical viewpoint, (7.14) makes the direct problem (7.11)–(7.13) a non-linear one so that, in principle, existence and uniqueness of the solution are not given a priori; nevertheless, it could be proven that the derivative $\frac{d|\mathbf{B}|}{d|\mathbf{H}|} = \mu(|\mathbf{H}|) + |\mathbf{H}| \frac{d\mu}{d|\mathbf{H}|}$ is bounded for any $|\mathbf{H}|$ and this makes the direct problem a well-posed one. To solve it numerically, the Newton-Raphson method (see Section 2.3.2) is applied.

Therefore, a bivariate identification problem is set up given the geometry of the pole and the current density in the winding, find (α, γ) in (7.14) such that $B_1(x_1(P), x_2) = B_0(x_2)$, $0 \leq x_2 \leq \lambda_2$, where B_0 is the known air-gap induction.

In practice, the error functional

$$f(\alpha, \gamma) = \sup_{x_2} |B_1(x_1(P), x_2, \alpha, \gamma) - B_0(x_2)|, \quad 0 \leq x_2 \leq \lambda_2 \tag{7.15}$$

is minimized with respect to (α, γ) , taking $\alpha > \frac{1}{2}$, $\gamma > 0$

The prescribed distribution of induction B_0 at the air-gap, coming from a finite-element solution of the direct problem, is shown in Fig. 7.4.

The finite-element mesh used for solving the direct problem is composed of 7,008 triangles with linear variation of the potential; it is shown in Fig. 7.5.

The minimization results are reported in Table 7.1; they have been obtained using the algorithm presented in Section 7.7.

The starting point corresponds to a permeability constant and equal to μ_{\max} (linear case).

The minimization trajectory in the design space is shown in Fig. 7.6.

The field solution, in terms of the flux lines corresponding to the optimal values of parameters (α, γ) , is represented in Fig. 7.7.

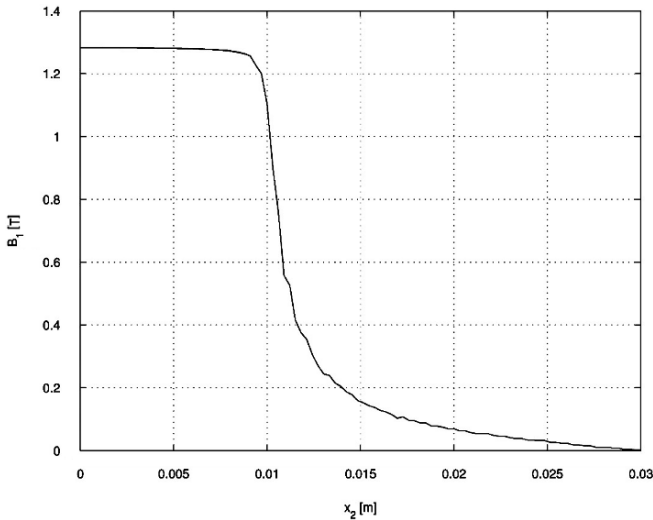


Fig. 7.4 Known air-gap induction

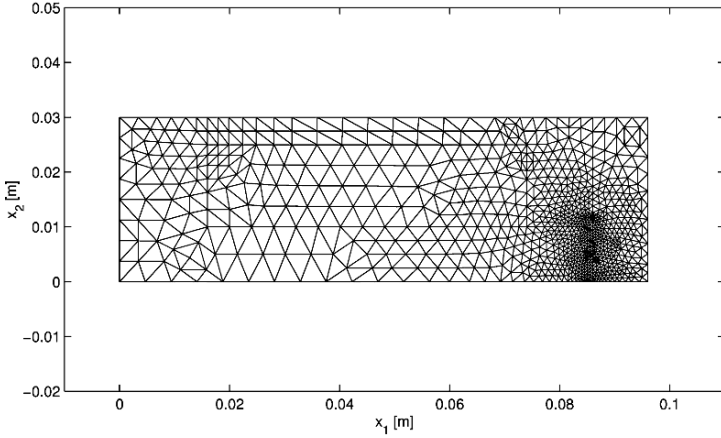


Fig. 7.5 Finite-element discretization of the computational domain

Table 7.1 B–H curve identification: Results

	γ	α	f
Start	0	0	1.43455
End	$3.8737 \cdot 10^{-2}$	5.2541	$9.71965 \cdot 10^{-4}$

Tolerance at convergence $< 10^{-6}$

Iterations 182

Runtime 14,107 [s]

Processor 2 GB, 2 GHz

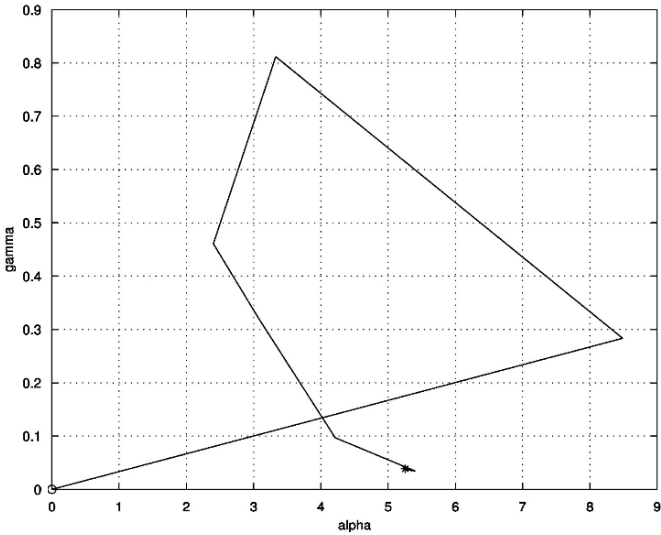


Fig. 7.6 Optimization trajectory in the design space (start, circle; end, star)

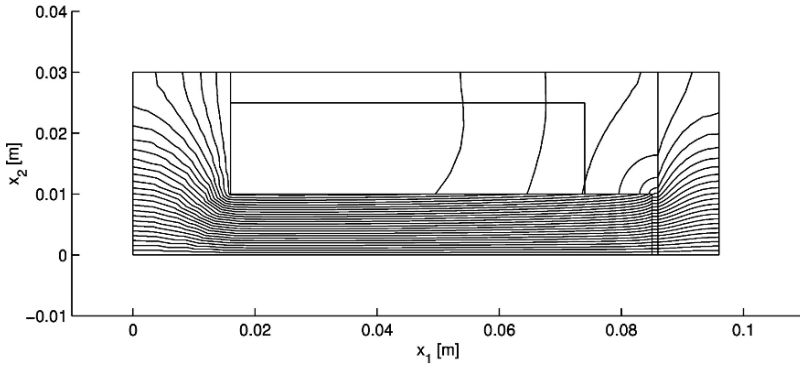


Fig. 7.7 Identification of B–H curve: geometry and flux lines

7.8.2 Shape Design of a Magnetic Pole (Static Optimization)

Let the vector $g = (a_1, a_2, a_3, a_4)$ of geometric variables as in Fig. 7.2 be defined, such that

$$\alpha_1 \leq a_1 < a_2 \leq \alpha_2 \quad (7.16)$$

and

$$\alpha_3 \leq a_3 < a_4 \leq \alpha_4 \quad (7.17)$$

with $\alpha_i > 0$, $i = 1, 4$. Then, the problem reads defined the objective function

$$f(g) = \sup_{(x_1, x_2) \in \Omega_1} |B_2(x_1, x_2, g)| \quad (7.18)$$

find the vector $\tilde{g} = [\tilde{a}_1, \tilde{a}_2, \tilde{a}_3, \tilde{a}_4]$ such that

$$f(\tilde{g}) = \inf f(g) \quad (7.19)$$

under the constraint

$$h(g) \geq k_1 > 0, \quad h(g) = |B_1(x_1(P), 0, g)| \quad (7.20)$$

The objective function (7.18) accounts for the maximum value of the fringing field in the winding, which is to be minimized, while (7.20) is the air-gap field at point P (Fig. 7.2) constrained by the threshold k_1 .

As far as the direct problem is concerned, the current density in the winding and the material properties are given; in particular, the non-linear relationship (7.14) with $(\alpha, \gamma) = (5, 5 \cdot 10^{-2})$ is assumed for the ferromagnetic material.

This is a problem of static optimization, because both direct and inverse problems do not depend on time.

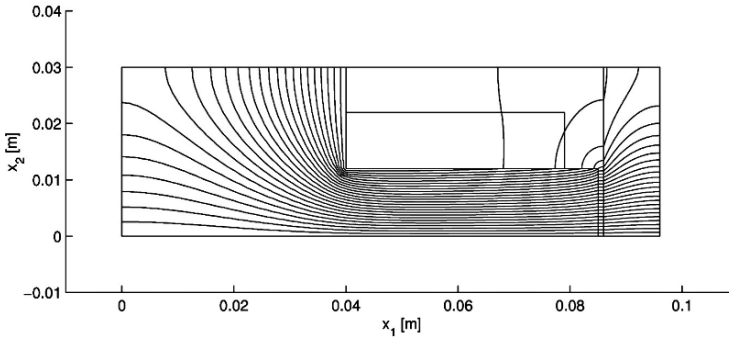


Fig. 7.8 Static optimization: initial geometry and flux lines

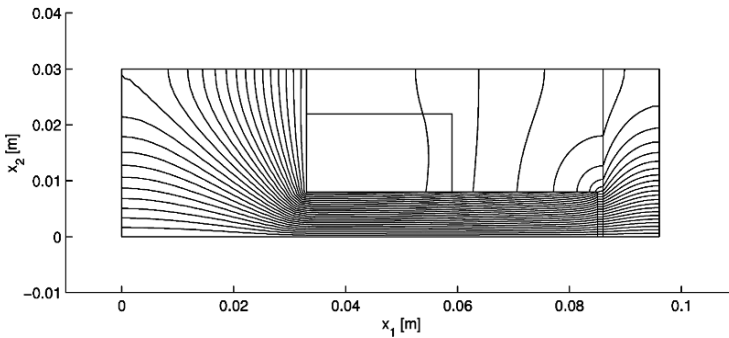


Fig. 7.9 Evolutionary algorithm: final geometry and flux lines

The initial geometry shown in Fig. 7.8 has been used to start the optimization.

Using the evolutionary algorithm, the results reported in Figs. 7.9 and 7.10 and Table 7.2 have been obtained.

For the sake of a comparison, the optimization has been repeated, using the simplex algorithm; in particular, the constraint $h(\mathbf{g}) > k_1$ has been taken into account by means of a penalty term added to the objective function (7.18). The results are reported in Figs. 7.11 and 7.12 and Table 7.3.

Comparing the two curves of the objective function vs iterations represented in Figs. 7.10 and 7.12, respectively, it can be remarked that the oscillating behaviour is particularly evident for more than 80 iterations in the former case while it disappears after 20 iterations in the latter case. This peculiarity can be attributed to the global search performed by the evolutionary algorithm with respect to the local search of the simplex algorithm. On the other hand, the latter requires a runtime remarkably shorter (see Tables 7.2 and 7.3).

Finally, comparing the results obtained by the two methods it can be remarked that two different final geometries are found, starting from the same initial geometry. Certainly, they represent an improvement with respect to the initial solution, but they

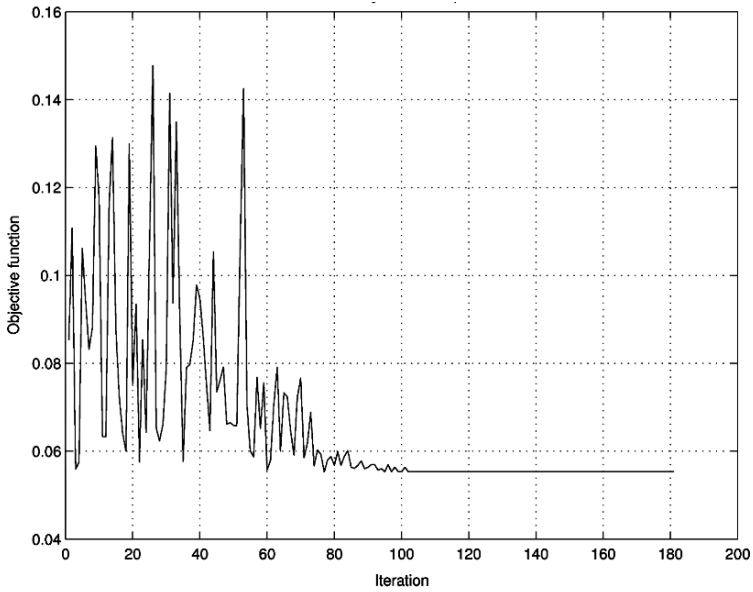


Fig. 7.10 Evolutionary algorithm: history of the objective function

Table 7.2 Evolutionary algorithm: Optimization results

	a_1 (mm)	a_2 (mm)	a_3 (mm)	a_4 (mm)	f (T)	h (T)
Start	40	79	12	22	$11.8191 \cdot 10^{-2}$	1.13239
End	33	59	8	22	$5.5324 \cdot 10^{-2}$	1.00014

Mesh triangles 6,752 (start), 5,712 (end)

Tolerance at convergence $< 10^{-6}$

Constraint threshold $k_1 = 1$ [T]

Iterations 182

Runtime 18,946 [s]

Processor 2 GB, 2 GHz

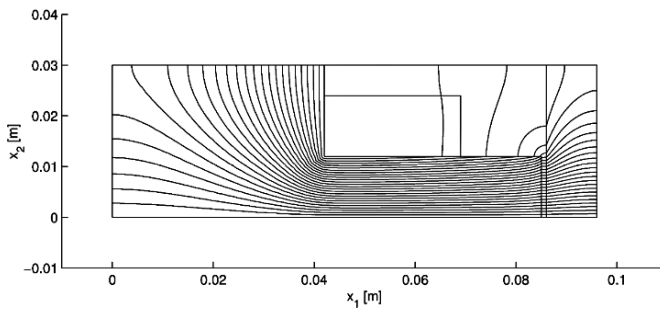


Fig. 7.11 Simplex algorithm: final geometry and flux lines

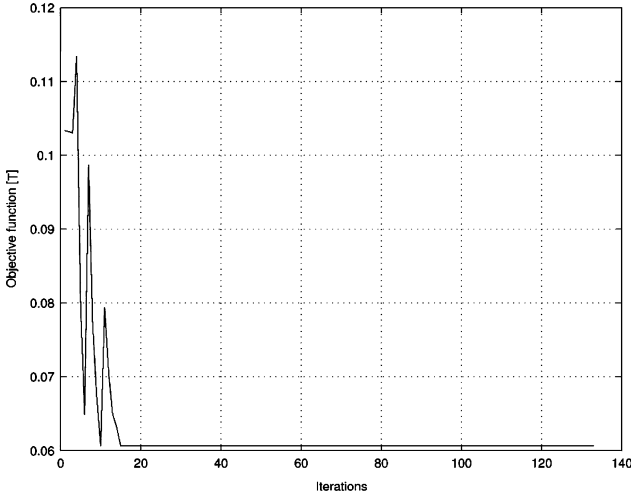


Fig. 7.12 Simplex algorithm: history of the objective function

Table 7.3 Simplex algorithm: Optimization results

	a ₁ (mm)	a ₂ (mm)	a ₃ (mm)	a ₄ (mm)	f (T)	h (T)
Start	40	79	12	22	11.8191 10 ⁻²	1.13239
End	42	69	12	24	6.0638 10 ⁻²	1.0114

Tolerance at convergence < 10⁻⁶
 Constraint threshold k₁ = 1 [T]
 Iterations 33
 Constraint violations 15
 Objective function calls 133
 Runtime 339 [s]
 Processor 2 GB, 2 GHz

are not coincident because they depend on the tuning knobs of the numerical algorithm; moreover, it cannot be stated that a unique end of the optimization procedure exists.

7.8.3 Shape Design of a Magnetic Pole (Dynamic Optimization)

The direct problem reads

find the magnetic potential $A(x_1, x_2, t)$ such that in $\Omega = \bigcup_{i=1}^4 \Omega_i$

$$\sigma \frac{\partial A}{\partial t} - \bar{\nabla} \cdot (\mu^{-1} \bar{\nabla} A) = J \chi_{\Omega_1} \tag{7.21}$$

where χ_{Ω_1} is the characteristic function of subdomain Ω_1 , subject to initial condition

$$A(x_1, x_2, 0) = 0 \tag{7.22}$$

and boundary conditions

$$A(x_1, 0, t) = 0 \quad (7.23)$$

and along $\partial\Omega \setminus \{x_2 = 0\}$

$$\frac{\partial A}{\partial \mathbf{n}} = 0 \quad (7.24)$$

A problem of transient magnetic diffusion under current step excitation is set up; the constitutive relationship of the ferromagnetic material is assumed to be linear.

The time integration of (7.21) is based on a standard Runge-Kutta routine.

As far as the inverse problem is concerned, let the vector $\mathbf{g} = (a_1, a_2, a_3, a_4)$ of geometric variables as in Fig. 7.2 be defined, such that

$$\alpha_1 \leq a_1 < a_2 \leq \alpha_2 \quad (7.25)$$

and

$$\alpha_3 \leq a_3 < a_4 \leq \alpha_4 \quad (7.26)$$

with $\alpha_i > 0$, $i = 1, 4$.

Then, the problem becomes defined the objective function

$$f(\mathbf{g}) = \sup_{(x_1, x_2) \in \Omega_1} |B_y(x_1, x_2, \mathbf{g}, \bar{t})| \quad (7.27)$$

find the vector $\tilde{\mathbf{g}} = [\tilde{a}_1, \tilde{a}_2, \tilde{a}_3, \tilde{a}_4]$ such that

$$f(\tilde{\mathbf{g}}) = \inf f(\mathbf{g}) \quad (7.28)$$

under the constraint

$$h(\mathbf{g}) \geq k_1 > 0, \quad h(\mathbf{g}) = |B_x(x_1(P), 0, \mathbf{g}, \bar{t})| \quad (7.29)$$

It is assumed that $\bar{t} = \frac{1}{2}T$, where $T = \lambda^2 \max_{i=1,4} (\mu_i \sigma_i)$ with $\lambda = \min(a_2 - a_1, a_4 - a_3)$ is the diffusion time constant.

In other words, the geometry which minimizes the fringing field at time \bar{t} for a given air-gap field at the same time instant is searched for. This is a problem of dynamic optimization, because both direct and inverse problems are time-dependent. It is important to underline that the actual value of T , and so \bar{t} , varies with the geometry \mathbf{g} considered; in turn, the ratio of the controlled time \bar{t} to the time constant T is prescribed. When $\bar{t} \rightarrow \infty$ the corresponding static case is set up, which was already developed in the previous Section 7.8.2.

The initial geometry considered for the optimization is shown in Fig. 7.13. The following data are assumed: $\mu_1 = \mu_3 = \mu_0$, $\mu_2 = \mu_4 = 10^3 \mu_0$, $J = 3 \cdot 10^6 \text{ A m}^{-2}$, $\lambda_1 = 96 \text{ mm}$, $\lambda_2 = 30 \text{ mm}$; the air-gap is 1 mm wide.

Using the evolutionary algorithm, the results reported in Fig. 7.14 and Table 7.4 are obtained.

Considering the distribution of flux lines in Figs. 7.13 and 7.14, it can be remarked that at time \bar{t} the magnetic field has not yet diffused completely through the ferromagnetic region. Moreover, from Table 7.4 it results that initial and final geometries are characterized by the same value of diffusion time constant $T = 628 \text{ ms}$.

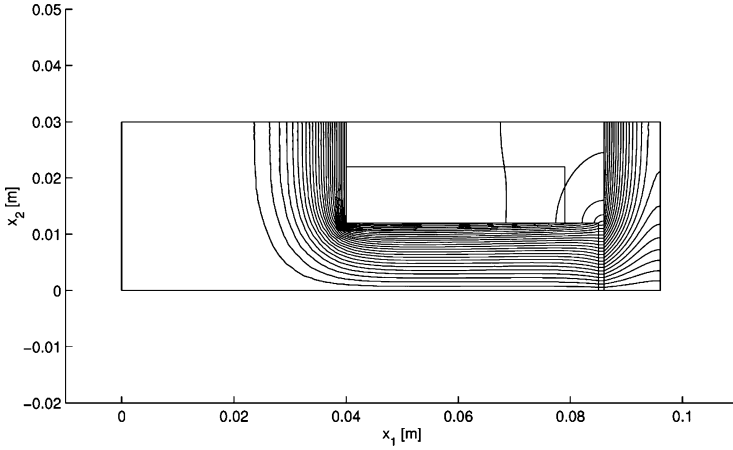


Fig. 7.13 Dynamic optimization: flux lines at time \bar{t} for the initial geometry

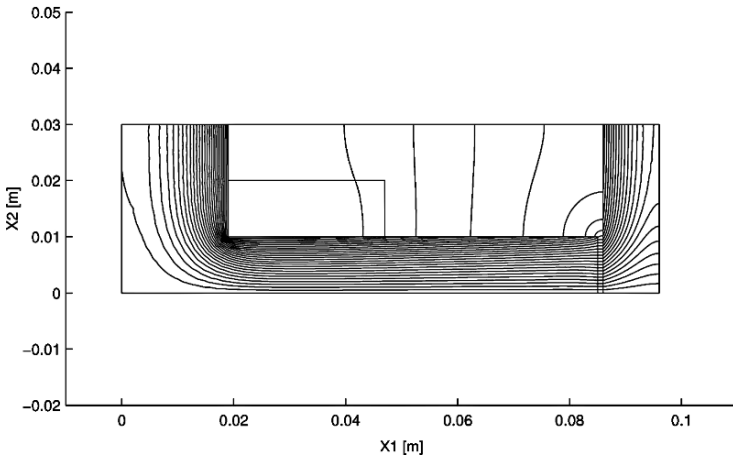


Fig. 7.14 Dynamic optimization: flux lines at time \bar{t} for the final geometry

Table 7.4 Dynamic optimization results ($t = \bar{t}$)

	a_1 (mm)	a_2 (mm)	a_3 (mm)	a_4 (mm)	f (T)	h (T)
Start	40	79	12	22	$7.41645 \cdot 10^{-2}$	0.70006
End	42	69	12	24	$3.66103 \cdot 10^{-2}$	0.60893

Mesh triangles 6,752 (start), 6,048 (end)

Tolerance at convergence $< 10^{-6}$

Constraint threshold $k_1 = 0.6$ [T]

Iterations 182

Runtime 6,128 [s]

Processor 2 GB, 2 GHz

7.8.4 A Multiobjective Approach to the Shape Design of a Magnetic Pole

Let the vector $g = (a_1, a_2, a_3, a_4)$ of geometric variables as in Fig. 7.2 be defined, such that

$$\alpha_1 \leq a_1 < a_2 \leq \alpha_2 \quad (7.30)$$

and

$$\alpha_3 \leq a_3 < a_4 \leq \alpha_4 \quad (7.31)$$

with $\alpha_i > 0$, $i = 1, 4$. Then, the following inverse problem is set up defined the objective functions

$$f_1(g) = |B_x(x_1(P), 0, g)| \quad (7.32)$$

and

$$f_2(g) = \sup_{(x_1, x_2) \in \Omega_1} |B_y(x_1, x_2, g)| \quad (7.33)$$

find the family of vectors $\tilde{g} = [\tilde{a}_1, \tilde{a}_2, \tilde{a}_3, \tilde{a}_4]$ such that

$$f_2(\tilde{g}) = \inf f_2(g) \quad (7.34)$$

under the constraint

$$f_1(g) \geq k_1 > 0 \quad (7.35)$$

or

$$f_1(\tilde{g}) = \sup f_1(g) \quad (7.36)$$

under the constraint

$$f_2(g) \geq k_2 > 0 \quad (7.37)$$

The problem formulation (7.34)–(7.35) or (7.36)–(7.37) leads to the associated Pareto front when thresholds k_1 or k_2 are varied, respectively.

A simple numerical procedure to identify the non-dominated solutions of a multiobjective optimization problem is given by the sample-and-rank method; to this end, a distribution of samples is generated in the feasible region of the design space, based on a uniform probability-density function. Samples are then mapped into the objective space via calculation of the objectives, so determining a distribution that in general is a non-uniform one. This way, the search space is explored exhaustively. The criterion of Pareto optimality is then applied and non-dominated solutions are extracted from the set of samples in the objective space; the corresponding points in the design space identify the optimal geometries.

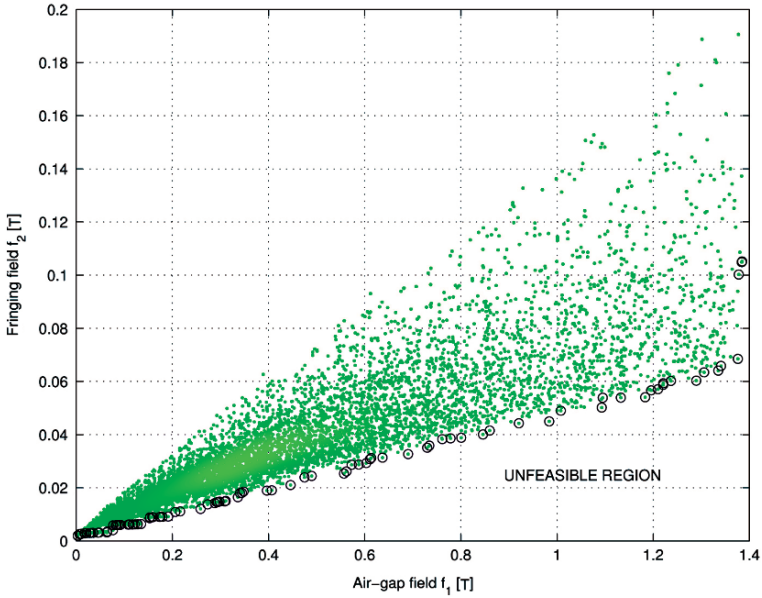


Fig. 7.15 Sampled objective space (dot) with non-dominated solutions outlined (circle)

The accuracy of the method in capturing the Pareto front depends on the density of samples in the design space; the whole computational cost c_1 of the method can be estimated as

$$c_1 \approx n_p^{n_v} \cdot n_f \cdot c_0 \tag{7.38}$$

where n_p is the number of points discretizing each of the n_v variables, n_f is the number of objectives and c_0 is the processor-dependent cost of a single finite-element analysis.

Fig. 7.15 shows a discrete representation of the objective space (f_1, f_2) obtained by random sampling the design space (a_1, a_2, a_3, a_4) . In particular, 10^4 points are generated assuming the following data: $\mu_1 = \mu_3 = \mu_0, \mu_2 = \mu_4 = 10^3 \mu_0, J = 3 \cdot 10^6 \text{ Am}^{-2}, \lambda_1 = 96 \text{ mm}, \lambda_2 = 30 \text{ mm}$; the air-gap is 1 mm wide.

For each point a finite-element mesh composed of about 6,000 triangles with linear variation of potential is generated and the subsequent analysis of the direct problem (7.11)–(7.13) is performed. After ranking all the points in the (f_1, f_2) plane, 146 out of 10^4 points approximate the Pareto front.

From the technical viewpoint, the Pareto front of non-dominated solutions corresponds to the set of geometries such that the fringing field in the winding is minimum for a given value of air-gap induction. A posteriori, a single non-dominated solution can be selected according to an additional criterion of decision making.

Chapter 8

Conclusion

At the end of this short excursion in the domain of static and quasi-static electromagnetism, looking back at the pathways run through, the authors realize that it was possible to highlight just some basic topics of the domain and to describe them in a very concise and essential way.

When possible, they tried to offer an original insight into well-known topics, but they do not pretend to have been exhaustive and are happy if they have been clear and hopefully correct.

The main intention was to provide the readers with methods for modelling electric and magnetic devices and systems, adopting a problem-solving approach. Both direct and inverse problems have been proposed and developed. In this respect, the Euclidean linear space, equipped with the usual norm, has been assumed to describe the geometry of the electromagnetic field. Therefore, all the analysis of Maxwell's equations has been based on the concepts of vector and relevant operators grad, div, curl. Accordingly, singularities due to lumped sources have been treated directly in terms of fields rather than potentials.

Throughout the book, in particular, a couple of magnetic test problems has been considered and solved by different methods. The comparison of the different approaches and of the relevant results is left to the readers; nevertheless, the leading idea is that different methods, both analytical and numerical, can be used to solve a given class of real-life problems: the actual choice depends on the acceptable trade-off between cost and accuracy of methods.

The authors will be satisfied if the readers, especially students, find the book helpful and not too heavy; in any case, they will be pleased to receive comments and suggestions for improvements.

Appendix

Delta Function

Let $f(x)$ be a given real function of real variable x . The so-called delta function $\delta(x - x_0)$ (or Dirac's delta) is an operator which transforms the given function $f(x)$, supposed to be continuous in x_0 , into $f(x_0)$, namely

$$\int_a^b f(x)\delta(x - x_0)dx = f(x_0), \quad a \leq x_0 \leq b \quad (\text{A.0})$$

Elementary Vector Analysis

In a three-dimensional domain, using rectangular coordinates, special vectors are the space vectors $\bar{r}_P = (x_P, y_P, z_P)$ and $\bar{r}_Q = (x_Q, y_Q, z_Q)$, defining field point P and source point Q, respectively (Fig. A.1).

The Euclidean distance between P and Q is

$$r = |\bar{r}| = \left[(x_P - x_Q)^2 + (y_P - y_Q)^2 + (z_P - z_Q)^2 \right]^{\frac{1}{2}} = |\bar{r}_P - \bar{r}_Q| \quad (\text{A.1})$$

A special function is $\frac{1}{r}$, $r \neq 0$; it turns out to be:

$$\bar{\nabla}_P \frac{1}{r} = -\frac{\bar{r}}{r^3}, \quad \bar{\nabla}_Q \frac{1}{r} = \frac{\bar{r}}{r^3} \quad (\text{A.2})$$

$$\bar{\nabla}_P \frac{1}{r} = -\frac{\bar{r}}{r^3}, \quad \bar{\nabla}_Q \frac{1}{r} = \frac{\bar{r}}{r^3} \quad (\text{A.3})$$

$$\bar{\nabla}_P \cdot \bar{r} = 3, \quad \bar{\nabla}_Q \cdot \bar{r} = -3 \quad (\text{A.4})$$

$$\nabla_P^2 \frac{1}{r} = -4\pi\delta(r) \quad (\text{A.5})$$

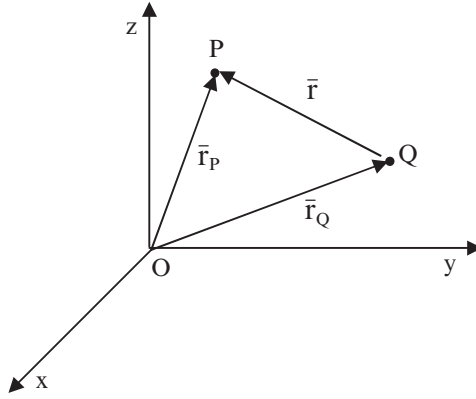


Fig. A.1 Field point P and source point Q

$$\bar{\nabla} \times \left(-\frac{\bar{r}}{r^3} \right) = \bar{\nabla} \times \bar{\nabla} \frac{1}{r} = 0 \quad (\text{A.6})$$

$$\int_{\Omega} \frac{\delta(\mathbf{r}_Q)}{r} d\Omega = \frac{1}{r} \quad (\text{A.7})$$

The following formulae hold:

$$\bar{\nabla} \cdot (\bar{\nabla} \times \bar{\nabla}) = 0 \quad (\text{A.8})$$

$$\bar{\nabla} \times \bar{\nabla} \phi = 0 \quad (\text{A.9})$$

Gauss's or divergence theorem

$$\int_{\Omega} \bar{\nabla} \cdot \bar{B} d\Omega = \int_{\Gamma} \bar{B} \cdot \bar{n} d\Gamma \quad (\text{A.10})$$

with $\Gamma = \partial\Omega$ closed surface enclosing Ω and \bar{n} outward normal vector.

Stokes's or circulation theorem

$$\oint_{\lambda} \bar{A} \cdot \bar{t} d\lambda = \int_{\Gamma} (\bar{\nabla} \times \bar{A}) \cdot \bar{n} d\Gamma \quad (\text{A.11})$$

with $\lambda = \partial\Gamma$ closed line representing the border of Γ and \bar{t} anticlockwise tangential vector.

Vector identities

$$\bar{\nabla} \times (\bar{\nabla} \times \bar{A}) = \bar{\nabla} (\bar{\nabla} \cdot \bar{A}) - \bar{\nabla}^2 \bar{A} \quad (\text{A.12})$$

$$\bar{\nabla} \cdot (\bar{\nabla}_1 \times \bar{\nabla}_2) = \bar{\nabla}_2 \cdot (\bar{\nabla} \times \bar{\nabla}_1) - \bar{\nabla}_1 \cdot (\bar{\nabla} \times \bar{\nabla}_2) \quad (\text{A.13})$$

$$\bar{\nabla} \cdot (\phi \bar{\nabla}) = \bar{\nabla} \cdot \bar{\nabla} \phi + \phi \bar{\nabla} \cdot \bar{\nabla} \quad (\text{A.14})$$

$$\bar{\nabla} \times (\bar{\nabla}_1 \times \bar{\nabla}_2) = \bar{\nabla}_1 \bar{\nabla} \cdot \bar{\nabla}_2 - \bar{\nabla}_2 \bar{\nabla} \cdot \bar{\nabla}_1 + (\bar{\nabla}_2 \cdot \bar{\nabla}) \bar{\nabla}_1 - (\bar{\nabla}_1 \cdot \bar{\nabla}) \bar{\nabla}_2 \quad (\text{A.15})$$

$$\bar{\nabla} \times \phi \bar{\nabla} = \phi \bar{\nabla} \times \bar{\nabla} + \bar{\nabla} \phi \times \bar{\nabla} \quad (\text{A.16})$$

In cylindrical coordinates

$$\bar{\nabla} \cdot \bar{\mathbf{V}} = r^{-1} \frac{\partial(r\mathbf{V}_r)}{\partial r} + r^{-1} \frac{\partial\mathbf{V}_\vartheta}{\partial\vartheta} + \frac{\partial\mathbf{V}_z}{\partial z} \quad (\text{A.17})$$

$$\nabla^2\mathbf{U} = \frac{\partial^2\mathbf{U}}{\partial r^2} + r^{-1} \frac{\partial\mathbf{U}}{\partial r} + r^{-2} \frac{\partial^2\mathbf{U}}{\partial\vartheta^2} + \frac{\partial^2\mathbf{U}}{\partial z^2} \quad (\text{A.18})$$

In spherical coordinates

$$\bar{\nabla} \cdot \bar{\mathbf{V}} = r^{-2} \frac{\partial(r^2\mathbf{V}_r)}{\partial r} + (r \sin\vartheta)^{-1} \frac{\partial(\mathbf{V}_\vartheta \sin\vartheta)}{\partial\vartheta} + (r \sin\vartheta)^{-1} \frac{\partial\mathbf{V}_\varphi}{\partial\varphi} \quad (\text{A.19})$$

$$\nabla^2\mathbf{U} = r^{-2} \frac{\partial}{\partial r} \left(r^2 \frac{\partial\mathbf{U}}{\partial r} \right) + r^{-2} (\sin\vartheta)^{-1} \frac{\partial}{\partial\vartheta} \left(\sin\vartheta \frac{\partial\mathbf{U}}{\partial\vartheta} \right) + (r \sin\vartheta)^{-2} \frac{\partial^2\mathbf{U}}{\partial\varphi^2} \quad (\text{A.20})$$

$$(\bar{\nabla} \times \bar{\mathbf{V}})_r = (r \sin\vartheta)^{-1} \left(\frac{\partial(\mathbf{V}_\varphi \sin\vartheta)}{\partial\vartheta} - \frac{\partial\mathbf{V}_\vartheta}{\partial\varphi} \right) \quad (\text{A.21})$$

$$(\bar{\nabla} \times \bar{\mathbf{V}})_\vartheta = (r \sin\vartheta)^{-1} \left(\frac{\partial\mathbf{V}_r}{\partial\varphi} - \frac{\partial(r \sin\vartheta \mathbf{V}_\varphi)}{\partial r} \right) \quad (\text{A.22})$$

$$(\bar{\nabla} \times \bar{\mathbf{V}})_\varphi = r^{-1} \left(\frac{\partial(r\mathbf{V}_\vartheta)}{\partial r} - \frac{\partial\mathbf{V}_r}{\partial\vartheta} \right) \quad (\text{A.23})$$

$$\bar{\nabla}\mathbf{U} = \left(\frac{\partial\mathbf{U}}{\partial r}, \frac{1}{r} \frac{\partial\mathbf{U}}{\partial\vartheta}, \frac{1}{r \sin\vartheta} \frac{\partial\mathbf{U}}{\partial\varphi} \right) \quad (\text{A.24})$$

References

- Binns K.J. and Lawrenson P.J.: Analysis and computation of electric and magnetic field problems. Pergamon, 1973.
- Bossavit A.: Computational electromagnetism. Academic, 1998.
- Chari M.V.K. and Silvester P.P.: Finite Elements in Electrical and Magnetic Field Problems. Wiley, 1980.
- Davies A.J.: The finite element method. Clarendon, 1980.
- Hameyer K. and Belmans R.: Numerical Modelling and Design of Electrical Machines and Devices. MIT, 1999.
- Hammond P.: Applied electromagnetism. Pergamon, 1971.
- Hammond P.: Energy methods in electromagnetism. Clarendon, 1981.
- Ida N. and Bastos P.A.: Electromagnetics and calculation of fields. Springer, 1997.
- Jeans J.: The mathematical theory of electricity and magnetism. Cambridge University Press, 1933.
- Lowther D.A. and Silvester P.P.: Computer-aided design in magnetics. Springer, 1986.
- Neittaanmaki P., Rudnicki M. and Savini A.: Inverse Problems and Optimal Design in Electricity and Magnetism. Oxford Science Publications, 1996.
- Panofsky W. and Phillips M.: Classical electricity and magnetism. Addison-Wesley, 1966.
- Reece A.B.J. and Preston T.W.: Finite element methods in electrical power engineering. Oxford University Press, 2000.
- Sadiku M.N.O.: Elements of electromagnetics. Oxford University Press, 2001.
- Seegerlind L.J.: Applied finite element analysis. Wiley, 1976.
- Silvester P.P.: Modern electromagnetic fields. Prentice-Hall, 1968.
- Silvester P.P. and Ferrari R.L.: Finite elements for electrical engineers. Cambridge University Press, 1983.
- Simonyi K.: Foundations of Electrical Engineering: Fields, Networks, Waves. Pergamon, 1963.
- Tikhonov A. and Arsénine V.: Méthodes de Résolution de Problèmes Mal Posés. MIR, 1976.
- Turowski J.: Elektrodynamika Techniczna. WNT, 1993.
- Woodson H.H. and Melcher J.R.: Electromechanical dynamics. Part II: Fields, Forces and Motion. Wiley, 1968.

Acknowledgements

The authors are indebted to various persons who have contributed to the preparation of the book.

In particular, they would like to thank Professor Alfredo Lorenzi (University of Milan) who reviewed the mathematical aspects of the manuscript and prepared the theoretical part of Section 3.1 about Green's functions. Thanks are due also to Professor Eugenio Costamagna, for his valuable comments and suggestions.

Moreover, the authors gratefully acknowledge the help of Maria Evelina Mognaschi, Ph.D., who prepared most of the figures in the books, and of Giuseppe Venchi, Ph.D., for his assistance in preparing the final manuscript.

Finally, the authors express their thanks to Springer for the friendly cooperation in the production of this book.

Index

- Ampère's equation, 102
- Analytic functions, 42
- Area coordinates, 83
- Automated optimal design, 2, 141

- Bandwidth, 88
- Bessel's function, 124
- Biot-Savart's law, 34, 128, 137
- Boundary conditions, 7, 13, 14, 31, 38, 42, 43, 67, 69, 70, 72–74, 78, 94, 102, 114, 118, 130, 131, 135, 136, 149, 157
- Boundary-value problem, 7, 10, 14, 48, 77

- Capacitance, 25
- Cauchy's problem, 136
- Cauchy-Riemann's equations, 42, 43
- Charge continuity, 102
- Charge-free, 12, 25, 108
- Charged sphere 20–21, 54–57, 63, 64
- Charge density, 11, 19, 20, 24, 56
- Coefficient matrix, 82, 84, 86, 87, 97
- Co-energy, 16, 22, 25, 26, 32, 34, 37, 79
- Complex variable, 42
- Condition number, 89, 139
- Conducting half-space, 60, 70
- Conducting plane, 70, 115–121
- Conduction
 - current, 101
 - field, 39, 40, 42
- Conductivity, 39, 102, 107, 115, 130
- Conductor, 11, 34, 42, 43, 57–59, 69, 73, 110, 115–117, 119–125, 137, 138
- Constitutive law, 10, 12, 28, 29
- Constrained optimization, 144
- Constraint, 153–159
- Convection current, 101
- Coulomb's gauge, 113
- Coulomb's method, 23, 25, 27
- Curl, 3, 5, 7, 8, 41, 85, 114, 161
- Curl-free field, 7
- Current density, 35, 39, 42, 58, 60, 79, 85, 87, 101, 102, 106, 107, 113, 115, 116, 119, 120, 122–125, 128, 131, 149–153
- Cylindrical
 - conductor, 42, 43, 59, 122, 123
 - coordinates, 3, 19, 33, 57, 77, 122, 165

- Delta function, 16
- Design variables, 143, 144, 147
- Deterministic, 146, 147
- Diagonal dominance, 88
- Differential approach, 33
- Dirac's distribution, 16, 17, 33
- Direct problems, 135
- Dirichlet's problem, 10, 14, 51, 52
- Displacement current, 101, 107, 113
- Divergence, 3, 5, 8, 9, 14, 36, 164
- Divergence-free, 6, 7
- Domain, 4, 5, 7, 10–17
- Double layer, 56
- Dual potentials, 113–115
- Dynamic optimization, 156–158

- Electric dipole, 18
- Electromagnet, 37, 97–99
- Electromagnetic
 - field, 101–103, 107, 110, 113, 114, 125, 161
 - wave, 105, 110
- Electrostatic
 - energy, 15, 23
 - field, 10, 15, 19, 22
 - images, 60–64
- Energy and forces, 22–24, 34–36
- Energy functional, 78–80

- Error norm, 92
- Euler's equation, 79
- Evolution strategy, 147
- Faraday's equation, 102
- Far field, 112
- Field
 - domain, 46, 72, 149
 - intensity, 10, 28, 39, 41, 101, 106, 127
 - point, 8, 45, 46, 57, 59, 110, 163, 164
- Finite elements, 80, 95
- Flux
 - density, 10, 15, 28, 32, 35, 65–67
 - surface, 4
- Force, 22–27, 34–38, 98, 99, 102
- Fredholm's equation, 137, 138
- Frequency domain, 103, 104, 106, 107, 110, 111, 121, 123
- Galerkin's method, 79
- Galilean transformation, 127, 132
- Gauge, 14, 30, 41, 108–111, 113, 114
- Gauss's electric equation, 102
- Gauss's magnetic equation, 102
- Generation, 147
- Genetic algorithm, 146
- Global coefficient matrix, 87
- Global minimum, 146
- Global shape function, 80, 81, 84
- Global source vector, 82, 84, 85, 94, 97
- Gradient, 14, 30, 41, 97, 108, 114, 145, 146
- Gradient-based method, 145, 146
- Gradient-free method, 145, 146
- Green's first identity, 9
- Green's formula, 9, 10, 45, 46, 56, 57,
- Green's function, 45, 46, 49–51, 54, 57, 59, 137, 138
- Grid, 80–82, 84–86, 88, 91–95, 144
- Hadamard's condition, 135, 136
- Harmonic, 13, 30, 41, 105, 113, 118
- Helmholtz's equations, 104
- Homogeneous medium, 12, 29, 40, 107, 108
- Identification, 135, 141, 150–153
- Ill-posed problems, 135–137
- Initial conditions, 113, 124, 130, 136
- Inner domain, 50
- Insulating medium, 10, 12, 105, 125
- Integral approach, 21, 57, 137
- Interface, 11, 12, 25, 27, 35, 61, 85
- Inverse problems, 135–141
- Irrrotational, 7, 11, 12, 29, 40
- Isotropic, 10, 11, 13, 15, 28, 32, 39, 113
- Kelvin's transformation, 46
- Kernel, 137, 138
- Kronecker's index, 53
- Laminar current density, 123, 125
- Laplace's equation, 13, 14, 31, 41, 71–73, 136
- Laplace's law, 58, 112
- Laplacian, 4, 47–49
- Least-square solution, 139–141
- Line
 - charge, 19, 21
 - current, 33, 57, 58, 64–70
- Local coefficient matrix, 84, 86, 87
- Local error, 91
- Local minimum, 144
- Local shape function, 82, 84, 95, 96
- Local source vector, 85
- Lorentz's equation, 102
- Lorentz's gauge, 109, 111, 113
- Lorentzian transformation, 132
- Magnet, 30
- Magnetic
 - diffusion, 129, 131, 157
 - dipole, 28
 - pole, 30, 150, 153, 156, 159
- Magnetostatic
 - energy, 32
 - field, 28–38
 - images, 64–67
- Maxwell's equations, 10, 28, 39, 101, 103, 106, 113, 127, 161
- Mechanical effect, 22
- Medium, 10–12, 15, 28, 29, 32, 39, 40, 61, 101, 102, 105–108, 113, 125
- Mesh, 95, 97, 98, 151, 155, 160
- Method of images, 60–70
- Minimization, 79, 143, 144, 146, 148, 151
- Moment, 18, 56
- Monopole, 19
- Motional effect, 102
- Multiobjective optimization, 145
- Multiply-connected domain, 14
- Mutation, 147
- Near field, 112
- Neumann's problem, 10, 14
- Newton-Raphson method, 31, 151
- Nodal
 - current, 82, 89
 - potential, 82

- Node, 80–82, 84–89, 91–94
- Non-deterministic, 146, 147
- Non-dominated solutions, 145, 159, 160
- Non-homogeneous medium, 12, 29, 40
- Non-linear, 15, 32, 131, 146, 150, 151, 153
- Norm, 119, 139, 161
- Normal versor, 5, 13, 23, 31, 35, 37, 46, 164

- Objective function, 143, 144, 146–149, 153–157
- Observer, 10, 28, 67, 125–131
- Optimization, 143–145, 152–159
- Ordinary differential equation, 72, 123
- Oscillating dipole, 110–112
- Outer domain, 52
- Over-determined system, 138, 139

- Pareto front, 145, 159, 160
- Pareto optimality, 159
- Partial differential equation, 72
- Penalty term, 144, 154
- Penetration depth, 118, 123, 125
- Permanent magnet, 28–30,
- Permeability, 28, 29, 31, 35, 37, 38, 57, 64, 65, 67, 68, 70, 71, 73, 77, 86, 97, 102, 113, 130, 150, 151
- Permittivity, 10, 11, 24, 26, 46, 60, 61, 102, 107, 113
- Phasor, 104, 105, 107, 110–112, 118, 121
- Plane wave, 105, 106
- Point charge, 16, 18, 21, 54, 57, 60–63, 110, 127
- Poisson's equation, 13, 45, 46, 72, 73, 79
- Potential, 8, 13, 16–19, 31, 34, 40–42
- Power loss, 42, 121
- Poynting's vector, 103, 104, 106, 112, 121
- Poynting's theorem, 103

- Radial vector, 61, 112
- Rectangular coordinates, 3, 4, 24, 30, 35, 41, 67, 71, 77, 80, 82, 95
- Reference frame, 3, 125
- Reluctivity, 28, 150
- Retarded potentials, 110
- Ritz's method, 79
- Rotational, 34

- Sample-and-rank method, 159
- Scalar potential, 8, 10, 14, 31, 108, 109, 111, 113, 114
- Selection, 147
- Separation of variables, 71, 123

- Shape
 - design, 141, 153, 156, 159
 - function, 80–84, 95, 96
- Simplex method, 147
- Simply-connected domain, 5, 77, 80, 102
- Simulated annealing, 146
- Single layer, 24, 56
- Singular value decomposition, 140
- Skin depth, 118
- Slot, 38, 39, 67–69, 73, 75, 86, 91, 93, 136, 149
- Slotted electrical machine, 38, 149
- Solenoidal, 6, 7, 12, 29, 40, 116
- Solid modeling, 95, 98
- Source
 - point, 8, 45, 46, 57, 59, 110
 - vector, 82, 84, 85, 88, 94, 97
- Sparse matrix, 84, 88
- Spherical coordinates, 3, 16, 18, 47, 111, 165
- Static optimization, 153, 154
- Steady
 - motion, 129
 - point, 78–80, 82
- Step excitation, 122, 157
- Stiffness matrix, 139
- Stress tensor, 23–26, 35, 37, 98
- Stokes's theorem, 34, 164
- Strong eddy current, 116
- Surface
 - charge, 11, 20, 21, 24
 - dipole, 56, 57
 - modelling, 95
- Symmetry, 16, 19, 21, 33, 38, 47, 73, 90, 92, 115, 117, 126
- Synthesis, 1, 135, 137, 141

- Tangential versor, 13, 14, 31
- Taylor's series, 31
- Time domain, 105, 106, 119
- Time-harmonic, 105, 113, 118
- Time-varying, 2, 101–103, 115, 119
- Torque, 22, 34, 35
- Trajectory, 144, 151, 152
- Transmission conditions, 11, 29, 61, 65
- Travelling charge, 128

- Unconstrained optimization, 143
- Under-determined system, 138, 139
- Unit source, 45, 49

- Variation, 22, 34, 77–79, 81, 82, 92, 113, 125, 137, 147, 151, 160
- Variational
 - equation, 78
 - formulation, 77

- Vector
 - field, 3, 5, 7
 - identities, 12, 29, 40, 77, 103, 104, 164
 - potential, 8, 14, 30, 31, 34, 38, 57, 71, 77, 108–111, 113, 114, 136, 138
- Virtual
 - displacement, 22, 34
 - work principle, 22, 26, 34
- Volume coordinates, 96
- Weak eddy current, 115
- Weak formulation, 77
- Well-posed problems, 135
- Work, 22, 23, 26, 34